JOURNAL OF GEOPHYSICAL RESEARCH

The continuation of

TERRESTRIAL MAGNETISM AND ATMOSPHERIC ELECTRICITY
(1896-1948)

An International Quarterly

VOLUME 62 September, 1957 NUMBER 3

CONTENTS

(Contents concluded on outside back cover)

Published at

THE WILLIAM BYRD PRESS, INC.

P. O. BOX 2-W, SHERWOOD AVE. AND DURHAM ST.

RICHMOND 5, VIRGINIA

Address all correspondence to

JOURNAL OF GEOPHYSICAL RESEARCH

5241 BROAD BRANCH ROAD, NORTHWEST

WASHINGTON 15, D.C., U.S.A.

SIX DOLLARS A YEAR

SINGLE NUMBERS, TWO DOLLARS

JOURNAL OF GEOPHYSICAL RESEARCH

The continuation of

Terrestrial Magnetism and Atmospheric Electricity

(1896-1948)

An International Quarterly

Founded 1896 by L. A. BAUER *Continued 1928-1948 by* J. A. FLEMING

Fields of Interest

Terrestrial Magnetism
Atmospheric Electricity
The Ionosphere
Solar and Terrestrial Relationships
Aurora, Night Sky, and Zodiacal Light
The Ozone Layer
Meteorology of Highest Atmospheric Levels
The Constitution and Physical States of the Upper Atmosphere
Special Investigations of the Earth's Crust and Interior, including experimental seismic waves, physics of the deep ocean and ocean bottom, physics in geology
And similar topics

This Journal serves the interests of investigators concerned with terrestrial magnetism and electricity, the upper atmosphere, the earth's crust and interior by presenting papers of new analysis and interpretation or new experimental or observational approach, and contributions to international collaboration. It is not in a position to print, primarily for archive purposes, extensive tables of data from observatories or surveys, the significance of which has not been analyzed.

Forward *manuscripts* to one of the Associate Editors, or to the editorial office of the Journal at 5241 Broad Branch Road, Northwest, Washington 15, D.C., U.S.A. It is preferred that manuscripts be submitted in English, but communications in French, German, Italian, or Spanish are also acceptable. A brief abstract, preferably in English, must accompany each manuscript. A *publication charge* of $8 per page will be billed by the Editor to the institution which sponsors the work of any author; private individuals are not assessed page charges. Manuscripts from outside the United States are invited, and should not be withheld or delayed because of currency restrictions or other special difficulties relating to page charges. Costs of publication are roughly twice the total income from page charges and subscriptions, and are met by subsidies from the Carnegie Institution of Washington and international and private sources.

Back issues and *reprints* are handled by the Editorial Office, 5241 Broad Branch Road, N.W., Washington 15, D.C., U.S.A.

Subscriptions are handled by the Editorial Office, 5241 Broad Branch Road, N.W., Washington 15, D.C., U.S.A.

Second-class mail privileges authorized at Richmond, Virginia

Journal of

GEOPHYSICAL RESEARCH

The continuation of

Terrestrial Magnetism and Atmospheric Electricity

VOLUME 62 SEPTEMBER, 1957 No. 3

REFRACTIVE CORRECTIONS TO SCATTER PROPAGATION

BY ALBERT D. WHEELON

The Ramo-Wooldridge Corporation,
Los Angeles 45, California

(Received October 17, 1956)

ABSTRACT

The role played by the ionosphere's mean electron density for scatter propagation is considered. An electron plasma at the scattering point (1) increases the effective wavelength and (2) decreases the scattering angle. These effects combine to modify the basic propagation variable

$$q' = \frac{4\pi}{\lambda} \sin\left(\frac{\theta}{2}\right)\left[1 - \frac{f_{\mathrm{MUF}}^2}{f^2}\right]^{1/2}$$

by a factor which depends only on the instantaneous maximum usable frequency for the path. Associated signal-level variations are found to be insignificant for conventional VHF scatter links. Such an analysis does provide an explanation for recent observations of *F*-layer scattered signals and their correlation with f_{MUF}/f. Apparent scattering-height changes caused by variable refractive pulse delay times are also studied.

I. INTRODUCTION

Thoroughgoing experimental studies of scatter propagation *via* the ionosphere at frequencies above the usual penetration frequency (MUF) are now published [see 1 and 2 of "References" at end of paper]. Daytime propagation is probably due to (single) scattering from turbulent concentrations of the ionosphere's electron

gas. Theoretical opinion now seems agreed [3, 4, 5] that turbulent convective mixing of ionization gradients exerts the strongest influence on these fluctuations.

D. K. Bailey has studied the changes of scattering propagation caused by tropospheric refraction [6]. The present study considers the mean (background) electron density at the scattering point, of which the fluctuations themselves are born and in the presence of which they must scatter waves. Previous treatments have tacitly assumed that free space plane waves fall on the turbulent blobs and are reradiated. This is equivalent to neglecting the mean electron density N_0 in the propagation equation.

$$\left[\nabla^2 + \frac{4\pi^2}{\lambda_0^2} - \frac{4\pi e^2}{mc^2}(N_0 + \delta N)\right]\vec{E} = 0 \quad \ldots\ldots\ldots\ldots\ldots\ldots (1)$$

It is just this mean density, however, which explains radio-wave reflection at the *vertical* incidence critical frequency.

$$f_c^2 = \frac{4\pi e^2}{m} N_0 \quad \ldots\ldots\ldots\ldots\ldots\ldots\ldots\ldots\ldots\ldots (2)$$

The same density and propagation path geometry set the maximum usable frequency (MUF) for reflection at oblique incidence.

$$f_{\text{MUF}}^2 = \frac{4\pi e^2}{m} N_0 \sec^2(i) \quad \ldots\ldots\ldots\ldots\ldots\ldots\ldots\ldots (3)$$

i is the angle which the rays make with the local vertical at the path midpoint (see Fig. 1) and is related to the free space scattering angle by $2i = \pi - \theta_0$.

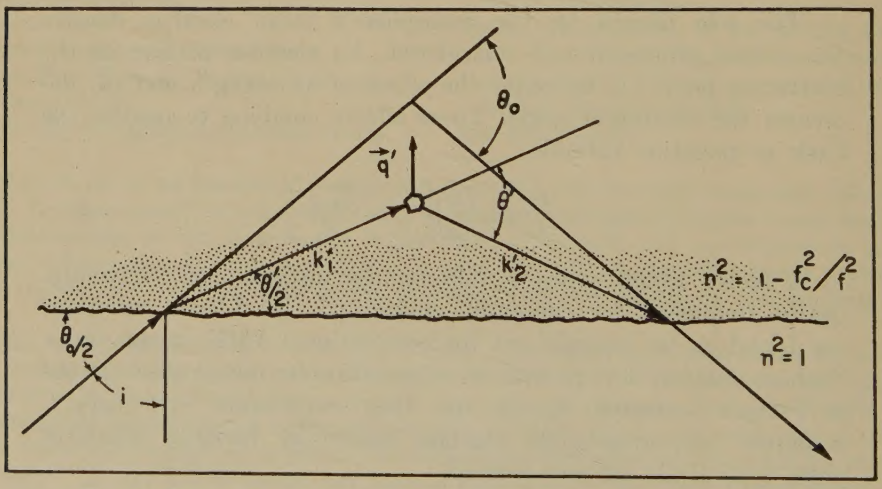

FIG. 1—Propagation geometry, showing refractive effects of scattering

This mean density also influences obliquely *penetrating* waves in two important ways: (1) it increases the effective wavelength in the scattering medium, and (2) refractive bending of the incident and scattered waves as they enter and leave the ionized region decreases the *effective* scattering angle θ'. From equations (1) and (2), we find for the first effect

$$\frac{2\pi}{\lambda'} = \frac{2\pi}{\lambda_0}\left[1 - f_c^2/f^2\right]^{1/2} \quad \ldots\ldots (4)$$

Snell's law applied to Figure 1 relates the free space incidence angle i to the effective scattering angle θ'.

$$1 \sin (i) = n \sin\left(\frac{\pi - \theta'}{2}\right)$$

From equation (1), the local index of refraction is $n = [1 - f_c^2/f^2]^{1/2}$, so that

$$\cos\left(\frac{\theta'}{2}\right) = \frac{\cos\left(\frac{\theta_0}{2}\right)}{\left[1 - f_c^2/f^2\right]^{1/2}} \quad \ldots\ldots (5)$$

The critical variable for scatter propagation is the scattering difference vector

$$\vec{q} = \vec{K}_2 - \vec{K}_1$$

defined by the incident and scattered wave propagation vectors $\vec{K}_1$ and $\vec{K}_2$ (that is, $|\vec{K}_i| = 2\pi/\lambda'$). For symmetric scattering, the direction of $\vec{q}$ is preserved and we need only consider its *local* magnitude.

$$|\vec{q}'| = q' = \frac{4\pi}{\lambda'} \sin\left(\frac{\theta'}{2}\right) = \frac{4\pi}{\lambda_0} \sin\left(\frac{\theta_0}{2}\right)\left\{1 - \left[\frac{f_c}{f} \csc\left(\frac{\theta_0}{2}\right)\right]^2\right\}^{1/2}$$

or

$$q' = \frac{4\pi}{\lambda_0} \sin\left(\frac{\theta_0}{2}\right)\left[1 - f_{\text{MUF}}^2/f^2\right]^{1/2} \quad \ldots\ldots (6)$$

It is significant that just this combination of f_c and θ_0 occurs, since the MUF is both measured and predicted for many oblique paths on a regular basis.

II. POWER CHANGES

The scattered power is proportional to the scattering cross-section $\sigma(k)$ evaluated at the wave-number $k = q'$. Further identification of $\sigma(k)$ with the (size) spectrum and space correlation of dielectric fluctuations involves only the classical electron radius $r_0 = e^2/mc^2 = 2.8 \times 10^{-13}$ cm [3].

$$\sigma(k) = r_0^2 S(k) = r_0^2 \int d^3R e^{i\vec{k}\cdot\vec{R}} < \Delta\epsilon^2 > C(R) \quad \ldots\ldots (7)$$

Analysis based on the "mixing-in-gradient" hypothesis suggests that the spectrum is [3, 5]

$$S(k) = \left(\frac{dN_0}{dh}\right)^2 \frac{1}{k^5} F\left(\frac{k}{k_s}\right), \qquad k > k_0 \quad \ldots\ldots (8)$$

where the function

$$F(x) = \frac{1}{[1 + x^{4/3}]^2} \frac{1}{[1 + x^4]^{4/3}} \quad \ldots\ldots (9)$$

describes the viscosity (diffusion) damping of the spectrum. dN_0/dh is the vertical gradient of mean ionization and k_0 the (largest blob) wave-number below which similarity considerations are not valid. Tropospheric line-of-sight phase measurements in the same (similarity) range tend to support a correlation function [7],

$$C(R) = \frac{R}{l_0} K_1\left(\frac{R}{l_0}\right)$$

where $l_0 \simeq 2\pi/k_0$. The equivalence of equation (7) suggests that expression (8) might be extended to smaller k by

$$S(k) = \left(\frac{dN_0}{dh}\right)^2 \frac{1}{[k_0^2 + k^2]^{5/2}} F(k/k_s) \quad \ldots\ldots\ldots\ldots\ldots\ldots (10)$$

The variation of scattered power with refractive conditions in the ionosphere is thus predicted by combining equations (6) and (9).

$$P_{rec.} = C \frac{F\left(\frac{4\pi}{\lambda k_s} \sin\left(\frac{\theta}{2}\right)\left[1 - \frac{f_{MUF}^2}{f^2}\right]^{1/2}\right)}{\left\{1 + \left[2\frac{l_0}{\lambda}\sin\left(\frac{\theta_0}{2}\right)\right]^2\left[1 - \frac{f_{MUF}^2}{f^2}\right]\right\}^{5/2}} \quad \ldots\ldots\ldots\ldots (11)$$

We must now inquire if there is experimental support for such an expression. The VHF scatter experiments of references [1] and [2] were made on a 1,250-km path (mostly), for which the vertical incidence critical frequency was always less than three (3) megacycles. Since csc $(\theta_0/2) \simeq 5$ for $h = 80$ km,* the MUF could not have been greater than 15 Mc and, hence, too small in comparison with the transmitted frequencies (28, 50, and 108 Mc) to play an effective role. Diurnal variations of signal level observed on this path(s) are too large (15 db) to be reconciled with corresponding changes in MUF *via* equation (11): it is likely that diurnal changes of dN_0/dh in equation (10) can explain this effect [8].

A recent series of propagation tests [9, 10] at 21.5 Mc over a 3,000-km path successfully established continuous F-layer transmission above the measured $F2$ MUF. It was suggested that this signal might represent scattering by F-region irregularities. An interesting correlation between field strength and f_{MUF}/f was observed, despite pronounced diurnal variations of both. The measured $F2$ MUF's at the path midpoint ranged from 6 to 15 Mc. Since these values are quite close to the transmitter frequency, a natural explanation for such correlation might be found in equation (11).

The propagation variable q' for such transmissions depends on the scattering height. It was stated [9] that earth curvature prevented the beams from intersecting below 200 km, while the MUF's were taken at a *virtual* height of 300 km. In the absence of pulse delay measurements, we shall assume $h = 250$ *km*, corresponding to $\theta_0 \simeq 36°$ and sin $(\theta_0/2) \simeq 0.3$. The wavelength was 15 m, so that

$$q_0 = \frac{4\pi}{\lambda} \sin\left(\frac{\theta_0}{\lambda}\right) \simeq 0.25 \text{ (meters)}^{-1}$$

*N.B. tan $(\theta_0/2) = 2h/d + d/4a$.

To determine the role of $F(k/k_s)$ in equation (11), we need to know the viscosity transition wave-number k_s at the scattering height. Booker [11] has studied this question, taking into account the earth's magnetic field. He suggests that the scales are different along and normal to the magnetic field: $L_s = (k_s)^{-1} = 10^{-2}$ m transverse, and $L_s' = (k_s')^{-1} = 10^4$ m longitudinally. The midpoint of the Dallas, Texas, to Caribou, Maine, path was near Ft. Belvoir, Maryland, where the magnetic field is inclined at 70° to the vertical. This means that the field $\vec{H}$ and $\vec{q}$ were within 20° of one another and that the small scale *along* the field was most effective. The viscosity function was therefore quite important and we set $F(x) = x^{-8}$. If one neglects values of f_{MUF}/f very near unity, the scattered power from equation (11) ought to behave as

$$P \simeq \frac{\text{constant}}{[1 - f_{MUF}^2/f^2]^{13/2}} \quad \ldots\ldots\ldots\ldots\ldots\ldots\ldots\ldots\ldots\ldots (12)$$

Experimental data [9] for 20–25 June 1955 and 25–30 July 1955 were selected for analysis. Simultaneous values of signal level in db and the quantity $1 - f_{MUF}^2/f^2$ are plotted on semi-log paper in Figure 2. A theoretical curve corresponding to

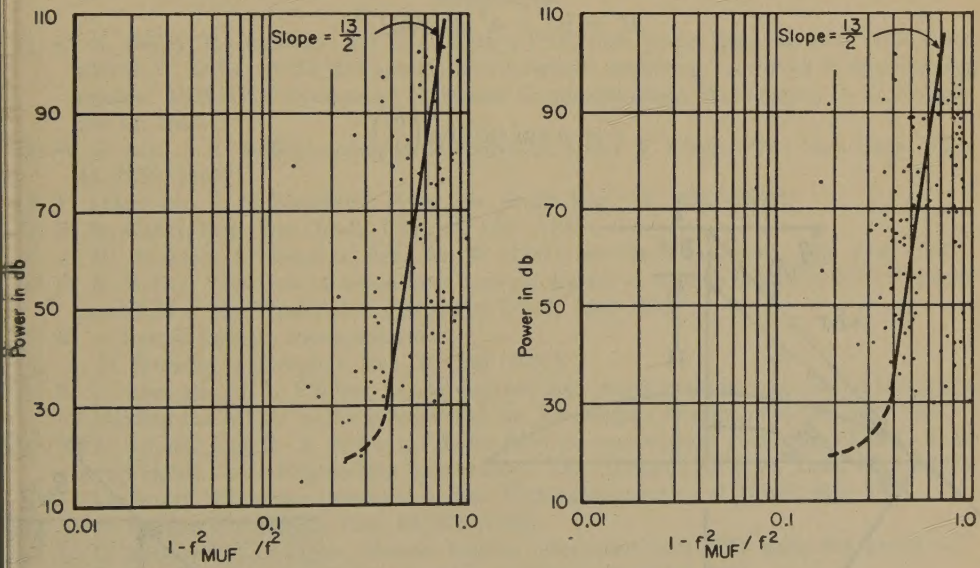

FIG. 2—Experimental and theoretical correlations of signal strength with simultaneous ratio of MUF to transmitter frequency for 3,000-km path, $f = 21.5$ Mc and $h = 250$ km, at intervals of one hour

equation (12) is also shown, and gives a possible fit for the data well above the MUF. The tendency for these power levels to saturate as the MUF approaches the transmitter frequency illustrates the role of l_0 in equation (11). If an approximate curve is fitted to the "knee" of these points (at about $1 - f_{MUF}^2/f^2 = 0.2$), one finds $l_0 > 100$ meters, which is in rough agreement with one's concept of the large blob size at such heights. From these data, it is clear that more experiments

need be performed. In the meantime, it should be clear that the dependence of such transmission on the midpoint MUF is associated with refractive effects.

III. HEIGHT CHANGES

The ionosphere's dispersive character ought also to influence measurements of scattering heights by pulse delay methods. Since pulses travel faster in an ionized medium, one would expect lower *apparent* scattering heights during daylight hours than at night (when the D and E regions sensibly collapse). This phenomenon is experimentally observed [1, 12] as a change from about 75 to 90 km at VHF. The *ray-path* change in the electron gas is

$$\delta r = \int_0^L \frac{ds}{[1 - f_c^2/f^2]^{1/2}} - L \simeq \frac{1}{2} L \left(\frac{f_c}{f}\right)^2 \quad \ldots\ldots\ldots\ldots\ldots\ldots (13)$$

where $L = b \csc(\theta/2)$ is the path length *in the ionization layer* of thickness b. Small changes in height are related to those in path length by $r\delta r = H\delta H$. H and r are given in terms of the scatter circuit's half-angle β and scattering angle θ_0 (see Fig. 3) by

$$H = [r^2 - a^2 \sin^2(\beta)]^{1/2}$$

and

$$r = a \sin(\beta) \sec\left(\frac{\theta_0}{2}\right)$$

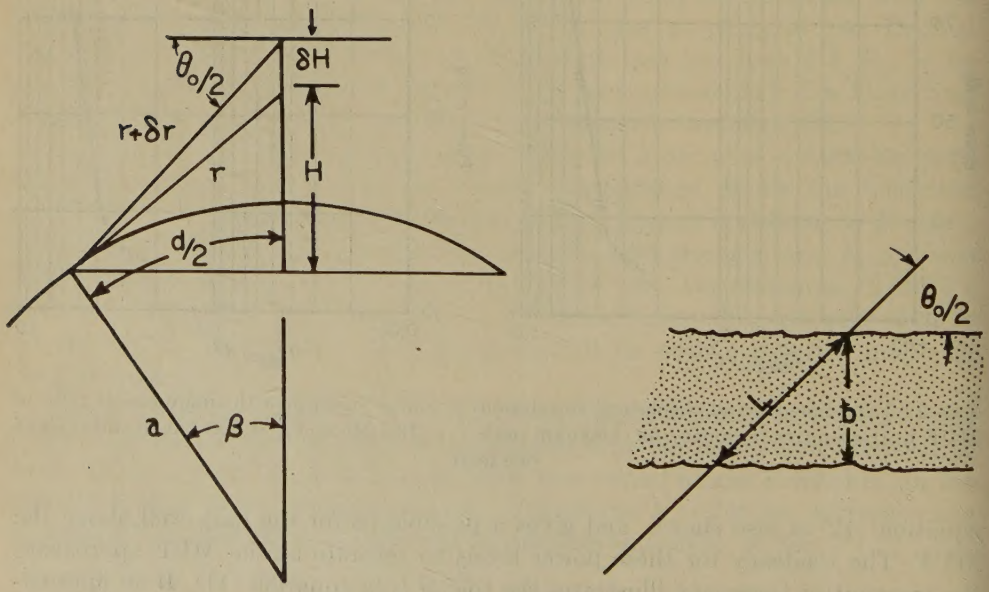

FIG. 3—Geometry for estimating refractive height changes

Combining all of these expressions,

$$\delta H = \frac{r}{H}\,\delta r = \frac{r}{[r^2 - a^2 \sin^2(\beta)]^{1/2}}\,\frac{1}{2}\,b \csc\left(\frac{\theta_0}{2}\right)\left(\frac{f_c}{f}\right)^2$$

or

$$\delta H = \frac{1}{2}\,b\left[\frac{f_{MUF}}{f}\right]^2 \qquad (14)$$

The refractive correction again depends only on the MUF. Applying this result to a 1,250-km path, with $f = 50$ Mc, $f_{MUF} < 12$ Mc, and $b = 20$ km, gives a height change which is ten times smaller than that observed. Evidently one must look elsewhere [8] for an explanation of this phenomenon. It would be very interesting to make pulse delay measurements on "*F*-scatter" paths, however, to see if changes in H there can be correlated with the ratio f_{MUF}/f, as are the changes in signal level.

ACKNOWLEDGMENTS

Dr. W. G. Abel kindly supplied copies of the 21.5-Mc data used in Figure 2 prior to publication.

References

[1] D. K. Bailey, R. Bateman, and R. C. Kirby, Proc. Inst. Radio Eng., **43**, 1181 (1955). See also R. C. Kirby, "VHF propagation by ionospheric scattering—A survey of experimental results," IRE-GWU Symposium on Scatter Communications, Washington, D. C., November 14, 1955.

[2] W. G. Abel, J. T. DeBettencourt, J. H. Chisholm, and J. F. Roche, Proc. Inst. Radio Eng., **43**, 1255 (1955).

[3] F. Villars and V. F. Weisskopf, Proc. Inst. Radio Eng., **43**, 1232 (1955).

[4] R. M. Gallet, Proc. Inst. Radio Eng., **43**, 1240 (1955).

[5] A. D. Wheelon, J. Geophys. Res., **62**, 93 (1957); see also Phys. Rev., **105**, 1706 (1957).

[6] D. K. Bailey, "The role of ionospheric forward scatter in oblique incidence MUF," paper presented at the Washington meeting of URSI, May 1955.

[7] K. A. Norton (private communication).

[8] A. D. Wheelon, J. Geophys. Res., **62**, 255 (1957).

[9] W. G. Abel and M. L. Phillips, "Long distance high power radio propagation at frequency exceeding the MUF," paper presented at the Washington meeting of URSI, May 1956.

[10] H. A. Schulke and R. A. Kulinyi, "Radio teletype transmission above the MUF," U. S. Army Signal Corps Engineering Laboratories, Fort Monmouth, N. J., Tech. Memo 1713 (November 1955); also presented at the Washington meeting of URSI, May 1956.

[11] H. G. Booker, J. Geophys. Res., **61**, 673 (1956).

[12] W. G. Abel and V. C. Pineo, "Scatter heights determined from VHF pulse measurements," paper presented at the Florida meeting of URSI, December 1955.

"MOLECULAR WEIGHT" OF AIR AT HIGH ALTITUDES

BY LEWIS E. MILLER

Geophysics Research Directorate, Air Force Cambridge Research Center, Air Research and Development Command, Laurence G. Hanscom Field, Bedford, Massachusetts

(Received August 31, 1956)

ABSTRACT

This report describes a method for obtaining the so-called "molecular weight" of air at high altitudes of the earth's atmosphere above the transition region for the dissociation of molecular into atomic oxygen. A reasonable working model, based upon the ratio of absolute temperature to molecular weight T/M, which is proportional to the slope of the $\log_e$ pressure *vs* altitude curve, is presented. The region considered is from 90 to 600 km, assuming that the composition of the atmosphere is constant up to 90 km.

The calculations are based upon experimental data reported by Byram, Chubb, and Friedman from Aerobee 16, 1 December 1953. Since the 1956 Model Atmosphere of the Air Research and Development Command employs a variable scale height gradient with altitude, the diffusive equilibrium and mixing formulas of Nicolet and Mange were modified to obtain the vertical distributions of the various atmospheric constituents. The mass densities are found by multiplying the number densities by the respective molecular mass of the individual components of the atmosphere.

The molecular weights at the various altitudes were calculated from the formula

$$\frac{\text{Total mass density}}{\text{Total number density}} \times N_0 \text{ (Avogadro's number)} = \text{Molecular weight}$$

Knowing the composition of the atmosphere at any altitude, it is possible to determine the temperature through the relationship of the scale height to temperature, $H = RT/Mg$.

INTRODUCTION

The need for knowing the quantitative composition of the earth's upper atmosphere is evident. An examination of the interrelationship among the quantities, (*a*) *pressure*, (*b*) *density*, (*c*) *altitude*, and (*d*) *temperature*, which describe the physical properties of the earth's atmosphere, reveals that any two of these parameters may be expressed in a formula as a function of either one of the other two quantities. Thus, the hydrostatic equation (1) below gives the pressure and density as a function of altitude. It may be observed, when temperature is related to either pressure and density, or to pressure and altitude in equations (2) and (3),

that the so-called mean *"molecular weight"** M of air also appears in the equation.

For low altitudes from the earth's surface up to about 90 km, it is generally assumed that the composition of the atmosphere does not change with height. Above this altitude, there is abundance of evidence that molecular oxygen dissociates into atomic oxygen and, as a result, the mean molecular weight of air changes with altitude. It is, therefore, of great importance to know the mean molecular weight of air above this transition region, in order to determine the temperature at high altitudes. As yet, there are no satisfactory direct experimental methods for measuring temperature in the upper atmosphere. Temperature in these regions must be determined indirectly through its relationship to pressure or density. The purpose of this report is to describe a method for obtaining the molecular weight of air in the upper regions of the atmosphere.

Experimental data from rocket flights are now available for the dissociation of molecular oxygen into atomic oxygen. Our calculations are based upon these observations. There are no quantitative measurements for the dissociation of molecular nitrogen and the amount of atomic nitrogen. However, there is observational evidence from rocket-flown mass ion-spectrographs, and from the spectra of the aurora and the night airglow for the occurrence of atomic nitrogen in the upper atmosphere.

THE BAROMETRIC FORMULA

The problem of the vertical distribution of the atmospheric constituents and the definition of such terms as *geopotential*, *geopotential altitude*, and *scale height* may be approached by the derivation of the *barometric formula*, which relates the decrease in atmospheric pressure with increasing height above the earth's surface. Consider a column of gas of one cm^2 cross-section extending upward into the atmosphere, and make the simplifying assumptions that the gas is at equilibrium in a constant gravitational field and constant temperature. Now consider a very thin horizontal layer of the gas of thickness dz. The difference in pressure $-(dp/dz)\,dz$ between the upper and lower surfaces is equal to the weight of the layer $\rho g\,dz$.

Therefore,

$$-dp = \rho g dz \qquad (1)$$

where ρ is the density of the gas, g is the acceleration of gravity, and the minus sign is used since the pressure of the earth's atmosphere decreases with increasing altitude z.

Equation (1) is the familiar hydrostatic or barometric formula. For an ideal gas,

$$\rho = \frac{pM}{RT} \qquad (2)$$

in which M is the molecular weight, R the universal gas constant, and T the temperature in degrees Kelvin. Substituting (2) into (1),

*"Molecular weight" is used throughout this paper in the sense that it represents the *mean mole mass*, that is, the mass of the Avogadro number of air particles.

$$-\frac{dp}{p} = \frac{Mg}{RT}dz = \frac{dz}{H} \quad \ldots\ldots\ldots\ldots\ldots\ldots\ldots\ldots\ldots\ldots (3)$$

Integrating between the limits p_0 at $z = 0$, and p at $z = z$

$$ln\frac{p}{p_0} = -\frac{Mgz}{RT} = -\frac{z}{H} \quad \ldots\ldots\ldots\ldots\ldots\ldots\ldots\ldots\ldots\ldots (4)$$

and

$$p = p_0 e^{-Mgz/RT} = p_0 e^{-z/H} \quad \ldots\ldots\ldots\ldots\ldots\ldots\ldots\ldots\ldots\ldots (5)$$

The latter equation was originally deduced by Boltzmann [see 1 of "References" at end of paper] and is merely an extension of the Distribution Law to include potential energy.

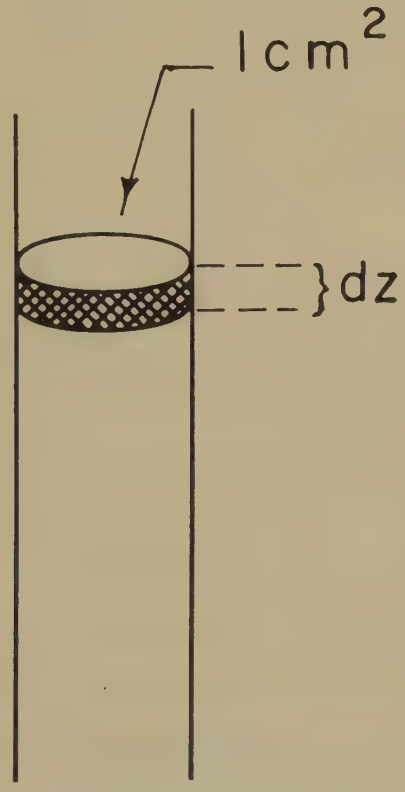

FIG. 1—The barometric formula

SCALE HEIGHT, GEOPOTENTIAL

The quantity RT/Mg in equation (3), which has the dimensions of length, is called the local *scale height* (the height of a homogeneous atmosphere of uniform density and at the temperature T). It is denoted by the symbol H. Mathematically, the quantity is defined as the reciprocal of the negative slope of the log$_e$ pressure *vs* altitude curve. This slope is proportional to the ratio of the absolute temperature

to molecular weight T/M, which is significant in the development of our method for determining the vertical distribution of the atmospheric constituents. The scale height may also be regarded as the increase in altitude necessary to reduce the pressure by $1/e$, where e is the base of Naperian logarithms.

The numerator Mgz of the exponent in the exponential equation (5) is simply the gravitational potential energy at the point z. The gravitational potential energy Φ per unit mass at any height z above the surface of the earth is termed the *geopotential.* It is defined to be the work required to bring unit mass to the height z from a standard position of zero potential, which conventially is taken to be at mean sea-level. It has the dimensions $cm^2\ sec^{-2}$. In many meteorological and aerological calculations, the unit adopted for geopotential altitude is called the *geopotential meter,* denoted by m′[2]. One thousand geopotential meters are termed the *geopotential kilometer* km′. Geopotential altitude Φ is related to geometric altitude z in meters through the following relationship:

$$\Phi = \frac{1}{9.80665}\int_0^z g\,dz \qquad (6)^*$$

Integration and solution of (6) through the substitution of Newton's inverse-square law of gravitation

$$g = g_0\left(\frac{r}{r+z}\right)^2 \qquad (7)$$

where g_0 is the acceleration of gravity at mean sea-level (980.665 cm sec^{-2}) corresponding with the latitude 45°32′40″, and r is the radius of the earth (6.356766×10^8 cm), reduces to the following simplified expressions for the relationship between geometric and geopotential altitudes:

$$z = \left(\frac{r\Phi}{r-\Phi}\right) \quad \text{in geometric meters} \qquad (8)$$

$$\Phi = \left(\frac{rz}{r+z}\right) \quad \text{in geopotential meters} \qquad (9)$$

where r is the radius of the earth in meters at the given latitude.

DIFFUSIVE EQUILIBRIUM AND MIXING FORMULAS

In 1932, Epstein [3, 4] derived a differential equation which controls atmospheric diffusion under the action of gravity. At lower altitudes, where the atmosphere is uniformly mixed, the densities of the components were shown to decrease with height z according to the equation

$$\rho = \rho_0 e^{-\mu z} \qquad (10)$$

in which the coefficient μ is equal to Mg/RT and M is the mean molecular weight of air as a whole. At high altitudes, the atmospheric gases were regarded to be

*The use of the factor 9.80665 in equation (6) is in keeping with the NACA Standard Atmosphere which will give Φ in standard geopotential meters.

completely unmixed. The density of each constituent gas decreases independently with height and tends to produce a concentration of each gas according to the law

$$\rho = \rho_0 e^{-\nu z} \quad \ldots\ldots\ldots\ldots\ldots\ldots\ldots\ldots\ldots\ldots (11)$$

where the coefficient ν is equal to mg/RT and m is the molecular weight of the individual gas.

More recently, Nicolet and Mange [5, 6, 7] have discussed diffusion processes in the thermosphere. The problem of the vertical distribution of molecular oxygen was considered as an example of diffusion in a region having sources and sinks. Formulas for three different modes of vertical distribution, (*a*) photoequilibrium, (*b*) mixing, and (*c*) diffusive equilibrium, were derived. The mass density ρ is defined by

$$\rho = nm \quad \ldots\ldots\ldots\ldots\ldots\ldots\ldots\ldots\ldots\ldots (12)$$

in which n is the total number density and m the mean mass of an average air particle.

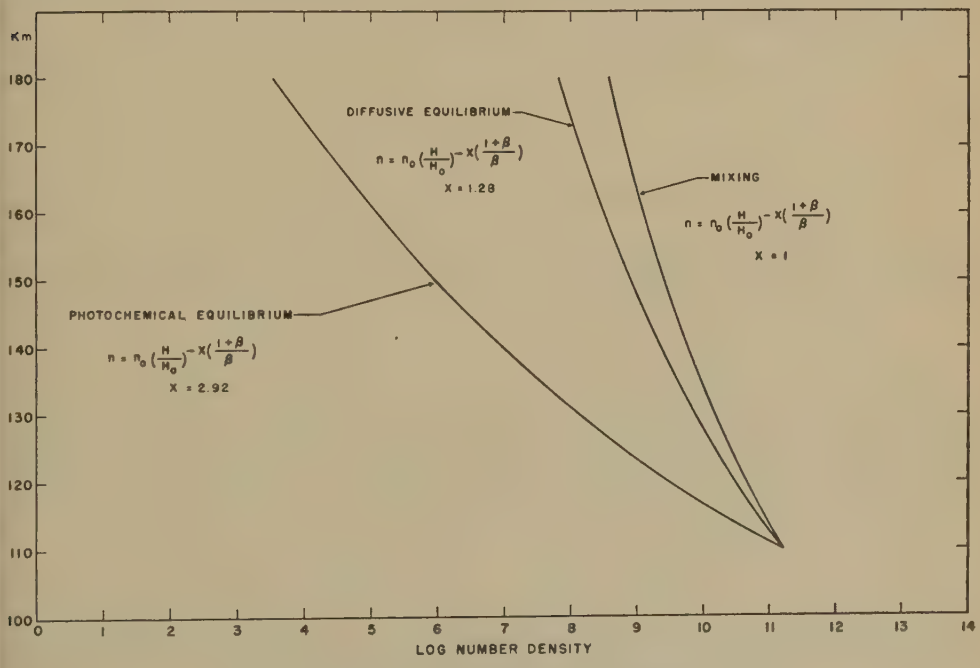

FIG. 2—Equilibrium distribution processes for O_2

For the ideal gas law,

$$p = nkT \quad \ldots\ldots\ldots\ldots\ldots\ldots\ldots\ldots\ldots\ldots (13)$$

in which n and k denote, respectively, the total number density cm^{-3} and the Boltzmann constant. Differentiation and solution of (13) yield

$$\frac{dp}{p} = \frac{dn}{n} + \frac{dT}{T} = -\frac{dz}{H} \quad \ldots\ldots\ldots\ldots\ldots\ldots\ldots\ldots (14)$$

where

$$H = kT/mg = RT/Mg \quad (15)$$

Assuming a constant gravitational field for a layer of definite thickness of uniform composition, H is taken to be proportional to T, and

$$\frac{dT}{T} = \frac{dH}{H} \quad (16)$$

The rearrangement of (14) may be written

$$\frac{dn}{n} = -\frac{dH + dz}{H} \quad (17)$$

Nicolet [8] introduced a linear scale height gradient β,

$$H = H_0 + \beta z, \quad \text{or} \quad \beta = dH/dz \quad (18)$$

which corresponds to a linear temperature variation, since both m and g are taken to be constant. Integration and solution of (14) and (17) give

$$\frac{p}{p_0} = \left(\frac{H}{H_0}\right)^{-(1/\beta)} = e^{-\zeta} \quad (19)$$

and

$$\frac{n}{n_0} = \left(\frac{H}{H_0}\right)^{-(1+\beta)/\beta} = e^{-(1+\beta)\zeta} \quad (20)$$

where p equals p_0 and n equals n_0 at the datum level where H equals H_0 . Zeta ζ is a new height variable introduced by Nicolet and Bossy [9], expressed by

$$H/H_0 = e^{\beta\zeta}, \quad \text{and} \quad \zeta = z/H \quad (21)$$

The utility of the zeta variable lies in the fact that this permits one to write theoretical exponential expressions for pressure and number density concentration for a non-isothermal atmosphere nearly analogous to the corresponding isothermal forms. The number density distribution of a minor atmospheric constituent was derived by Nicolet [10] and Mange [11], and shown to obey the diffusion law

$$\frac{n}{n_0} = \left(\frac{H}{H_0}\right)^{-X(1+\beta)/\beta} = e^{-X(1+\beta)\zeta} \quad (22)$$

The parameter X has a value of unity when complete mixing conditions obtain. For diffusive equilibrium, where thermal diffusion is not effective, X has the following value:

$$X = \frac{\left(\frac{m}{\bar{m}} + \beta\right)}{1 + \beta} \quad (23)$$

where m is the molecular mass of the minor atmospheric constituent, $\bar{m}$ is the mean molecular mass of an average air particle at the altitude of the reference level, and β is the scale height gradient per kilometer.

VERTICAL DISTRIBUTION OF ATMOSPHERIC CONSTITUENTS

The 1956 Model Atmosphere of the Air Research and Development Comman (ARDC) introduces a linear temperature-distribution profile based upon a new temperature variable with altitude. The geopotential meter is employed to denote height. Thus, the scale height variation will be non-linear as compared to the linear scale height assumed by Nicolet and Mange. Accordingly, it was necessary to modify the Nicolet-Mange method for obtaining the vertical distribution of the various gases in the atmosphere in order to be consistent with the ARDC Model Atmosphere.

A new temperature variable was defined for altitudes above 90 geopotential kilometers, the height at which molecular oxygen begins to dissociate into atomic oxygen. As a result, the mean molecular weight of air changes with altitude above this level and the molecular weight becomes an unknown parameter. This new temperature term was called the *molecular-scale temperature* and denoted by the symbol T_M . In the expression for scale height, $H = RT/Mg$, T, M, and g are all variables above the transition region. The ratio of absolute temperature to molecular weight T/M was multiplied by the constant, the mean molecular weight of air at low altitudes (0 to 90 geopotential kilometers), in order to give the dimension of temperature for the T_M parameter:

$$\frac{T}{M} \times 28.966 = T_M \quad \ldots\ldots (24)$$

The following gradients were adopted for the T_M-altitude profile.

Altitude range in km'	*Temperature gradient in degree C per km'*
Sea-level to 11	−6.5
11 to 25	isothermal
25 to 47	+3.0
47 to 53	isothermal
53 to 75	−3.9
75 to 90	isothermal
90 to 126	+3.5
126 to 175	+10.0
All altitudes above 175	+5.8

Solving the expression $H = RT/Mg$ for the variable non-linear scale height *vs* altitude,

$$H = \frac{R}{28.966} \times \frac{T_M}{g} = 0.28704 \times \frac{T_M}{g} \quad \ldots\ldots (25)$$

where R, the gas constant, has the value 8.31439 ergs deg^{-1} mole^{-1} (gm cm^2 sec^{-2} deg^{-1} mole^{-1}). The scale height values were computed employing the appropriate T_M and g values at different altitudes. Assuming that diffusive equilibrium for all of the atmospheric constituents begins with 180 km (geometric), except molecular oxygen, which was assumed to follow diffusive equilibrium beginning with 140 km, the $m/\bar{m}$ values of the various atmospheric gases were calculated.

Constituent	$m/\bar{m}$ *values*
O_2	1.33645
N_2	1.17006
O	0.668224
N	0.585030
A	1.66822
Ne	0.842923
Kr	3.49982
Xe	5.48361
He	0.167181
H	0.0420981

The substitution of the $m/\bar{m}$ values into equation (23) and using the various β values computed from the results of equation (25) will give the X parameter for different heights. Equation (22) may now be solved either for complete mixing or for diffusive equilibrium to determine the vertical distribution of number density for each of the various atmospheric gases. Linear scale height gradients were assumed for each 5-km increment in altitude up to 300 km. Above the latter altitude, the scale height was assumed to be linear in 10-km intervals in height.

OXYGEN DISTRIBUTION

The values for number density distribution of molecular oxygen in the region 108 to 130 km are those reported by Byram, Chubb, and Friedman [12]. It may be observed from Figure 3, in the region from 110 to 120 km, where the percentage dissociation of molecular oxygen increases rapidly with altitude, that the vertical distribution of molecular oxygen follows the diffusive equilibrium formula. Above 120 km, the experimental data are in agreement with the mixing formula which was used in computing $n(O_2)$ up to 140 km. It was assumed that diffusive equilibrium for molecular oxygen becomes effective beyond 140 km. Later results from rocket firings on October 18 and 21, 1955, were reported by Friedman at the Conference on Chemical Aeronomy, 25–28 June 1956, sponsored by the Geophysics Research Directorate of the Air Force Cambridge Research Center, Air Research and Development Command. Although tentative, the data indicated complete mixing for molecular oxygen up to 140 km, and probably even to higher altitudes.

According to Byram, Chubb, and Friedman, the percentage dissociation of molecular oxygen from about 110 to 130 km is obtained from the expression

$$\text{Per cent dissociation} = 1 - \frac{\rho_{(O_2)}}{0.23\rho_{(air)}} \qquad (26)$$

One can thus calculate the number density cm^{-3} for atomic oxygen $n(O)$. Multiplying the number densities of $n(O_2)$ and $n(O)$ by their respective molecular and atomic masses, the corresponding mass densities are obtained. The vertical distribution of atomic oxygen was assumed to follow the complete mixing law above 120 km. Below this altitude, the values of $n(O)$ were calculated from the results of equation (26).

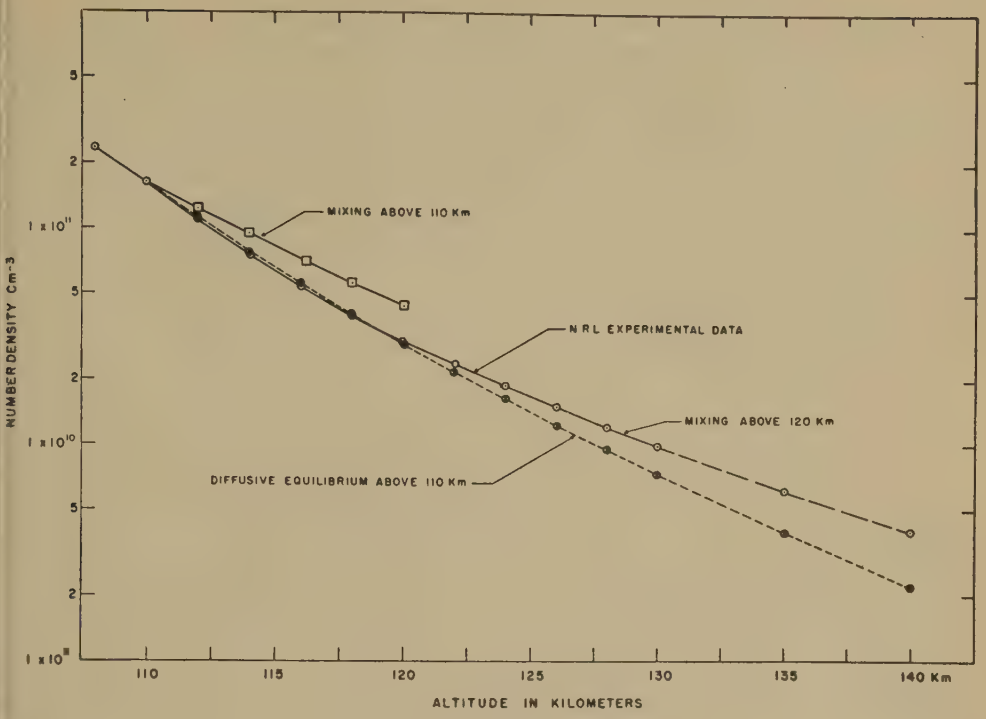

FIG. 3—Vertical distribution of O_2

NITROGEN DISTRIBUTION

The following relation obtains for the atmosphere as a whole.

$$\rho_{(air)} - (\rho_{(O_2)} + \rho_{(O)}) = \rho_{(N_2)} + \rho_{(N)} + \rho_{(A)} \quad \ldots\ldots\ldots\ldots (27)$$

Knowing the densities of air, molecular and atomic oxygen in the region 110 to 130 km [assuming n(N), the number density of atomic nitrogen, to be negligible in this region in comparison to that of molecular nitrogen], the mass densities and the number densities of molecular nitrogen and argon were obtained. Townsend, Meadows, and Pressly [13] have found that the ratio of argon to molecular nitrogen up to approximately 140 km does not change as a function of altitude from the value at the surface of the earth. The vertical distribution of these latter constituents was found by the use of formula (22) with the substitution of the appropriate X values for N_2 and argon. The values obtained from formula (22) are in close agreement if one obtains the number densities for N_2 and argon from densities in equation (27).

At about 160 km and higher altitudes, the sum of the mass densities of N_2 and argon becomes appreciably less than the difference of densities on the left-hand side of equation (27). The difference was assumed to be the mass density of atomic nitrogen. The value of the number density for atomic nitrogen was calculated and substituted into equation (22), using the X value for atomic nitrogen. These calculations were extended to both higher and lower altitudes, since in a

region where there are sources and sinks the light constituents will diffuse downwards and the heavy constituents will diffuse upwards. Figure 4 illustrates the diffusive equilibrium values for $n(\mathrm{N})$ beginning with 180 km. The number density values were also calculated by using the constants given by Deb [14]. The $n(\mathrm{N})$ curve was extrapolated downwards from 180 km and called the ARDC reference curve for atomic nitrogen. The value of the ratio $n(\mathrm{N})/n(\mathrm{N}_2)$ at 180 km is about 1/10, a value in close agreement with that suggested by Mitra [15], which he considered to be reasonable.

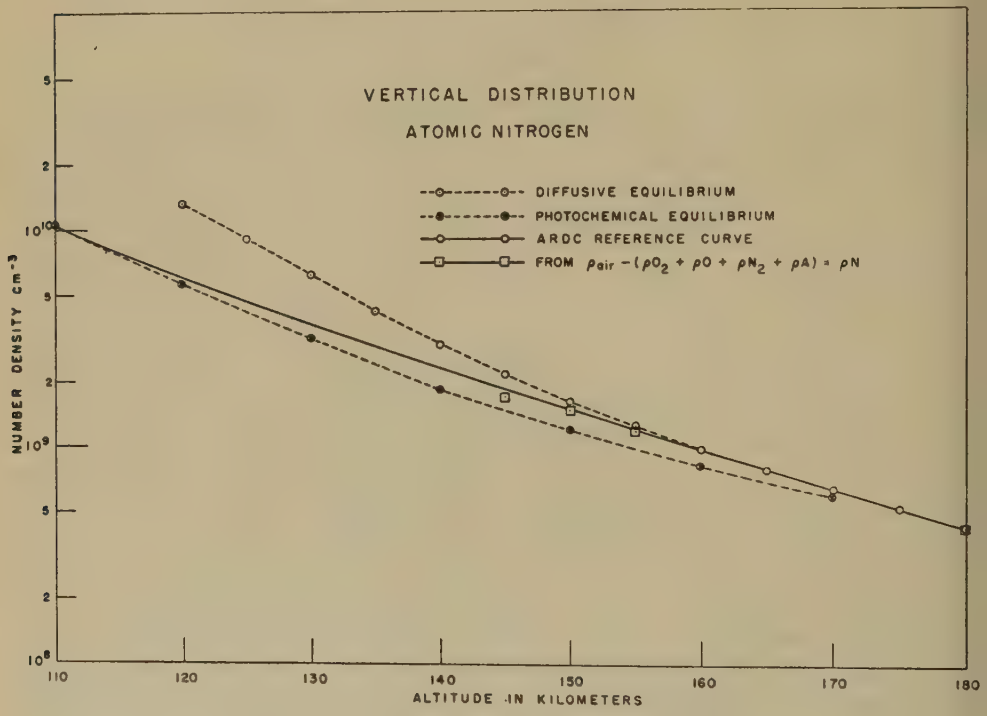

FIG. 4—Vertical distribution atomic nitrogen

CALCULATION OF MOLECULAR WEIGHTS

After obtaining the various vertical number-density distributions for the individual atmospheric constituents, the individual mass densities may be calculated from the respective molecular and atomic masses. The total number and mass densities are found as a function of altitude by the addition of these values. The molecular weights at various altitudes may readily be computed from the relation

$$\frac{\text{Total mass density}}{\text{Total number density}} \times N_0 \text{ (Avogadro's number)} = \text{Molecular weight}$$

TABLE 1—*Number density of atmospheric constituents*

Altitude	$n(O_2)$	$n(O)$	$n(N_2)$	$n(N)$	$n(A)$
km	cm^{-3}	cm^{-3}	cm^{-3}	cm^{-3}	cm^{-3}
0	5.34×10^{18}	.....	1.99×10^{19}	.....	2.37×10^{17}
10	1.80×10^{18}	.....	6.71×10^{18}	.....	7.99×10^{16}
20	3.87×10^{17}	1.61×10^{8}	1.44×10^{18}	.....	1.72×10^{16}
30	7.78×10^{16}	8.66×10^{9}	2.90×10^{17}	.....	3.45×10^{15}
40	1.74×10^{16}	2.97×10^{10}	6.50×10^{16}	.....	7.74×10^{14}
50	4.72×10^{15}	3.45×10^{10}	1.76×10^{16}	.....	2.09×10^{14}
60	1.52×10^{15}	6.42×10^{10}	5.67×10^{15}	.....	6.75×10^{13}
70	4.37×10^{14}	1.90×10^{11}	1.63×10^{15}	.....	1.94×10^{13}
80	9.43×10^{13}	2.15×10^{11}	3.52×10^{14}	.....	4.17×10^{12}
90	1.74×10^{13}	2.30×10^{11}	6.49×10^{13}	3.71×10^{10}	7.73×10^{11}
100	1.40×10^{12}	3.40×10^{12}	1.16×10^{13}	2.09×10^{10}	1.37×10^{11}
110	1.62×10^{11}	1.06×10^{12}	2.58×10^{12}	1.07×10^{10}	3.06×10^{10}
120	3.00×10^{10}	3.13×10^{11}	6.95×10^{11}	6.02×10^{9}	8.23×10^{9}
130	9.08×10^{9}	9.46×10^{10}	2.10×10^{11}	3.65×10^{9}	2.49×10^{9}
140	2.62×10^{9}	3.12×10^{10}	6.94×10^{10}	2.28×10^{9}	8.21×10^{8}
150	8.61×10^{8}	1.29×10^{10}	2.87×10^{10}	1.43×19^{9}	3.40×10^{8}
160	3.41×10^{8}	6.19×10^{9}	1.38×10^{10}	9.75×10^{8}	1.63×10^{8}
170	1.54×10^{8}	3.30×10^{9}	7.33×10^{9}	6.35×10^{8}	8.68×10^{7}
180	7.73×10^{7}	1.90×10^{9}	4.23×10^{9}	4.24×10^{8}	5.01×10^{7}
190	4.32×10^{7}	1.37×10^{9}	2.52×10^{9}	3.17×10^{8}	2.46×10^{7}
200	2.51×10^{7}	1.01×10^{9}	1.55×10^{9}	2.41×10^{8}	1.27×10^{7}
210	1.50×10^{7}	7.62×10^{8}	9.84×10^{8}	1.85×10^{8}	6.80×10^{6}
220	9.27×10^{6}	5.82×10^{8}	6.41×10^{8}	1.45×10^{8}	3.78×10^{6}
230	5.87×10^{6}	4.51×10^{8}	4.27×10^{8}	1.15×10^{8}	2.16×10^{6}
240	3.81×10^{6}	3.54×10^{8}	2.90×10^{8}	9.28×10^{7}	1.28×10^{6}
250	2.52×10^{6}	2.81×10^{8}	2.01×10^{8}	7.54×10^{7}	7.72×10^{5}
260	1.70×10^{6}	2.25×10^{8}	1.42×10^{8}	6.18×10^{7}	4.78×10^{5}
270	1.17×10^{6}	1.83×10^{8}	1.01×10^{8}	5.11×10^{7}	3.03×10^{5}
280	8.16×10^{5}	1.49×10^{8}	7.36×10^{7}	4.26×10^{7}	1.95×10^{5}
290	5.78×10^{5}	1.23×10^{8}	5.42×10^{7}	3.58×10^{7}	1.28×10^{5}
300	4.15×10^{5}	1.02×10^{8}	4.03×10^{7}	3.03×10^{7}	8.58×10^{4}
320	2.21×10^{5}	7.19×10^{7}	2.31×10^{7}	2.20×10^{7}	3.98×10^{4}
340	1.24×10^{5}	5.19×10^{7}	1.38×10^{7}	1.64×10^{7}	1.96×10^{4}
360	7.20×10^{4}	3.82×10^{7}	8.49×10^{6}	1.25×10^{7}	1.01×10^{4}
380	4.32×10^{4}	2.87×10^{7}	5.39×10^{6}	9.63×10^{6}	5.44×10^{3}
400	2.68×10^{4}	2.20×10^{7}	3.52×10^{6}	7.56×10^{6}	3.04×10^{3}
420	1.70×10^{4}	1.71×10^{7}	2.35×10^{6}	6.00×10^{6}	1.75×10^{3}
440	1.11×10^{4}	1.34×10^{7}	1.60×10^{6}	4.83×10^{6}	1.04×10^{3}
460	7.38×10^{3}	1.07×10^{7}	1.12×10^{6}	3.92×10^{6}	6.33×10^{2}
480	5.02×10^{3}	8.58×10^{6}	7.92×10^{5}	3.23×10^{6}	3.97×10^{2}
500	3.47×10^{3}	6.97×10^{6}	5.70×10^{5}	2.68×10^{6}	2.54×10^{2}
520	2.44×10^{3}	5.71×10^{6}	4.16×10^{5}	2.24×10^{6}	1.65×10^{2}
540	1.74×10^{3}	4.72×10^{6}	3.08×10^{5}	1.88×10^{6}	1.09×10^{2}
560	1.25×10^{3}	3.93×10^{6}	2.30×10^{5}	1.59×10^{6}	7.37×10^{1}
580	9.17×10^{2}	3.30×10^{6}	1.74×10^{5}	1.36×10^{6}	5.04×10^{1}
600	6.80×10^{2}	2.78×10^{6}	1.34×10^{5}	1.17×10^{6}	3.50×10^{1}

TABLE 2—*Total number and mass densities, pressure, temperature, and molecular weight*

Altitude	Total n	Total ρ	Pressure	Temperature	Molecular weight
km	cm^{-3}	$gm\ cm^{-3}$	*dynes* cm^{-2}	*deg Kelvin*	(*gm/mole*)
0	2.55×10^{19}	1.23×10^{-3}	1.013×10^{6}	288.16	28.966
10	8.60×10^{18}	4.14×10^{-4}	2.649×10^{5}	223.26	(Constant
20	1.85×10^{18}	8.89×10^{-5}	5.528×10^{4}	216.66	up
30	3.71×10^{17}	1.79×10^{-5}	1.185×10^{4}	231.24	to
40	8.32×10^{16}	4.00×10^{-6}	2.997×10^{3}	260.91	90 km)
50	2.25×10^{16}	1.08×10^{-6}	8.784×10^{2}	282.66	
60	7.26×10^{15}	3.49×10^{-7}	2.581×10^{2}	257.55	
70	2.09×10^{15}	1.00×10^{-7}	6.320×10^{1}	219.33	
80	4.50×10^{14}	2.17×10^{-8}	1.223×10^{1}	196.86	
90	8.31×10^{13}	4.00×10^{-9}	2.257×10^{0}	196.86	28.966
100	1.65×10^{13}	7.12×10^{-10}	4.629×10^{-1}	203.06	25.975
110	3.83×10^{12}	1.59×10^{-10}	1.187×10^{-1}	224.28	24.957
120	1.05×10^{12}	4.28×10^{-11}	3.609×10^{-2}	250.09	24.632
130	3.20×10^{11}	1.30×10^{-11}	1.260×10^{-2}	285.13	24.511
140	1.06×10^{11}	4.30×10^{-12}	5.343×10^{-3}	364.19	24.378
150	4.42×10^{10}	1.80×10^{-12}	2.697×10^{-3}	441.79	24.225
160	2.14×10^{10}	8.56×10^{-13}	1.531×10^{-3}	517.94	24.062
170	1.15×10^{10}	4.57×10^{-13}	9.429×10^{-4}	593.87	23.942
180	6.69×10^{9}	2.65×10^{-13}	6.178×10^{-4}	669.37	23.842
190	4.28×10^{9}	1.65×10^{-13}	4.110×10^{-4}	695.89	23.229
200	2.85×10^{9}	1.07×10^{-13}	2.831×10^{-4}	720.97	22.636
210	1.95×10^{9}	7.16×10^{-14}	2.007×10^{-4}	744.29	22.072
220	1.38×10^{9}	4.94×10^{-14}	1.461×10^{-4}	766.76	21.537
230	1.00×10^{9}	3.50×10^{-14}	1.089×10^{-4}	788.33	21.038
240	7.41×10^{8}	2.53×10^{-14}	8.281×10^{-5}	809.16	20.574
250	5.60×10^{8}	1.87×10^{-14}	6.417×10^{-5}	829.75	20.146
260	4.31×10^{8}	1.41×10^{-14}	5.055×10^{-5}	850.03	19.753
270	3.37×10^{8}	1.08×10^{-14}	4.061×10^{-5}	874.20	19.395
280	2.67×10^{8}	8.44×10^{-15}	3.278×10^{-5}	890.87	19.067
290	2.14×10^{8}	6.66×10^{-15}	2.698×10^{-5}	911.37	18.769
300	1.73×10^{8}	5.33×10^{-15}	2.230×10^{-5}	931.92	18.498
320	1.17×10^{8}	3.51×10^{-15}	1.576×10^{-5}	974.1	18.031
340	8.22×10^{7}	2.41×10^{-15}	1.154×10^{-5}	1017.0	17.644
360	5.93×10^{7}	1.71×10^{-15}	8.68×10^{-6}	1061	17.324
380	4.38×10^{7}	1.24×10^{-15}	6.68×10^{-6}	1106	17.059
400	3.31×10^{7}	9.25×10^{-16}	5.26×10^{-6}	1151	16.838
420	2.54×10^{7}	7.03×10^{-16}	4.20×10^{-6}	1198	16.653
440	1.98×10^{7}	5.44×10^{-16}	3.41×10^{-6}	1244	16.496
460	1.57×10^{7}	4.27×10^{-16}	2.80×10^{-6}	1291	16.364
480	1.26×10^{7}	3.40×10^{-16}	2.33×10^{-6}	1340	16.265
500	1.02×10^{7}	2.74×10^{-16}	1.96×10^{-6}	1387	16.155
520	8.37×10^{6}	2.23×10^{-16}	1.66×10^{-6}	1435	16.070
540	6.91×10^{6}	1.84×10^{-16}	1.41×10^{-6}	1483	15.988
560	5.81×10^{6}	1.52×10^{-16}	1.22×10^{-6}	1519	15.809
580	4.88×10^{6}	1.27×10^{-16}	1.05×10^{-6}	1565	15.737
600	4.13×10^{6}	1.07×10^{-16}	9.18×10^{-7}	1611	15.670

DISCUSSION

Obviously, different models are obtained, depending upon the altitude at which it may be supposed that the major atmospheric constituents will begin to follow the diffusive equilibrium law. In a quiet atmosphere, in the absence of winds and other disturbing factors, diffusive equilibrium may be assumed to begin at lower levels. While in the presence of upper atmospheric turbulence, winds, and other factors, mixing may be the dominant mode of vertical distribution. In the model presented in this paper, it was assumed that diffusive equilibrium for the main constituents of the atmosphere becomes effective at 180 km. Likewise, different vertical distributions are obtained, depending upon the temperature profile adopted. The temperature and scale height profiles were those from the ratio of the absolute temperature to molecular weight, employing the molecular-scale temperature T_M defined in the 1956 ARDC Model Atmosphere.

It should be emphasized that the two modes of vertical distribution, complete mixing and diffusive equilibrium, define what might be called a lower and an upper limit. It should not be construed that the actual vertical atmospheric distribution is an *either/or* process, but it is probably a *both/and* process, in which both diffusive equilibrium and mixing forces are in operation. As yet, no satisfactory intermediate process has been derived for the main constituents of the atmosphere. There are also several other forces which would modify the vertical distribution of the individual atmospheric gases, such as the diffusion transport velocity, the effect of thermal diffusion, the effect of basic flow, and the effect of ions and the magnetic field of the earth. This explains the reason why a simplified working model will give slightly different pressures and densities from those calculated from the T/M ratio by considering the atmosphere as a whole.

The effect of the rare gases, except argon, and other minor components of the atmosphere has been neglected in the molecular weight determination. In the lower regions of the atmosphere, the effect is insignificant. In extending the model to 500 km and above, the inclusion of neon, helium, and atomic hydrogen would only introduce about a one per cent difference. Argon was included, since in the D and E regions it is more abundant than atomic oxygen and comparable in abundance to molecular oxygen above the transition region. The first ionization potentials for the various atmospheric gases are given.

Constituent	*First ionization potential (ev)*
O_2	12.1
N_2	15.6
A	15.7
NO	9.25
O	13.6
N	14.5

It is conceivable that argon may enter into ionization processes in the upper atmosphere.

Having determined the mean molecular weight of air at various altitudes,

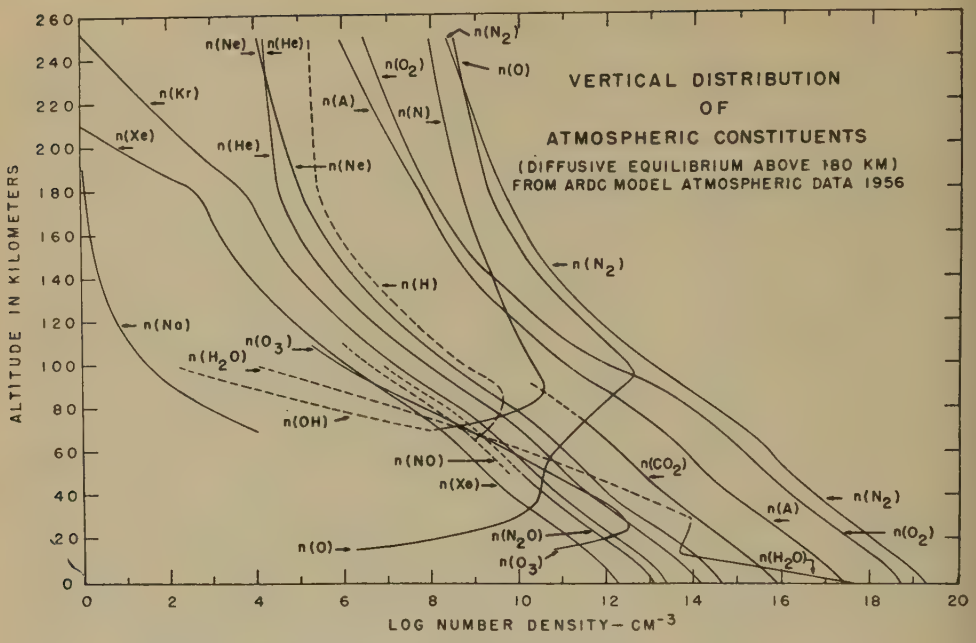

FIG. 5—Vertical distribution of atmospheric constituents, 0 to 260 km

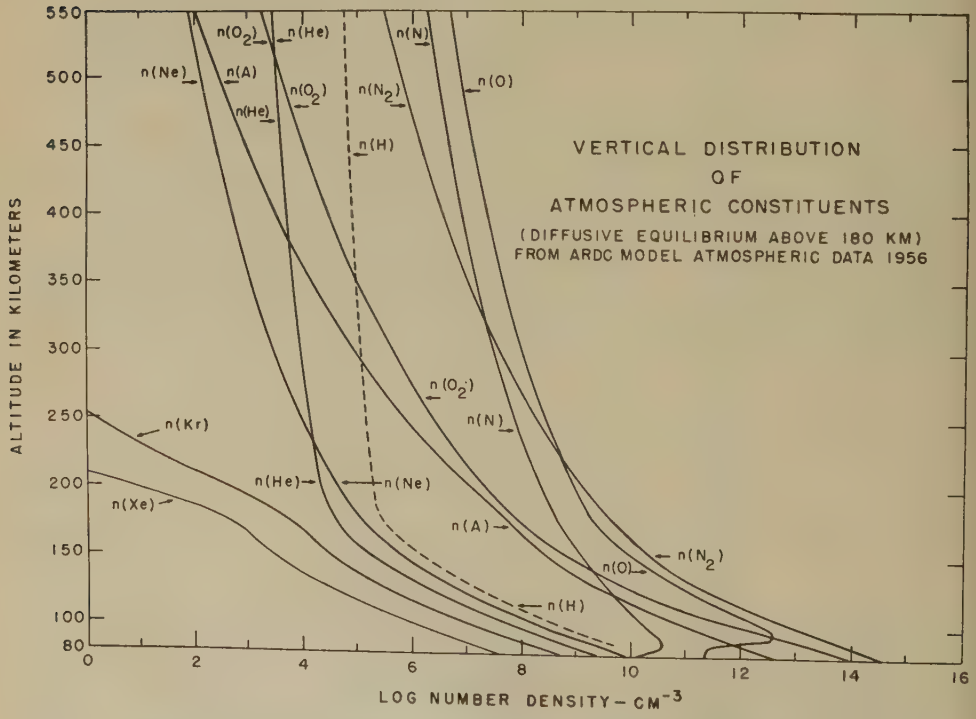

Fig. 6—Vertical distribution of atmospheric constituents, 80 to 550 km

one may compute the upper atmospheric temperatures from the corresponding scale height values.

$$T = HMg/R$$

From the ideal gas law (equation 12), when both the total number density and temperature are known as functions of altitude, values of the pressure may be derived. It is evident that quantitative data upon the dissociation mechanisms for molecular nitrogen and the amount of atomic nitrogen in the upper atmosphere would be most valuable. The intensive experimental investigations planned for the International Geophysical Year 1957–58 should contribute to the better understanding of the composition of the earth's atmosphere.

ACKNOWLEDGMENTS

The author's appreciation is extended to Mr. R. A. Minzner and Mr. W. S. Ripley of the Geophysics Research Directorate, Air Force Cambridge Research Center, who supplied the data on the molecular-scale temperatures and densities at low altitudes from their extensive tabulations for the 1956 Model Atmosphere of the Air Research and Development Command. Thanks are also due Dr. R. Penndorf,* of the Geophysics Research Directorate, who read the manuscript, for his many helpful discussions, criticisms, and suggestions.

References

[1] L. Boltzmann, Wien, SitzBer. Ak. Wiss., math.-naturw. Kl. K., II, **72**, 427 (1875); II, **74**, 503 (1876); II **78**, 7 (1879); II, **95**, 153 (1887).
[2] Smithsonian Meteorological Tables, edited by R. J. List, 6th rev. ed., Washington, D. C.; pp. 217, *et seq.*
[3] P. S. Epstein, Phys. Rev., **33**, 269 (1929).
[4] P. S. Epstein, Beitr. Geophysik, **35**, 153 (1932).
[5] M. Nicolet and P. Mange, J. Geophys. Res., **59**, 15 (1954).
[6] M. Nicolet, J. Atmos. Terr. Phys., **5**, 132 (1954).
[7] P. Mange, Ann. Géophys., **11**, 153 (1955).
[8] M. Nicolet, Mém. R. Met. Belgique, **19** (1945).
[9] M. Nicolet and L. Bossy, Ann. Géophys., **5**, 275 (1949).
[10] M. Nicolet and P. Mange, Pennsylvania State University, Ionosphere Res. Lab., Sci. Rep. No. 56 (Feb. 1, 1954).
[11] P. Mange, Pennsylvania State University, Ionosphere Res. Lab., Sci. Rep. No. 64 (June 15, 1954).
[12] E. T. Byram, T. A. Chubb, and H. Friedman, Phys. Rev., **98**, 1594 (1955).
[13] J. W. Townsend, Jr., E. B. Meadows, and E. C. Pressly, Rocket Exploration of the Upper Atmosphere, edited by R. L. F. Boyd and M. J. Seaton, Pergamon Press, Ltd., London (1954); p. 169.
[14] S. Deb. J. Atmos. Terr. Phys., **2**, 309 (1952).
[15] A. P. Mitra, Indian J. Phys., **28**, 269 (1954); Pennsylvania State University, Ionosphere Res. Lab., Sci. Rep. No. 53 (Nov. 10, 1953).

*Now at Electronics Research Laboratory, Advanced Research and Development Division, AVCO Manufacturing Company, Boston, Massachusetts.

DISCUSSION OF THE BOOKER AND COHEN PAPER, "A THEORY OF LONG-DURATION METEOR ECHOES BASED ON ATMOSPHERIC TURBULENCE WITH EXPERIMENTAL CONFIRMATION"

BY L. A. MANNING AND V. R. ESHLEMAN

Radio Propagation Laboratory, Stanford University, Stanford, California

(Received March 18, 1957)

ABSTRACT

The experimental evidence offered in support of Booker and Cohen's theory is examined point-by-point. It is concluded that the theory does not accurately represent the properties of meteoric echoes.

In their paper [see 1 of "References" at end of paper], Booker and Cohen attribute most of the properties of long-duration meteor echoes to the action of atmospheric turbulence having a velocity of three meters per second at a scale as small as 1.3 meters. In a forthcoming series of papers, one of the writers will present a theory of long-duration meteor echoes which, when compared with experiment, indicates that the pertinent properties of long-duration echoes result from scales of about one kilometer and larger (similar to the distortions of meteor trains photographed by Whipple [2]). The comparison of this large-scale theory with experiment also indicates that small-scale turbulence of the size and velocity assumed by Booker [3] does not exist at meteoric heights. In the present note, the experimental basis of Booker and Cohen's theory is examined. It is concluded that their theory is not in good agreement with experiment.

1. Booker and Cohen assume that Greenhow's observation [4] of a 0.4 second average delay in the start of fading of long-enduring echoes signifies the beginning of incoherent scattering in the trails, a result of mixing by meter-size eddies. McKinley and Millman [5] have found from combined visual and radar observation, however, that aspect sensitivity (a measure of coherence) persists for an average of ten seconds after trail formation.

These two delays, differing by 25 to 1, are explicable using a single large-scale model. In the Booker-Cohen theory, however, the times of onset of fading and incoherence are hypothesized as being the same.

2. Booker and Cohen present measurements of long-enduring meteor echo amplitude *versus* time on logarithmic coordinates. These graphs are intended for comparison with their predicted inverse-cube echo-decay. It will be noted that the experimental curves depart systematically from this prediction. If they are replotted on linear coordinates, however, it will be found that they decay almost linearly. One of the results of the large-scale theory is a predicted linear decay of echo amplitude with time.

To illustrate the comparison of the inverse-cube and linear predictions with the experimental results of Booker and Cohen, Figure 1 of this note has been prepared. Assuming linear decay to zero at a time t_0 , it follows that at time t a signal-strength curve will have a negative slope of $t/(t_0 - t)$ on doubly-logarithmic

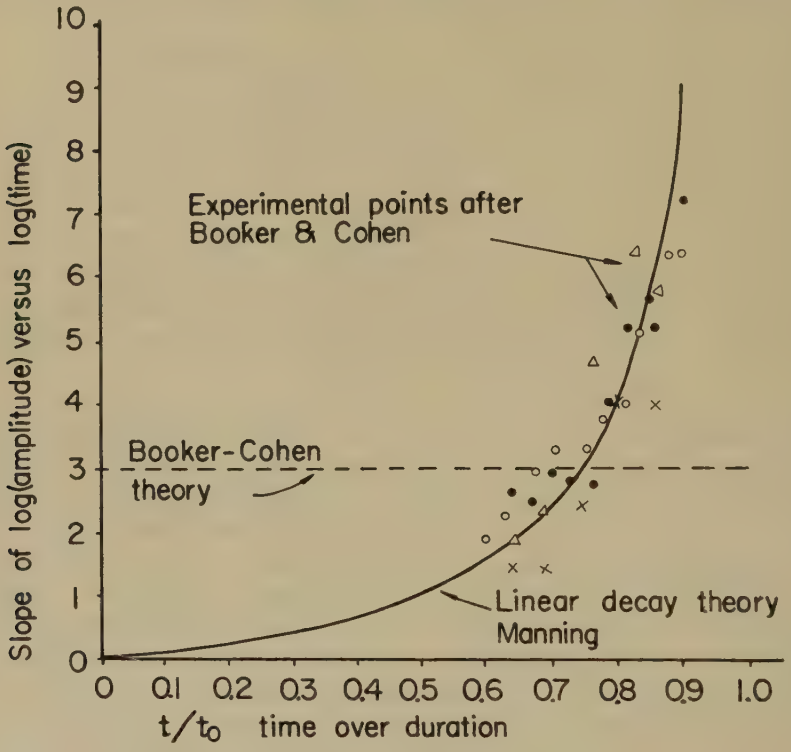

FIG. 1—Plot of the magnitude of the slope on doubly-logarithmic coordinates of echo amplitude *versus* time. The solid line is the slope $t/(t_0 - t)$ expected for linear echo decay, while the dotted line is the slope of three predicted by the Booker-Cohen theory. The experimental points are slopes scaled from Booker and Cohen's Figures 5 and 7; crosses from Figure 5 at 30.38 Mc, circles from Figure 5 at 17.31 Mc, triangles from Figure 7 at 49.78 Mc, dots from Figure 7 at 30.38 Mc.

coordinates. In Figure 1, the solid curve is this relation. Booker and Cohen's inverse-cube law is described by the dashed horizontal line shown in the Figure. The plotted points correspond to the slopes scaled from Booker and Cohen's experimental results, as presented in their Figures 5 and 7. It appears that the linear theory gives a much better description of Booker and Cohen's measurements than does their inverse-cube theory.

If Booker and Cohen's hypothesis of a seven-second attachment time-constant is accepted, their theoretical negative slope becomes $(3 + t/7)$. Since in the examples the maximum times scaled are 3.0, 6.9, 2.7, and 5.7 seconds, the influence on slope is insufficient to change appreciably the comparison in the accompanying Figure.

3. Booker and Cohen found it necessary to invoke the *ad hoc* assumption of a seven-second attachment time-constant to bring their theory into agreement with

McKinley's experimental results on high- *versus* low-power meteor durations (Booker and Cohen, p. 723). An alternative explanation of these experimental results can be found based upon standard over-dense echo theory and linear decay of signal strength. That is, excellent agreement is obtained with McKinley's results assuming linearly-decaying echoes whose durations vary directly with line-density, and whose peak amplitudes vary with the one-fourth root of line-density. No arbitrary constants are required in this explanation.

While the hypothesis of a seven-second attachment time-constant brings the theory of Booker and Cohen into agreement with McKinley's experimental results, recall from paragraph 2 that this added factor does not bring their theory into good agreement with their own measurements. The linear decay theory based on large-scale turbulence is consistent with both experiments.

4. Booker and Cohen present on page 727 a curve that is interpreted as the frequency dependence of the meteoric scattering cross-section. The exponent of the power law they find is then identified with the exponent in the Kolmogoroff-Heisenberg theory of turbulence. It is pertinent to observe, however, that the scaled results they obtain can be reproduced for any meteoric echo theory giving a decay characteristic possessing two key properties: first, an approximately $(1/f^2)$ frequency dependence of duration; second, a signal strength *versus* time behavior of the same functional form at all frequencies. For example, the method of record scaling used in preparing their Figure 10, if applied to the specular over-dense theory of Kaiser and Closs [6], yields a result very similar to that shown in the Figure despite the determination of no experimental constants. Therefore, it appears unwise to associate these results with the turbulent state of the upper atmosphere.

5. It is stated by Booker and Cohen on page 731 in connection with ionospheric scatter-communication that "The explanation originally suggested by Eshleman and Manning [7] was that atmospheric turbulence was not involved, and that the phenomenon could be explained entirely by specular reflection from rectilinear meteor trails. It should be stated that the authors who originally supported [this] explanation have subsequently taken the view that other factors ··· may be important." Careful reading of the cited paper of Eshleman and Manning shows that they did not exclude the possible importance of irregularities in the ionosphere caused by turbulence. According to the paper by Eshleman and Manning, "Turbulent wind motion is also believed to be responsible for temporal and spatial variations in the average electron density" although "at very high frequencies scattering from meteor trails has been found to be at least an important contributing factor ···" Contrary to the impression given by Booker and Cohen, the writers think that the specular meteoric reflection theory is of even greater application than they originally claimed.

It was also suggested by Eshleman and Manning that the off-path maximum of specular meteor contributions might be used "to assess the relative importance of meteoric scattering and scattering due to turbulence or other factors." These tests have now been performed [8]. The results indicate that during at least most of the diurnal period a greater ionospheric forward-scatter background signal can be obtained by aiming the antennas to one side of the path, rather than to the

midpoint. The optimum beam intersection region varies from one side of the path to the other with time of day in accordance with predictions based upon the behavior of meteoric radiants. These findings are a clear proof that the aspect-sensitive specular meteor contribution dominates any component associated with incoherent turbulent scattering.

6. Booker and Cohen on page 732 conclude from data of McKinley [9] that incoherent scattering from large meteors is more important to the background signal in VHF scatter than specular reflections from small meteors. It appears that Booker and Cohen have overlooked the 30-db difference in system gain between the VHF and radar results in their comparison. The higher sensitivity of the VHF scatter circuits results in a great increase in the number of small, weakly-reflecting specular echoes. The number of large meteors detected is not a strong function of system gain. Taking into account the difference in system sensitivity, the relative importance of large and small meteors is assessed in the following Table 1:

TABLE 1—*The number of seconds per hour that meteor echoes are present*

	Particulars	Short duration, $t < 3$ sec	Long duration, $t > 3$ sec
A	33-Mc/s radar data (McKinley)	150 sec/hr	400 sec/hr
B	Effect of 30 db on duration of above meteors	450 sec/hr	800 sec/hr
C	New short-duration meteors due to 31.6 times increase in sensitivity	31.6×150 $= 4{,}750$	None
D	Total radar results corrected for sensitivity	5,200	800
E	Corrected to oblique path at 50 Mc/s	$\gg 5{,}000$ $(> 3{,}600)$	> 800 $(< 3{,}600)$

In line *A* are McKinley's data on the number of seconds per hour on 33 Mc/s during which signal was present due to echoes of short and long durations. In line *B*, these durations have been corrected for the increased echo duration of the individual meteors at higher power, after McKinley's results. In line *C*, the theoretical 31.6 times rate increase due to small meteors brought out of the noise by the 30-db system gain is included. Line *D* is the sum of lines *B* and *C*. Line *E* should be obtained by multiplying by the 33- to 50-Mc/s frequency correction, and 5-times duration-increase-factor due to obliquity. The short-duration (specular) signals are seen to supply the continuous background. It may also be noted that, since McKinley and Millman's measurements indicate that meteor echoes exhibit some degree of specularity for an average of ten seconds after trail formation,

the division between specular and non-specular echoes for the comparison in the Table should be made at a duration somewhat greater than three seconds.

From the foregoing remarks, it appears that the small-scale meteor turbulence theory of Booker and Cohen is in serious contradiction with experiment. The writers will show in later papers that the existing experimental results, as well as new results on the space diversity and detailed fading properties of enduring echoes, are consistent with a large-scale wind structure similar to that photographed by Whipple. However, the theoretical method in Booker and Cohen's paper appears sound. If small-scale turbulence did exist, their conclusions would doubtless be valid. Thus, it appears that they have proved that small-scale turbulence of significance velocity does not exist in the ionosphere at meteoric heights.

References

[1] H. G. Booker and Robert Cohen, J. Geophys. Res., **61**, 707 (1956).
[2] F. L. Whipple, J. Met., **10**, 390 (1953).
[3] H. G. Booker, J. Geophys. Res., **61**, 673 (1953).
[4] J. S. Greenhow, Proc. Phys. Soc., B, **65**, 169 (1952).
[5] D. W. R. McKinley and P. M. Millman, **37**, 364 (1949).
[6] T. R. Kaiser and R. L. Closs, Phil. Mag., **43**, 1 (1952).
[7] V. R. Eshleman and L. A. Manning, Proc. Inst. Radio Eng., **42**, 530 (1954).
[8] V. C. Pineo, "Experimental observations of the contribution of meteoric ionization to the propagation of VHF radio waves by ionospheric forward scatter," in publication.
[9] D. W. R. McKinley, Can. J. Phys., **32**, 450 (1954).

A METHOD FOR OBTAINING LF OBLIQUE-INCIDENCE REFLECTION COEFFICIENTS AND ITS APPLICATION TO 135.6-KC/S DATA IN THE ALASKAN AREA

BY JOHN E. BICKEL

U. S. Navy Electronics Laboratory,
San Diego 52, California

(Received April 1, 1957)

ABSTRACT

A method is presented for obtaining the amplitude of an obliquely reflected one-hop sky-wave from recordings of a continuous transmission of a low-frequency radio signal. The reflection coefficient is obtained from the ratio of the one-hop sky-wave to the calculated unabsorbed one-hop sky-wave. The method is applied to a 135.6-kc/s signal recorded in the Alaskan area. The $\|R\|$ component of the reflection coefficient is obtained.

Introduction

In order to determine the ionospheric reflection coefficient of LF sky-waves, the one-hop sky-wave must be separated from other modes of propagation that are received. Several methods have been developed for doing this. Many workers have used the pulse method of separating the one-hop sky-wave from the various other modes of propagation and thereby determining its amplitude. Others have used the "Hollingworth interference-pattern" method, which has given measurements out to 1,000-km ground distance.

In this paper is presented a method for obtaining the ionospheric reflection coefficient of the obliquely reflected one-hop sky-wave received at a point near its limiting distance. The reflection coefficient is determined on a continuing basis, so that its mean hourly value throughout the night-time is obtained. The r.m.s. value of the daytime reflection coefficient over a period of several weeks is also obtained. The signal from an uninterrupted transmission is used.

The mean amplitude of the received signal is shown to approximately equal the amplitude of the major mode of propagation, which was primarily the one-hop sky-wave during the night and the ground-wave during the day. For daytime propagation conditions, the standard deviation of the signal is shown to equal the r.m.s. value of the one-hop sky-wave.

The data were obtained from a project conducted by the Naval Research Laboratory and maintained jointly by the Naval Research Laboratory and the U. S. Navy Electronics Laboratory. During this project, a 135.6-kc/s signal was recorded continuously from November 1953 to December 1954 in the Alaskan area.

The Data

The data analyzed in this report were recorded from 9 August to 28 November 1954 at Nome and Kodiak. The transmitter was located at Adak. Figure 1 shows the location of the propagation paths. The Adak-Nome path is 1,550 km long, entirely over sea water. The Adak-Kodiak path is 1,670 km long with about 300 km of the distance being over mountainous terrain.

FIG. 1—A map of Alaska, showing the location of the two propagation paths for which the data were taken

The continuous transmission was recorded by Esterline-Angus recorders. The signal was received with top-loaded vertical long-wire antennas feeding Navy model RBA receivers. The calibration for the system was obtained from field-intensity measurements made with a Navy model URM/6 field-intensity receiving set, using the procedure recommended in the instruction book. The URM/6 field-intensity receiver is designed for an accuracy of ± 10 per cent. This is the estimated accuracy of the data.

At the Kodiak receiving station, two recorders were used simultaneously with appropriate instrumentation so that the deflection of one was directly proportional to the field intensity and the deflection of the other was proportional to the logarithm of the field intensity. At Nome, only the logarithmic recording was obtained. Figure 2 shows samples of the night-time records obtained at Kodiak. The first sample of Figure 2 is a logarithmic recording, where the amplitude range is from 15 db to 48 db above 1 μV/m during the night-time period and from 3 db to 36 db during the daytime and the periods of transition between daytime and night-time. The night-time recording condition began at 0533 and ended at 1638 in the sample of Figure 2. The other samples of Figure 2 are from the linear recordings. The amplitude range is from 0 to 215 μV/m.

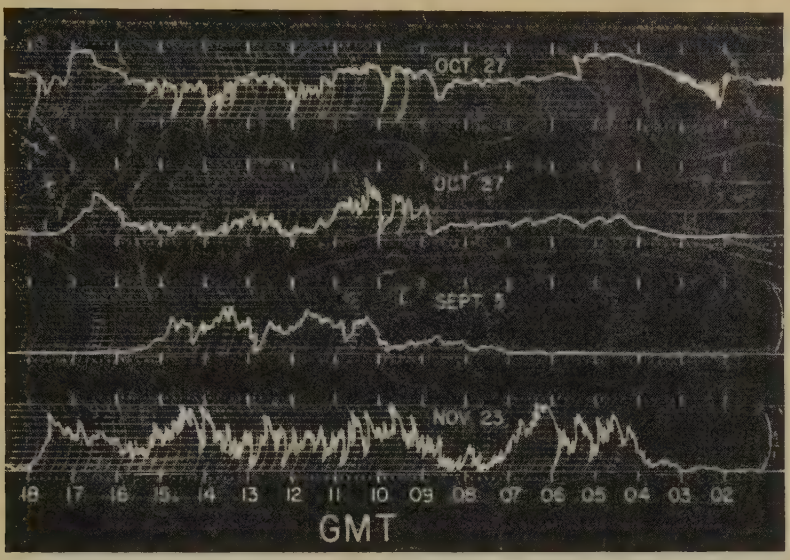

FIG. 2—Typical night-time data samples recorded at Kodiak on 135.6 kc/s. The first sample is a logarithmic recording obtained on 27 October 1954 with an amplitude range from 15 db to 48 db above 1 μV/m, between 0533 and 1638. The daytime recording range was 12 db lower. The other data samples are linear recordings, where the amplitude range is from 0 to 215 μV/m.

Basis of the Analysis

Variation in the field intensity is caused by fluctuations of the amplitude of the individual sky-wave modes and changes in the phase relation between the various modes of propagation. The second and third data samples of Figure 2, where the amplitude is relatively low or high for several hours and where there does not appear to be any periodicity to the amplitude variations, are assumed to be examples of amplitude changes caused by absorption along the path. Figure 3 shows an

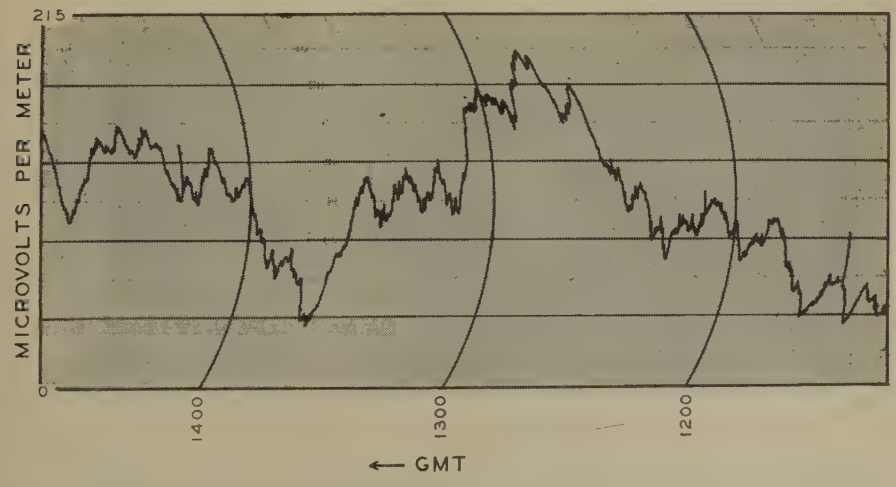

FIG. 3—A sample of the linear recording obtained at Kodiak on 11 September 1954, showing the detail of the amplitude variations of the 135.6-kc/s signals

example of the type of variations caused by phase interference. It is a sample of the linear recording obtained on 11 September at Kodiak. From inspection, it appears that the detail of this recording can be reproduced by summation of the various sine waves tabulated in Table 1. This type of record would be produced

TABLE 1—*Individual modes of propagation estimated from Figure 3*

Amplitude of mode	Cycles/hour	Period/cycle	Ratio of periods
3μV/m	100	0.6 min/cycle	
			 6
4μV/m	25	3.5 min/cycle	
			 3
16μV/m	6	10 min/cycle	
			 4
36μV/m	1-1/2	40 min/cycle	
			 3
70μV/m	1/2	120 min/cycle	

if the height of reflection of the sky-waves varied uniformly over the propagation path, the lower amplitude variations with the shorter periods being produced by the sky-waves with the greater number of hops. For 135 kc/s with a wavelength of 2.2 km, a change in height of reflection of $3\frac{1}{2}$ km between 50 km and 150 km would be sufficient to produce a phase change of 2π between the two major propagation modes, whether they were one-hop and two-hop sky-waves or one-hop sky-wave and ground-wave. Most of the variation of the data shown in the last sample of Figure 2 is apparently due to phase interference also.

If it is assumed the height of reflection of the sky-waves varies randomly within a $3\frac{1}{2}$-km range, a randomness in the phase relationships of the various modes received at the receiving site will be produced. Under these conditions, the mean amplitude of the strongest mode can be determined. The method is illustrated by a simple analysis of the mean value of resultants from two vectors of constant amplitude with a random variation of their phase difference.
Thus,

$$\bar{R} = \lim_{n\to\infty} \frac{\sum R}{n} = \int_0^{2\pi} \frac{\sqrt{A^2 + B^2 + 2AB\cos\theta}\,\mathrm{d}\theta}{2\pi}$$

where A and B are the amplitudes of the two vectors, θ is their phase difference, and $\bar{R}$ is the mean value of the resultants. The value of $\bar{R}$ can be represented by the curve of Figure 4, where A is assumed to be the amplitude of the largest vector and B the amplitude of the smaller vector.

The type of analysis that has been applied to the data shown in Figure 3 was applied to other data samples picked at random. On the basis of these rough estimates, it is concluded that most of the time A is twice the value of B, where B is considered to be the resultant amplitude of all the minor modes of propagation. Therefore, from the curve of Figure 4, it was concluded that the mean signal amplitude is predominantly less than 6 per cent above the mean amplitude of the major mode of propagation. The group of data samples from which the mean is obtained must be such that a random distribution of phases is represented.

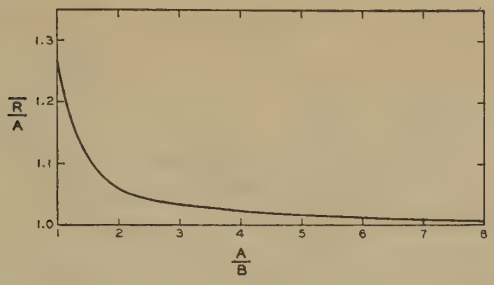

FIG. 4—Curve showing the relation between the two ratios $\bar{R}/A$ and A/B

For most of the daytime data, the major mode of propagation is the ground-wave, which is of constant amplitude. It will be shown that the daytime reflection coefficient is about an order of magnitude smaller than the night-time reflection-coefficient value. As a result, the two-hop sky-wave is highly attenuated. Under these conditions, the amplitude of the one-hop sky-wave can be estimated from the standard deviation of a group of signal amplitude measurements, provided the measured values represent a random distribution of phase differences between the one-hop sky-wave and the ground-wave. Consider the standard deviation σ of the resultant amplitudes R of two vectors A and B of constant amplitude with random phase relationship,

$$\sigma^2 = \frac{\sum (R - \bar{R})^2}{n} = \frac{\sum R^2}{n} - \bar{R}^2$$

$$= \int_0^{2\pi} \frac{(A^2 + B^2 + 2AB \cos\theta)\, d\theta}{2\pi} - \bar{R}^2$$

$$= A^2 + B^2 - \bar{R}^2$$

or

$$B^2 = \sigma^2 + \bar{R}^2 - A^2$$

On the basis of the curve of Figure 4, let $A \approx \bar{R}$ for a first approximation to B. This gives an approximate value for the ratio A/B needed to obtain a correction-factor from Figure 4. This process of successive approximations can be repeated until satisfactory values for A and B are obtained.

Under conditions in which the value of B varies as a function of time, the resultant value obtained from the standard deviation will be the r.m.s. value of the distribution of amplitudes of B.

Results

From the linear recording made at Kodiak, signal amplitude values were read off the *E-A* charts at three-minute intervals during the night-time period. The means of these amplitude values were obtained for the last three to five hours of each night-time period and are plotted in Figure 5. Data from the sunrise period were not included in these values.

The values plotted in Figure 5 represent the amplitude of the one-hop sky-wave.

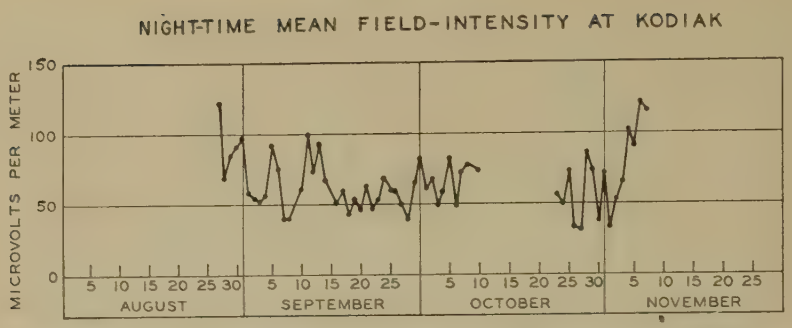

FIG. 5.—Mean values of the Kodiak data for the last three to five hours of each night-time period

The ground-wave was calculated from K. A. Norton [see 1 of "References" at end of paper] to be 8 μV/m. Some of the means may have been obtained from data for which the requirement of random distribution of phase between the modes of propagation was not satisfied. However, it appeared from the data that, in general, the random phase condition is sufficiently satisfied. Figure 5 shows a variation of one-hop sky-wave amplitude over about a two-to-one range.

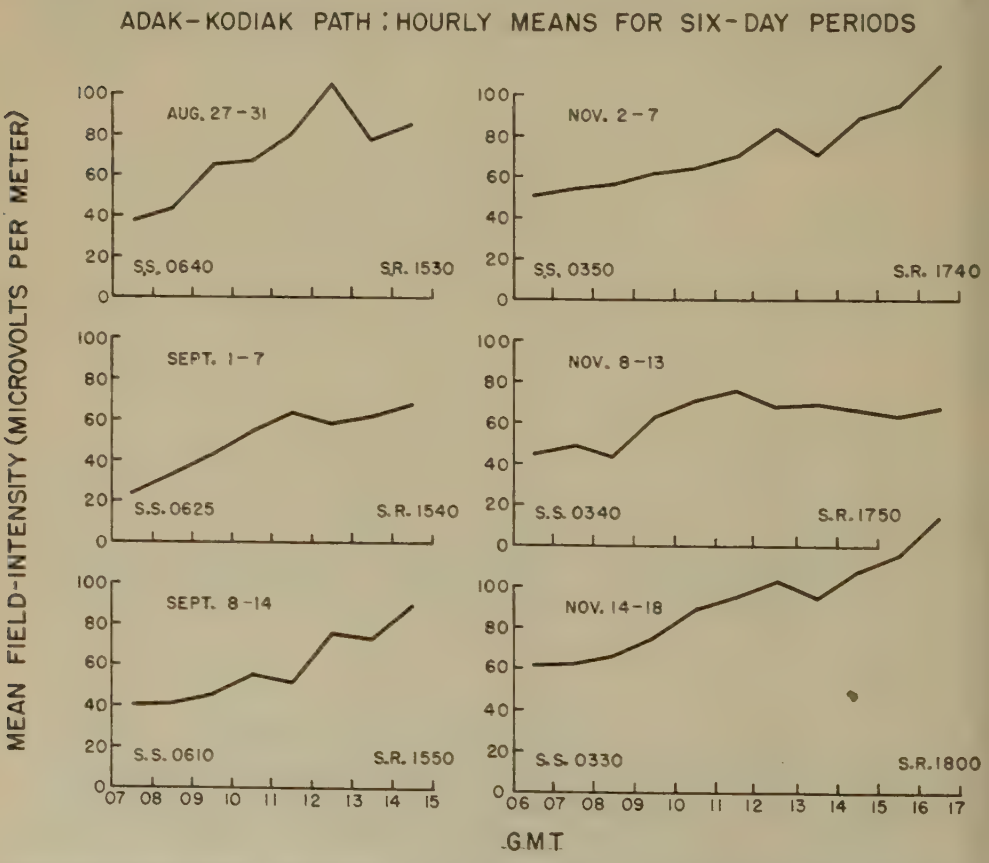

FIG. 6.—Average one-hop sky-wave intensity throughout the night-time period. The values plotted are the mean values of data recorded at Kodiak during the indicated hour for four to six consecutive days.

The amplitude values obtained from the *E-A* charts were also used to obtain the average amplitude of the one-hop sky-wave throughout the night-time period. Figure 6 shows the results of these calculations. The hourly means were determined from the amplitude values obtained at three-minute intervals throughout the indicated hour for about six consecutive days. The random phase relation is well represented in each of these groups of data samples.

Figure 6 shows the general increase of one-hop sky-wave amplitude throughout the night-time period to a value about two or three times what it is at the beginning of the night. The sunrise-sunset times indicated in Figure 6 are the approximate beginning and end of total darkness along the entire path at 80-km altitude.

The daytime data recorded at Nome were analyzed in a similar way. However, the daytime data are not subject to the relatively rapid fluctuations in amplitude that were recorded during the night. Apparently the height of reflection during the daytime was more stable. Values of signal amplitude were obtained only every hour from the daytime data. Figure 7 shows the daily means obtained from these data where only 5 to 10 signal-amplitude values were used. Because of the relative stability of the height of reflection, the daily means shown in Figure 7 do not necessarily represent the amplitude of the major mode of propagation. For this reason, the daytime signal-amplitude values were divided into groups representing approximately three-week periods. The horizontal lines of Figure 7 represent the mean signal amplitudes for each of the periods. The mean signal amplitude is also a good approximation to the amplitude of the major mode of propagation.

The approximate amplitude of the minor mode of propagation was obtained from the data for each three-week period by the method discussed in the section

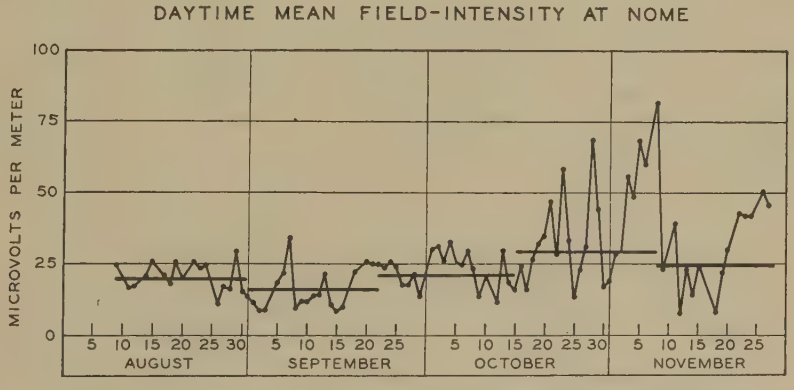

Fig. 7—Daytime mean field-intensity recorded at Nome. The horizontal lines represent the means of hourly amplitude values for the period of time indicated by their length.

"*Basis of the Analysis.*" Table 2 presents results of these calculations made with the daytime data. The values of A in Table 2 are the means of the data that are shown in Figure 7.

The values of A for the first three-week periods represent the amplitude of the ground-wave. The average of these three values is 18.5 μV/m, which agrees well with the ground-wave amplitude of 17 μV/m calculated from the results of

K. A. Norton [1]. The value of B for the first three periods and the value of A for the last two periods represent the mean amplitude of the one-hop sky-wave. The value of B for the last two periods is not significant, since it is influenced by the amplitude fluctuations of the one-hop sky-wave.

TABLE 2—*Amplitude of propagation modes received at Nome during the daytime and associated reflection coefficients*

Three-week period	$A(\mu V/m)$	$B(\mu V/m)$	$\|R_\|$
8–31 Aug.	19.5†	6.6*	0.009
1–22 Sep.	14.9†	10.0*	0.013
23 Sep.–15 Oct.	21.2†	11.3*	0.014
16 Oct.– 8 Nov.	29,2*	34.4	0.037
9–28 Nov.	24.9*	26.0	0.032

*Amplitude of one-hop sky-wave.
†Amplitude of ground-wave.

Estimate of the Reflection Coefficient

The $\|R_\|$ component of the reflection coefficient is obtained from the ratio of the amplitude of the one-hop sky-wave to the calculated unabsorbed one-hop amplitude. The intensity of the unabsorbed one-hop sky-wave at the receiver is calculated using the inverse-distance relationship, doubled to account for the ground reflected ray at the receiving antenna, and increased by 5 db to account for the focusing effect of a spherical ionosphere, as given by Pierce [2]. This gives a value of 775 μV/m for the unabsorbed intensity at Kodiak. Due to the presence of a 2,500-foot mountain, 1.5 miles from the receiving antenna, it is estimated this field-intensity value will be attenuated 3 to 6 db. The value used to obtain reflection coefficients is 470 μV/m $\pm$ 20 per cent.

The reflection coefficient calculated from the night-time data at Kodiak is shown in Table 3.

TABLE 3—*Night-time reflection coefficients for Adak-Kodiak path**

Item	Mean field-intensity	$\|R_\|$
Lowest one-hop intensity	35μV/m	0.074
Mode of distribution of values	60μV/m	0.13
Highest one-hop intensity	125μV/m	0.26

*From data of Figure 5.

The daytime reflection coefficients calculated for the Adak-Nome path are tabulated in Table 2 with the amplitude of the one-hop sky-wave. The unabsorbed sky-wave amplitude used is 775 μV/m.

Conclusions

1. Oblique-incidence reflection coefficients can be obtained from the continuous recording of a distant CW signal in the 135-kc/s frequency range.

2. The mean night-time oblique-incidence reflection-coefficient values (as defined in this report) at 135 kc/s increase by the end of the night to two or three times their value at the beginning of the night. Hourly and nightly variations over about a two-to-one range occur. The mode of the distribution of night-time reflection coefficients is estimated to be 0.13.

3. A greater seasonal variation of the daytime reflection coefficient than the night-time value occurred. Daytime reflection coefficients at 135 kc/s range from 0.009 to 0.032.

4. The daytime reflection height of sky-wave modes of propagation is more stable than the night-time reflection height.

References

[1] K. A. Norton, The calculation of ground-wave field intensity over a finitely conducting spherical earth, Proc. Inst. Radio Eng., **29**, 623–639 (1941).

[2] J. A. Pierce, Sky-wave field intensity, low and very-low radio frequencies, Harvard University, Cruft Laboratory, Tech. Rep. No. 158 (Sept. 1952).

THE RELATION OF FORWARD SCATTERING OF VERY HIGH FREQUENCY RADIO WAVES TO PARTIAL REFLECTION OF MEDIUM FREQUENCY WAVES AT VERTICAL INCIDENCE

By J. B. Gregory

Physics Department, Canterbury University College, Christchurch, New Zealand

(Received April 23, 1957)

ABSTRACT

A comparison is made between published VHF forward-scatter data and results of vertical-incidence investigations of the lower ionosphere, mainly at a frequency of 1.75 Mc/s. The received waves in each type of transmission are shown to have many similar characteristics, such as temporal variations, and to originate in the same height regions. It is concluded that the two types of transmission have a common origin.

I—INTRODUCTION

In a recent paper, Pineo [see 1 of "References" at end of paper] has given information on the heights in the ionosphere at which forward scattering of VHF waves occurs. The sample records shown in his paper bear a marked resemblance to records obtained by the author, using waves of frequency 1.75 Mc/s at vertical incidence [2]. Less extensive observations by Gardner and Pawsey [3] at a frequency of 2.28 Mc/s have produced similar records.

In succeeding paragraphs, reasons will be given for considering that essentially the same phenomenon has been revealed by both the oblique VHF and the vertical MF studies. The data to be compared include that given by Bailey, Bateman, and Kirby [4]; and also further results obtained at 1.75 Mc/s by the writer during a two-year period of observation.

II—COMPARISON OF DATA

For convenience, the VHF and the MF results may be compared under the following headings:

(*a*) *Nature of Received Signals*

The essential continuity of the VHF forward-scattered signal is matched by a similar continuity of reflection of 1.75-Mc/s waves from a region whose lower boundary height lies between 80 and 90 km. Periods when reflection from these heights have not been detected include occasions of excessive noise level at night, when the presence of the region may still be inferred with reasonable confidence; intervals of increased absorption (SID's), when reflections are still received from heights usually between 60 to 70 km; and parts of winter days of high absorption,

when lower height reflections again persist. (This latter effect is described in detail in reference [2], where the presence of an 85-km region throughout these days is inferred.) In addition to the 80- to 90-km reflections throughout day and night, other lower reflections are detected at 1.75 Mc/s during day only, down to a minimum of about 50 km.

Both the VHF and the MF signals show rapid fading, with quasi-periods of the order of a few seconds. The fading period at 1.75 Mc/s has been shown to change at different heights up to the *E*-region, and to vary from day to day. Information regarding fading rates at different heights for VHF scatter does not appear to be available. The mean strengths of both types of signals vary widely. At 1.75 Mc/s, the change in mean strength is greatest in the night 85-km region, and is then of the order of 20 to 30 db. An analysis of these variations is planned.

The VHF scattering process has been described in terms of a scattering cross-section per unit volume, as defined by Villars and Weisskopf [5], and experimental values range from 0.2 to 40 $\times$ 10^{-16} cm^{-1}. At 1.75 Mc/s, partial reflections are returned from regions whose voltage reflection coefficient lies between the minimum detectable value of 5 $\times$ 10^{-6}, at heights near 50 km, and an upper limit of about 10^{-3}, in the 85-km region. A comparison of these two sets of data is scarcely possible in view of present lack of understanding of the processes involved; and it is perhaps coincidence that, on considering the 1.75-Mc/s results as due to isotropic scattering, cross-sections similar to the VHF values are obtained.

(*b*) *Heights of Reflection*

It is interesting to compare sample records obtained by oblique pulse transmissions at VHF, and by vertical pulse transmissions at 1.75 Mc/s. Plate *A* is reproduced from the paper by Pineo, and shows VHF scattering, during a winter morning of 1953, from heights of about 73 and 89 km. Plate *B* shows 1.75-Mc/s

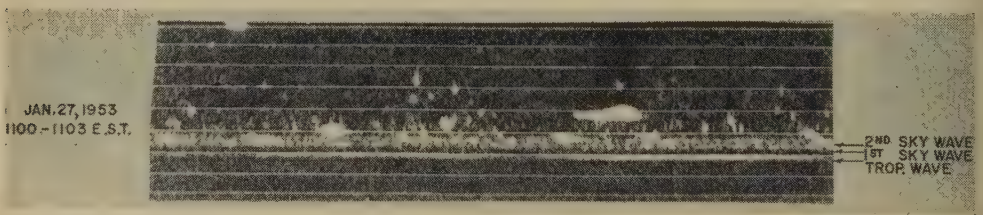

Plate *A*—Sky-wave *vs* tropospheric delay records made at 49.8 Mc/s over the 810-km Sterling, Va.,-Bluffton, S. C., path. Time delay markers are at intervals of 100 microseconds. (Reproduced from Pineo, J. Geophys. Res., 61, 165, 1956.)

Plate *B*—1.75 Mc/s *h't* record, July 30, 1955. At left, partial reflections at 61 km, 71 km, and 84 km. At right, where receiver gain has been reduced in successive 6-db steps, with short switching interval between each step, the *E*-region reflects partially at 98 km and totally at 107 km. (Height markers commence at 45 km and are at 10-km intervals.)

reflections at similar time of day and season in 1955. Partial reflections with differing fading rates may be seen at about 61 and 71 km. At the right of the record, during an interval of receiver gain reduction by successive steps of approximately 6 db, the lower boundary of a much stronger region may be seen at about 84 km. The *E*-region has a partially reflecting "ledge" at about 98 km, and reflects totally at about 107 km. It is perhaps necessary to emphasize the great day-to-day variation in the reflections below 80 km at 1.75 Mc/s. The record shown in Plate *B* has been selected as providing a reasonable comparison with that of Plate *A*; and all its features have been observed many times in other records taken by the author with the same equipment.

A comparison of the diurnal occurrence of reflection heights as observed by Pineo and by the author is likewise of interest. Figure 1 is reproduced from the

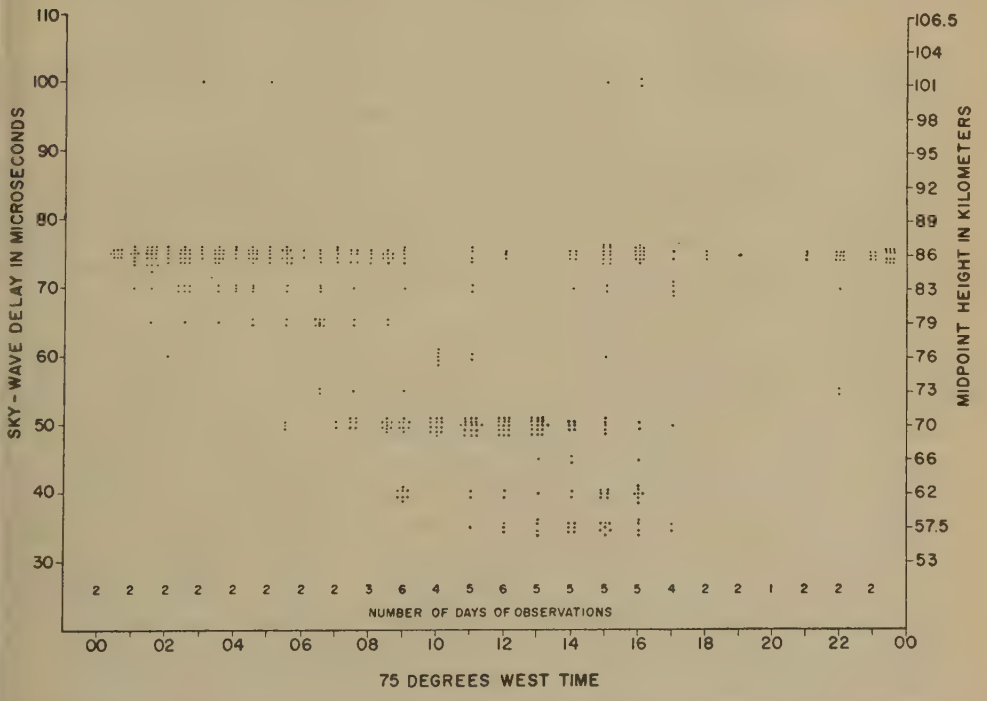

FIG. 1—Diurnal characteristics of sky-wave delays observed during the period of October 31 to November 13, 1952, at 49.8 Mc/s over an 810-km path. (Reproduced from Pineo, J. Geophys. Res., 61, 165, 1956.)

data given by Pineo, and shows VHF scatter heights for the period October 31 to November 13, 1952. Although the 1.75-Mc/s observations did not start until January 1955, and observing schedules differed from those of Pineo, it appears that a three-day period of continuous observation for May 16 to 19, 1955, is sufficiently similar in season and sunspot activity to permit comparison. A mass plot of heights of lower boundaries of reflecting regions, excluding the *E*-region, at regular half-hourly intervals throughout this period, is shown in Figure 2.

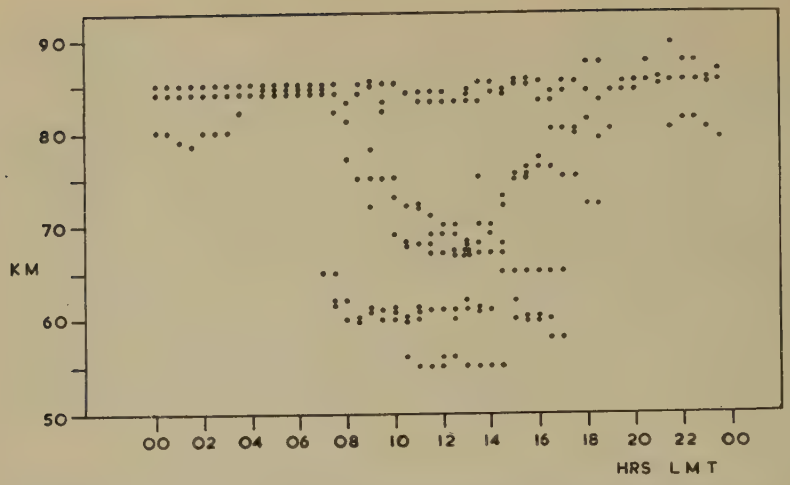

Fig. 2—Diurnal characteristics of 1.75-Mc/s vertical-incidence reflection heights below *E*-region, observed for period May 16–19, 1955

The VHF results are for latitude 36° north, and the MF results for latitude 43.5° south. The agreement is surprising, particularly at about 85 km, where reflections of 1.75-Mc/s waves are always observed. This suggests that the ionospheric structure causing the two phenomena might be determined more simply from the MF than from the VHF observations.

A similar measure of agreement is scarcely to be expected below 85 km, since, apart from the separation in time and place of the observations, a great variation in the height and strength of the 1.75-Mc/s reflection is encountered. The 1.75-Mc/s $h't$ records also show that reflections often occur throughout a range of heights above each boundary, usually increasing in strength with height. It is thus the lower boundary characteristics of the 1.75-Mc/s partially reflecting regions which are being compared with the VHF scatter sources. Reflection heights at 1.75 Mc/s are constant with time for periods of many minutes duration, and in this respect resemble the VHF scattering strata. Both the VHF and the MF results show the presence of lower scattering heights during daytime only. The VHF data did not indicate whether new scattering levels were formed in daytime below the night levels, or whether a transfer from upper to lower levels occurred. The 1.75-Mc/s results have shown that, in general, new heights of reflection appear below 80 km in daytime. However, it is possible that a transfer from upper to lower heights occurs on winter days of excessive MF absorption. This trend may be seen in Figure 2, since the period of observation included such days. The over-all patterns of Figures 1 and 2 are sufficiently similar to suggest that a close relationship exists between the two types of phenomena.

(c) *Effect of Meteors*

In both types of transmission, the presence of meteors has been detected. Plate *A* shows transient reflections of VHF waves which are believed to be due to meteors at heights above 100 km. Similar reflections of 1.75-Mc/s waves may

be seen in Plate *C*, which is reproduced from the author's paper [2]. These reflections are also believed to be of meteoric origin, and extended observations have failed to reveal any below 95 km. In the 1.75-Mc/s studies, the presence of meteors may be detected only when normal *E*-region or sporadic-*E* reflections do not obscure the levels in question.

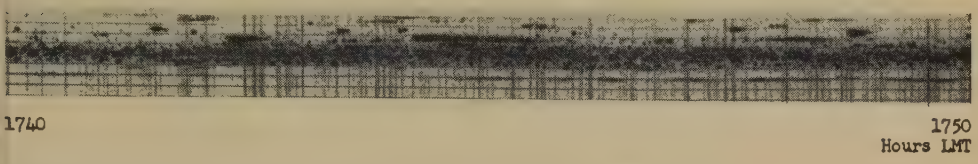

Plate *C*—1.75 Mc/s *h't* record, March 26, 1955. Meteor reflections are visible above 100 km. The 85-km region, and weak reflections at 74 km, are also visible. (Height markers commence at 55 km and are at 10-km intervals.)

The extent of the contribution of reflections from meteor trails to the weak continuous forward-scattered VHF signal, as distinct from strong bursts correlating with meteor showers, is not yet known. It is clear that the direct effect of meteors must be confined to heights above 75 to 80 km, since below these heights solar control of reflecting regions is evident. Both the VHF and the MF results emphasize the responsibility of the region near 85 km for continuous signals, but the origin of this region is still undetermined. Villard, Manning, Eshleman, and Peterson [6] have shown that the overlapping effects of many weakly ionized meteor trails could account for the magnitude of the weak continuous VHF signal. It is not readily apparent how such trails, which tend to be somewhat random in time and height, might give rise to a continuous 85-km region which, at 1.75 Mc/s, often presents a sharp underside. Further, on rare occasions, the 85-km region has been observed to return 1.75-Mc/s waves in a manner resembling sporadic-*E* reflections from greater heights. The possibility of an indirect contribution to ionization at these levels by meteoric material, however, is not excluded.

(*d*) *Seasonal Effects*

The main seasonal effect so far noted in the 1.75-Mc/s observations is the enhancement of daytime reflections below 85-km height during winter months. A decrease in the heights of these reflections also occurs in this season. This effect is matched by a winter enhancement of scatter signal strength for VHF paths in mid-latitudes. A summer maximum of signal strength occurs in all VHF forward-scatter paths for which data are available, but a corresponding summer increase is not apparent at 1.75 Mc/s. There can be little doubt that the winter maxima of the VHF and the MF reflections at mid-latitudes have a common origin, but a closer comparison will be possible only when data on the relative contributions of different heights to the total VHF scatter strength become available.

The suggestion of Bailey and his colleagues that the VHF winter maximum is related to excessive MF absorption in that season is supported by the 1.75-Mc/s results, but the latter show that this absorption is only one aspect of the over-all behavior of the lower part of the ionosphere in winter. The same results also lend

support to a comment by Dieminger [7] that structural changes in the lower ionosphere will be found to account for this absorption anomaly. It seems likely that such changes are the cause of the low-height winter-reflection increase in general.

The winter effect discussed above has been noted at mid-latitudes. At higher latitudes, the VHF winter noon maximum is much less pronounced. It would be interesting to determine whether the MF winter increase is also less evident at high latitudes, and it is to be hoped that further MF studies, using vertical-incidence apparatus of sufficient sensitivity, will be made at several latitudes.

III—CONCLUSION

In the foregoing, a comparison, largely qualitative in nature, has been drawn between the results which can be obtained from vertical-incidence studies using apparatus of sufficient sensitivity at medium frequencies, and those so far published regarding the VHF forward-scatter process. It is believed that sufficient evidence has been presented to show that these apparently diverse effects have a common origin in scattering processes in the lower part of the ionosphere. The extent to which quantitative studies of these processes are still required is obvious from the preceding paragraphs. In future studies, the medium frequency and the very-high-frequency approaches to the problem of the nature of the scattering processes should be regarded as complementary.

IV—ACKNOWLEDGMENT

It is a pleasure to acknowledge a number of helpful discussions with Squadron-Leader J. Mawdsley, New Zealand Defence Scientific Corps.

References

[1] V. C. Pineo, J. Geophys. Res., **61**, 165 (1956).
[2] J. B. Gregory, Aust. J. Phys., **9**, 324 (1956).
[3] F. F. Gardner and J. L. Pawsey, J. Atmos. Terr. Phys., **3**, 321 (1953).
[4] D. K. Bailey, R. Bateman, and R. C. Kirby, Proc. Inst. Radio Eng., **43**, 1181 (1955).
[5] F. Villars and V. F. Weisskopf, Proc. Inst. Radio Eng., **43**, 1232 (1955).
[6] O. G. Villard, Jr., V. R. Eshleman, L. A. Manning, and A. M. Peterson, Proc. Inst. Radio Eng., **43**, 1473 (1955).
[7] W. Dieminger, J. Atmos. Terr. Phys., **2**, 340 (1952).

JOURNAL OF GEOPHYSICAL RESEARCH VOLUME 62, NO. 3 SEPTEMBER, 1957

LYMAN ALPHA AND X-RAY EMISSIONS DURING A SMALL SOLAR FLARE

BY T. A. CHUBB, H. FRIEDMAN, R. W. KREPLIN, AND J. E. KUPPERIAN, JR.

U. S. Naval Research Laboratory,
Washington 25, D. C.

(Received April 24, 1957)

ABSTRACT

A rocket instrumented to measure Lyman alpha and X-rays was fired while a small flare was in progress on June 20, 1956. The rocket reached peak altitude about ten minutes after the flare was first seen visually. An unusually high X-ray flux was observed extending to a short wavelength limit of 3A. Although the flare was still visible in Hα, Lyman alpha was not appreciably different from normal.

Of all the types of activity observed on the sun, the solar flare is the phenomenon which appears to have the most direct effect at the earth. One of the most striking consequences of a flare is an immediate increase in ionization density in the *D* layer of the ionosphere with resultant radio fadeout (SID), sudden increase in atmospherics (SEA), and sudden phase anomaly in reflected long-wave radio signals (SPA). It is now well established that normal *D* layer is caused by the hydrogen Lyman α line always present in the solar emission spectrum. This line is unable to ionize the primary atmospheric constituents (O_2 , N_2 , A, CO_2 , H_2O), but is capable of ionizing nitric-oxide gas, presumably present as a trace constituent of the atmosphere in *D* region. There is reason to doubt that the increased ionization produced in *D* region during a solar flare is caused by a simple increase in solar Lyman α emission [see 1 of "References" at end of paper], however, both because of the unreasonably large increases required to account for the observed lowering of the base of the *D* layer and because of the imperfect correlation between the time duration of observed Hα emission and the duration of anomalous *D*-layer ionization. In addition, it has been known for several years that the sun normally produces a flux of soft X-rays, sufficiently intense to account for most of *E*-region ionization. This X-ray flux has been shown to vary considerably in magnitude and character in accordance with ground measurements of coronal excitation spectra [2]. Since an extension of the sun's normal X-ray emission spectrum to slightly shorter wavelengths could produce the increase in *D*-layer ionization observed during a flare, an X-ray theory of the origin of SID appeared to be an attractive alternative to the Lyman α theory. The present paper describes a direct measurement made last summer of both the Lyman α flux and the short wavelength X-ray flux reaching *D* layer during a solar flare that could be described as a large subflare or a flare of barely Class 1 magnitude.

OPERATIONAL PROCEDURE

In order to determine whether an increase of Lyman α radiation or X-ray radiation from the sun was responsible for the increase in *D*-layer ionization during a flare, it was planned to fly rocket-borne instrumentation to 100-km altitude in conjunction with ground measurements of flare activity. Since the scheduling and safety requirements of available land-based rocket ranges were likely to cause serious delays in attempts to launch rockets at times of flares, it was decided to carry out the measurements using balloon-borne six-inch solid-propellant rockets (Rockoons) fired at sea [3]. With this technique, it was possible to maintain a rocket suspended below a balloon in readiness for firing for a period of several hours. The operation was carried out from the U.S.S. *Colonial* (LSD-18), approximately 350 miles southwest of San Diego. The operational procedure was to launch a balloon and rocket in the morning. Once the balloon reached an altitude of 70,000 feet, the sun was observed continuously for evidence of a solar flare. The rocket could be command fired at floating altitude by radio. If no flare was observed by the time the balloon drifted to the boundary of the assigned firing area, the rocket had to be fired. During the operation, one rocket was successfully fired during a solar flare and two additional rockets gave background data on the level of solar Lyman α emission at the present stage of the solar cycle.

SUPPORTING MEASUREMENTS OF SOLAR FLARES

In order to determine when to launch the balloon-borne rockets, it was necessary to monitor concurrently the flare activity of the sun. Three methods of flare monitoring were attempted. Flares producing significant radio fadeout in the 6 to 15 Mc region were detected by monitoring the signal strength of four short-wave radio stations. The stations were so chosen that their signals were received via an ionospheric reflection occurring at a point on the sunlit side of the earth. During the operating period of the expedition, two such fadeouts were observed, but, unfortunately, they occurred on the one day during which no rocket launchings had been planned.

The detection of solar flares by means of radio fadeout is limited, in that it is capable of detecting only the infrequent larger flares producing intense low-level *D*-layer ionization. Since it appeared that the probability of encountering a large flare was small, direct observation of the sun was essential. We were fortunate in obtaining the cooperation of two solar observatories. Direct radio communication was established between the U.S.S. *Colonial* and the solar observatory at Sacramento Peak, Sunspot, New Mexico. Radio communication between the solar observatory at Climax, Colorado, and Sacramento Peak also permitted observations at Climax to be relayed to the operating ship. At Sacramento Peak, the solar disk was observed through a narrow band pass Lyot filter tuned to Hα. Measurements at Climax were made by means of a spectrohelioscope. Visual measurements were also attempted from shipboard by means of a narrow band filter and telescope assembly [4], mounted on a pointing control and utilizing television monitoring of the solar Ca K line emission. Constant cloud cover prevented visual observation of the sun from shipboard, and intermittent clouding also hampered observations from Sacramento Peak and Climax. The one flare during which a rocket was suc-

cessfully launched was observed at Climax. Without the generous cooperation of the people at both Climax and Sacramento Peak, these results could not have been obtained.

ROCKET INSTRUMENTATION

Four types of radiation detectors were flown in each of the rockets. An ion chamber with a LiF window and filled with nitric-oxide gas was used to measure the incident intensity of solar Lyman α radiation; a Geiger counter with a 14.7 mg/cm^2 Be window was used to measure X-rays of wavelength less than 8A; a partially shielded scintillation counter, using a NaI (Tl) crystal 1-1/8 inches in diameter and 1/2 inch thick, combined with a 6199 photomultiplier, was flown as an X-ray pulse amplitude spectrometer to measure any hard X-ray flash that might be encountered during a flare. Two photocells sensitive to visible light were flown to determine rocket orientation in space [5]. One photocell measured the angle between the direction of the sun and the view plane of the detectors during each roll of the spinning rocket; the second photocell determined the phasing between horizon sweeps and views of the sun. The detector outputs were continuously recorded on the ground by means of a conventional four-channel FM, FM telemetering link with the rocket. The telemetering system was calibrated throughout the flight by use of a commutator in the rocket, which placed a 0 volt and a 2.64 volt signal on each channel input once every six seconds. The time of rocket firing was identified with signals from WWV.

The instrumentation in several of the rockets encountered varying problems of sudden failure at the time of rocket ignition. The failures affected individual information channels only. The channels that remained operating after rocket firing were in no way compromised by failures in other channels.

DESCRIPTION OF THE FLARE DURING WHICH ROCKET OBSERVATIONS WERE MADE

Rocket measurements were made during a flare reported to have begun between 19:05 and 19:07 UT, on July 20, 1956. This flare was observed on a spectrohelioscope by R. Hansen, at the High Altitude Observatory, Climax, Colorado. The information that the flare was in progress was immediately transmitted to our ship by radio via Sacramento Peak. At 19:15 UT, the Hα from the affected region was still considerably brighter than preflare Hα, but its strength was declining. At 19:20, there were still signs of a flare in progress, and shortly afterwards all evidence of a flare had disappeared. The flare was too small to produce a detectable radio fadeout. Unfortunately, no record of the flare is known to have been recorded at other solar observatories. The flare was considered by the High Altitude Observatory as being something between Class 1 and a subflare.

The rocket measurements were made between 19:16 UT and 19:18 UT. The rocket measurements did not, therefore, cover any initial flash excitation that may have occurred during this short-lived solar event. However, evidence of unusually intense coronal excitation was obtained.

EXPERIMENTAL RESULTS

The rocket measurements made during the flare of July 20 are shown in Figure 1. Curve *A* shows the current passed by the Lyman α ion chamber as a function

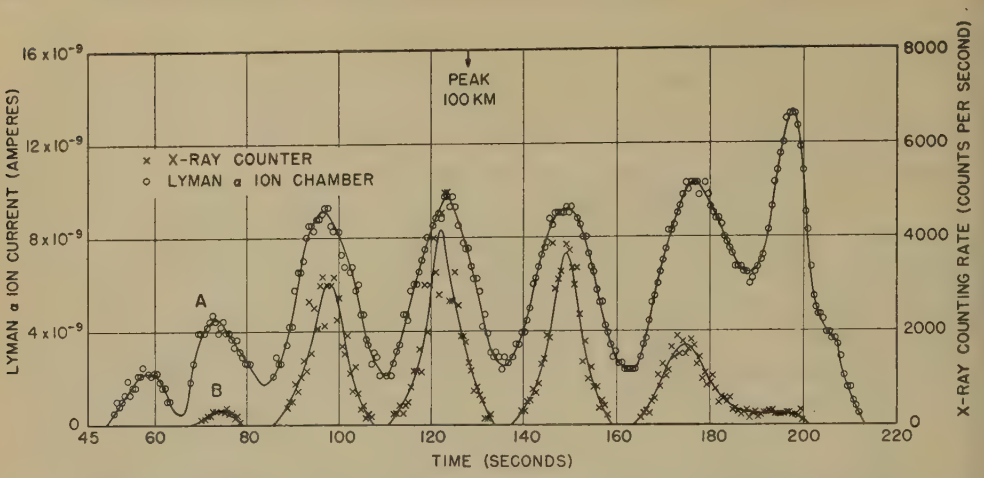

FIG. 1—Responses obtained from a nitric-oxide ion chamber and a beryllium window X-ray counter late in a Class 1 to 1— solar flare. The response of the X-ray counter has been corrected for circuit time constant and counter dead-time.

of flight time. The plotted points are the peak currents in the ion chamber corresponding to each complete roll of the rocket. This current is affected by the angle between the view plane and the sun. The current peaks observed at 97 seconds, 123 seconds, and 149 seconds were caused by the precession of the rocket, which at these altitudes behaved almost as a free-falling rigid body spinning mainly about its smallest moment of inertia. The rocket roll rate was 5.0 revolutions per second. The Lyman α ion currents have been corrected only for a very slight non-linearity in the frequency shift of the FM modulator.

Curve *B* of Figure 1 shows the count rate response of the Be window Geiger counter. There is a considerable statistical variation in the individual response peaks of the Geiger counter, caused by the relatively small number of counts contributing to each counter response. The magnitude of the statistical fluctuations is attributable to the relatively brief view of the sun obtained during each roll. Each data point shown for Curve *B* is based on the average amplitude of three adjacent response peaks. The data have been corrected for the small non-linearity of the FM modulator, for circuit time constant (20 per cent), and for counter dead-time (450 μ-seconds).

The photomultiplier and aspect photocell information channels failed on rocket ignition.

LYMAN α RADIATION DURING THE FLARE

The determination of the intensity of Lyman α radiation as measured by the "flare" rocket was complicated by lack of aspect photocell information. Despite this lack of direct aspect information, it proved possible to determine the incident Lyman α intensity with fair accuracy. The manner by which the data were treated is described in the Appendix. Based on this treatment, the intensity of the above atmosphere flux of Lyman α radiation was 6.1 ergs/cm^2 sec.

Table 1 shows a comparison between the incident Lyman α flux measured in the flare rocket and the fluxes measured in other rockets utilizing the nitric-oxide

ion-chamber technique. The figure of ±20 per cent reflects the confidence of the authors in the validity of the trajectory solution described in the Appendix.

TABLE 1—*Solar Lyman α emission as measured by nitric-oxide ion chambers*

Rocket	Time of firing (UT)	Sun condition	Incident flux of Lyman α
			ergs/cm² sec
A-34	2250, 10/18/55	Quiet	5.7 (−1 + 3)
A-35	0015, 10/22/55	Quiet	4.0 (±0.8)
A-36	1530, 11/4/55	Quiet	9.2 (±3)
D-5	1915, 7/17/56	Quiet	6.1 (±0.3)
D-8	1917, 7/20/56	Late in Class 1 flare	6.1 (±1.4)
D-13	2113, 7/25/56	Quiet	6.7 (±0.3)

Clearly, there was no evidence of an unusually high value of Lyman α radiation during the flare flight. It is not known whether the result indicates that small flares of the type encountered cause only a negligible percentage change in the over-all Lyman α emission from the solar disk, or whether the Lyman α emission accompanying the flare had decayed to negligible levels by the time the rocket measurements began. A comparison between the amplitudes of the Lyman α maxima accompanying free-fall precession of the rocket, namely, those shown in Curve *A* of Figure 1 at 97 seconds, 123 seconds, and 149 seconds, shows that no major change in Lyman α emission occurred during the flight.

SOLAR X-RAY EMISSION DURING THE SOLAR FLARE

In order to determine the intensity and to analyze the characteristics of the incident flux of solar X-ray radiation observed during the flare flight, it was necessary to correct the observed responses of Curve *B*, Figure 1, for variations in angle between the sun and the plane of view. The method of making this aspect correction is described in the Appendix. The large angle between the direction of the sun and the detector view plane which occurred during most of the flight resulted in a shift of the spectral sensitivity curve of the counter, as shown in Figure 2. The X-ray counting rates corrected for aspect are shown in Figure 3.

The X-ray intensities found in the flare flight are indicative of an exceptionally high state of coronal excitation. A comparison between the X-ray responses obtained during this flight and all previous flights for which we have X-ray data is shown in Table 2. The flare rocket received a 3A to 8A X-ray flux several times as intense as any flux previously measured. The high X-ray emission intensities found during the V-2 #49 flight may have been influenced by a Class 1 solar flare, which peaked 160 minutes before the flight. The relatively high energy value indicated for flight A-9 is partially the result of using a computation based on a 2×10^6 degree K emission distribution. A computation based on a higher temperature would be justified for a Be window as thick as 47 mg/cm². In contrast, the intensities observed since January 1953, flights A-14, A-16, and A-34, show that very low values of coronal emission below 8A occur during the sunspot minimum.

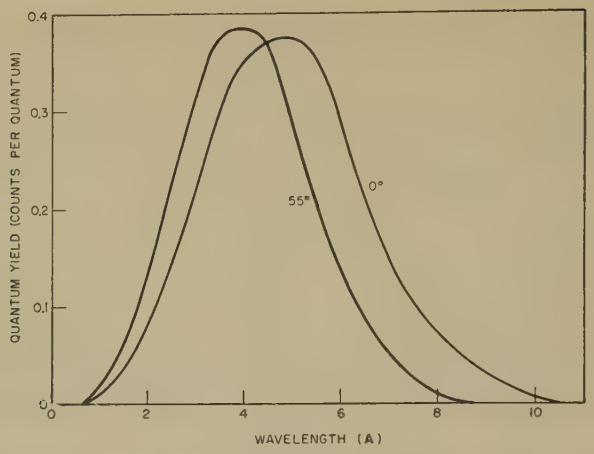

FIG. 2—Spectral response characteristics of 14.7 mg/cm² Be X-ray counter flown in the flare rocket. The spectral response is calculated from window and gas absorption coefficients for normally incident X-rays and for X-rays incident at an angle of 55°.

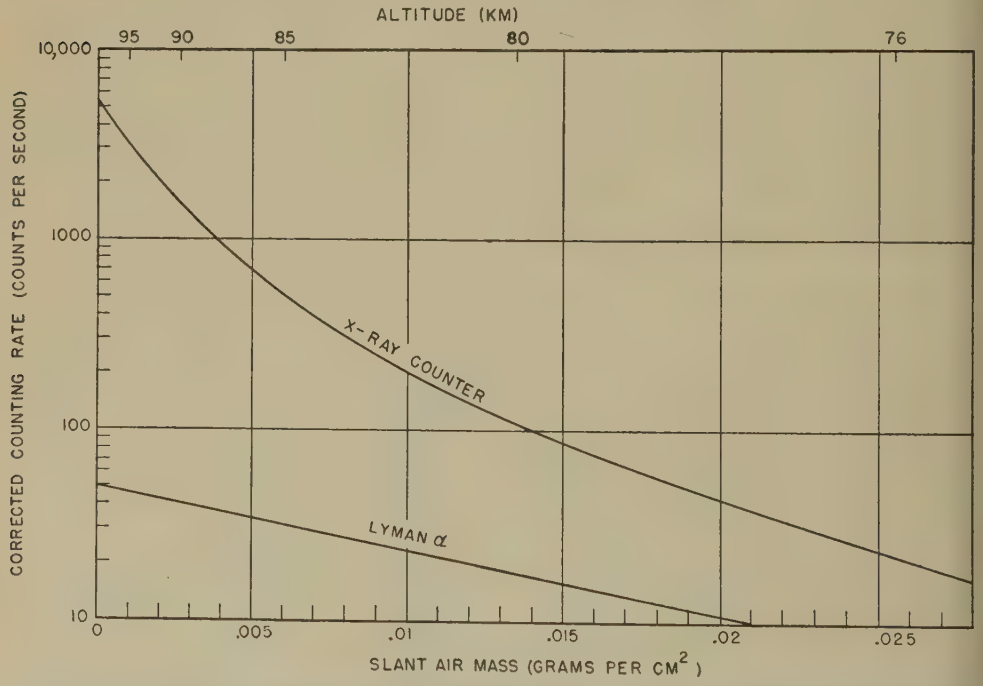

FIG. 3—Counting rate *vs* slant air mass for the Be window X-ray counter flown in the flare flight. The counting rates have been corrected for changes in the angle between the detector view plane and the sun.

The A-14, A-16, and A-34 data are believed to be more reliable than those obtained previously.

ENERGY DISTRIBUTION OF FLARE

From the X-ray counting rate *vs* air mass curve of Figure 3, it has been possible to determine a smoothed energy spectrum of X-ray intensities. Such a spectrum

TABLE 2—*Solar X-ray emission as measured by beryllium and aluminum Geiger counters*

Rockets	Time of firing (UT)	Sun condition	Counter window material and surface density	Be counters response above atmosphere	Al counters response above atmosphere	Energy** below 8A	Energy** 8A to 20A
			mg/cm²	*counts/cm² sec*	*counts/cm² sec*	*erg/cm² sec*	*erg/cm² sec*
V-2 #49	1730, 9/29/49	160 min after Class 1 flare	Be 13	1.0×10^4	.....	0.0015	.....
A-9	1459, 5/1/52	Quiet	Be 47	495	.....	0.0017	.....
A-10	1344, 5/5/52	Quiet	Be 47	< 125	.....	< 0.0005	.....
Viking 9	2138, 12/15/52	Quiet	Be 13	$< 1.5 \times 10^{3*}$	.....	<0.0006	.....
			Al 1.59	.....	$2.9 \times 10^{6*}$	.....	0.2
A-14	2240, 11/15/53	Quiet	Be 13	< 40	.....	$< 6.7 \times 10^{-6}$	.....
			Al 1.59	.....	$< 3.1 \times 10^{4*}$	.....	< 0.0015
A-15	1546, 11/25/53	Quiet	Be 13	332	.....	2.9×10^{-6}	.....
			Al 1.59	.....	$< 2.6 \times 10^{4*}$	.....	< 0.0013
A-16	1529, 12/1/53	Quiet	Al 1.59	.....	4.5×10^4	.....	0.0004
A-34	2250, 10/18/55	Quiet	Al 1.59	.....	1.4×10^5	.....	0.0012
D-8	1915, 7/20/56	Late in Class 1 flare	Be 14.7 at 55° aspect	1.2×10^5	.....	0.005	.....

*These counters were filled with He + quench agent. Other counters were filled with Ne + quench agent. The Be window counters using He have about 1/20 the sensitivity of the Ne counters. The Al window counters using He have about 1/5 the sensitivity of the Ne counters.

**A2 $\times 10^6$ deg K gray-body emission curve is assumed for the sun. The spectrum is normalized to give the experimentally observed counting rates. The Table shows the energy of the normalized emission curve that falls within the indicated spectral limits.

can be calculated because the air absorption coefficients of the incident X-rays form a single valued and rapidly varying function of wavelength. Thus, we can subdivide the spectral region 3A to 9A into small spectral bands, each band having a unique range of air absorption coefficient. By approximating the curve of Figure 3 by a series of straight-line segments, each corresponding to a single absorption coefficient, we can determine the number of counts contributed by quanta in each spectral band. From the spectral sensitivity curves of Figure 2, the energy distribution of the incident flux can then be determined.

The results of such an analysis are shown in Figure 4. The energy spectrum determined in the above manner is not capable of showing any structure in the coronal emission characteristics, but does distinguish between thermal and non-thermal emission sources. For example, it is possible to distinguish a constant-emissivity (gray-body) single-temperature thermal emission from the non-thermal *Bremsstrahlung* produced by a monoenergetic electron beam injected into a cold gas. Similarly, a non-thermal synchrotron emission, analogous to that studied by C. Y. Fan, as a source of cosmic radio noise [6], is easily distinguished from the thermal emissions. On the other hand, it is not possible to differentiate between gray-body thermal emission and the *Bremsstrahlung* emission of a high-temperature electron cloud in a cold gas. Nor is it possible to differentiate between a constant emissivity source and one in which rapid fluctuations in emission occur with wavelength, so long as no single emission line overwhelmingly predominates in the spectral region covered.

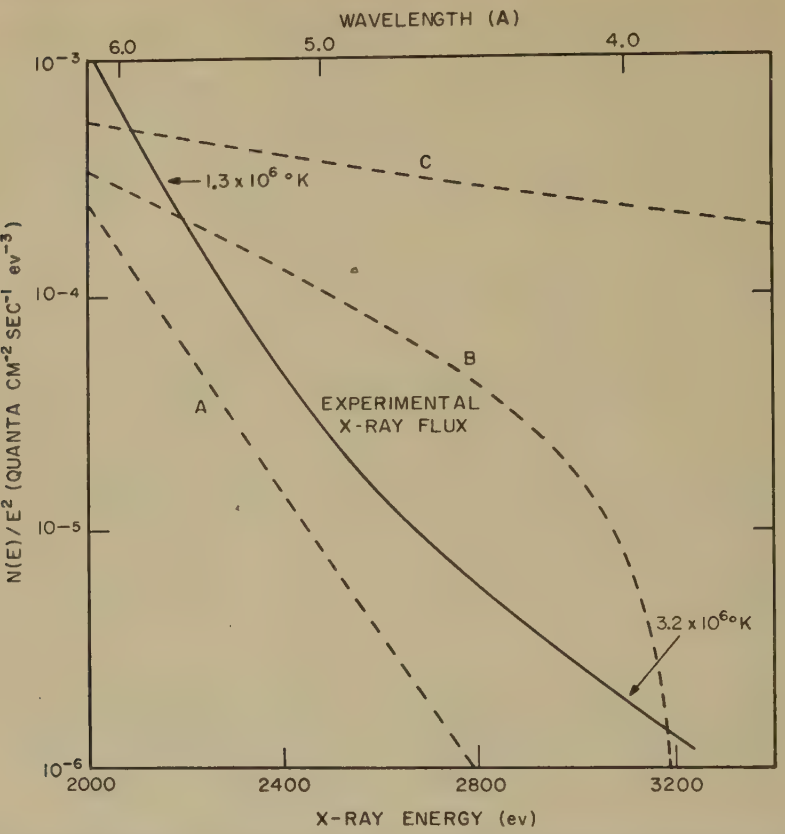

Fig. 4—Spectral distribution of incident X-ray quanta as a function of quantum energy. The plot of log $E^{-2}N(E)$ *vs* E, where $N(E)$ is the number of quanta per cm² per sec per unit energy interval, gives a straight line for gray-body emission for $\lambda T < 0.3$. The heavy solid line is a plot of the experimental energy distribution observed during the solar flare. The three broken-line curves show the relative emission spectrum from (*A*) a 2×10^6 degree K electron cloud in a cool gas, (*B*) a stream of 3,200 eV monoenergetic electrons injected into a cool gas, and (*C*) a high energy E^{-3} distribution of electrons radiating in synchrotron fashion due to acceleration in a magnetic field.

The observed emission spectrum of the coronal X-rays most closely approximates the thermal type with the form to be expected from a collection of solar regions at different states of temperature excitation. If the results are interpreted in terms of emission from gas of approximately constant emissivity, emission from regions of $T = 1.3 \times 10^6$ degrees K predominated at 6A, and emission at $T = 3.2 \times 10^6$ degrees K predominated at 4A. If the results are interpreted in terms of *Bremsstrahlung* emission from a highly excited electron gas in a much colder scattering medium, emission from regions of electron temperature $T_e = 1.6 \times 10^6$ degrees K predominated at 6A, and emission from regions of $T_e = 4.41 \times 10^6$ degrees K predominated at 4A. This general form of coronal emission is in agreement with the interpretation of data obtained at longer wavelengths in Aerobee 16.

CONCLUSIONS

On the basis of measurements of 3A to 8A X-rays and Lyman α radiation made

rom a rocket flown late in a Class 1 to Class 1− solar flare, there was observed n unusually large amount of X-ray emission below 8A. The character of the emission in the 3A to 8A region resembles a collection of thermal sources at temperatures ranging from 1.0×10^6 degrees C to 3.5×10^6 degrees C. The intensity of Lyman α radiation during the flight was comparable to that observed from other rockets fired in the same two-week period. In view of the fact that the visible emission of Hα from the flare region had almost returned to normal by the time of the rocket measurements, the emissions observed are indicative of a strong intensification of the normally present coronal excitation. The measurements would seem to indicate that the coronal excitation lingers long after the primary flare event has dissipated. They also lend strong support to the theory that a hardening of the coronal X-ray spectrum is the source of the low-level D-layer ionization responsible for SID.

It is planned to fire additional rockets coincident with direct observations of solar flares in the summer of 1957. The development of an island-based launching facility will permit ground launchings. With this arrangement, attempts will be made to obtain measurements during various phases of larger SID producing flares.

References

[1] H. Friedman and T. A. Chubb, The Physics of the Ionosphere Report of 1954 Cambridge Conference, Physical Society, London (1955); p. 58.
[2] E. T. Byram, T. A. Chubb, and H. Friedman, J. Geophys. Res., **61**, 251 (1956).
[3] J. A. Van Allen and M. B. Gottlieb, Rocket Exploration of the Upper Atmosphere, edited by R. L. F. Boyd and M. J. Seaton, Pergamon Press, Ltd., London (1954); p. 53.
[4] D. E. Billings, R. Lee, and G. A. Newkirk, Astr. J., **62**, 8 (1957).
[5] J. E. Kupperian, Jr., and R. W. Kreplin, Rev. Sci. Inst., 28, 14 (1957).
[6] C. Y. Fan, Astroph. J., **123**, 491 (1956).
[7] The Rocket Panel, Phys. Rev., **88**, 1027 (1952).

APPENDIX

Treatment of Data

The basic data upon which the incident intensities of solar X-ray and Lyman α radiation were determined are shown in Figure 1. In order to reduce these data to absolute energy values, it was necessary to determine the angle between the detector view plane and the sun. The solution of the problem was greatly facilitated by knowledge of the typical behavior of the type of rocket flown, as determined from other flights during which photocell aspect information was obtained. It was also facilitated by the relatively wide angular response of the ion chamber, which made the response relatively insensitive to small changes in aspect when the aspect was good.

The key to the reduction of the Lyman α data for the flare rocket, Curve *A*, Figure 1, lies in the Lyman α response peak observed at 197.5 seconds and the shoulder observed at 207 seconds, combined with a knowledge that the other Deacon rockets of comparable spin rate tumbled due to air drag at altitudes above the altitude at which solar Lyman α radiation disappeared. As the rocket tumbles and subsequently swings, it must pass through perfect aspect at least

once. The solution of the rocket aspect problem in this case is based on the assumption that the rocket had perfect aspect both at the 197.5 second peak and at the 207 second shoulder. The difference in the amplitudes of the two response peaks must then be due to atmospheric attenuation. Since the rocket peaked within a few seconds of 128 seconds, its vertical velocity in the neighborhood of 200 seconds was known fairly accurately. Thus, from a knowledge of the scale height in D region, the atmospheric attenuation at 197.5 seconds was determined. The atmospheric attenuation at 197.5 seconds determined in this manner was 0.51. The corresponding above atmosphere incident flux of Lyman α radiation was 6.1 ergs/cm^2 sec. The trajectory determined by this solution gives a peak altitude of 100.1 km and a peak time of 128 seconds. This trajectory was very similar to that of another Deacon flight in the same series, which had a peak altitude of 102.5 km and a peak time of 128 seconds, as determined from matching aspect corrected ascent and descent Lyman α data in conjunction with Rocket Panel [7] pressure data. An independent check of the accuracy of the flare rocket trajectory solution can be gained from a comparison in the computed altitudes of the last observed Lyman α responses for these two rockets. Since the rockets are both tumbling rapidly at these altitudes, differences in aspect are unlikely to have major effects on the results. The last response of the flare rocket was noted at 212 seconds, corresponding to 66.6 km. The last response of the comparison flight occurred at 215 seconds, corresponding also to 66.6 km.

In order to reduce the X-ray data, it was necessary to correct the observed X-ray responses, Curve B, Figure 1, for the continually varying angle between the detector view plane and the sun. This aspect correction was made by using the response of the Lyman α ion chamber, corrected for atmospheric attenuation as a measure of the rocket aspect. The relative response of this type of ion chamber as a function of the angle between its direction of view and the sun was determined from the responses obtained in flights with operating photocells. By using this angular response curve, it was determined that at the aspect peak of 123 seconds, the sun was 55° above the plane of view swept out by the detectors. All data obtained at times such that the aspect angle was greater than 55° were adjusted on the basis of an aspect correction curve obtained by plotting Lyman α ion-chamber response *vs* counter response for points obtained within 51 seconds of peak time. These data were obtained at almost constant altitude, that is, within 1.0 km of peak. This method of correction required no knowledge of either the angular response curve of the ion chamber or of the counter. All data obtained at times such that the angle between sun and detector view plane was less than 55° were corrected on the basis of the ion-chamber angular-response curve deduced from other flights and from an X-ray angular-response curve calculated from the counter geometry. Calculations showed that the counter angular response was determined mainly by the free window area projected on a plane perpendicular to the line between detector and sun. In addition, there was a shift in spectral response due to increased effective window thickness and an increased path length through the absorbing counter gas. This shift in spectral response is shown in Figure 2. The X-ray counting rates plotted in Figure 3 have been corrected in this manner to a constant aspect angle of 55°.

STUDIES OF TRANSEQUATORIAL IONOSPHERIC PROPAGATION BY THE SCATTER-SOUNDING METHOD*

BY O. G. VILLARD, JR., SIDNEY STEIN, AND K. C. YEH

Radio Propagation Laboratory, Stanford University, Stanford, California

(Received May 18, 1957)

ABSTRACT

Echoes of exceptionally long delay detected by a HF radar located in the West Indies are interpreted as ground backscatter propagated by two or more successive reflections from the *F*-region of the ionosphere, without intermediate ground reflection. Propagation of this sort is associated with tilts in the reflecting layers. Pronounced tilts are encountered regularly in equatorial regions; one occurs almost daily at approximately 1900 local time over the geomagnetic equator; another occurs around noon in the vicinity of the subsolar point. It is shown that tilt-supported propagation can take place at frequencies considerably in excess of the MUF predicted in the usual way. It is believed that these results may explain the reports by radio amateurs of anomalous propagation between North and South America.

Introduction

For many years, radio amateurs have reported ionospheric propagation from North to South America at frequencies which appreciably exceed the calculated F2-layer MUF [see 1 of "References" at end of paper]. These transmissions have the following unusual properties: (1) They occur primarily in the hours between 1800 and midnight, although some occur during the afternoon; (2) the signals display a moderately rapid fade, voice transmissions being characterized by severe selective fading; and (3) the propagation appears to take place by one reflection from the *F*-layer over paths whose length exceeds the normal maximum of 4,000 km. Ferrell, who collected many of these reports, has presented evidence that the afternoon propagation tends to occur during, or just after the end, of magnetic storms [2].

The experience of commercial services and other workers appears to be conflicting. Wilkins and Minnis [3] report that MUF predictions tend to be conservative over transequatorial paths, and this conclusion is emphasized by Bennington and others [4]. On the other hand, Appleton and Beynon [5] attribute discrepancies between calculated and actual MUF's to the effects of sporadic-*E*. And Allcock [6],

*This work was supported in part by the Army, the Navy, and the Air Force under contract with Stanford University, and in part by a research grant of the General Electric Company. One of the authors (S.S.) was the holder of a National Science Foundation fellowship during the period of this work. A preliminary version of this paper was presented at the IRE National Convention in March, 1957.

in studying a Pacific transequatorial path, concludes that actual MUF's fall consistently below MUF's calculated by the usual prediction methods.

It is the purpose of this paper to present evidence suggesting that ionospheric tilts can significantly affect *F*-layer propagation in equatorial regions, and, accordingly, must be taken into account in any analyses of transequatorial propagation. These tilts appear to be able not only to account for transmission over unusual distances without intermediate ground reflections, but also for appreciable increases in MUF's above the values calculated in the usual manner.

Experimental Arrangements

During the months of August and September, 1956, two fixed-frequency backscatter-sounders were operated simultaneously on the island of St. Croix in the U. S. Virgin Islands (longitude 64° 45′, latitude 17° 45′). One sounder operated continuously at a radio frequency of 23.1 Mc; the other was operated at either 30.66, 40.68, or 46.2 Mc. Both sets had power outputs of approximately two kilowatts peak, and used rotatable three-element Yagi antennas. Pulse length was 2 milliseconds (approximately) and the PRF was 9.37 cps. The operating site was at the top of a hill, roughly 500 feet high. In the south direction, the view was unobstructed and the edge of the Caribbean Sea only some three or four miles away. To the east and west, there were no hills projecting above the horizontal, but to the north there was some screening due to a structure in the immediate vicinity of the antennas. These antennas, mounted one above the other, executed a complete scan in azimuth once each minute. Range-azimuth information was recorded on 16-mm movie-film.

Figure 1 is a map of Central and South America, showing the position of St. Croix and a scale of distance up to 7,000 km in the south direction. Positions of vertical-incidence ionospheric sounders are noted.

Description of Records Obtained

Ionospheric sounders, utilizing ground backscatter and located at temperate latitudes, will normally register echoes corresponding to one-hop *F*-layer transmission at delay times corresponding to free-space slant ranges up to a maximum of about 4,000 km [7]. Echoes corresponding to multiple hops are seen at times of day when ionospheric absorption is low. At St. Croix, however, examination of the records revealed the presence of a new class of echoes having delay times corresponding to free-space slant ranges varying between 5,500 and 11,000 km.

Echoes of this sort were seen virtually daily in a southerly direction between 1500 and 2100 local time (Atlantic Standard Time). Examples are designated by the arrows in Figures 2 and 3. They were almost invariably visible on 23, 31, and 41 Mc/s, and on a number of occasions on 46 Mc/s, as in Figure 3. One of their most striking characteristics is that their equivalent slant range (between 6,000 and 8,000 km) was approximately the same even when the operating radio frequencies differed by as much as two to one (see Fig. 3). This behavior is in sharp contrast with that of one-hop ground-scatter propagated by the *F*-layer of the ionosphere in the usual way; the equivalent range of such echoes normally increases linearly with operating frequency. Another striking characteristic of the evening echoes is that they were often seen, at the higher frequencies, by

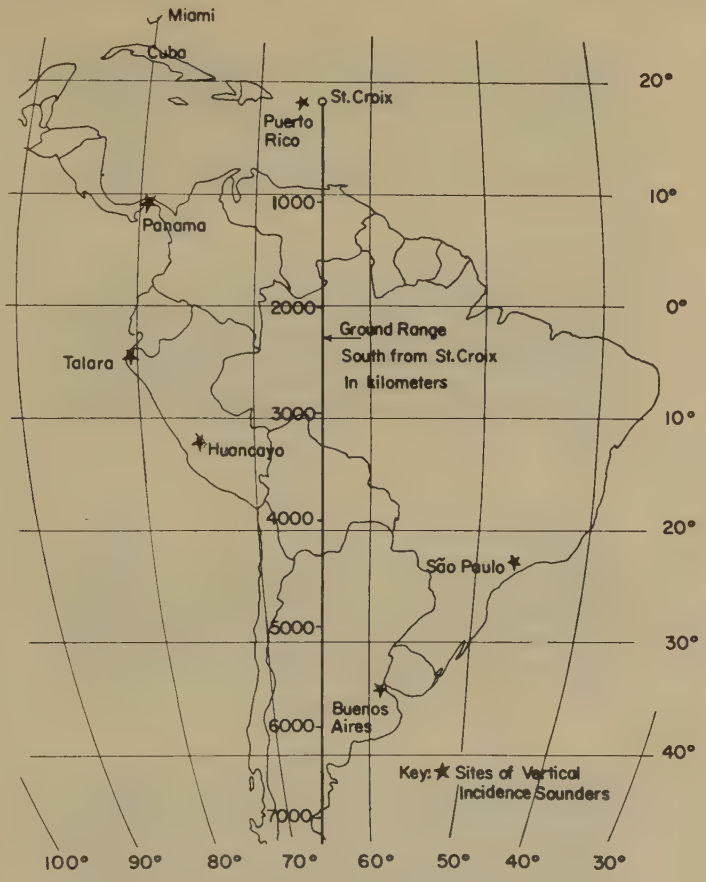

FIG. 1—Map of transequatorial region

themselves alone without any other echoes being present whatsoever (note the 16.2 Mc record of Fig. 3).

During the afternoon hours, long-range echoes were seen regularly at 41 Mc. An example is designated by the arrows in Figure 4. These echoes generally appeared in the hours immediately preceding local noon, and usually in an easterly to southeasterly direction. They were not, in general, observed at the other radio frequencies. Since their ranges varied from 7,000 up to 12,000 or more kilometers, they were often difficult to identify, owing to the fact that the 9.37 cps PRF afforded a maximum range interval of only 8,000 km. However, careful examination of a sequence of records usually permitted around-the-time-base echoes to be identified as such. For example, an echo seen at 1,000-km slant range on 41 Mc (as in Fig. 4) could be the result of sporadic-*E* propagation; if an equivalent echo is not simultaneously registered on 23 Mc, however, sporadic-*E* is ruled out, and the 41-Mc echo is presumably around-the-time base. Nevertheless, there were several days when long-range echoes *may* have been present, but owing to the presence of sporadic-*E* they could not be positively identified as such.

Other long-range echoes were observed at various times during the day. Of

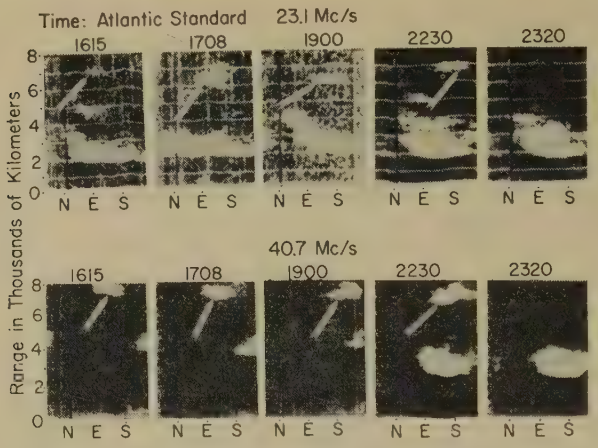

FIG. 2—Examples of evening long-range echoes, September 2, 1956 (St. Croix)

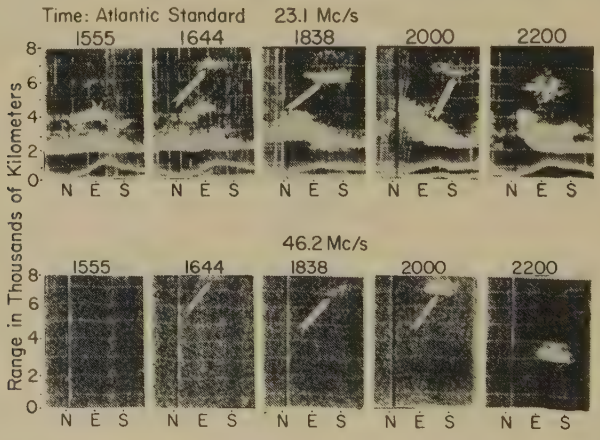

FIG. 3—Examples of evening long-range echoes, September 10, 1956 (St. Croix)

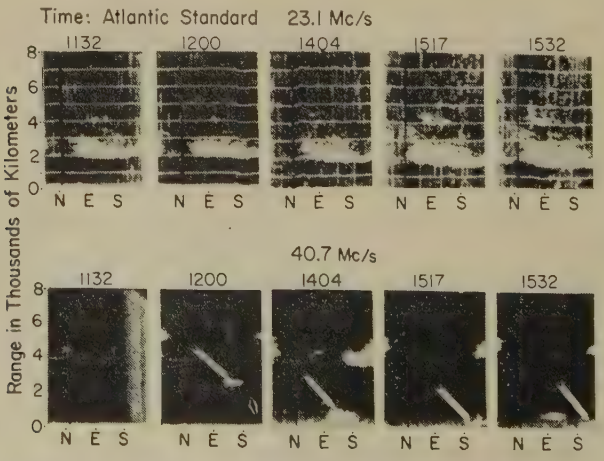

FIG. 4—Examples of noon long-range echoes, September 2, 1956 (St. Croix)

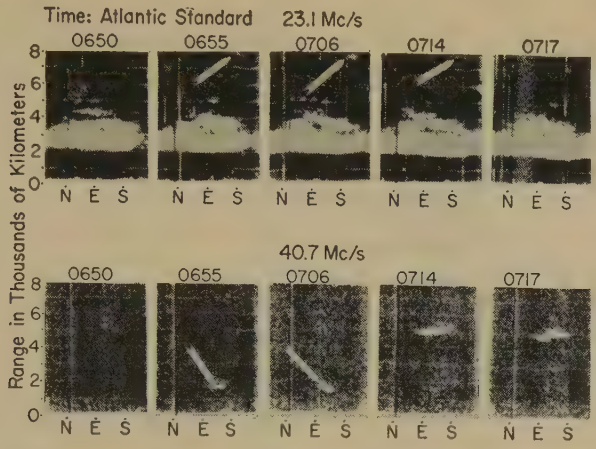

FIG. 5—Examples of transient long-range echoes, September 8, 1956 (St. Croix)

short duration, these echoes were seen most frequently at 41 Mc. Figure 5 shows such an echo, visible on both 23.1 and 40.7 Mc, which appeared at 0655 on September 8, 1956.

Figure 6 shows the number of hours during which long-range echoes of any category were seen, during the operating period of August 8 through September 11.

Interpretation of the Records

All echoes of unusually long range are interpreted as being ground backscatter propagated by the ionosphere, and not as direct reflections from a scattering or reflecting region within the ionosphere. The long-range echoes appeared to have roughly the same fading frequencies and Doppler shifts as normal *F*-layer-propagated backscatter. They also showed the same marked dependence of amplitude on pulse length that is characteristic of ground backscatter. These properties were not studied systematically, however. An opportunity did not present itself to correlate the existence of these echoes with the existence of strong direct transmission from the ground areas presumably being illuminated by the radar. The possibility of the echoes being around-the-world transmission of the sounding pulses was ruled out by varying the PRF and observing the effect on apparent echo range. (Around-the-world transmission was actually observed and positively identified on several occasions, however.) Figures 7 and 8 illustrate the time variation of the equivalent range of the long-range echoes seen on the four frequencies. For convenience, the 23-Mc echoes have been divided into two periods, August 8–31 and September 1–11. Plots for the other three frequencies represent all of the available data.

It is suggested that the propagation giving rise to the echoes consists of one or more successive reflections from the *F*-region of the ionosphere, without intermediate reflection from the ground [8]. Such reflections are designated as "*F* modes. They may arise whenever the ionosphere can be considered to have an equivalent tilt from the standpoint of the reflection of radio waves. Thus, an equivalent tilt might arise owing to a localized increase in height of a layer, without any other alteration in the contours of ion density, or (in the case of a thick layer) it might

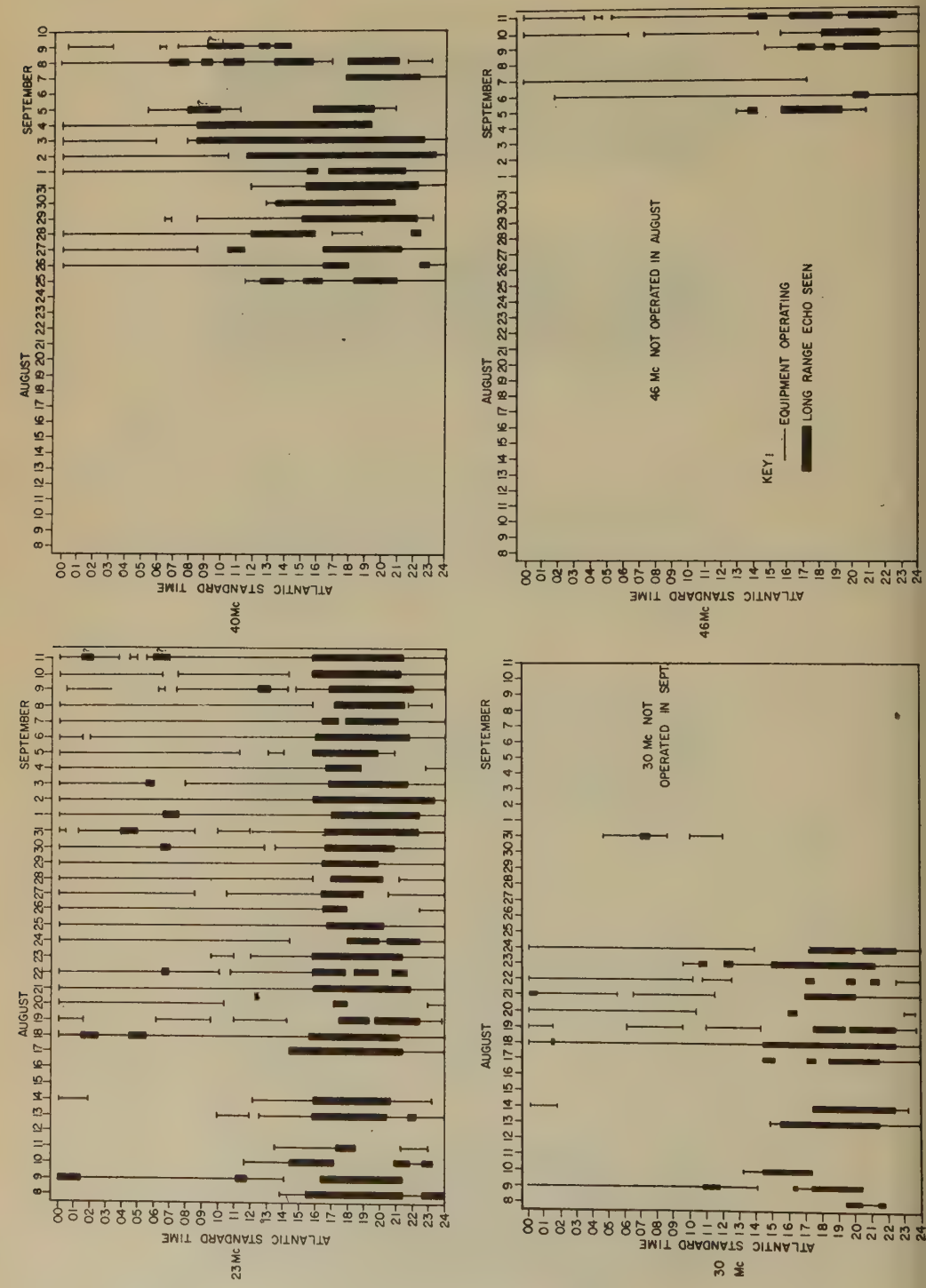

FIG. 6—Hours during which long-range echoes were seen

be caused by a change in ion density in the horizontal direction, without any change in the height of the maximum ion density or in the layer thickness.

One of the striking features of the equatorial ionosphere is the sharp, transitory rise in minimum virtual height ($h'F2$) which occurs daily at approximately 1900

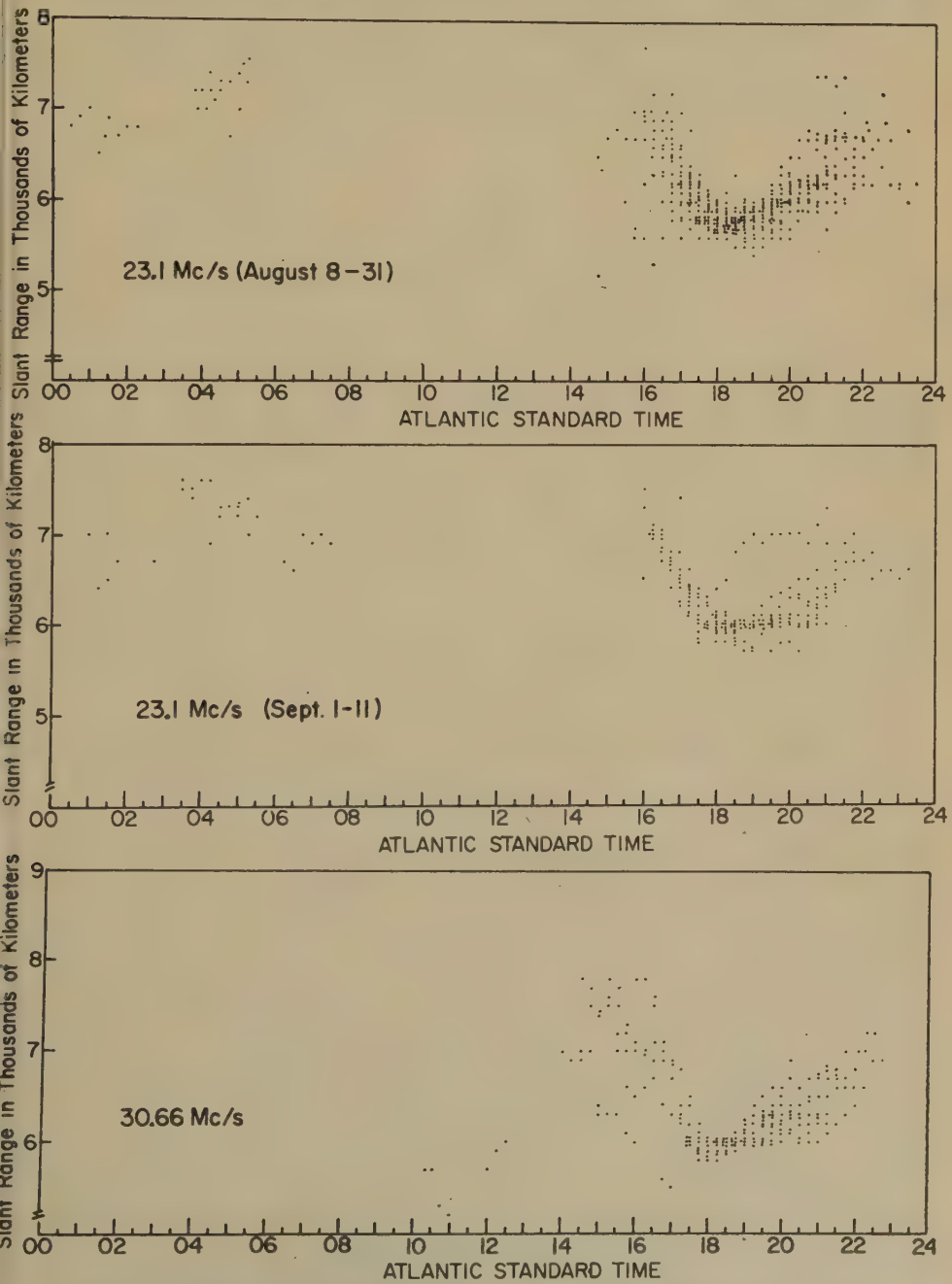

FIG. 7—Long-range echo ranges *versus* local time, August 8–September 11, 1956

local time in a belt extending some ten to fifteen degrees north and south of the geomagnetic equator. Contours of f_0F2 and $h'F2$ *versus* time and geographical location are shown in Figure 9 for the month of August, 1956. Note that geomagnetic coordinates have been used. This plot is derived by extrapolating monthly median ionospheric characteristics reported from Puerto Rico, Panama, Talara, and Huancayo, Peru, and São Paulo, Brazil. (Owing to the absence of August data, it was necessary to use September data from the São Paulo station.) The increase in height around 1900 local time is apparent.

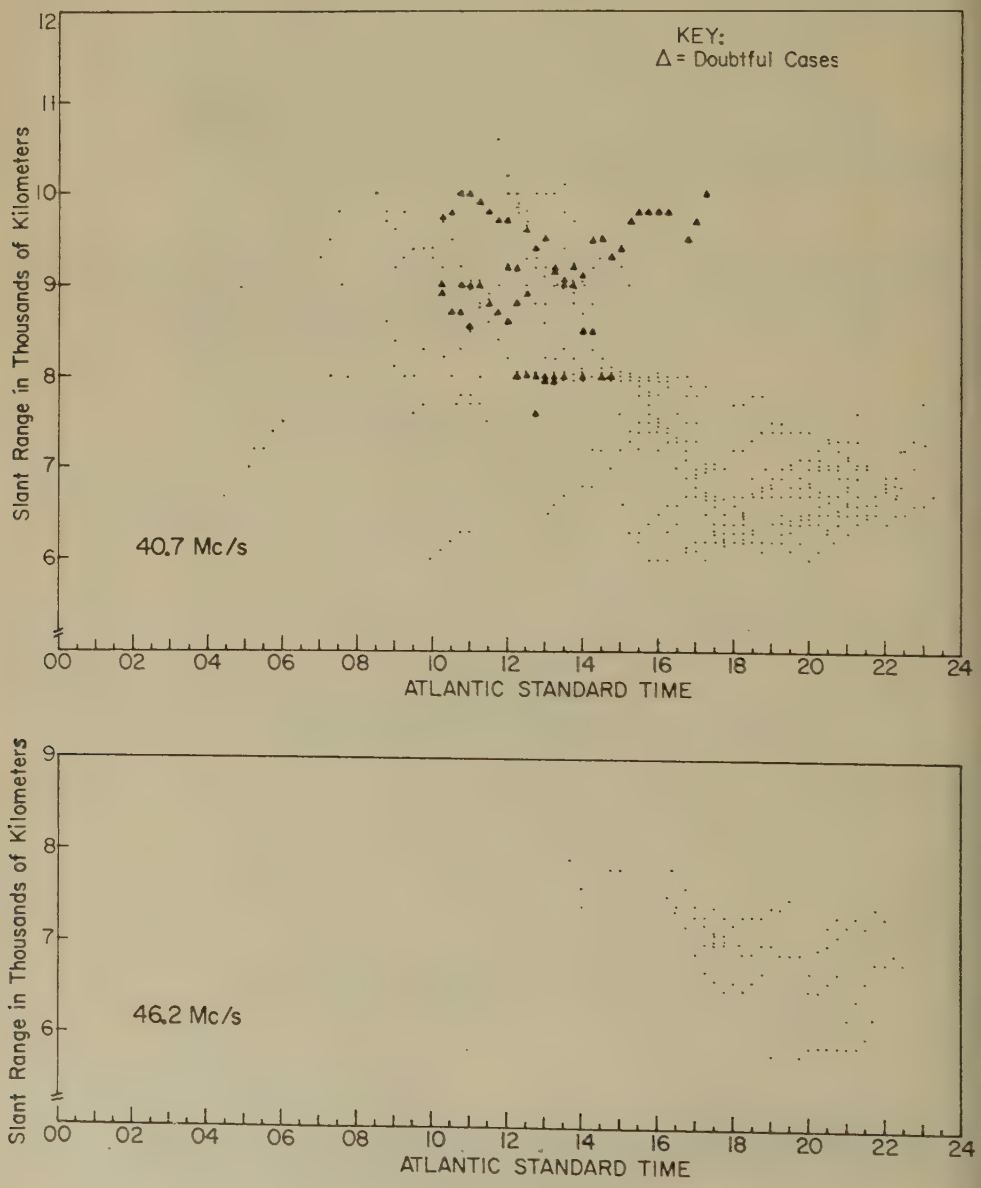

FIG. 8—Long-range echo ranges *versus* local time, August 8–September 11, 1956

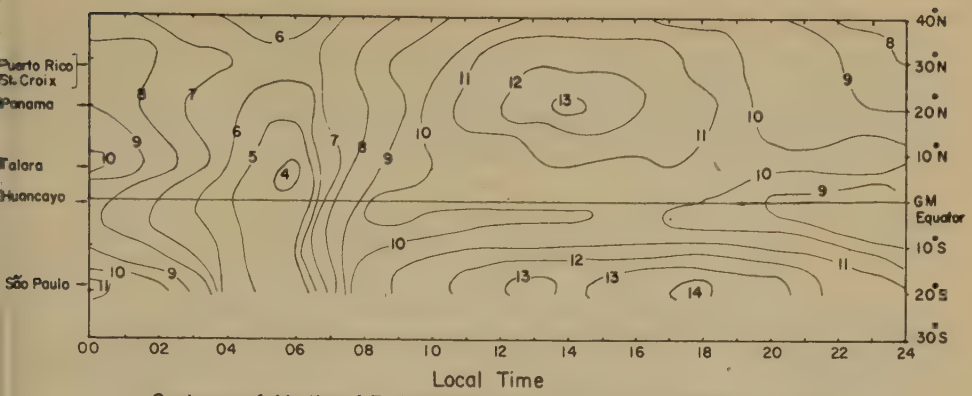

Contours of Median f_0F_2 Values in Mc/s for August, 1956, Plotted in Geomagnetic Coordinates, Based on Reported Data

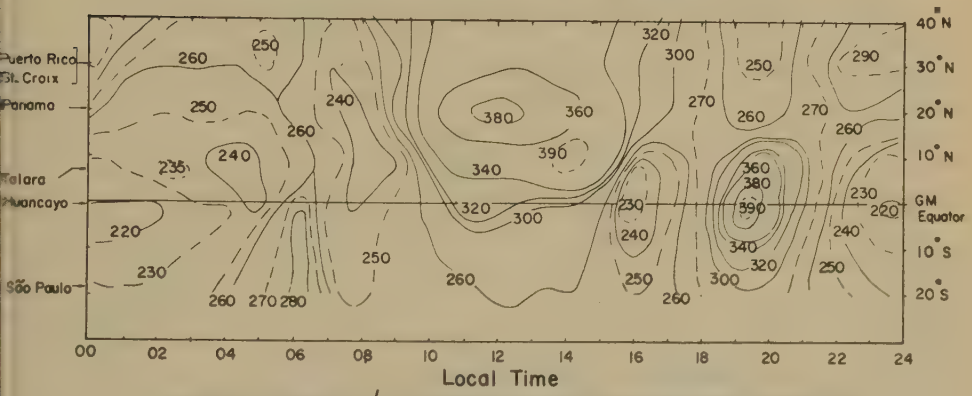

Contours of Median $h'F_2$ Values in Km for August, 1956, Plotted in Geomagnetic Coordinates, Based on Reported Data (September Data Used for São Paulo Station)

FIG. 9

In order to investigate propagation through this region at this particular hour, a "typical" day was chosen for detailed study. Magnetic activity occurred on September 2, 1956, but the principal properties of the ionosphere, as registered at equatorial sounders, do not appear appreciably to have been affected. On this day, the various classes of echoes observed at St. Croix are readily distinguishable, and it was chosen for this reason. From the original ionograms made at Panama and Talara, the true height of reflection was determined as a function of frequency using the approximate method of Manning [9]. The earth's magnetic field and frictional losses were neglected. From the true-height curves, shown in comparison with the original ionograms in Figure 10, the refractive index as a function of height can be found for a fixed operating frequency. This was done for both the Panama and the Talara ionospheric sounders at a time corresponding to 1900 Atlantic Standard Time on September 2, 1956. The refractive index at intermediate points was derived by interpolation, using the data from these stations and assuming a linear variation of ionospheric parameters with latitude. Symmetry of the ionosphere about the geomagnetic equator was assumed.

Next, contours of constant refractive index were drawn on a chart showing a cross-section of the earth and the ionosphere in the south direction from St. Croix. This chart has a scale of one inch per 100 km. The contours of constant refractive index corresponded to one per cent increments in refractive index. Within each contour interval, the refractive index was assumed to be constant. Rays were

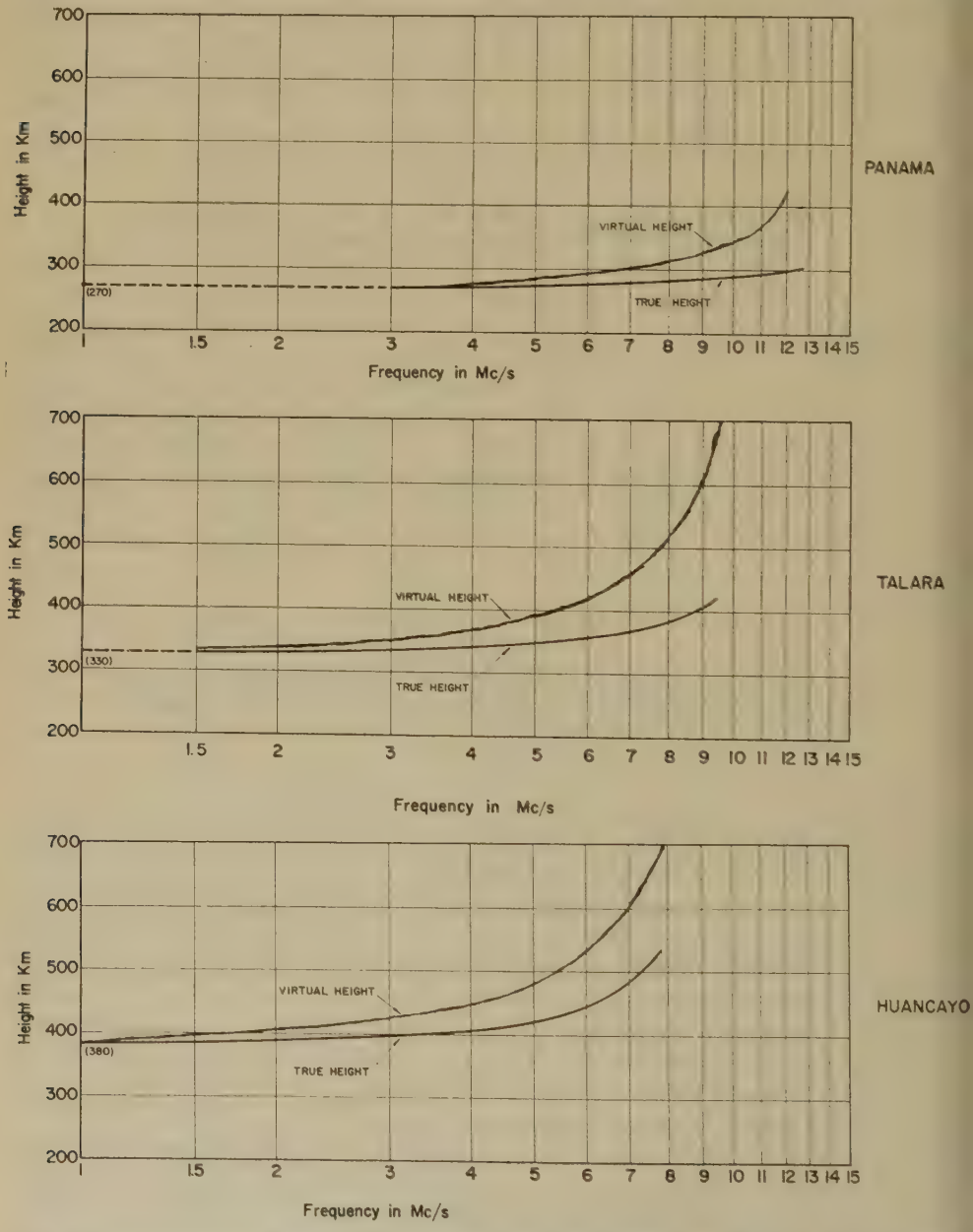

FIG. 10—Reproductions of Panama, Talara, and Huancayo ionograms showing true heights as a function of frequency (1900 local time, Sept. 2, 1956)

then traced on a step-by-step basis, the appropriate refractive index being used within each contour interval.

The graphically-determined ray paths for 23 Mc at 1900 AST on September 2, 1956, are shown in Figure 11. Note that the ray taking off at a vertical angle of 10° is returned to the earth approximately 2,500 km away. This ray can give

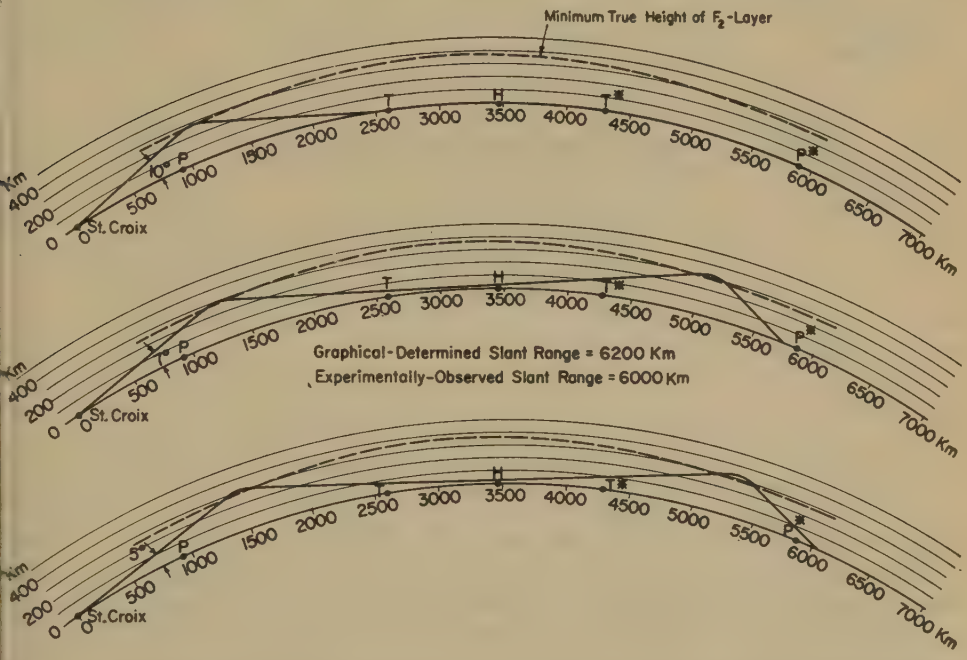

FIG. 11—Graphically-determined ray paths for 23.1 Mc/s, south from St. Croix, based on ionospheric observations at 1900 hour local time, at Panama, Talara, and Huancayo (Sept. 2, 1956)

ise to normal one-hop ground-scatter. Energy taking off at 7°, however, passes verhead at the equator and is not returned to earth until it reaches a point 5,750 m distant from the transmitter. A ray taking off at 5° travels over a similar but omewhat longer path. This mode of propagation is called ^2F.

Figure 12 presents the situation when the operating frequency is increased to 0.7 Mc. At this frequency, a ray taking off at 9° penetrates the ionosphere completely. The 7°-ray, however, executes two successive reflections and returns to he earth at a point 6,750 km from the transmitter. It should be noted that energy aking off at the lower angle of 5° also penetrates the ionosphere and is not returned.

An additional piece of evidence which may be adduced in support of the mode f propagation illustrated in Figures 11 and 12 is a noticeable tendency for a gap o appear in the outer edge of the one-hop F-layer ground-scatter in the south irection at the 23-Mc frequency. This effect is visible, to some extent, in Figures and 3. In any given direction, the portion of the one-hop F-layer-propagated round-scatter echo at minimum slant range corresponds to energy taking off rom the transmitter at a relatively high vertical angle. The portions of the echo t greater slant range correspond to energy taking off at lower vertical angles.

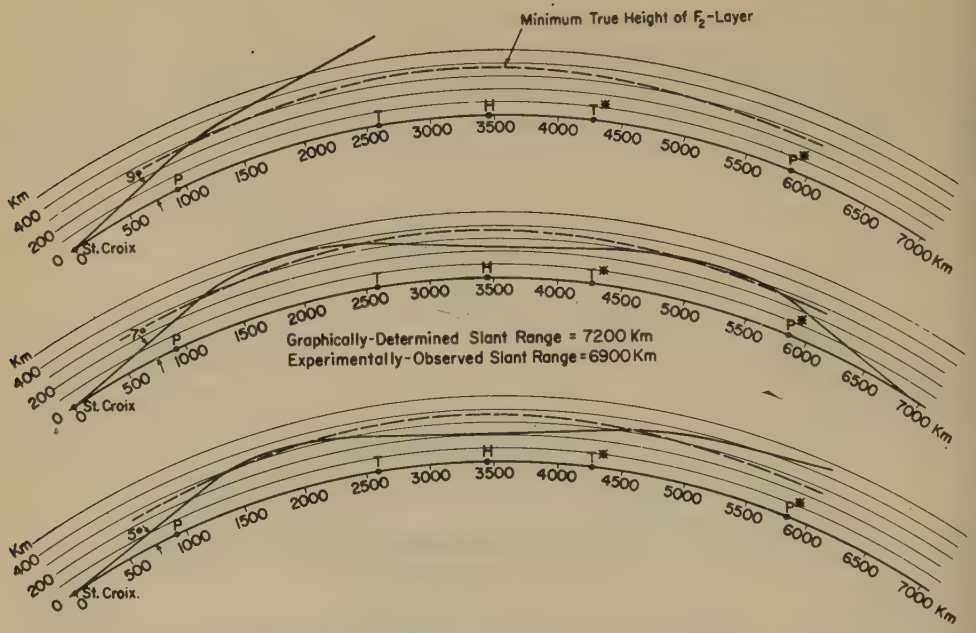

FIG. 12—Graphically-determined ray paths for 40.7 Mc/s, south from St. Croix, based on ionospheric observations of 1900 hour local time, at Panama, Talara, and Huancayo (Sept. 2, 1956)

In Figures 2 and 3, when the long-range echo to the south is seen simultaneously with the one-hop F-layer echo (which is always the case at 23 Mc), the longer-range portion of the normal one-hop echo tends to be missing, suggesting that energy taking off at the lower vertical angles in the south direction is somehow not being bent down to the ground in the usual way. Since it is unlikely that such rays will fail to be reflected somewhere, the most logical explanation for the missing portion of the echo is that the corresponding energy is not immediately bent downward, but travels on farther south, owing to the effect of a tilt at the point where reflection from the ionosphere would otherwise occur (see Fig. 12).

Ionospheric tilts capable of influencing the interpretation of backscatter records occur with some regularity even at temperate latitudes. Their effect on the interpretation of long -range echoes from auroral ionization observed at Stanford University has already been pointed out [10]. Study of the ionosphere at temperate latitudes for ^nF modes is being continued [8].

It will be noted in the range histograms of Figures 7 and 8 that the echoes occurring around midday and in the early afternoon hours have ranges well in excess of 8,000 km. Thus, it appears that they must originate by a ^3F mode, since the maximum distance for ^2F propagation cannot greatly exceed 8,000 km.

The "equivalent tilt" which launches ^3F propagation during the noontime hours may be due to a horizontal gradient of ionization resulting from the great increase in thickness of the F-region over the equator in the hours around noon. This increase in thickness is probably not accompanied by an appreciable change in the height of the lower edge of the layer.

The conventional "F-4,000 MUF" is based upon a symmetrical layer and has to do with the ray which is nearly tangent to the earth. If there is a horizontal

gradient in the ionosphere in the region where reflection takes place, part of the ray system may miss the earth (this may be seen in Figs. 11 and 12). It is evident that propagation utilizing the rays which miss the earth may be carried out at frequencies higher than the maximum for a conventional 4,000-km path.

The extent to which the evening-type transequatorial propagation observed in the present series of tests actually exceeded the MUF as calculated in the usual way is shown in Figure 13. The comparison is made for 1900 Atlantic Standard

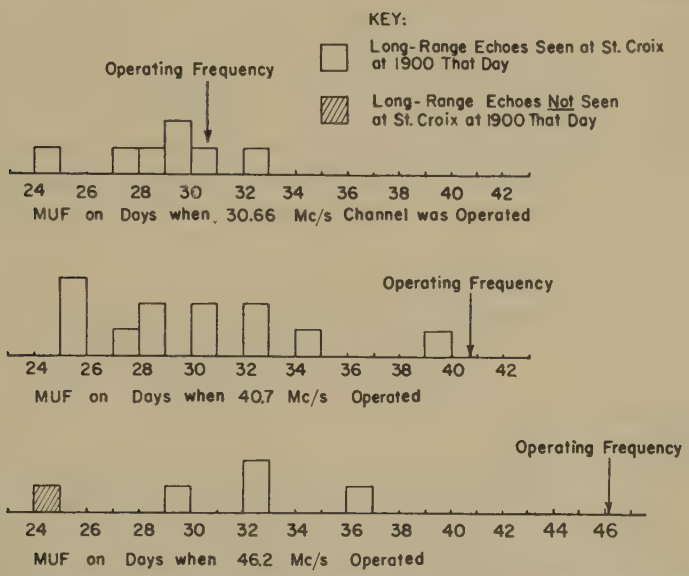

FIG. 13—1900-hour 3,000 MUF at a point 1,500 km south of St. Croix (extrapolation based on Panama and Talara ionograms)

time each day. Since the long-range echoes corresponded to propagation over a ground distance somewhat in excess of 6,000 km, on the average, the normal MUF calculated for a path of this length would assume propagation by means of two hops, each 3,000 km in length. The 3,000-km MUF at the first reflection point, 1,500 km south of St. Croix, was found by interpolating the Panama and Talara ionospheric data. Symmetry of the ionosphere north and south of the equator was assumed, so that if the northern end of the path propagates it follows that the southern end would also.

If long-range echoes were seen at St. Croix at 1900 on a particular day, an empty square was entered on the histogram for the appropriate operating frequency, at a position on the frequency scale corresponding to the calculated MUF at that time. If long-range echoes were *not* seen, a cross-hatched square was entered at a point corresponding to the calculated two-hop MUF. Note that there was only one instance in the latter category. Certain days for which scatter-sounding data were available had to be omitted owing to the absence of ionospheric data.

It can be seen that the calculated two-hop MUF tends to fall consistently below the operating frequency at which the long-range transmission was actually observed. The effect is most noticeable, of course, on the days when 46.2 Mc was

operated, although the data are meager. Averaging the 41- and 46-Mc results suggests that the tilt-supported propagation took place at frequencies at least 1.3 to 1.4 times the two-hop MUF predicted in the usual way.

Conclusions

It is concluded that echoes of exceptionally long delay, detected by a scatter-sounder located in the West Indies, are ground backscatter propagated by two or more successive reflections from the ionospheric *F*-region without intermediate reflection from the ground. These reflections are called ^{n}F modes. An ionosphere having an equivalent tilt is required in order to launch such successive reflections. In equatorial regions, equivalent tilts occur with regularity. One of these is the daily rise in $h'F2$, occurring around 1900 hours local time. A second is a consequence of the midday thickening of the *F*-layer, in the general vicinity of the subsolar point.

Evidence is presented indicating that this tilt-supported propagation takes place at frequencies of the order of 1.4 times the MUF for the same path calculated in the conventional manner from the records of vertical-sounding stations.

It is believed that equatorial tilts may account for reports by amateurs of anomalous long-range propagation between North and South America at frequencies considerably in excess of the MUF. Study of ^{n}F modes at temperate latitudes is under way.

Acknowledgment

The assistance of Richard S. Rich in the experimental work is gratefully acknowledged. Thanks are also due to the Boulder Laboratories of the National Bureau of Standards for ionograms, to Prof. L. Q. Orsini of São Paulo, Brazil, for ionospheric data, and to Mr. and Mrs. Douglas S. Armstrong and Mr. William C. Thomas of St. Croix.

References

[1] Q. P. Ferrell, Very-high-frequency propagation in the equatorial region, paper presented at the April 1951 URSI meeting, Washington, D. C., and abstracted in Proc. Inst. Radio Eng., **39**, 719 (1951).

[2] O. P. Ferrell, Enhanced trans-equatorial propagation following geomagnetic storms, Nature, **167**, 811 (1951).

[3] A. F. Wilkins and C. M. Minnis, Comparison of ionospheric radio transmission forecasts with practical results, Proc. Inst. Elec. Eng., **98**, Pt. 3, 209 (1951).

[4] Discussion on above paper, Proc. Inst. Elec. Eng., **99**, Pt. 3, 148 (1952).

[5] E. V. Appleton and W. J. G. Beynon, Radiocommunication on frequencies exceeding predicted values, Proc. Inst. Elec. Eng., **100**, Pt. 3, 192 (1953).

[6] G. McK. Allcock, The prediction of maximum usable frequencies for radiocommunication over a transequatorial path, Proc. Inst. Elec. Eng., **103**, Pt. B, 547 (1956).

[7] E. D. R. Shearman, The technique of ionospheric investigation using ground back-scatter, Proc. Inst. Elec. Eng., **103**, Pt. B, 210 (1956).

[8] S. Stein, Effects of ionospheric layer tilts on high frequency radio propagation, paper presented at the May 1957 URSI meeting, Washington, D. C.

[9] L. A. Manning, A survey of the literature of the ionosphere, Final Report, Contract AF 19(604)-686, Radio Propagation Laboratory, Stanford University (July 31, 1955).

[10] S. Stein and O. G. Villard, Jr., On the interpretation of long-range radio echoes from auroral ionization, paper presented at the Berkeley, California, meeting of URSI, July 31, 1955.

ATMOSPHERIC DRAG ON THE SATELLITE

BY R. JASTROW AND C. A. PEARSE
U. S. Naval Research Laboratory, Washington 25, D. C.

(Received June 11, 1957)

ABSTRACT

The drag exerted on the satellite in its orbit arises partly from collisions with neutral air particles and partly from losses associated with the passage of a charged sphere through an ionized medium. It is found that the charged and neutral effects are comparable under the atmospheric conditions expected at an orbital altitude of 300 miles.

I. INTRODUCTION

Observations on the deceleration of the satellite can provide a sensitive measure of atmospheric density at the expected orbital altitudes of 500 km [see 1 of "references" at end of paper]. A discussion of the theory of the atmospheric drag on the satellite will be presented below. It will be seen that in addition to the drag exerted by neutral air molecules and atoms, collisions with charged particles must also be considered. The charged drag is, in fact, found to be comparable with the neutral drag under the most probable conditions of atmospheric density, temperature, and ionization [2].

II. NEUTRAL DRAG

At an altitude of 500 km, the air density is estimated [3] to be 10^7 particles/cm^3. The corresponding mean free path of air particles is large in comparison with the satellite diameter of 50 cm. Under this condition, the rate of momentum transfer to the satellite by impinging air particles has been shown by Epstein [4] to be

$$F = -\frac{4\pi}{3} R^2 nm\bar{v}V \qquad (1)$$

when the satellite velocity is smaller than the mean thermal velocity of the air particles. (R = satellite radius, n = particle density, m = particle mass, $\bar{v}$ = mean thermal velocity, V = satellite velocity.) In the present problem, V is larger than $\bar{v}$, a case for which we find

$$F = -\pi R^2 nmV^2\left[1 + \frac{\pi}{4}\frac{\bar{v}^2}{V^2} + 0\left(\frac{\bar{v}}{V}\right)^4\right] \qquad (2)$$

For a probable air temperature of 1000° or 0.1 ev, we have $\bar{v} = 10^5$ cm/sec, while $V = 8 \times 10^5$ cm/sec. Thus, the corrections to the leading term in (2) contribute 1 per cent.

To (2) must be added the reaction of the recoiling particles. We note that air particles have a kinetic energy of 6 ev relative to a satellite moving at 10^6 cm/sec. Measurements by Wehner [5], on the recoil momentum distributions of somewhat more energetic particles, suggest that at energies $\sim$10 ev, and on dirty surfaces, the coefficient of reflection is close to unity, and incident and reflected velocities are comparable. We assume, therefore, that the reflection is approximately elastic. Since the angular distribution of reflected particles is uncertain, we consider the extremes of *specular elastic* and *diffuse elastic* reflection. On these assumptions, we have for the total momentum transfer rate due to neutral particles, that is, the neutral drag,

$$f_n = -\pi R^2 n m V^2 \quad \text{(specular elastic)} \ldots\ldots\ldots\ldots\ldots\ldots (3a)$$

$$f_n = -\frac{4\pi}{3} R^2 n m V^2 \quad \text{(diffuse elastic)} \ldots\ldots\ldots\ldots\ldots\ldots (3b)$$

III. CHARGED DRAG

1. *Mechanism for charging the satellite*

The satellite moves through a partly ionized medium composed of O and N atoms, O^+ and N^+ ions, and electrons [6]. For comparable ion and electron temperatures, the thermal velocities of the electrons will be $\sim$60 times greater than the ion velocities, and the incident flux of electrons on the satellite surface correspondingly larger than the ion flux, tending to charge the satellite to a negative potential on the night side of the earth. On the day side, this effect will be opposed by photoejection of electrons. The photoefficiency of the satellite surface has not been measured, but a calculation based on a plausible assumption for its value indicates that the two charging rates are comparable. Therefore, the sign of the satellite potential is uncertain in the daytime. However, we will continue our discussion on the assumption that the satellite is also negative on the day side.

2. *Estimate of the satellite potential*

To determine the satellite potential φ_0, we note that φ_0 must rise to a value such that the flux of electrons with energies above $e\varphi_0$ is equal to the flux of positive ions across the satellite surface. Since the electron velocities are larger than the thermal velocities of the ions by several orders of magnitude, we may anticipate that a small number of energetic electrons in the tail of the velocity distribution will be sufficient to balance the ion flux; hence the satellite potential will be substantially greater than the average electron energy.

For the present, we assume a Maxwellian distribution of electron energies at a temperature T_e, although the actual distribution may depart appreciably from Maxwellian. We then have for the flux of electrons with energies above $e\varphi_0$,

$$\pi R^2 n_e \sqrt{\frac{\pi kT}{2m}} \int_{e\varphi_0}^{\infty} \sqrt{\frac{E}{kT_e}} \frac{dE}{kT_e} e^{-E/kT_e} \ldots\ldots\ldots\ldots\ldots\ldots (4)$$

and for the flux of positive ions,*

$$\pi R^2 n_i V \ldots\ldots\ldots\ldots\ldots\ldots\ldots\ldots\ldots\ldots (5)$$

*Note that $v_e \gg V \gg v_i$.

where n_e , T_e , and v_e are the electron density, temperature, and mean thermal velocity, n_i is the ion density, and V is the satellite velocity. We take $kT_e = 1.5$ ev, $n_i = n_e$, and $V = 8 \times 10^5$ cm/sec. Equating (4) to (5) and inserting these values, we obtain

$$\frac{e\varphi_0}{kT_e} \approx 7$$

and $\varphi_0 = 10$ volts.

The source of ionospheric electrons is believed to be radiation from the solar corona at a black-body temperature of 70 ev [7]. Therefore, on the day side, the distribution of electron velocities will include a high-energy tail extending to ~60 ev. The fraction of the electron population at such high energies is of course small, the energy of a fast electron being quickly degraded by ionization and electronic excitation until it reaches the threshold for the latter at 2 volts. In order to estimate the population at high energies, we observe that the ionization cross-section [8] is 10^{-16} cm^2, and the time required for energy degradation of a 60-volt electron is therefore ~10 seconds, *versus* 10^4 seconds required for radiative electron capture. Thus, 10^{-3} of the electrons have energies of the order of 60 volts. At these electron energies, the ratio of electron to ion velocities is 10^3; hence the flux of 60-volt electrons into the satellite is comparable to the flux of ions. Thus, the satellite potential may be as high as 60 volts on the day side. The population of very energetic electrons disappears in 10 seconds when the sun departs; hence the potential cannot be greater than 10 volts on the night side of the orbit.

In the following discussion, we assume a range of satellite potentials between 10 and 60 volts.

3. *Shielding of the satellite*

The negatively charged satellite will polarize the atmosphere in its neighborhood. The distribution of charge, with density ρ, and of potential φ is given by Poisson's equation, $\nabla^2\varphi = -4\pi\rho$, in which

$$\rho = e[n_i e^{-e\varphi/kT} - n_e e^{e\varphi/kT}] \quad \ldots\ldots (6)$$

In the present case, we note that $v_i \ll V$, hence the ion distribution cannot adjust itself to the oncoming satellite in accordance with (6). Thus, (6) must be replaced by

$$\rho = e[n_i - n_e e^{e\varphi/kT}] \quad \ldots\ldots (7)$$

Setting $n_i = n_e$, we obtain for Poisson's equation,

$$\nabla^2\varphi = -4\pi n_e[1 - e^{e\varphi/kT_e}] \quad \ldots\ldots (8)$$

Introducing the dimensionless variables $u = (r/\lambda_D)(e\varphi/kT_e)$ and $x = r/\lambda_D$, where $\lambda_D = \sqrt{kT_e/4\pi ne^2}$, (8) becomes

$$d^2u/dx^2 = x[e^{u/x} - 1] \quad \ldots\ldots (9)$$

If $u/x \ll 1$ everywhere, the solution to (9) is $u = u_0 e^{-x}$, that is, a screened potential with shielding length given by λ_D , the Debye length. For the typical values of $kT_e = 1.5$ ev, $n_e = 2 \times 10^5/\text{cm}^3$, we find $\lambda_D = 2$ cm.

In the present problem, $e\varphi/kT = 7$ at the satellite surface, and the linear Debye approximation is inapplicable. However, a simple qualitative argument will give the shielding distance. We observe that, while the ion distribution maintains its normal value in the neighborhood of the sphere, the electron density must drop to zero within a distance l from the satellite such that the positive charge in the shell between R and $R + l$ cancels the negative charge Q on the sphere (Fig. 1.):

$$\frac{4\pi}{3} ne[(R + l)^3 - R^3] = -Q \quad \text{.....(10a)}$$

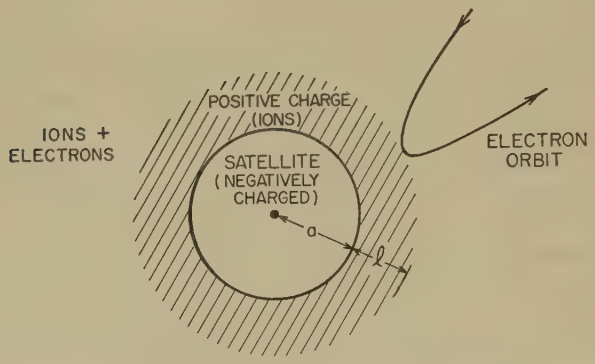

FIG. 1—Qualitative estimate of the sheath thickness, l. The charge in the shaded area cancels the charge on the sphere.

Q is related to the potential φ by $E = 4\pi\sigma$, or

$$-\partial\varphi/\partial r\,|_R = Q/R^2 \quad \text{.....(10b)}$$

and φ is obtained from the spherically symmetric solution to Poisson's equation,

$$\varphi = -\frac{2\pi}{3} ner^2 + \frac{a}{r} + b \quad \text{.....(10c)}$$

The constants a and b are determined by the conditions,

$$\varphi(R) = \varphi_0 \quad \text{.....(10d)}$$

$$\varphi(R + l) = 0 \quad \text{.....(10e)}$$

We solve for l in (10a) to (10e), and find, if $l \ll R$,

$$l = \sqrt{2\frac{e\varphi_0}{kT_e}}\,\lambda_D \quad \text{.....(11)}$$

where λ_D is the Debye length. In the present case, $\varphi_0 = 30$ volts, $kT_e = 1.5$ ev, and $\lambda_D = 2$ cm; hence $l = 12.6$ cm. With this estimate, the effective cross-section of the satellite for ion encounters is, therefore, $(25 + 12.6)^2/(25)^2 = 2.25$ times its value for collisions with neutral atoms.

Numerical integrations of (9) on the Naval Research Laboratory computer yield a shielding distance close to the result of our qualitative argument. Figure 2

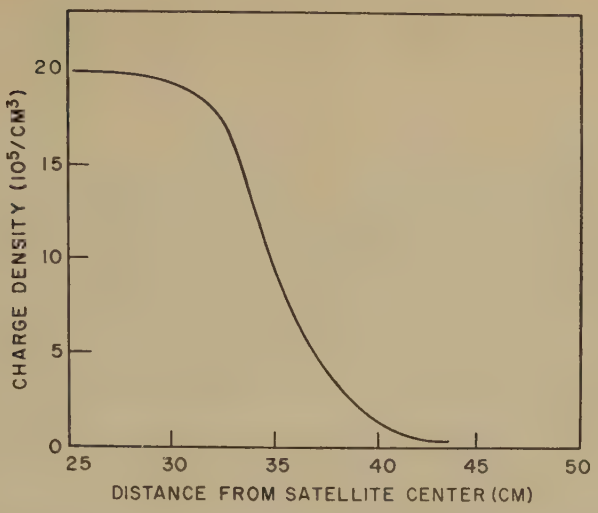

FIG. 2—Density of total charge around the satellite. The curve represents $(n_i - n_e)/n_i$, where n_i and n_e are the ion and electron densities, respectively, obtained by integration of equation (9). ($\varphi_0 = -30$ volts; $kT_e = 1.5$ ev.)

shows the charge distribution obtained from a typical integration of (9) for $n_e = 2 \times 10^5/\text{cm}^3$, $kT_e = 1.5$ ev, and $\varphi_0 = -30$ volts.

4. Calculation of the charged drag

The rate of momentum transfer from the ions to the satellite is calculated in three steps:†

(*a*) We first determine the momentum taken out of the incident beam by those ions which impinge on the satellite surface. If b_m is the largest impact parameter for which contact of the ion with the surface is possible, the number of ions per second striking the sphere is $(\pi b_m^2)n_i V$. Since each ion has originally the momentum $m_i V$, the rate of momentum transfer is

$$\pi m_i n_i V^2 b_m^2 \quad \ldots\ldots (12)$$

From the potential distributions obtained by integration of (9), we learn that

$$b_m \approx R + \alpha\lambda_D \quad \ldots\ldots (13)$$

in which R = satellite radius, λ_D = Debye length, and α depends primarily on the satellite potential. We find that α varies from 6 to 10 for satellite potentials between 10 and 60 volts.

(*b*) If the impinging particle leaves the surface, it imparts an additional momentum to the satellite. Experimental studies indicate that almost all of the incident ions are reflected [5], but as neutral atoms and not as ions [9], the overwhelmingly probable process being neutralization of the ion shortly before impact, by extraction of an electron from the satellite surface. Thus, the ion of incident energy E_i is accelerated by the satellite field to a kinetic energy $E_i + e\,|\,\varphi_0\,|$ on approaching the

†The following discussion refers to a coordinate system moving with the satellite.

sphere, and after impact departs as a neutral atom with the full energy $E_i + e \mid \varphi_0 \mid$. The contribution of the recoiling particles to the momentum transfer rate is then

$$n_i m_i v_f V \int_0^{b_m} 2\pi b \cos \theta(b)\, db \qquad (14)$$

in which $v_f = \sqrt{2(E_i + e \mid \varphi_0 \mid)/m_i}$, and $\theta(b)$ is the angle between the incident beam and the reflected particle. $\theta(b)$ must be determined by numerical integration of the equations of motion of the ion in the satellite potential given by the solutions to (9). A typical set of ion trajectories is shown in Figure 6.*

(*c*) When $b > b_m$, the ion is deflected by the potential without striking the surface. Calculation of the ion trajectories for this case indicates that the corresponding contribution to the momentum transfer is less than one per cent of that from (*a*) or (*b*).

Finally, we may expect the electron contribution to the charged drag to be negligible. The analysis of Epstein for the case of large thermal velocities indicates the electron drag to be approximately

$$\pi R^2 n_e m_e \bar{v}_e V$$

larger than the ionic drag by a factor of $\bar{v}_e/V = 500$ but smaller by $m_e/m_i = 1/32{,}000$. Thus, the electronic contribution is 500/32,000 or about one per cent of the ionic contribution.

5. *Contribution of antennas to the charged drag*

We represent the satellite antennas by four cylinders, 75 cm in length and 4 mm in mean radius, located 90° apart on the satellite surface. As in our preliminary discussion of the spherical problem, we assume that all electrons are excluded from a region of thickness l around the cylinder. Appendix *A* contains the details of the procedure for solving Poisson's equation in this approximation. We find the following result for the thickness of the sheath around each antenna:

$$l \approx 4\lambda_D$$

For $n_e = 6 \times 10^5$ and $kT_e = 1.5$ ev, we have $\lambda_D = 1.2$ cm; hence $l = 4.8$ cm. Thus, the cross-section presented to ions by the antennas will make an appreciable contribution to the charged drag (Fig. 5).

IV. COMPARISON OF CHARGED AND NEUTRAL DRAG

The results of the calculations described in the preceding section are given in Figures 3 and 4, which show f_c/f_n, where f_c is the charged drag, that is, the rate of momentum transfer to the satellite by charged particles, and f_n is the neutral drag, calculated from (3*a*). The total drag on the sphere is $f_c + f_n$.

Figures 3 and 4 do not include the contribution of the antennas to f_c. The antenna contribution is shown in Figure 5 for a representative choice of parameters.

The charged drag is seen to vary from 10 per cent to 150 per cent of the neutral

*Figure 6 suggests that the ion density is negligible for several sphere diameters behind the satellite. The resulting perturbation of the spherically symmetric potentials is found by an approximate calculation to have little effect on those trajectories for which $b < b_m$.

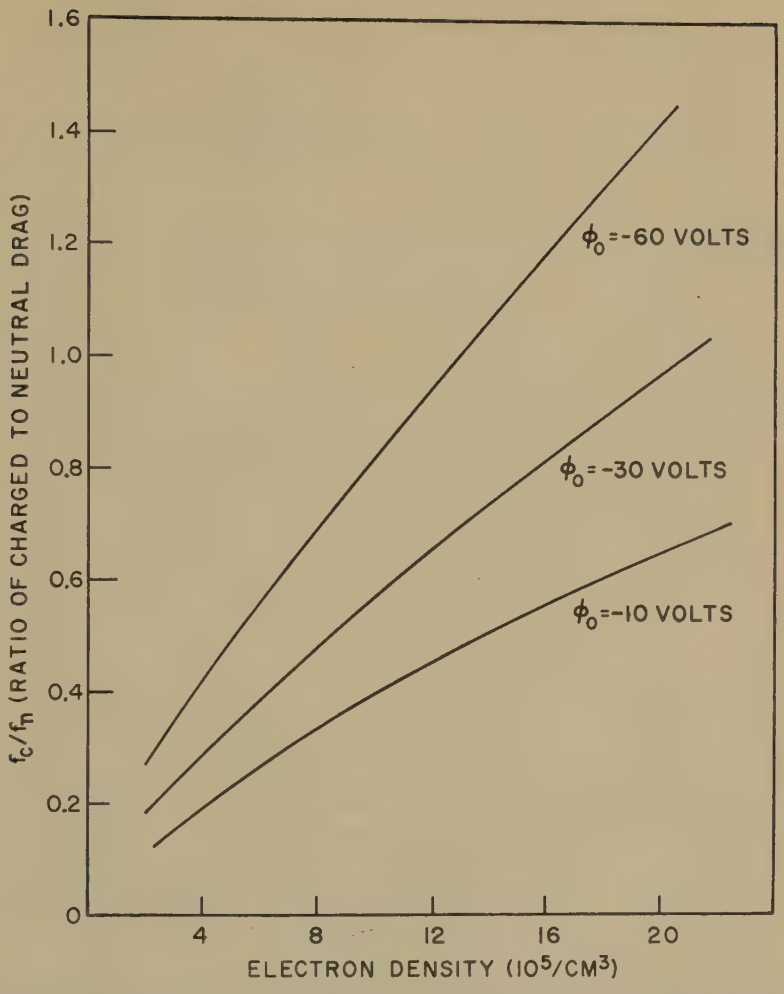

FIG. 3—Dependence of charged drag on satellite potential and electron density (kT_e = 1.5 ev). The ordinate is the ratio of charged drag (f_c) to neutral drag (f_n). Note that the ratio of total drag to neutral drag is 1 + (f_c/f_n).

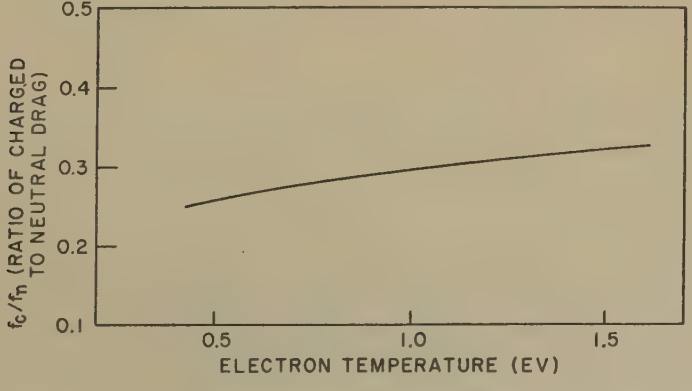

FIG. 4—Dependence of charged drag on electron temperature. ($\varphi_0 = -30$ volts; $n_e = 6 \times 10^5$/cm^3.)

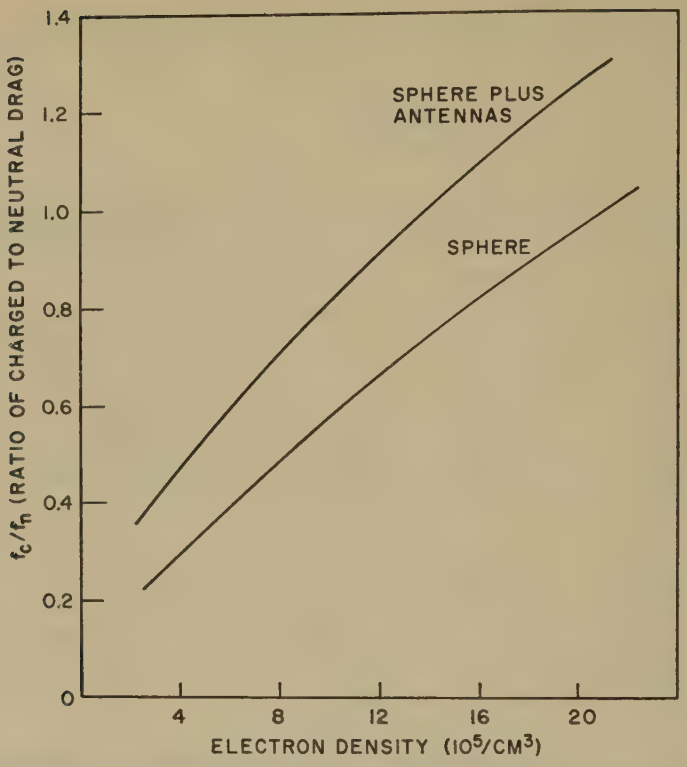

FIG. 5—Contribution of the antennas to the charged drag. ($\varphi_0 = -30$ volts; $T_e = 1.5$ ev.)

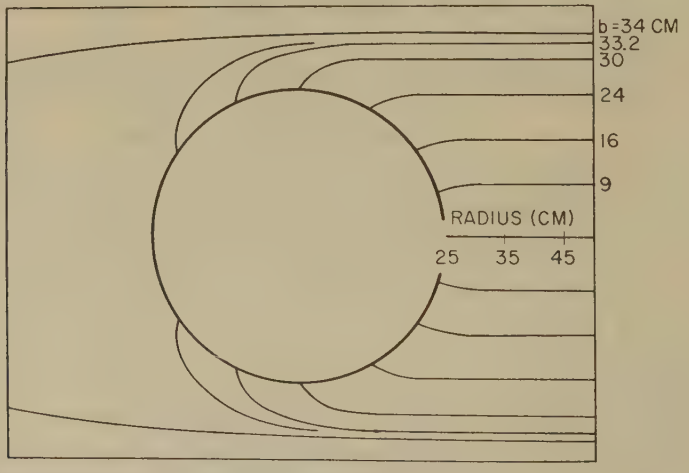

FIG. 6—Ion trajectories in the field of the charged satellite. ($\varphi_0 = -30$ volts; $n_e = 2 \times 10^5$/cm^3.)

drag for the assumed range of electron densities. If the atmospheric density is 2×10^7/cm^3 or less, the contribution of f_c substantially reduces the density values deduced from the observed drag force. Figure 7 indicates the magnitude of the reduction, assuming $\varphi_0 = -30$ volts and a range of electron densities extending to 2×10^6/cm^3.

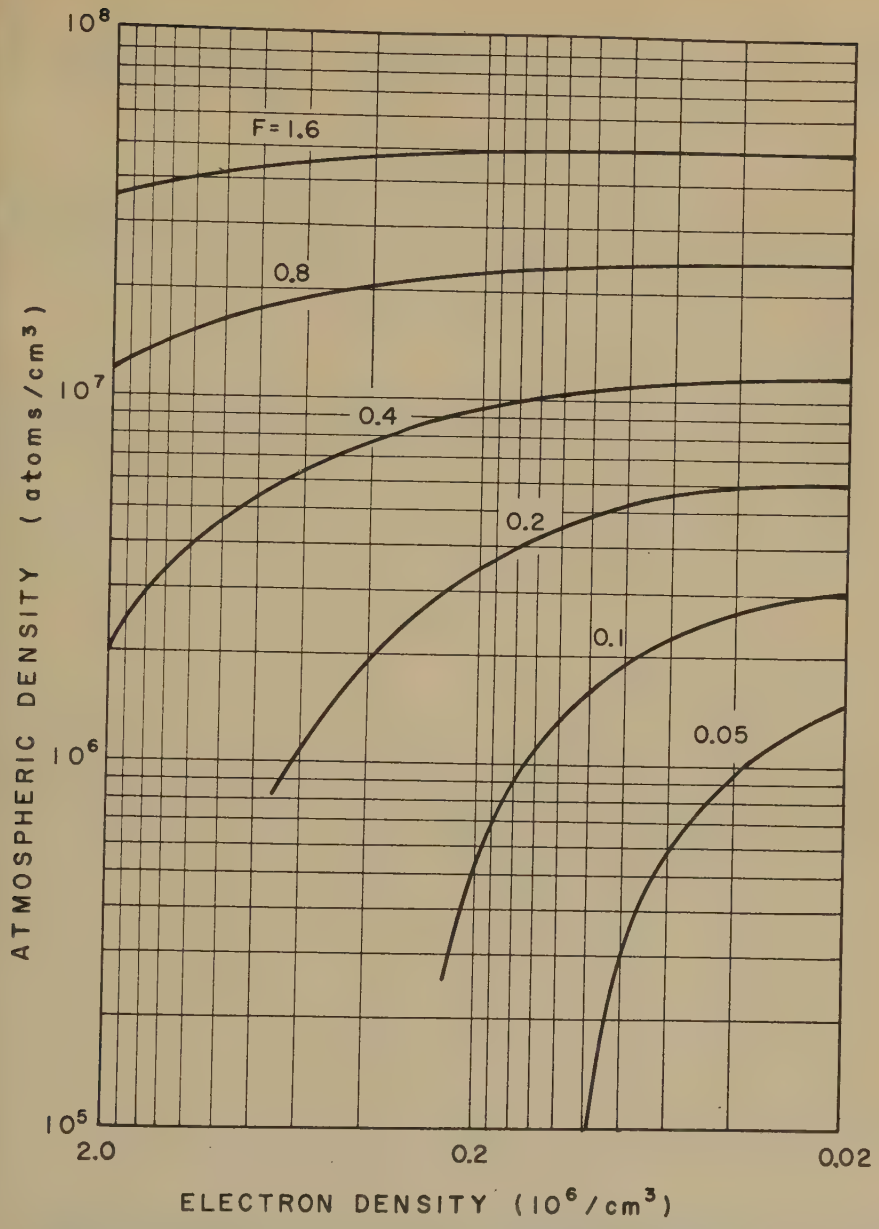

FIG. 7—Atmospheric density *vs* drag force and electron density. Satellite velocity = 8×10^5 m/sec; $\varphi_0 = -30$ volts. $F = f_e + f_n$ (dynes), with f_n taken from (3*a*) and f_e from Figure 5.

V. ACKNOWLEDGMENTS

We are indebted to Dr. I. Harris for his assistance in all phases of these calcu-ations, to Dr. R. H. Kraichnan for his very helpful criticism, and to Drs. J. W. iry, J. F. Clark, H. Friedman, and Mr. J. C. Seddon for several informative iscussions on the properties of the upper atmosphere. We also wish to thank Ir. H. V. O'Neill and Mrs. L. F. Shapiro for the preparation of the integration

routines on the Naval Research Laboratory digital computer (NAREC), and Dr. B. Lepson and the members of the NAREC staff for their cooperation in executing these computations.

References

[1] J. A. Van Allen (Editor), Scientific Uses of Earth Satellites, University of Michigan Press. Ann Arbor (1956); Chap. 10 (L. M. Jones and F. L. Bartman) and Chap. 11 (L. M. Spitzer).
[2] H. E. Newell, Ann. Géophys., **11**, 115 (1955); E. O. Hulburt, Naval Research Laboratory, Washington, D. C., NRL Rep. 4600 (Oct. 25, 1955).
[3] Reference [1], Chap. 10, p. 88.
[4] P. S. Epstein, Phys. Rev., **23**, 710 (1924).
[5] G. Wehner, private communication.
[6] R. J. Havens, H. Friedman, and E. O. Hulburt, Report of the Physical Society Conference on The Physics of the Ionosphere, held at Cavendish Laboratory, Cambridge, September 1954, Physical Society (1955); p. 237.
[7] E. T. Byram, T. A. Chubb, and H. Friedman, J. Geophys. Res., **61**, 251 (1956).
[8] H. S. W. Massey and E. H. S. Burhop, Electronic and Ionic Impact Phenomena, Oxford, Clarendon Press (1952); p. 3.
[9] H. D. Hagstrum, Phys. Rev., **96**, 325 (1954).

APPENDIX A

Potential distribution around the antennas

As in our preliminary discussion of the sheath around the sphere, we assume a uniform distribution of electrons for $r > R + l$, and zero electron density for $R > r > R + l$. Here R is the antenna radius and l is the sheath thickness, taken such that the amount of positive charge in the annular region between R and $R + l$ cancels the negative charge on the sphere. Thus, we must solve

$$\left.\begin{aligned} \nabla^2\varphi &= -4\pi ne, \qquad R < r < R + l \\ \nabla^2\varphi &= 0, \qquad\quad r \geq R + l \end{aligned}\right\} \quad \ldots\ldots\ldots\ldots\ldots\ldots (1)$$

with the conditions

$$\varphi = 0, \qquad r \geq R + l \quad \ldots\ldots\ldots\ldots\ldots\ldots (2)$$

$$\varphi = \varphi_0 \qquad r = R \quad \ldots\ldots\ldots\ldots\ldots\ldots (3)$$

The desired solution to (1) is

$$\varphi = a + b \log r - \pi ner^2 \quad \ldots\ldots\ldots\ldots\ldots\ldots (4)$$

with a and b determined by substitution of (4) into (2) and (3). For the determination of l, we have the equation stating the cancellation of charge,

$$q = -\pi ne[(R + l)^2 - l^2] \quad \ldots\ldots\ldots\ldots\ldots\ldots (5)$$

in which q is the charge/cm on the antenna. The quantity q is eliminated by the relation, $E = 4\pi\sigma$, where E = electric field intensity and σ = charge/cm^2 on the antenna surface. Since $E = -\partial\varphi/\partial r$ and $\sigma = q/2\pi R$, we have

$$-\frac{\partial\varphi}{\partial r} = -\frac{b}{R} + 2\pi neR = -\frac{2q}{R} \quad \ldots\ldots\ldots\ldots\ldots\ldots (6)$$

From (2) through (6), we eliminate a, b, and q to obtain the following transcendental equation in l:

$$R + l = 2\lambda_D \sqrt{\frac{e \mid \varphi_0 \mid}{kT_e}} \left[\log \left(\frac{R + l}{R} \right)^2 - 1 \right]^{-1/2} \quad \ldots\ldots\ldots\ldots (7)$$

Setting $\varphi_0 = -30$ volts, $kT_e = 1.5$ ev, $n_e = 6 \times 10^5/\text{cm}^3$, $R = 0.3$ cm, as a typical assignment of parameters, we find by graphical solution of (7),

$$l \approx 4\lambda_D = 4.8 \text{ cm}$$

PARAMETERS

Satellite velocity (V): 10^6 cm/sec
Atmospheric density (n): $10^7/\text{cm}^3$
Electron density (n_e): between $2 \times 10^5/\text{cm}^3$ and $2 \times 10^6/\text{cm}^3$
Per cent ionization: between 2 per cent and 20 per cent
Electron temperature (T_e): between 0.5 ev and 2.0 ev
Ion temperature (T_i): 0.1 ev
Potential on the satellite (φ_0): between -10 and -60 volts

A POSSIBLE TROPOSPHERE-IONOSPHERE RELATIONSHIP

BY SIEGFRIED J. BAUER

U. S. Army Signal Engineering Laboratories, Fort Monmouth, New Jersey

(Received April 30, 1957)

ABSTRACT

Minimum virtual height and critical frequency of the ionospheric $F2$-layer are analyzed by means of the superposed epoch method. Results of this analysis, on the basis of their statistical significance, suggest a relationship between frontal passage in the troposphere and $F2$-layer characteristics. The observed effects are interpreted qualitatively in the light of a hypothesis suggested by Martyn, and seem to be consistent with the concept of dynamic coupling between lower and upper atmosphere. The results of this analysis are also found to agree with previously reported troposphere-ionosphere correlations.

INTRODUCTION

Correlations between meteorological variables in the lower atmosphere and ionospheric characteristics such as virtual height and critical frequency have been reported by various investigators within the past two decades. A summary of some weather-ionosphere relationships has been given by Mitra [see 1 of "References" at end of paper]. The majority of the reported correlations, however, have not been verified by independent sources, so there is not as yet sufficient evidence from which to form definite conclusions about the reality of such relationships. For this reason, an independent investigation of this subject seemed well justified.

DATA ANALYSIS

In a pilot study covering a period of three months (July, August, and September, 1955), height data of the ionospheric $F2$-layer, $h'F2$ (approximate sunrise), for Washington, D. C., were analyzed by means of the superposed epoch method. The key day or 0-day was selected as a day when a cold front passed through Washington, D. C. Height data were analyzed for 11 days, consisting of the key day and the five days before and after it. Since there were 14 cases of cold-front passage for the sample under consideration, the mean of 14 values for each of the 11 days was calculated. Figure 1 (solid line) shows the response of $h'F2$ with respect to the passage of a cold front as established by the superposed epoch method. It can be seen that the passage of a cold front seems to be associated with a drop in height, $\Delta h'F2 = -20$ km. In addition, values of the critical frequency of the $F2$-layer, f_0F2, for the same period of time were analyzed by means of the superposed epoch method. The response of f_0F2 with respect to the key day (Fig. 1,

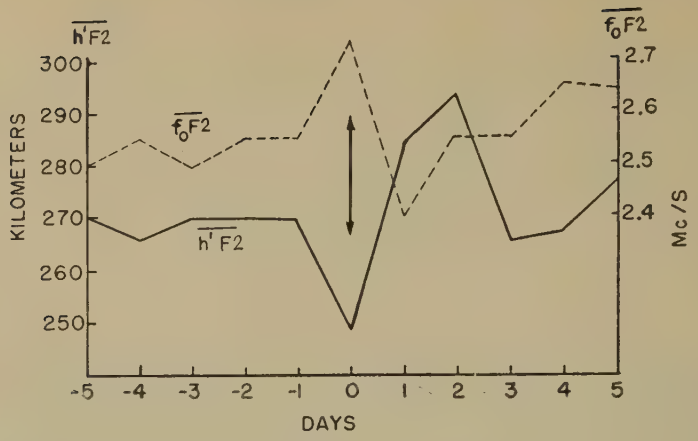

FIG. 1—Superposed epoch analysis of $h'F2$ and f_oF2 for Washington, D. C.; 14 cases of cold-front passage

dashed curve) was found to be opposite to that of $h'F2$; that is, it showed an increase in critical frequency, $\Delta f_oF2 = 0.18$ Mc/s (see Fig. 1, dashed line). This effect is to be expected from the generally inverse relationship between critical frequency and virtual height.

Since the small sample of data had indicated a possible association between ionospheric characteristics and the passage of cold fronts, an investigation covering a greater time interval was undertaken to determine whether results obtained from a larger sample would be consistent with the original results. The result of the superposed epoch analysis for this larger sample (nine months with 44 cold-front passages) is presented in Figure 2. A comparison between the pilot study and the larger sampling shows agreement with regard to the drop in height on 0-day and

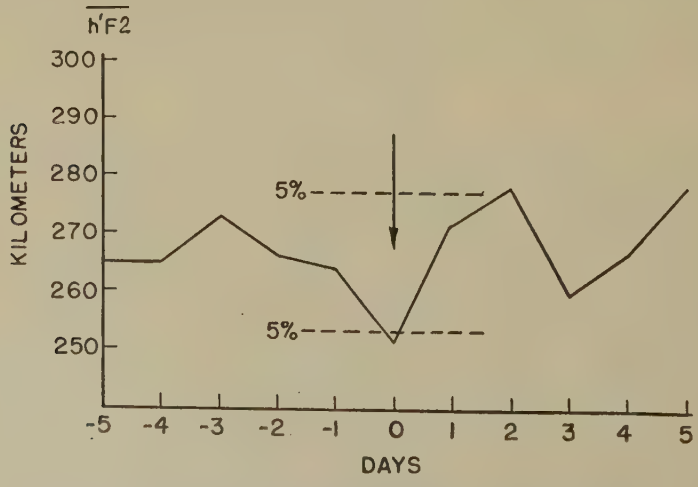

FIG. 2—Superposed epoch analysis of $h'F2$ for Washington, D. C.; 44 cases of cold-front passage. The 5 per cent significance level is indicated by dashed lines.

the maximum height on +2-day. (A superposed epoch analysis of noon values of $h'F2$ and f_0F2 for the larger sample also shows essentially the same features as found in the pilot study.) The larger sample, which covers the months July, August, September, and December of 1955, and January to May of 1956, is not a strictly independent sample because it includes the earlier data. However, since a superposed epoch analysis of the six-month sub-sample, excluding July, August, and September of 1955, also shows good agreement with the earlier survey, it is apparent that the consistent results obtained for the nine-month sample are not solely the effect of bias by the original data.

In order to determine whether the minimum on the key day is caused by a true or a chance relationship between the passage of cold fronts in the troposphere and the minimum virtual height of the ionospheric $F2$-layer, this effect was tested for its statistical significance. The use of Student's t-test (after its applicability had been established by a preceding F-test) showed that the drop in $h'F2$ on the key day exceeds the 5 per cent level of significance for the given degrees of freedom; that is, the probability of a chance occurrence of an effect as observed (difference of mean values) is less than 0.05. (The 5 per cent level of significance is indicated in Figure 2 by dashed lines.) On the basis of this result, it is concluded that the observed height drop on the key day is "probably significant" and might therefore be the result of a real relationship between lower and upper atmosphere.*

Assuming the reality of such a relationship, one could try to explain the general features of the curve obtained by the superposed epoch method (Fig. 2). The curve shows two minima—one on the key day and a smaller one on +3-day; and two maxima—one on +2-day and another one on +5-day. Since the minimum on the key day has been shown to be associated with the passage of cold fronts or polar air, it seems reasonable to assume that the second minimum might have been caused by the same effect. The inspection of meteorological data showed that there was a tendency toward a three-day period in occurrence of cold fronts; that is, in some cases, a second cold front followed the first one three days later. On the other hand, the two maxima seemed to correspond to the existence of a tropical air mass, since generally about two days after the cold-front passage a tropical or modified polar-air mass was prevalent. These results, although of a somewhat speculative nature, seem to verify results of Gherzi [2], who obtained echoes from the lower part of the F-region when polar air was present and from the upper part of the F-region when tropical air was prevalent. He claimed that by this technique he was able to determine the type of air mass which was to be responsible for the weather in an area of about 400 km around his station in China. Up to now, Gherzi's technique has not been verified at other places.

Since the result of this study (representing mean conditions) seemed to correspond with Gherzi's findings, the possible correlation between minimum virtual height of the $F2$-layer and the air-mass type was briefly investigated. The departures of $h'F2$ from their monthly mean, $D(h'F2) = h'F2 - \overline{h'F2}$, were calculated

*It should be noted that the great majority of key days and their close neighbors corresponded to "magnetically quiet days." For the sake of completeness, the few key days corresponding to "magnetically disturbed days" were included in the superposed epoch analysis, although inspection of these cases showed that they tended to reduce the observed drop in $h'F2$ on the key day.

and two samples—one representing three summer months, the other four months of winter and spring—were investigated separately. The frequencies of occurrence of the departure values $D(h'F2)$ were determined for both continental polar (cP) and maritime tropical (mT) air masses. For the summer sample, the $D(h'F2)$ values showed an approximately normal distribution for cP as well as mT air masses. The mean value of the distribution representing cP air mass was slightly on the negative side of the $D(h'F2)$ scale, while the mean value of the distribution representing mT air mass was slightly positive. The difference between the two mean values, however, did not seem to be significant. For the sample representing winter and a transitional season (spring), the means of the distributions of $D(h'F2)$ for cP and mT air masses showed a significant separation. The distribution representing cP air mass had a mean value of $D(h'F2)_{cP} = -10$ km, while the mT distribution had a mean $D(h'F2)_{mT} = +70$ km. The standard deviation in both cases was about 15 km. From these results, it seems that in summer, when the differences between air masses in our area are not so pronounced as in winter and spring, the distributions of $D(h'F2)$ behave correspondingly. Although a day-by-day relationship between $h'F2$ and air-mass type as reported by Gherzi (*loc. cit.*) could not be observed, this relationship is apparent for the mean. The relationship between $h'F2$ and frontal passage discussed above, however, seems to produce better results, since it was found that even in individual cases a cold front will be associated with a drop in $h'F2$. These results, however, are based on a not too large sample of data and, therefore, should not be considered conclusive.

HYPOTHETICAL CONCEPTS

Martyn [3] has suggested that dynamic coupling might be a possible mechanism whereby there could be a connection between troposphere and ionosphere. It is a well-known fact that there is no complete stoppage at any barrier if the wavelength is very long compared with the thickness of the barrier. The wavelength of atmospheric circulation at the ground is in the order of 1,000 km, while the barrier between troposphere and ionosphere is only about 100 km in thickness. Thus, most likely, there will be penetration of energy from troposphere to ionosphere. In the two atmospheric models whose mathematical treatment is relatively simple, (1) an atmosphere having an adiabatic gradient with expansions taking place adiabatically, and (2) an isothermal atmosphere with isothermal expansions, the energy flow is concentrated mainly near the ground. These two cases, however, are not of such great importance, since they actually do not exist in the atmosphere, which has a temperature gradient varying with height and where expansions take place adiabatically. Such a temperature structure brings in rotational components which create, in effect, a cavity resonator. This serves as a wave-duct in which the circulation takes place between two boundary surfaces: the earth and some level in the upper atmosphere. In such a duct, there is a tendency for the energy flow to be constant with height. Consider a simple illustration for a compressional wave: The energy flow at any level in a duct is proportional to ρv^2, where ρ is the density at that height and v the velocity of movement in the wave. In the atmosphere, ρ falls off exponentially with height, so that the amplitude of motion must increase exponentially in order to maintain a constant energy flow at any level.

If there is any coupling between troposphere and ionosphere, an amplification in the ionosphere in the order of 10^3 to 10^4 could be expected for a wave traveling horizontally in the troposphere. This amplification-factor is verified by atmospheric tidal effects which are magnified to that extent in the ionosphere [4]. Therefore, it should be expected that, even with damping or partial blockage in the stratosphere, large-scale movements in the troposphere would appear magnified in the ionosphere, especially in the F-region. Complications, however, may arise because of the possibility that more than one cell may be formed within the duct and as the result of the effect of the earth's magnetic field on the motion in the ionosphere.

DISCUSSION OF RESULTS AND SPECULATION

For an additional comparison of meteorological and ionospheric variables, the mean pressure difference $\overline{\Delta p}$ between -1-day and 0-day was calculated for the nine-month sample analyzed by the superposed epoch method. It was found that, on the average, the surface pressure on the key day decreases about 10.5 mb with respect to the preceding day. On the other hand, it was established that $h'F2$ shows a drop of about 12 km on the key day.* Since a change in surface pressure of about 10 mb corresponds to a change in height of about 80 meters, it appears (in the light of the hypothesis on dynamic coupling between lower and upper atmosphere) that such an effect at the ground is magnified by a factor in the order of 10^2 in the ionosphere. Compared with the expected amplification, this result seems reasonable, in view of the fact that damping most certainly will occur and because of other complications which may be expected.

The values of critical frequency f_oF2 for the -1-day and 0-day for the nine-month sample were also analyzed. The mean difference between these two days was found to be about 0.25 Mc/s. Hence, the change in pressure between -1-day and key day, $\overline{\Delta p} = -10.5$ mb, corresponds to an increase in critical frequency, $\overline{\Delta f_oF2} = 0.25$ Mc/s. This result is in agreement with the negative correlation between surface pressure and critical frequency of the E- and $F2$-layers found by Beynon and Brown [5] and also corresponds in order of magnitude with their values.

In the light of Martyn's hypothesis [3], one could try to explain a troposphere-ionosphere relationship such as the one between frontal passage in the troposphere and ionospheric characteristics of the $F2$-layer in the following manner: The exchange of air masses is associated with a wave motion aloft, represented by (cold) troughs of low pressure and (warm) ridges of high pressure. Since these waves are long in comparison to the thickness of the barrier region between troposphere and ionosphere, energy will be able to leak through. If the temperature structure of the upper atmosphere provides a period of free oscillation corresponding

*According to J. W. Jackson (J. Geophys. Res., **61**, 107, 1956), large variations in virtual height of the $F2$-layer are sometimes not accompanied by changes in the true height of the layer. This effect is attributed to signal retardation in the lower regions and will occur when the electron density of the $F2$-layer is not much greater than the densities of the E- and $F1$-layers. At the time for which the data under consideration are representative, that is, at about sunrise, this is evidently not the case. We may therefore assume that changes in minimum virtual height indicate changes in true height of the $F2$-layer.

to the period of the tropospheric wave, resonance will occur and a tropospheric effect appears amplified in the ionosphere.

The reason why most known weather-ionosphere relationships are more pronounced or observable only in certain seasons (mainly during local winter and spring) may be that in these seasons the conditions in the lower atmosphere are more favorable for providing strong coupling. Actually, it has been found [6] that the zonal index, measured by the mean pressure difference between 35° and 55° north, characterizing the circulation in the mid-latitude belt, shows much larger variations in winter than in summer.

CONCLUSIONS

Results of a statistical analysis suggest the existence of a relationship between frontal passage in the lower atmosphere and virtual height and critical frequency of the ionospheric $F2$-layer. A speculative interpretation of these results in the light of a hypothesis suggested by Martyn [3] shows that the observed effects are consistent with the concept of dynamic coupling between troposphere and ionosphere as used in the theory of atmospheric oscillations [4]. Although the relationship between tropospheric frontal passage and minimum virtual height of the ionospheric $F2$-layer was shown to be statistically significant, it should not be considered conclusive before verification by an extensive investigation. The observed effects, however, have been found to be in agreement with previously reported troposphere-ionosphere correlations [2, 5].

It is hoped that future investigations will shed further light on the existence of troposphere-ionosphere relationships which, if substantiated, could eventually lead to a unified picture of the behavior of the atmosphere.

References

[1] S. K. Mitra, The Upper Atmosphere, Asiatic Society, Calcutta, 2nd ed. (1952). [Vol. 5, Asiatic Society Monograph Series.]

[2] E. Gherzi, Ionosphere and weather, Nature, **165**, 38 (1950).

[3] D. F. Martyn, in Proceedings of the Conference on Ionospheric Physics, July 1950, Part *B* (edited by L. Katz and N. C. Gerson), Geophysical Research Division, Air Force Cambridge Research Center, Geophy. Res. Papers, No. 12, pp. 31–33, 62–64 (April 1952).

[4] M. V. Wilkes, Oscillations of the Earth's Atmosphere, University Press, Cambridge (1949).

[5] W. J. G. Beynon and G. M. Brown, Geophysical and meteorological changes in the period January-April 1949, Nature, **167**, 1012 (1951).

[6] S. Petterssen, Weather Analysis and Forecasting, McGraw-Hill Book Co., Inc., New York, 2nd ed. (1956); Vol. 1, p. 281.

DISTURBANCES IN THE LOWER IONOSPHERE OBSERVED AT VHF FOLLOWING THE SOLAR FLARE OF 23 FEBRUARY 1956 WITH PARTICULAR REFERENCE TO AURORAL-ZONE ABSORPTION

BY D. K. BAILEY

Page Communications Engineers, Inc.,
Washington 5, D. C.

(Received June 17, 1957)

ABSTRACT

Observations at the time of the great solar flare of 23 February 1956 of oblique-incidence signal intensities and simultaneous observations of the background cosmic noise were made at VHF for a number of high-latitude communication links employing the ionospheric-scatter mode of propagation. During the flare and for some hours afterward, all paths lay in the dark hemisphere. Virtually synchronously with the arrival of solar cosmic rays, a sharp signal-intensity enhancement was observed, which is tentatively explainable if it is supposed that the first-arriving solar cosmic rays were predominantly of positive charge. The unusually stable night-time absorption which developed in one to three hours after the flare and the much greater following daytime absorption are explained in some detail as consequences of the deposition in the *D* region of moderately heavy solar atomic ions, such as calcium, having ionization potentials low compared with the normal atmospheric constituents. The absorption effects, which were limited to fairly high geomagnetic latitudes, gradually died away over a period of several days. The absence of significant magnetic disturbance and unusual auroral activity for nearly 48 hours after the flare is shown to be in accord with the suggested explanation of the absorption effects. Asymmetry about local noon was observed in the absorption effects on signal intensity, for which an explanation is suggested.

I. INTRODUCTION

The world-wide effects of the great solar event which was first observed as an unusually intense solar flare, beginning at about 0331 UT on 23 February 1956, are being reported in current scientific literature. The cosmic-ray intensity increases which began within 20 minutes of the beginning of the solar flare are perhaps the most spectacular effect reported. However, the consequences of this event in the lower ionosphere in high latitudes as observed on operational communications systems employing the ionospheric-scatter mode of propagation at VHF were also spectacular. The departures from normal conditions were enormous and

quite unique for the comparatively short period—since 1951—that systematic observations of ionospheric scattering at VHF have been made.

II. OBSERVATIONAL MATERIAL

It has been possible to examine the effects of the event on six two-way communications circuits which were in operation at the time of the event. Five of the circuits were in the region of eastern North America and the North Atlantic, and the sixth was in Alaska. These circuits varied in length from about 900 to 1,600 km and were operating on frequencies between 31.5 and 38.0 Mc/s. All employed transmitters having output powers of about 40 kw and high-gain directional antennas for both transmitting and receiving. The antennas were of the 60° corner-reflector type, employing four horizontal collinear full-wave elements [see 1 and 2 of "References" at end of paper]. Thus, horizontal polarization was used. By a suitable choice of antenna height, the main ground-reflection lobes were directed toward a point in the ionosphere at a height of about 85 km above the midpoint of the path. The plane-wave gains of the antennas varied somewhat, but were of the order of 18 to 20 db with respect to a horizontal half-wave dipole at the same height. Continuous recordings were made of the signal intensity at each receiving point, and the background cosmic noise was recorded four times a day by shutting off the transmitter for a period of two minutes each time. In addition to this, at two of the three receiving terminals at Søndre Strømfjord, Greenland, particular care was taken in the data recording and the cosmic noise was observed every half-hour without traffic interruption by detuning the recording receiver to an adjacent portion of the spectrum which was usually free of radio-frequency energy of terrestrial origin.

III. SELECTION AND ANALYSIS OF THE DATA

On the basis of an examination of the recordings for completeness and accuracy, the better of the two receiving terminals of each circuit was selected for a detailed analysis. In general, the signal behavior at the two terminals of a particular path is sufficiently similar that there is no need to make a detailed study of the observations for both terminals. Table 1 contains the path lengths, operating frequencies, and, for the midpoints of the paths, the geographic coordinates, the geomagnetic latitudes, and the magnetic inclinations. Because of operational complications, the recordings for the circuits between Goose Bay, Labrador, and Limestone, Maine, were unusable during much of the period of interest, although the presence of some of the effects and the time of their onset could be established. On several of the circuits, tests and adjustments were in progress, which necessitated the application of corrections of somewhat uncertain magnitude to some of the observations.

The recording techniques and methods of analysis are sufficiently similar to those already published [3] to require little further discussion. In general, the observed points shown in Figures 1 and 2 are hourly medians for the intensity of the scattered signal, except when abrupt changes were taking place. Quarter-hourly values are shown, for example, between 0330 and 0430 UT on 23 February.

TABLE 1—*Path characteristics*

Path	Length	Frequency	Midpoint coordinates			
			Lat.(N)	Long.(W)	Geomag. lat.(N)	Inclin. (1955)
(*Transmitter to receiver*)	*km*	*Mc/s*	°	°	°	°
Thule to Søndre Strømfjord	1,224	31.5	72.0	57.3	82.8	83.2
Goose Bay to Søndre Strømfjord	1,575	32.2	60.3	56.5	72.4	78.9
Keflavik to Søndre Strømfjord	1,328	32.4	66.1	35.8	74.5	78.2
Narsarssuak to Goose Bay	1,244	37.0	57.5	53.7	68.4	78.1
Limestone to Goose Bay	915	33.0	50.2	64.6	61.2	76.0
Kenai to Juneau	977	36.4	59.7	142.6	61.0	74.5
Cedar Rapids to Sterling	1,243	49.8	40.6	84.4	51.6	72.0

In the case of the detailed background cosmic-noise observations made only at Søndre Strømfjord as shown in Figure 1, the observational points plotted are determined during the short breaks occurring each hour on the half hour, unless the intensity was changing rapidly, when intermediate points are shown. On a few occasions, the cosmic-noise observations are missing because of interference.

Both the signal and cosmic-noise intensities could be measured with decreasing precision down to the level of receiver noise, shown at −25 db in Figure 1. Some estimates were attempted down to −30 db. The probable errors of the plotted signal and cosmic-noise intensity observations for values greater than −22 db are estimated to be, respectively, 1-1/2 and 1 db. The probable errors increase markedly for lower intensity values. Values shown are relative, and systematic effects for the period of time represented by the plots are believed to be unimportant. The greater probable error for the observed signal intensities results from the difficulty of estimating the median signal intensity for periods of one hour.

In order to obtain control or reference standard observations of the intensity of the scattered signal, the medians of the hourly medians for the 11 days immediately prior to 23 February were used. The control values of signal intensity are shown as fine lines in Figures 1 and 2. Control values of cosmic-noise intensity, shown as a similar fine line in the lower half of Figures 1(*a*) and 1(*b*), were obtained as medians of the observations for the four days before 23 February and the two days following 27 February.

A comparison of the normal cosmic-noise intensities shown in Figures 1(*a*) and 1(*b*) demonstrates, apart from marked differences in the diurnal variation, a general difference in level. The latter is the result in part of differences in transmission-line lengths for the two antennas. The antenna directed toward Thule

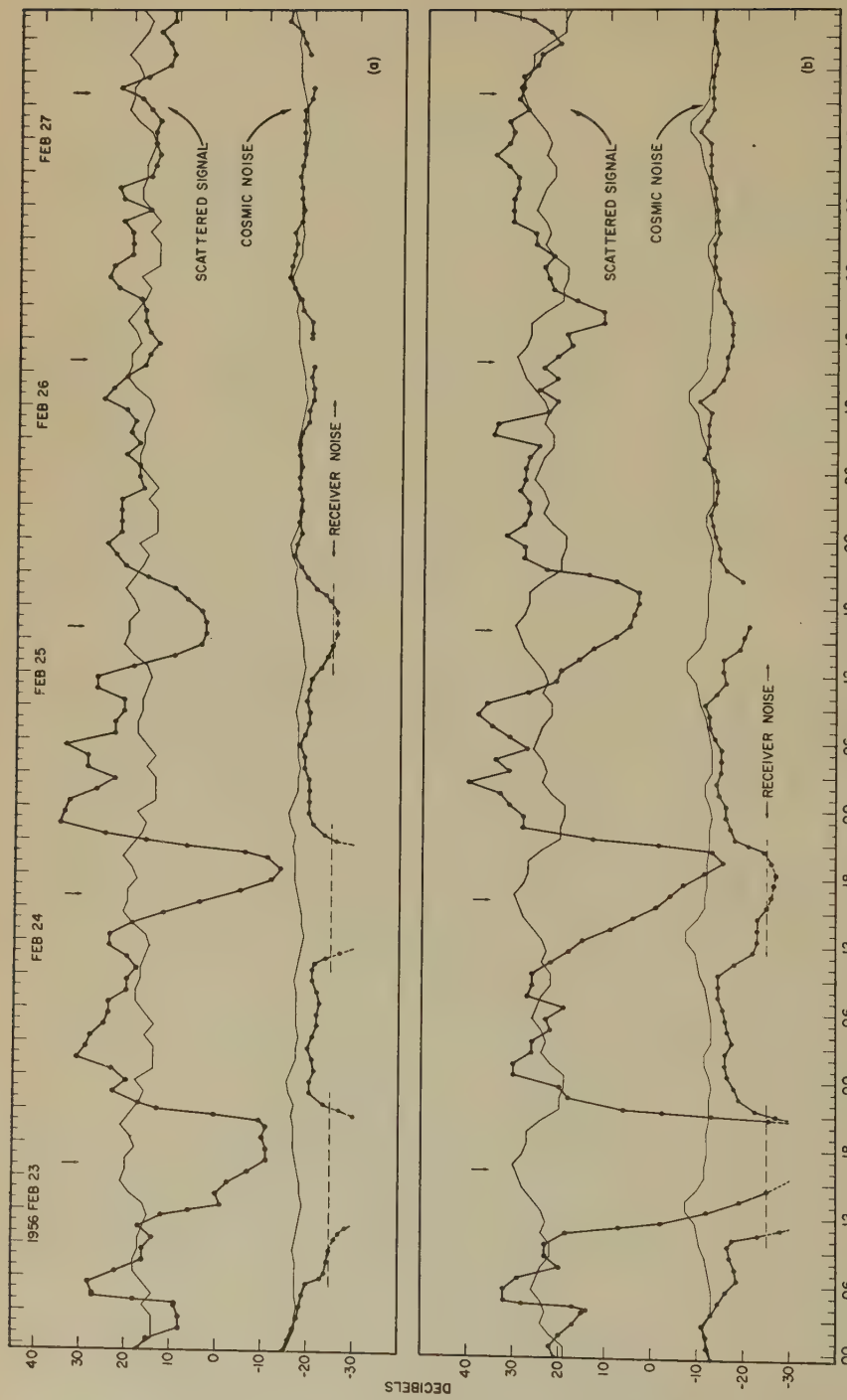

FIG. 1—Observed variations with time of intensity of signals and background cosmic noise at the same frequency with the same antenna. Normal variations indicated by the thin line. Vertical arrows indicate local apparent noon at path midpoint.
(*a*) Observations at Søndre Strømfjord, Greenland, of signals from Thule, Greenland, and background cosmic noise, at 31.5 Mc/s.
(*b*) Observations at Søndre Strømfjord of signals from Goose Bay, Labrador, and background cosmic noise, at 32.2 Mc/s.

as a longer transmission line with between 2 and 3 db more loss. Furthermore, e main lobe of the Thule antenna sweeps the sky in declination +26.3°, whereas e antenna directed toward Goose Bay sweeps the sky at declination −18.6°. he balance of the general difference between the normal cosmic-noise intensities, erefore, can be attributed to the generally lower noise intensities observed in the gher declination. The conspicuous peak of the cosmic noise observed in the direc- on of Goose Bay occurs at the time of year under study at about 1300 UT and rresponds to the passage through the main antenna lobe of the Milky Way st north of Sagittarius. Table 2 contains information about the position of the

TABLE 2—*Position of main lobe of receiving antennas used for cosmic-noise absorption observations*

Location	Directed toward	Azimuth	Elevation	Position angle	Declination	Right ascension at 00 UT on 23 February
		°	°	*h m*	°	*h m*
ndre Strømfjord	Thule	338.0	5.3	10 22	+26.3	20 23
ndre Strømfjord	Goose Bay	202.6	2.9	01 36	−18.6	05 08

in-lobe maximum for each of the two antennas for which detailed cosmic-noise formation is available. As a result of the combination of naturally higher cosmic- ise intensities and lower transmission-line losses for the antenna directed toward oose Bay, it was possible to observe the absorption of the cosmic noise over a der range of intensity in the direction of Goose Bay than in the direction of ule.

Detailed observations are shown in Figures 1 and 2 for the entire period from through 27 February, since aftereffects of the event were still significantly bservable on the 26th. Local apparent noon at the midpoint of each path is dicated each day by a small vertical arrow.

IV. DESCRIPTION OF THE OBSERVED EFFECTS

The Initial Enhancement of the Signal

The first effect attributable to the solar event on the signal-intensity recordings as an enhancement of the signal intensity. The enhancement was abrupt and of rge magnitude on all the paths except one, that from Keflavik to Søndre Strøm- ord. On this path, two separate and smaller enhancements occurred, the second which, though less distinct, is perhaps the more significant, judged by the nature the change in the character of the recording. Table 3 gives limits for the probable mes of onset of the initial enhancements for the different paths, together with a mewhat arbitrary number, expressed in decibels, to indicate the amplitude and eepness of the rise. Uncertainties in the times shown are not considered to exceed ne or two minutes. The uncertainty implied by the limits arises not from errors of mekeeping but from the difficulty of defining and identifying an instant when he enhancement may be said to have begun. During the course of the enhance-

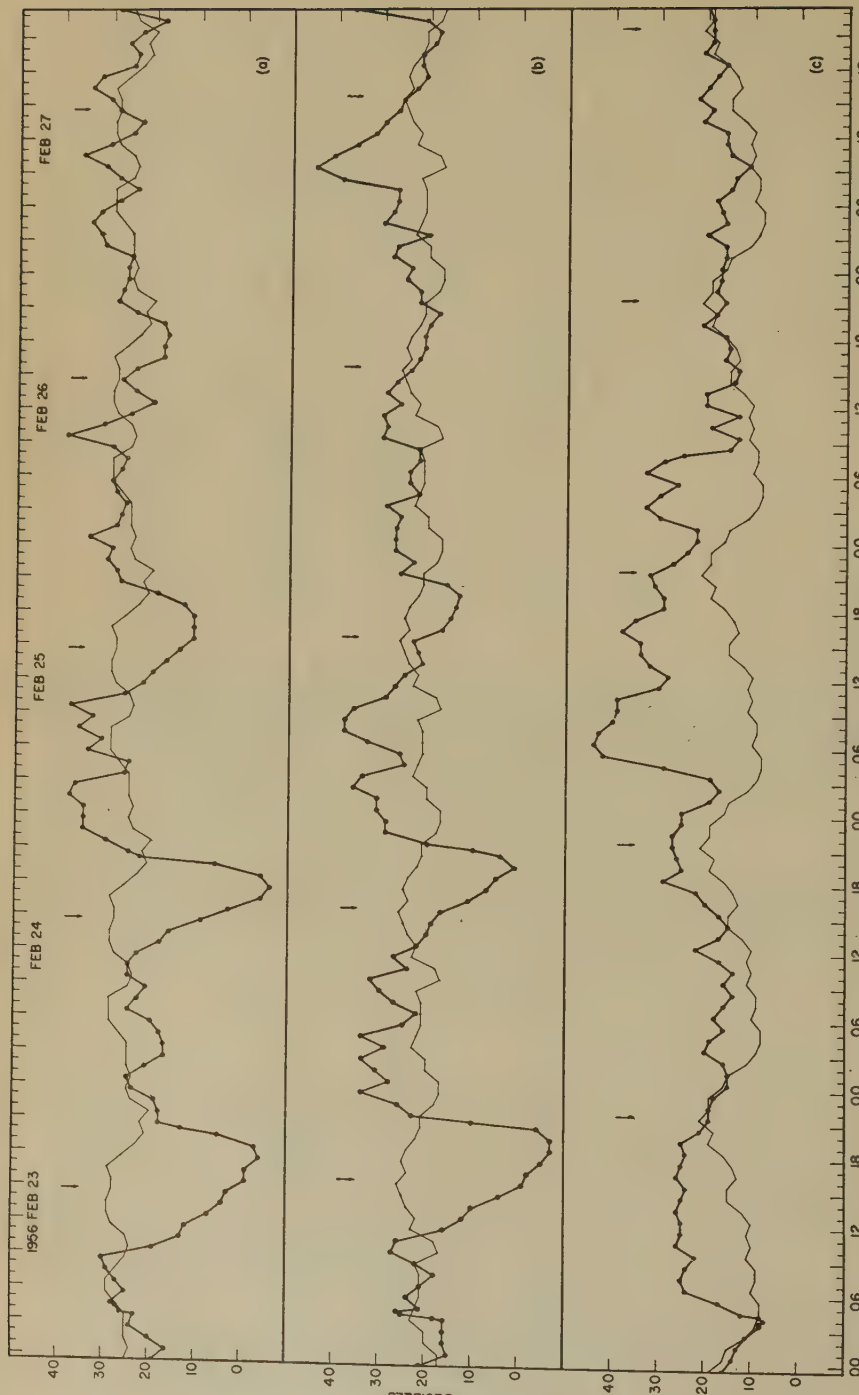

FIG. 2—Observed variations with time of intensity of signals. Normal variations indicated by the thin line. Vertical arrows indicate local apparent noon at path midpoint.

(*a*) Observations at Søndre Strømfjord, Greenland, of signals from Keflavik, Iceland, at 32.4 Mc/s.
(*b*) Observations at Goose Bay, Labrador, of signals from Narsarssuak, Greenland, at 37.0 Mc/s.
(*c*) Observations at Juneau, Alaska, of signals from Kenai, Alaska, at 36.1 Mc/s.

TABLE 3—*Initial enhancement*

Path	Limits for probable time of onset, UT		Amplitude
	h m	*h m*	*db*
Thule to Søndre Strømfjord	03 49	03 54	20
Goose Bay to Søndre Strømfjord	03 56	04 00	14
Keflavik to Søndre Strømfjord	03 31	03 37	5
	03 55	04 05	3
Narsarssuak to Goose Bay	03 42	03 49	17
Limestone to Goose Bay	04 13	04 17	11
Kenai to Juneau	04 12	04 19	6

ments, the appearance of the trace altered noticeably from the rather weak levels, which are heavily influenced by meteoric ionization in the ionospheric volume common to the main lobes and principal side lobes of the antennas, to the more stable daytime type of trace usually interpreted as resulting from the dominance of true midpoint scattering from ionospheric irregularities. At their maxima, the enhanced-signal recordings not only looked like daytime records, but exhibited signal intensities which equalled or exceeded typical daytime values. This remarkable change took place within an hour of *local midnight* at all the path midpoints except on the Alaskan path. On the latter path, the beginning of the enhancement occurred at about 1828 local apparent time at the path midpoint—a time of day when the signal intensities were approaching their lowest normal diurnal levels. While the enhancements were not simultaneous, all occurred within a period of half an hour, and the earliest occurred about 15 minutes after the start of the flare.

2. *The Night Absorption*

For the present discussion, absorption is taken to be measured by the difference between the observed intensity of the cosmic noise at a particular time and the normal value at the same time. For the two paths shown in Figure 1, for which detailed observations of background cosmic noise are available, a gradual decrease in the intensity of the background noise was observed to begin at about the same time as the sudden signal enhancement. The absorption, presumed to be of the non-deviative kind occurring mostly below the 90-km level,* continued to increase for about three hours, that is to say, until about 0630 UT, by which time it had attained a value of about 6 db. For the more southerly path, Goose Bay to Søndre Strømfjord, Figure 1(*b*), the absorption then remained nearly constant until 0950 UT, when sunrise took place at heights of 70 to 80 km in the absorbing region (true zenith angle of the sun, $\chi \approx 99.5°$) and a very rapid increase in the

*Confirmed by the reports of total blackout during the night for the ionosphere recorder at Tromsö, Norway [4], and elsewhere in high latitudes.

absorption occurred. This is discussed in the next Section. For the more northerly path, Thule to Søndre Strømfjord, Figure 1(*a*), the absorption continued to increase slowly until layer-sunrise at about 1000 UT, at which time it had reached about 9 db.

Ignoring for the moment the much greater daytime absorption, it is seen in Figure 1 that a remarkably uniform and stable but gradually decreasing night absorption was observed in the direction of the midpoint of both paths for the two nights following the night of the solar event. Some traces of night absorption may even have been present on the third night.

3. *The Great Daytime Absorption*

From about the time of sunrise to sunset in the 70- to 80-km height region, additional absorption of the background cosmic noise of extraordinary magnitude was observed at Søndre Strømfjord in the direction of the midpoint of both the path to Thule and to Goose Bay. During the day of 23 February, the absorption was too great to measure except when the sun was near the horizon. It was again too great to measure during most of the period of daylight in the absorbing region on 24 February in the Thule direction. In the Goose Bay direction, it could be estimated. The daytime absorption decreased from day to day until, by 27 February, its presence could no longer be recognized with certainty.

Figure 3 illustrates in more detail the circumstances of the abnormal increases in the absorption observed at sunrise at Søndre Strømfjord. In it, the differences between the observed and the normal cosmic-noise intensities have been plotted as a function of time and the vertical lines through the observed points represent their estimated probable errors. The pre-sunrise observations are nearly constant and are represented by a horizontal line. The increasing absorption during the first hour after its onset at sunrise has been represented by a sloping line. The intersection of the lines is taken as giving the approximate time of layer sunrise. The actual times of sunrise at the path midpoints have been computed, making the necessary allowances for refraction in the lowest 20 km of the atmosphere, for the visible red and near infrared part of the spectrum as a function of height of the absorbing layer. These sunrise times are labeled with the letter "D" (for photo-detachment). For such sunrises, the sun's rays graze the earth's surface, so that the rays first reaching the ionosphere will have lost by scattering and absorption practically all of their energy represented by wavelengths shorter than the yellow region of the visible spectrum. The first rays having any substantial ultraviolet content must have grazed the top of the ozone layer. The latter is somewhat difficult to define, and an arbitrary height of 40 km was selected to represent the closest approach of these rays to the surface of the earth. The times of ultraviolet sunrise are designated according to ionospheric heights by the letter "I" (for photo-ionization). Even making full allowance for the arbitrariness and uncertainties in the lines whose intersection has been used to fix the time of onset of the absorption increase, it seems quite certain that solar ultraviolet radiation was not responsible for the onset of the daytime absorption increase. From the sunrise times labeled "D" it will be seen that the onset of the absorption increase can probably be attributed to the arrival of solar photons at the red and infrared end of the solar spectrum at *D*-region heights. The sunrise effect for 23 February for

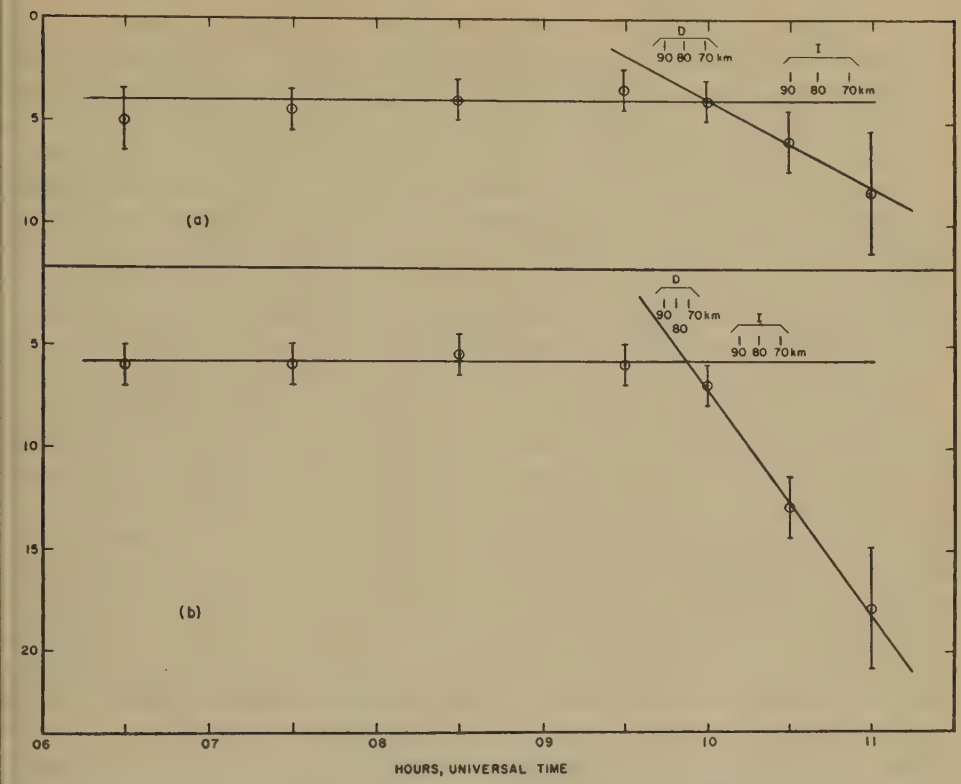

IG. 3—Variations with time of cosmic-noise absorption observed at sunrise at Søndre Strømfjord, Greenland.

a) With antenna directed toward Thule, Greenland, on 24 February 1956, at 31.5 Mc/s.

b) With antenna directed toward Goose Bay, Labrador, on 23 February 1956, at 32.2 Mc/s.

mes of earth-grazing sunrise at 70, 80, and 90 km, including effects of refraction up to a height 20 km, are labeled "D". Times of ozone-layer grazing sunrise at 70, 80, and 90 km, assuming effective upper limit of height of 40 km, are labeled "I".

ie antenna directed toward Thule could not be well determined because the night bsorption was still increasing at sunrise. Accordingly, in Figure 3(*a*), the observaons for 24 February are shown. Figure 3(*b*) shows the observations for 23 Febuary for the antenna directed toward Goose Bay. Similar findings govern the isappearance of the abnormal daytime absorption at sunset, but the times are ss clearly defined by the observations.

Although the VHF observations cannot be regarded as conclusive, they are onsistent with an absorption which is approximately symmetrical about local oon. Thus, they strongly suggest a dependence of the daytime absorption on the osine of the zenith angle χ of the sun.* Independent support for an approximate

*A simple classical dependence such as $\cos^n \chi$, where n might lie between 1/2 and 1, is inufficient, since it does not take account of the observed absorption at times when χ approaches exceeds 90°. The observations would appear to be satisfied by a cos χ-dependence having a rm, $(a + b \cos \chi)^n$, like that of the empirical absorption index used for many years by the ational Bureau of Standards (see, for example, NBS Circular 462), in which $a = 0.142$, $b =$ 858, and $n = 1.0$.

cos χ-dependence is provided by the observations at vertical incidence at HF during the day of 23 February at Inverness, Scotland, by Minnis, Bazzard, and Bevan [5], and at Kjeller (near Oslo), Norway, by Lied [4], near the southern limits of the region showing the effect, where the intensity of the absorption was insufficient to produce a complete blackout.

In order that the importance of the daytime absorption event can be appreciated, it is to be noted that on no occasion since such observations began in the Arctic in 1951 has anything approaching such an enormous absorption event been observed. The intensity of the absorption during the local midday of 23 February was at least eight times as great as any previously observed by the same techniques and adjusted to equivalent conditions of illumination. Based on examination of the signal-intensity behavior of the scattered signals and the discussion in the following section, it has been possible to reconstruct approximate values for the maximum absorption, assumed to have occurred at about local noon, on each day following the event. For the antenna directed toward Goose Bay, a plausible sequence of maximum values is 48, 23, 14, and 6 db, respectively, for 23, 24, 25, and 26 February. In arriving at these values, certain additional corrections have been made to take account of the effect of the sec i-variation of the absorption which results in a systematic underestimate of the true absorption, characteristic of the receiving antenna pattern, when absorption is measured as the difference between the observed intensity of the cosmic noise at a particular time and the normal value at the same time. The values after 24 February were probably influenced by the sudden-commencement geomagnetic storm which began shortly after 0300 UT on 25 February. The later values, therefore, cannot with confidence be considered to form a homogeneous sequence with the earlier values.

Non-deviative absorption A in decibels at a particular frequency and for a particular main-lobe position is approximately proportional to $\int N \nu \, dh$, where dh is an element of height in the absorbing region, N is the electron density, and ν is the electron collision frequency. For convenience, suppose that most of the absorption takes place in a layer 10-km thick, lying between 70 and 80 km. Next, instead of considering N and ν as functions of h, replace them by suitable mean values $\bar{N}$ and $\bar{\nu}$, such that $\int N\nu \, dh = 10\bar{N}\bar{\nu}$. A suitable value $\bar{N}$ for local noon on 23 February, *under normal conditions*, for the midpoint of the Goose Bay to Søndre Strømfjord path is 200 electrons/cm^3. Under such normal circumstances, the absorption of cosmic noise at 32.2 Mc/s would be about 0.5 db. Assuming that $\bar{\nu}$ is not very different from its normal value* in the absorbing layer on 23 February 1956, the absorption of 48 db, which is estimated to have occurred, would require about a 100-fold increase in $\bar{N}$.

4. *Abnormalities in the Scattered Signal Intensity*

Following the initial signal-intensity enhancement, which is discussed separately above because of its independence of local time, the behavior of the signal intensity for the several days following may be characterized in the following way. At night, the signal intensities were unusually high [except somewhat anomalously for the night of 23–24 February for the Keflavik to Søndre Strømfjord path shown in Figure 2(*a*)]. For all the paths (including Limestone to Goose Bay) except Kenai

*Possibly about 5×10^6 collisions per second.

o Juneau, the signal intensity decreased fairly uniformly from shortly after sunrise until a minimum was reached, usually some two or three hours after local noon. During the three to four hours of remaining daylight in the layer, the signal intensity returned to enhanced night levels at a rate which in all but one case (Thule to Søndre Strømfjord, 25 February) considerably exceeded the rate of decline earlier in the day. The magnitude of the daytime phenomenon was greatest on 23 February for three out of five paths showing the effect, and it decreased progressively over the following three days. By 26 February, the effect had virtually disappeared. For the Thule to Søndre Strømfjord and the Keflavik to Søndre Strømfjord paths, the depth of the daytime minimum was slightly greater on the second day, 24 February, although the duration of the period of substantially weakened signal was greater on the first day.

It has already been established [3] that during an intense polar blackout the scattering stratum lies above the region of most of the non-deviative absorption. It was simultaneously established that the absorption varied inversely as the square of the frequency, so that the absorbing layer must have been mostly above 50 km, below which the absorption, if any, tends to become independent of frequency. It has also been established [3, 6] for temperate latitudes in winter that the principal night-time scattering level, usually between 85 and 90 km, persists weakly during the day, but that most of the signal received by day is scattered from a lower stratum at a height between 70 and 80 km. The exact height of the daytime scattering stratum and its effectiveness as a scattering medium varies from day to day and even from hour to hour. Nevertheless, a certain diurnal regularity does exist. Assuming that a somewhat similar state of affairs exists in winter in the lower ionosphere in the Arctic where no direct height determinations have yet been undertaken, the following explanation of the daytime signal-intensity behavior can be advanced. First let it be accepted, in accordance with earlier discussion of the daytime absorption, that the abnormal daytime absorption was cos χ-dependent and therefore essentially symmetrical about local noon. Also assume that most of the abnormal daytime absorption takes place in the atmospheric region between 70 and 80 km. Then, as the absorption begins to increase at sunrise, the intensity of the signals scattered from heights of 85 to 90 km or higher decreases rapidly, since the signals received from these levels traverse the absorbing stratum twice. Let it also be supposed that active scattering begins to occur at sunrise at about the 70-km level. Scattering from this level will suffer relatively little absorption. Now suppose that in the course of the day the scattering level slowly rises through the absorbing layer and that by midafternoon it reaches a height such that the increase in absorption resulting from its further rise is just offset by the decrease of absorption resulting from the decrease of cos χ. This height is probably near the top of the region in which the main absorption takes place. Such a behavior would produce a minimum signal intensity displaced as observed into the afternoon period, with a consequent asymmetry of the kind observed.* The observance of daytime minima less deep on 23 February than on

*This simplified explanation is offered merely to be illustrative. A complete explanation would need to provide not only for changes in the scattering height, but also for the possibility of important contributions to the total signal from more than one height, for variations with time in the vertical distribution of the absorption, and for variations with time of the scattering efficiency.

24 February, for the Thule to Søndre Strømfjord and Keflavik to Søndre Strømfjord paths, as shown in Figures 1(*a*) and 2(*a*), may now be accounted for by supposing that the daytime scattering layer rose more slowly than usual through the absorbing layer on the first day, and only reached a height corresponding to about the middle of the absorbing layer by midafternoon.* During the day of 25 February, the Thule to Søndre Strømfjord signal intensity exhibited a minimum at about local noon and showed a more rapid morning decline than afternoon rise. This would be explained by assuming that the daytime scattering layer formed at a somewhat higher level on this day and remained at a nearly constant height. Such day-to-day variations in behavior would not have been considered unusual in a lower latitude, and are probably associated with meteorological processes at the heights involved.

In the light of the above explanation, it is now desirable to reexamine the position with respect to abnormal signal-intensity enhancements. Experience during lesser blackouts in the Arctic, particularly at higher frequencies, has shown not only that an enhancement of the absorption occurs, but also that an enhancement of the intensity of the scattered signals takes place. The latter effect is observed whenever the absorption enhancement is insufficient to overcome the effect of the enhanced scattering. Figures 1 and 2 show that, notwithstanding the absorption directly observed in Figure 1, enhancement was, in fact, observed at night. While there is no reliable means of assessing the magnitude of the enhancement of the scattered signal intensity which would have been observed by day in the absence of absorption, it seems very likely that it was considerable—perhaps as much as 20 db at times. This could have been determined experimentally if simultaneous observations had been made at a substantially higher frequency, since the increase in scatter efficiency (in decibels) under such circumstances seems to be independent of frequency,** whereas the absorption (in decibels) which varies roughly inversely as the square of the observing frequency would be substantially reduced.

Some further interpretation is now possible of the signal-intensity behavior between the time of the initial enhancement and sunrise, as shown in Figures 1(*a*) and 1(*b*). The initial enhancement was of about 20 db or 100 to 1 in power. According to the earlier theories of ionospheric scattering, this could be explained by a 10-fold increase in the electron density in the scattering layer. The scattering layer at night is presumed to have been situated at 85 to 90 km or higher. The

*Two other possible explanations may be mentioned. First, there might have been a saturation effect in the absorption on the first day. This seems unlikely. A more likely possibility is that the unattenuated signal intensities on the first day were so greatly enhanced compared with the second day that in spite of greater absorption the resultant signal intensities were higher. See the discussion in the following paragraph.

**According to the various theories discussed by Bailey, Bateman, and Kirby [3], the scattered power is directly proportional to f_N^4, and therefore to N^2, where f_N is the critical plasma frequency corresponding to the electron density N in the scattering stratum. Thus, fractional changes in the scattered power caused by changes in N are independent of the frequency at which they are observed. More recent views on the nature of the scattering process [7] do not relate the scattered power so simply to the electron density in the scattering stratum. However, fractional changes in the scattered power caused by changes in meteorological or ionospheric parameters in the expression for the scatter coefficient are probably approximately independent of frequency.

rop of 10 to 12 db in signal intensity which took place some three hours after
e enhancement may perhaps be attributed to the development of the night
bsorption of about 6 db in a region below the scattering level so that the signal
ssed through the absorbing layer twice and experienced therefore an attenuation
about 12 db.

Turning now to the signal-intensity observations for the Kenai to Juneau
th, as shown in Figure 2(*c*), it is seen first that the initial enhancement, which
ok place in the local evening, persisted throughout the night and continued well
to the following day. By noon, however, the signal intensity had decreased to
rmal levels. The decrease may reflect some low-level absorption, but of a much
naller magnitude than observed on the other paths. This could not be ascertained
th certainty from the noise observations, which were few in number and of
or quality. On 25 February, between 0300 and 0600 UT, a tremendous signal
hancement of about 30 to 35 db took place, corresponding in the earlier scattering
eories to an increase of electron density in the scattering stratum by a factor
perhaps 50, and coinciding accurately with the onset shortly after 0300 UT of a
dden-commencement geomagnetic storm, somewhat doubtfully associated with
e solar flare event 48 to 50 hours earlier. The importance of the storm can be
lged by the increase which took place in the three-hourly planetary magnetic
dex *Kp* [8]. *Kp* was 1− for the period 00-03 UT, 6o for the period 03–06 UT,
d 8+ for the period 06–09 UT. The effects of the storm are less apparent in the
gnal-intensity observations for the more northerly paths. This enhancement
s by far the strongest observed for the path in a year of operation. Signal inten-
ies on this path, as on the others, did not become normal until 26 February.

V. GEOGRAPHICAL EXTENT OF THE DISTURBANCES

The initial enhancement effects as observed in high geomagnetic latitudes
8° to 83°N) in the dark hemisphere occurred nearly simultaneously with the
smic-ray event, within the general uncertainties of identifying the actual onset
nes. For example, Forbush [9] reports that the cosmic-ray increase was observed
begin at Godhavn, Greenland, at about 0353 UT. Godhavn is 330 km to the
utheast of the midpoint of the Thule to Søndre Strømfjord path. It should be
ted, however, that the enhancements last much longer in the case of the scattered
gnals. For lower geomagnetic latitudes (about 60°N) in the dark hemisphere,
e onsets of the enhancements occurred about 20 minutes later. The observational
terial is insufficient to place limits on the occurrence and characteristics of the
hancements. It may be said that enhancement effects were observed well to
e south of locations at which absorption effects took place. In particular, there
s a considerable enhancement of the 49.8-Mc/s scattered signal received by
e National Bureau of Standards at Sterling, Virginia, from Cedar Rapids,
wa [10], during the period of the cosmic-ray event. Unfortunately, an enhance-
ent of unknown origin but of a type occasionally observed began about 18 to
minutes before the cosmic-ray event, so that any particular enhancement
sociated in time with the cosmic-ray event is obscured.

In the case of the absorption features of the event, as exhibited in Figures 1 and
by intensity observations of both the scattered signal and the background cosmic

noise, somewhat more definite limits can be set. Table 1 indicates the geographic and magnetic coordinates of the ionospheric regions observed. The greatest effects were observed for paths with their midpoints near or inside the region of maximum auroral frequency. At geomagnetic latitudes south of 60° to 62°, large effects were not observed. It is of interest to note that moderate daytime absorption was observed for the Limestone to Goose Bay path in geomagnetic latitude 61.2°N on 23 and 24 February, whereas significant absorption effects were apparently absent from the signal-intensity observations for the Kenai to Juneau path, far to the west in geomagnetic latitude 61.0°N. The magnetic inclinations for the midpoints of these two paths will apparently provide a better basis for establishing the southern extent of the effect. These are shown in Table 1 as 76.0° and 74.5°, respectively. Thus, a southern boundary for the effect seems to have existed in the North American-North Atlantic region at about magnetic inclination 75°. Further confirmation for this approximate boundary is found in the observations for the Cedar Rapids to Sterling path, already alluded to, which showed no significant absorption effects. The absorption effects clearly extended as far south as the northern part of the British Isles and Southern Norway. Minnis, Bazzard, and Bevan [5] have analyzed the vertical incidence $h'f$ observations made at Inverness, Scotland, and Slough, near London. At Inverness, a significant increase in $f_{\min}$ was observed during the daylight hours of 23 February; no such absorption effect was observed at Slough. Lied reports [4] vertical-incidence results from Kjeller (near Oslo) similar to those from Inverness. From Tromsö, however, a complete blackout was observed for about 48 hours from about 0500 UT on 23 February. No low-level absorption effect was found in the $f_{\min}$ observations made by the Central Radio Propagation Laboratory at Fort Belvoir, Virginia [11]. The apparent absorption effect reported by Forbush and Burke [12] from a station near Washington must have had its cause at much higher levels in the ionosphere. Finally, the lack of evidence for a large absorption effect for the Kenai to Juneau path can neither be taken as indicating that abnormal absorption was completely absent nor that a large absorption effect was absent farther north in Alaska. The Geophysical Institute at College, near Fairbanks, has, in fact, reported heavy absorption effects [13].

In summary, important absorption effects of the type observed at VHF are known to have occurred at locations having geomagnetic latitudes greater than about 60° to 62° in the northern hemisphere over the longitude range 19°E (Tromsö) to 148°W (Fairbanks) from which observations have been reported.

VI. TENTATIVE PHYSICAL EXPLANATIONS

1. *Introduction*

It has been customary to regard abnormal changes in the ionosphere as being the result either of abnormal ionizing photon radiation or of abnormal ionizing "corpuscular" radiation, both of solar origin. More recently, the arrival and presence of meteoric matter has been recognized as having importance as well. Other processes may, however, be effective. For example, increases in non-deviative absorption may result not only from an increase in electron density in a region

high collision frequency, but also from the presence of an electrostatic field ross a slightly ionized gas. Such a field can increase the electron temperature d therefore the electron collision frequency at levels where the collision frequency normally too low to produce much absorption [14]. Recently, Chapman and ttle [15] have proposed a still different mechanism for unusual increases in low-vel ionization. They attribute the ionization responsible for very intense auroral-gion absorption in part to *Bremsstrahlung* X-rays produced by the impacts auroral electrons having energies in the range 10^4 to 10^5 ev.

A detailed interpretation of the ionospheric consequences of a great solar event ch as that of 23 February 1956 must await the assemblage of much more informa-on than is at present available. Nevertheless, with respect to the lower ionos-ere, the VHF observations represented by Figures 1 and 2 provide sufficiently tailed evidence to allow the formulation of some tentative physical explanations.

The Initial Enhancement of the Signal

The initial enhancements would seem to require close association with the rld-wide cosmic-ray increase which occurred during and was superposed on the overy phase of a broad Forbush-type of cosmic-ray intensity decrease which gan about 12 February. The latter is believed to have been associated with a nerally high level of solar activity some weeks earlier. Meyer, Parker, and npson [16] have provided a comprehensive discussion of the 23 February cosmic-event, together with a model designed to account not only for the fact that the reases were observed on the dark side of the earth, but also that the increases gan some 5 to 10 minutes after the peak of the flare. A different model has been cussed by Brown [17]. Both models indicate that the trajectories of high-energy arged particles in the solar system may involve magnetized clouds of ionized tter as suggested by earlier workers and thus be much more complex than therto believed. The model of Meyer, Parker, and Simpson leads to the interesting ggestion that particles emitted from the invisible hemisphere of the sun may ch the earth.

Enhancements of VHF signals propagated by ionospheric scattering are served fairly frequently in the auroral regions at night. They are sometimes sociated with increased non-deviative absorption giving rise to the polar blackout enomenon at lower frequencies, and then are often associated with magnetic-y disturbances. They have not been satisfactorily related to particular solar nts. Wells [18] has described the characteristics of such blackouts, but it is to noted that he excludes daytime blackout phenomena. The enhancement of February does not fit the classification of a normal magnetic-bay type in the llowing respects:

(1) Enhancement was observed over a much wider area than is usual with a magnetic-bay disturbance.
(2) The absorption during the first one to two hours did not increase sufficiently rapidly.

The close association in time between the initial signal-intensity enhancements d the onset of the enhanced cosmic-ray flux provides the basis for the following

suggestion. Suppose that the cosmic-ray primaries of which the enhanced flux at onset was composed were preponderantly particles of positive charge.* A consequence would be the accumulation of a net positive charge in the lower atmosphere. By this means, a vertical electric field would be temporarily established. The effect of such a field might be to polarize the lower ionosphere by drawing electrons downward in such a way as to increase N or dN/dh in a turbulent region, thereby giving rise to an increase in the intensity of the scattered signals. This hypothesis has the following interesting properties:

(1) It does not require any direct interaction in the ionosphere with the cosmic-ray primaries or charged particles of lower energy.
(2) It requires that ionospheric effects shall occur with a geographic distribution similar to the cosmic-ray event and thus extend to middle and, perhaps weakly, to low geomagnetic latitudes.

The above or any other tentative explanation should be examined particularly in the light of events observed at VLF and possibly of events in the F region of the ionosphere as well. Whatever explanation is eventually found acceptable, it must take account of the following observations:

(1) The initial enhancement phenomenon was more widespread in geomagnetic latitude than the subsequent absorption phenomena.
(2) The signal-intensity enhancement began later and proceeded more slowly in geomagnetic latitudes 60° to 62° than in higher geomagnetic latitudes.

3. *The Cosmic-noise Absorption Phenomena*

The daytime absorption events of 23 February and the following days were perhaps the most impressive and enduring single phenomenon of the lower ionosphere associated with the great solar event. The residual night-time absorption was almost certainly closely related to the daytime absorption and it will be so explained. The effects of the low-lying absorption on the intensity of the scattered signals will not be further discussed.

Any working hypothesis or mechanism, to be acceptable, must provide adequately for certain facts. The first, having to do with magnetic and auroral activity, is established by magnetic and auroral information from various sources [8, 19, 20]. The remaining facts are more or less well established by observations, as shown in Figures 1, 2, and 3, and also by observations for 23 February reported by Minnis, Bazzard, and Bevan [5] and by Lied [4]. Among the various facts, the most pertinent are:

(1) The absence of significant magnetic disturbance or unusual auroral activity during 23 and 24 February.
(2) The restriction of the excessive absorption to high geomagnetic latitudes;

*At the relativistic velocities and therefore very high energies associated with cosmic-ray primaries, the requirement for net neutrality of charges in space is probably not stringent for volumes the size of perhaps the inner solar system. Thus, for periods of time up to an hour or more, before complete isotropy is established for solar cosmic rays [16], the arrival of particles having charges of predominantly positive charge is not unreasonable.

absorption effects were either minor or not observed at geomagnetic latitudes below about 60°.

(3) The approximate cos χ-dependence of the daytime absorption with consequent symmetry about a maximum near local noon and with the daytime effect beginning in the morning and ending in the evening when $\chi \approx 99.5°$.

(4) The repetition of the event for several successive daylight periods with decreasing intensity.

(5) The local geographical uniformity and great geographical extent of the absorption as compared with ordinary polar blackout absorption.

(6) The unusual stability of the night-time absorption.

Point (4) embodies the most striking features of Figures 1 and 2; it indicates that a decay process was involved. The main question that arises is whether the decay took place on the sun or in the ionosphere.* If the abnormal ionization is assumed to have resulted from the continuing arrival and action of charged particles [required by point (2)] of solar origin, then the observed decay would have to result from the dwindling of the supply of solar particles of suitable energy that can reach the earth. If the decay is of ionospheric origin, the abnormal ionization must have resulted from the presence of unusual particles of solar origin in the absorbing region on which the normal solar radiation and ordinary ionospheric processes could act. In accordance with point (2), these particles must have been charged during their travel from the sun. The observed decay in this case would result from a removal or deactivation process.

In an attempt to account for the observational facts, two physical hypotheses, identifying the seat of the decay process as occurring on the sun and in the ionosphere, respectively, will be described and discussed. The first has recently been proposed by Chapman and Little [15] to account for the commonly observed daytime polar blackout absorption. It is not necessarily applicable in its present form to the daytime absorption observed following such an event as that under discussion. The second hypothesis, proposed below, is specifically applicable to the circumstances of the particular and unusual solar event. It is not *prima facie* applicable to the much commoner but less extensive daytime blackout absorption observed in high geomagnetic latitudes. An outline and discussion of each hypothesis is now given.

. *Ionization by X-rays Resulting from Continuing Electron Impact*

a. Outline of the hypothesis—Based on the observational work of Van Allen and co-workers [21], a mechanism has been proposed in some detail by Chapman and Little which requires that the ionosphere undergo bombardment by rather patchy streams of electrons having energies between about 10^4 and 10^5 ev, and depths of penetration corresponding to heights from about 105 to 79 km.** Much of the ionization responsible for the absorption is attributed directly to the particle bombardment. About one in 1,000 of these electrons is thought to produce by impact an X-ray photon (*Bremsstrahlung*) which, having a considerable range,

*The possibility that the seat of the decay process may have been elsewhere will be the subject of a subsequent short communication.

**See Figure 4, described and discussed below in connection with the second hypothesis.

tends to disperse the ionization process, as well as carry it down into lower atmospheric levels, thereby giving rise to a fairly uniformly distributed abnormal absorption. Chapman and Little take the particle bombardment to be more intense by night than by day, but account for the stronger absorption by day by having the low-level electrons produced at night removed by attachment, forming negative ions. By day, they invoke photo-detachment to keep down the ratio of negative ions to electrons.

b. Discussion—Certain difficulties can be raised concerning the mechanism in general and, more particularly, concerning its applicability to the events of 23 February and the days immediately following. Three such difficulties are now indicated and discussed.

(1) A detailed comparison of the 1953, 1954, and 1955 "rockoon" results [21, 22] from the Davis Strait area with VHF scatter signal-intensity and cosmic-noise intensity observations for the Goose Bay to Søndre Strømfjord path, situated in the same geographical region and made at the same time, has demonstrated no significant correlation of high and off-scale rockoon counting rates with unusual enhancements of the intensity of the scattered signals or with abnormal cosmic-noise absorption. It may, of course, be argued that the rockoon results represent highly localized events in both time and space.

(2) Appreciable magnetic disturbance and auroral activity were not observed on 23 and 24 February. It is thus difficult to see how intense and continuing electron bombardment could have been occurring.

(3) The mechanism in its present form makes no provision for the repetition, with declining intensity on successive days, of the daytime absorption. To account for such repetition, continuing but declining electron bombardment must be inferred.

This last point is in itself a general kind of difficulty with the Chapman-Little mechanism, since such constancy or regular variation in electron emission and arrival is most difficult to reconcile with other solar and magnetic observations. This difficulty is particularly pertinent to the situation under study, as it would seem to be necessary to assume that the particles giving rise to the ionospheric events were associated with the great solar flare of 23 February. This flare occurred near the western limb of the sun and the region associated with it disappeared behind the solar limb in less than two days. It is thus very difficult to imagine any mechanism capable of continuous ejection of high-speed electrons (velocities a few tenths of the velocity of light) that could have remained effective for three or four days. Most ejection mechanisms which have been proposed require the most efficient particle ejection to take place normal to the solar surface. It might be suggested that the absorption remaining on 25 and 26 February resulted from particles associated with the sudden-commencement geomagnetic storm which began shortly after 0300 UT on 25 February. If these latter particles began their travel at the time of the flare of 23 February, they must have been positively charged to have penetrated even to heights somewhat above the E-region maximum. While these particles may surely be related to the large enhancement in

e signal intensity observed on the Kenai to Juneau path on 25 February, they are nlikely to have given rise to much non-deviative absorption observable at VHF.

None of these difficulties is necessarily fatal to the Chapman-Little mechanism, hich may well prove to be valid for the common type of polar blackout absorption. he Chapman-Little mechanism is, however, provisionally considered inapplicable the event under study. No other detailed mechanism seems to have been pro-osed, and the second hypothesis, believed to be free of these difficulties, is there-re proposed and discussed in the following Section.

Penetration into the D Region of Moderately Heavy Solar Atomic Ions

a. Outline of the hypothesis—Since it was possible for the sun, by a flare-asso-ated mechanism, to eject a burst of primary cosmic rays which gave rise to the creased flux observed following the solar flare of 23 February, the writer suggests at the sun may also have ejected at that time charged matter having a velocity energy spectrum extending downward to values appropriate to auroral particles. his spectrum need not have been continuous or uniform. It is therefore suggested at atomic ions from the solar atmosphere intermediate in energy between auroral rticles and cosmic rays were deposited, like cosmic rays with local geographical iformity, in high latitudes in the terrestrial atmosphere to depths corresponding a height of about 70 km and perhaps in some concentration between 70 and 80 n.* Since the daytime absorption was fully developed on 23 February, it is further ggested that the deposition of solar ions was essentially complete by sunrise that date. Thus, a maximum travel time of about six hours may be inferred. om the observations shown in Figures 1(*a*) and 1(*b*), a somewhat more precise vel time may be estimated. It would seem plausible to interpret the gradual crease of the cosmic-noise absorption, beginning at about the time of the initial nal enhancement, and its subsequent leveling-off to an approximately constant lue between one and three hours after the solar flare, as defining the period en most of the ions arrived in the atmosphere following a fairly short period ejection during the flare. The great daytime absorption and intervening night-ne absorption observed on 23 February and the days immediately following uld then be explained by considering the nature and probable behavior of gatively charged atmospheric particles required for electrical neutrality in the sence of very slowly disappearing positive atomic ions of solar origin. Negative-formation in the lower ionosphere is now believed to be an important, perhaps most important, process for the removal of free electrons [23]. At night, there-re, most of the negative charges can probably be identified as negative molecular

*In interpreting absorption observations using cosmic noise in the auroral zone, considerable understanding can arise if the rather patchy or local nature of the commonly observed blackout sorption is not understood. The absorption events reported in this paper are the greatest ob-ved quantitatively at oblique incidence thus far. In order, therefore, that the results of this per may be compared with the absorption discussed in reference [15], the values of vertical-idence absorption of cosmic noise at 30 Mc/s that would have been observed at the midpoint the Goose Bay to Søndre Strømfjord path during the first night just before sunrise and at the t noon have been computed. For a pencil beam, they are 1.1 and 8.4 db, respectively. For ple antennas having broad main lobes directed vertically upward, the apparent absorption uld have been about 1.5 and 11 db, respectively. The point is that the absorption following cosmic-ray event was remarkably uniform, stable, and widely distributed.

oxygen ions O_2^- rather than O^-, since the population of oxygen atoms, resulting from dissociation, relative to oxygen molecules is small at heights below about 90 km [24]. However, the electron affinity for O_2^- molecules is probably about half that for atomic oxygen [25]. The latter has recently been found experimentally by Branscomb and Smith [26] to be about 1.45 ± 0.15 ev. The electron affinity of the O_2 molecule, while not known precisely, can thus be taken to be about 0.5 ev. At night, therefore, the process of collisional detachment would be expected to prevent the complete disappearance of the electrons and thus might account for the residual night-time absorption.* The observed stability of the night-time absorption would result if mutual neutralization of positive and negative ions by charge exchange or associative recombination were negligible or very slow. This matter is further discussed below. By day, the photo-detachment process, the extent of which would be cos χ-dependent, would free the electrons required to account for the observed absorption. Since 1 ev corresponds to a photon wavelength of 12378 angstrom units, it is clear that photo-detachment would become significant as soon as the red and near infrared rays of the sun reached the negative ions.** This is confirmed by the observations shown in Figure 3, where the appropriate sunrises for photo-detachment are indicated by the letter "D". Removal or deactivation processes having a half-period of the order of a day would then be invoked to account for the gradual decay of the observed effects. These are further discussed below. The explanation just outlined in a highly simplified form appears to meet the requirements listed above for an acceptable working hypothesis, while at the same time avoiding difficulties encountered in attempting to apply the Chapman-Little mechanism.

b. Discussion

(1) *Independent evidence for the slow recombination of certain atomic ions in the ionosphere*

Observational evidence for the slow recombination of atomic ions of meteoric origin deposited in the ionospheric E region mostly at heights between about 85 and 120 km has been provided by long-duration meteor echoes. Kaiser and Greenhow [27] and Kaiser [28] review the evidence which indicates that, while the effective recombination coefficient of the E region is of the order of 10^{-8} cm^3/sec, the recombination coefficient for various meteoric ions having ionization potentials considerably lower than the atmospheric constituents is not less than about 4×10^{-12} cm^3 sec, which is of the order of 10^{-12} cm^3 sec obtained from theoretical calculations of the radiative recombination coefficient for such atomic ions. The much higher E-region coefficient is explained, following Bates [29], by assuming that molecular oxygen ions O_2^+ are present in sufficient numbers for dissociative recombination with a coefficient of the order of 10^{-5} cm^3/sec to predominate. Recently, arguments have been advanced by Kaiser [30] linking the very slow recombination of meteoric ions with summer sporadic-E ionization and by Nicolet [31] linking it with residual night-time E-layer ionization.

*Collisional detachment may also be of importance in connection with the persistent night-time signal-intensity enhancements.

**The significance of this process for the formation or activation of daytime scattering in the 70- to 80-km region should be noted.

(2) *Identity of possible ions*

The identity of the ions which could have been responsible for the long-enduring bsorption effects cannot be established uniquely from the observational material vailable. Protons and helium ions can probably be eliminated because of the high onization potentials of hydrogen and helium, and the consequent high electron ffinities which will cause their ions to undergo charge transfer with ordinary tmospheric constituents [31]. This does not imply that protons or helium ions vere necessarily absent from the incident particle stream. This leaves principally lkali and alkali-earth metals, among which Ca^+ is perhaps the likeliest, with Ca^+ a possibility of interest. Magnesium, aluminum, iron, and silicon are comaratively abundant elements that should not be excluded from any list of possiilities. For the moment, it is assumed that the arriving atomic ions are singly harged and that in their penetration of the atmosphere very few lose their identity hrough disruptive nuclear collisions.

Calcium, together with hydrogen and helium, is known to be plentiful in the olar chromosphere. Much of the calcium exists there in the singly ionized state s Ca^+. Kiepenheuer [32] has discussed the emission of corpuscles from the sun ith particular respect to the Milne mechanism [33], which is applicable efficiently ly to Ca^+. He indicates that calcium may well be expelled from the sun as Ca^+ uring solar flares.* Some not altogether satisfactory spectroscopic observations ave been made during magnetic storms which suggest the presence of fast-moving a$^+$ ions between the sun and the earth [34, 35]. Furthermore, a report by Bowen 6] may be cited referring to work of Wild in Australia on radio-frequency outursts from the sun coincident with flares, which suggests the emission of particles ith velocities of one- or two-tenths of the velocity of light. Finally, Dodson, edeman, and Chamberlain [37] have published evidence for the ejection by the n of Ca^+ ions at velocities exceeding the escape velocity at the time of *onset* five flares near the solar limb.

Sodium is well known to be a constituent of the terrestrial atmosphere as a sult of airglow studies [38, 39]. Recent rocket work has confirmed that its main stribution is below the *E*-layer maximum [40]. It also occurs mostly as Na^+ the solar atmosphere. The source of the sodium in the terrestrial atmosphere has t been satisfactorily identified, but the sun cannot be eliminated as a possible urce.

(3) *Possible role of photo-ionization*

The time of the sunrise effect shown in Figure 3 suggests that photo-ionization not of prime importance. However, its possible role requires some comment. or photo-ionization to take place in the 70- to 80-km region of the atmosphere, is necessary that the atoms have a sufficiently low ionization potential to be nizable by photons reaching that level. Because of oxygen absorption and the pid decline in the solar continuum, very few solar photons below about 1900 gstrom units can reach the 70- to 80-km level. Above about 1900 to 2000 ang-

*Most views on possible mechanisms of solar-flare ejection require that the most efficient ction be normal to the solar surface. It is, therefore, of unusual interest that the great solar re of 23 February 1956 occurred within 20° of the western limb of the sun.

strom units, the atmosphere is moderately transparent down to the ozone layer, as confirmed by rocket observations [41]. Thus, atoms having ionization potentials greater than about 6.5 ev and requiring photon wavelengths shorter than 1900 angstrom units for photo-ionization need not be considered.* This restriction also leaves the choice primarily among the various alkali and alkali-earth elements. Of these, sodium and calcium, being comparatively abundant and having ionization potentials of 5.1 and 6.1 ev, respectively, are considered the most likely. Nicolet [31] has calculated the rate coefficients for the photo-ionization by sunlight of sodium and calcium atoms, using the laboratory measurements of absorption cross-sections near the threshold [42, 43] and rocket results on the number of solar photons available. He finds the coefficient for sodium to be 1.1×10^{-5} per second, and for calcium about 10^{-6} per second. For other possible metals, it is much smaller. The half-life in seconds of a population of photo-ionizable atoms in sunlight is $\log_e 2$ divided by the rate coefficient. For sodium, the half-life comes to 18 hours, and for calcium it is about 200 hours. Photo-ionization is thus seen to be of small or even negligible importance, except possibly for sodium. In the latter case, it may serve slightly to replenish the supply of ions during the daytime, always assuming that sodium is a constituent of the incident stream of ions, thus retarding the decay of the absorption.

(4) *Penetration depths in the atmosphere*

The hypothesis that the abnormal absorption resulted from the presence in the *D* region of very slowly disappearing solar ions concentrated in the 70- to 80-km region of the atmosphere requires that the ions shall have arrived at the limit of the earth's atmosphere within six hours and more probably within one to three hours of their ejection as a result of the solar flare. The evidence for this has already been discussed. For vertical incidence on the atmosphere, the depths of penetration of various particles known or believed to be associated with auroral phenomena, namely, electrons, protons, and He^+, as well as Na^+ and Ca^+, have been determined or estimated as a function of their velocities and energies and are shown in Figure 4. For this purpose, the atmospheric pressure as a function of height determined, from rocket flights, by Havens, Koll, and LaGow [44] was adopted. Neither the subsequent rocket measurements in the Arctic [45] nor the modifications suggested by Kallmann [46] changes the results appreciably. To the extent possible, published measurements of ranges in air under standard conditions have been used. Values for electron ranges were taken from Heitler [47]. For proton ranges, the data published by Livingston and Bethe [48] were used. The slight divergences between more recent measurements of proton ranges leave the earlier measurements as typical. The ranges for He^+, Na^+, and Ca^+ were determined in accordance with Rossi's curves [49] for singly charged particles and can be considered only as upper limits. Experimental values do not appear to exist. For these ions, ranges thus found are likely to be considerably too great, since stripping is not taken into account. To make a detailed allowance for the effect on the ranges of stripping (the removal by collision of some or all of the remaining electrons during passage through the ionosphere) would apparently

*Solar X-rays are not considered in this connection.

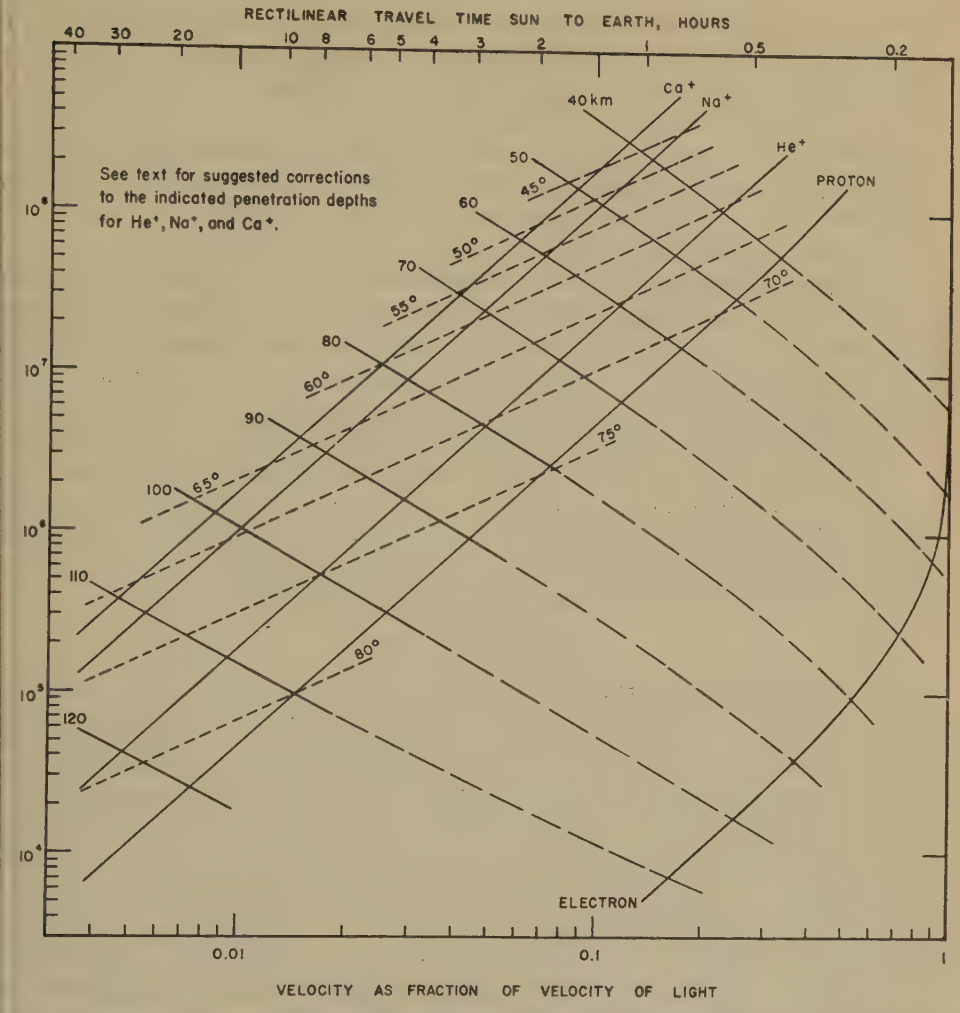

Fig. 4—Atmospheric depths of vertical penetration expressed as heights above ground for electrons, protons, and He^+, Na^+, and Ca^+ ions, as a function of their kinetic energies or velocities. Dashed curves indicate geomagnetic latitudes below which single particles or particle streams of very low density cannot arrive as a result of the magnetic dipole field of the earth.

quire application of the Monte Carlo technique. Although the atmosphere is ighly exponential in nature, it is thought, nevertheless, that the penetration pths shown in Figure 4 may represent overestimates by as much as 25 km for dium and calcium actually reaching the 70- to 80-km region. This view is derived m an extrapolation of the results for the ranges of light and heavy fission fragnts and for various ions, all lighter than sodium, as given by Knipp and Teller 0]. To a degree of approximation which is sufficient for present purposes and stified by the limited experimental data, improved estimates of the depth of netration of ions heavier than the hydrogen ion (proton) can be obtained from gure 4 by adopting the proton depths as a reference (they are probably fairly curate) and assuming that heavier ions of the *same velocity* penetrate to the

same depth. This is equivalent to saying that the curves of constant depth in Figure 4 should extend vertically upward from their intercepts with the kinetic energy *versus* velocity curve for the proton. The result of this procedure is in accord for the He^+ ion, since it is well known that protons and α-particles (He^{++}) of the same velocity have about the same range. This type of correction seems to be reasonable for depths between about 70 and 100 km. For depths corresponding to heights above 110 km, the differences between the plotted depths and the correct depths are probably less.

The energies of the ions reaching the 70- to 80-km region probably lie somewhat above 10^8 ev, but are probably less than 10^9 ev. Ions of such energy lie in the very soft cosmic-ray spectrum and may well be more than singly ionized on arrival at the atmosphere. The importance of nuclear collisions at energies below 10^9 ev during the stopping process is believed to be very small.

The dashed curves labeled in degrees indicate the lowest geomagnetic latitudes at which singly charged *single* particles of the energies shown can reach the earth's atmosphere when influenced by the earth's magnetic dipole field. These curves are computed on the basis of a relation given in a simple form by Störmer [51] for auroral particles and given in a more complete form by Alpher [52] for cosmic-ray particles. For the present purpose, the relation may be written

$$R = 14.7 \cos^4 \lambda \quad \ldots\ldots(1)$$

where R is the magnetic rigidity of the particle in units of 10^9 volts and λ is the geomagnetic latitude. The applicability of these curves to streams of ionized particles is discussed below in connection with the estimate of the density of the incident stream. Bearing in mind that the trajectories of the ions somewhat exceed one astronomical unit in length, and allowing 20 to 25 km for the possible correction to the penetration depth, it is seen from Figure 4 that either Ca^+ or Na^+ within reasonable tolerances would penetrate to depths of the order of 70 to 80 km in geomagnetic latitudes as low as 50°. Since magnetic rigidities are inversely proportional to the particle charge, arriving particles of a given energy of more than single charge would be confined to higher geomagnetic latitudes. Furthermore, ions arriving much later than five to six hours after the flare would come to rest above the absorbing region and could, therefore, only be important as possible causes of enhancement of the signal intensity.

(5) *Negative ions and electron-detachment processes*

Assuming that the mechanism proposed is correct, an attempt is now made, employing equilibrium considerations, to arrive at some quantitative results characterizing the daytime maximum and the stable night-time absorption. Neglecting photo-ionization of neutralized solar ions, the detailed relationships which must be examined are as follows:

$$\frac{dN}{dt} = q - (\alpha_e)_d N N_a^+ - (\alpha_e)_r N N_s^+ - \eta n N + \kappa n N^- + \rho S N^- \quad \ldots\ldots(2)$$

$$\frac{dN^-}{dt} = -(\alpha_i)_a N^- N_a^+ - (\alpha_i)_s N^- N_s^+ + \eta n N - \kappa n N^- - \rho S N^- \quad \ldots\ldots(3)$$

y adding (2) and (3), the following relationship is obtained:

$$\frac{dN^+}{dt} = q - (\alpha_e)_d N N_a^+ - (\alpha_e)_r N N_s^+ - (\alpha_i)_a N^- N_a^+ - (\alpha_i)_s N^- N_s^+ \quad \ldots\ldots(4)$$

hich is a consequence of the requirement that the ionosphere be electrically eutral, or

$$N^+ = N_a^+ + N_s^+ = N + N^- \quad \ldots\ldots(5)$$

he somewhat complex notation arises from the need to keep separate the reactions volving normal atmospheric constituents, subscripts "a" and "d", and the reign particles of solar origin, subscripts "s" and "r". The meanings are as follows:

- n = particle density of neutral particles to which electrons attach themselves (mainly O_2) and which can detach electrons by collision
- N = electron density
- N^- = negative-ion density
- N^+ = total positive-ion density
- N_a^+ = positive-ion density resulting from photo-ionization of normal atmospheric constituents
- N_s^+ = positive-ion density resulting from the deposition of positive-ions of solar origin
- $(\alpha_e)_d$ = dissociative recombination coefficient for collisions between electrons and O_2^+ ions
- $(\alpha_e)_r$ = radiative recombination coefficient for collisions between electrons and positive ions of solar origin
- $(\alpha_i)_a$ = coefficient of mutual neutralization for collisions between negative ions and positive ions of atmospheric origin
- $(\alpha_i)_s$ = coefficient of mutual neutralization for collisions between negative ions and positive ions of solar origin
- q = rate of electron production by photo-ionization of normal atmospheric constituents (mainly O_2)
- η = attachment coefficient of electrons for molecules having electron affinity, here primarily O_2
- κ = coefficient of collisional detachment of electrons from negative ions, mostly detachment from O_2^-
- ρS = photo-detachment coefficient of electrons from negative ions, again mostly O_2^-
- S = intensity of solar radiation involved in the process, a function of cos χ

In the present instance, the half-life of the removal or deactivation processes sponsible for the gradual disappearance of the absorption will be regarded as ig with respect to a period of daylight or darkness. Furthermore, in the 70- to -km region, the normal atmospheric ionization processes may be disregarded, ce their total contribution to the first daylight absorption maximum is less by actor of about 10^{-2} than the contribution from the mechanism proposed, and ir contribution to the observed night-time absorption is vanishingly small. us, (2) and (3) can be simplified at once to the following:

$$\frac{dN}{dt} = -(\alpha_e)_r NN_s^+ - \eta nN + \kappa nN^- + \rho SN^- \quad (6)$$

$$\frac{dN^-}{dt} = -(\alpha_i)_s N^- N_s^+ + \eta nN - \kappa nN^- - \rho SN^- \quad (7)$$

Further simplification is now possible. In (6), the term involving $(\alpha_e)_r$ is at most some 10^{-3} times the value of any of the terms following it, even taking pessimistic values for the various coefficients and admitting the unlikely possibility that the negative-ion density in the daytime may be as much as ten times the electron density. The position is similar at night. In (7), at night, the term involving $(\alpha_i)_s$ is at most some 10^{-2} times the value of either of the two following terms (ρSN^- vanishes at night), as determined by a similar method of estimation. By day, the disparity is even greater. Therefore, to a sufficient degree of approximation for the exploratory considerations which follow, (6) and (7) may be still further simplified to

$$\frac{dN}{dt} = -\eta nN + \kappa nN^- + \rho SN^- \quad (8)$$

$$\frac{dN^-}{dt} = +\eta nN - \kappa nN^- - \rho SN^- \quad (9)$$

For the moment, (4) may be regarded as trivial, since each term is taken to be zero, and (8) and (9) merely express the temporary assumption that N^+ is constant and equal to N_s^+, so that $dN/dt = -dN^-/dt$. Now using subscripts N and D for night and midday, respectively, and parentheses where necessary for clarity, two cases are distinguished.

Case 1: At night, $dN/dt = 0$, and photo-detachment cannot take place. Therefore, defining λ_N as the night-time value of N^-/N,

$$\lambda_N = \left(\frac{N^-}{N}\right)_N = \frac{\eta}{\kappa} \quad (10)$$

Case 2: By day, $dN/dt = 0$ near local noon, and similarly defining λ_D as the noon value of N^-/N,

$$\lambda_D = \left(\frac{N^-}{N}\right)_D = \frac{\eta n}{\kappa n + \rho S} \quad (11)$$

From (10) and (11), it follows that

$$\frac{(N)_D}{(N)_N} = \frac{1 + \lambda_N}{1 + \lambda_D} \quad (12)$$

But the ratio of the noon to the night value of mean electron density in the absorbing layer may be established from the absorption observations in Figure 1 and the reconstructed values of the maximum midday absorption already stated. Making allowance for the observed rate of decay, this ratio may be taken as about 10. Table 4 has been constructed for a selected range of values of λ_D with the aid of this observationally determined ratio and relations (10), (11), and (12). It is

TABLE 4—*Interrelationships between coefficients in the absorbing region (h = 75 km) required by the observations*

λ_D	λ_N	η	ρS	κ
		$cm^3\ sec^{-1}$	sec^{-1}	$cm^3\ sec^{-1}$
0.1	10	1.5×10^{-15}	3.6	1.5×10^{-16}
		1.5×10^{-14}	36	1.5×10^{-15}
0.3	12	1.5×10^{-15}	1.2	1.2×10^{-16}
		1.5×10^{-14}	12	1.2×10^{-15}
1	19	1.5×10^{-15}	0.34	7.9×10^{-17}
		1.5×10^{-14}	3.4	7.9×10^{-16}
3	39	1.5×10^{-15}	0.12	3.8×10^{-17}
		1.5×10^{-14}	1.2	3.8×10^{-16}
10	109	1.5×10^{-15}	0.033	1.4×10^{-17}
		1.5×10^{-14}	0.33	1.4×10^{-16}
30	309	1.5×10^{-15}	0.011	4.9×10^{-18}
		1.5×10^{-14}	0.11	4.9×10^{-17}

given for a height of 75 km, where the particle density of O_2 molecules, n, is taken to be $2.4 \times 10^{14}/cm^3$ [44]. Two values of η have been used. The value 1.5×10^{-14} cm^3/sec is based on a value considered likely by Bates and Massey [53] for the height under study. The lower value 1.5×10^{-15} cm^3/sec is derived by Mitra [54] from Biondi's laboratory measurements [55].* Assuming that a maximum likely value for ρS is about 0.5/sec [56, 53] and that Biondi's measurements are likely to have provided a better value for η, it would appear from Table 4 that the proposed interpretation of the observations is consistent in the 70- to 80-km region with a value of λ_D of about unity or a little more. A value for κ of about 10^{-16} cm^3/sec or a little less is then required. The latter is about a tenth of the value indicated by Mitra [57], but is in accord with the "likely value" given by Mitra and Jones [23]. In view of the well-known uncertainties about ionospheric collisional processes and their associated rate coefficients, the proposed interpretation is regarded as quantitatively satisfactory.

It is now possible to estimate the particle density of the solar ions in the model absorbing layer. It has already been demonstrated that the absorption observed at Søndre Strømfjord in the direction of Goose Bay at local noon on 23 February 1956 was about 100 times the normal D-region value. The latter corresponds to a mean electron density of about 200 electrons/cm^3. Thus, at noon on 23 February, it is inferred that the electron density in the model uniform absorbing layer between 70 and 80 km was about 2×10^4 electrons/cm^3, since $\bar{\nu}$ is assumed to have been

*The actual value given by Bates and Massey is 1.6×10^{-14}. A rederivation from Biondi's cross-section gives 1.4×10^{-15} rather than 1.5×10^{-15} given by Mitra. The values 1.5×10^{-14} and 1.5×10^{-15} are used in Table 4 for their convenience, as they differ by an exact factor of 10.

unaffected by the flux of solar particles. In accordance with the discussion above, a value of $\lambda_D \sim 1$ at noon means that an equal density of negative ions was simultaneously present. From (5), then, the particle density of the positive atomic ions of solar origin must have been about $4 \times 10^4/\text{cm}^3$. When the atomic ions arrived some ten hours earlier, their mean particle density, making allowance for the decay processes, must have been of the order of $6 \times 10^4/\text{cm}^3$. Thus, a column of the absorbing layer 10-km high and 1 km^2 in cross-section would have contained initially about 6×10^{20} atomic ions, which would have had a mass of about 40 mg if calcium and 24 mg if sodium.*

(6) *Decay processes*

It is now necessary to consider processes whereby the positive atomic ions of solar origin are deactivated or removed, since the preceding simplified analysis is only justified if the half-life of the effectiveness of the ions is long compared with a period of daylight or darkness. The processes of radiative recombination and photo-ionization have already been discussed. They are too slow to be of much importance. The question of mutual neutralization by charge exchange between positive and negative ions must next be considered. The process may be indicated as

$$A^+ + B^- \rightarrow A \text{ (excited)} + B \text{ (excited)} \quad \ldots\ldots\ldots\ldots (13)$$

For the present purpose, (4) can be simplified as above and it becomes

$$\frac{dN^+}{dt} = -(\alpha_i)_s N^- N_s^+ \quad \ldots\ldots\ldots\ldots (14)$$

Since $\lambda_D \sim 1$ and $\lambda_N \sim 19$, N^- will be equal to about $\frac{1}{2}N_s^+$ by day and N_s^+ by night. From (5), since N_a^+ is practically zero, $N_s^+ = N^+$. It is therefore possible to write for (14) the relation

$$\frac{dN^+}{dt} = -(\alpha_i)_s (N^+)^2 \quad \ldots\ldots\ldots\ldots (15)$$

where it must be noted that the decay by day will proceed more slowly than indicated by (15), which is essentially correct at night. At time $t = 0$, taken to be the approximate time of arrival of the solar atomic ions, the value of N^+ was previously found to be $N_0^+ = 6 \times 10^4$ ions/cm^3. The solution of (15) is given by

$$N^+ = \frac{N_0^+}{1 + (\alpha_i)_s N_0^+ t} \quad \ldots\ldots\ldots\ldots (16)$$

The half-life τ is defined as the time required for N^+ to reach $\frac{1}{2}N_0^+$ and is written

$$\tau = \frac{1}{(\alpha_i)_s N_0^+} \quad \ldots\ldots\ldots\ldots (17)$$

*It is of interest to compare this number with that derived for airglow sodium. Most of the airglow sodium lies in a layer with its maximum at 85 km but extending from about 70 to 95 km [40, 58]. For the present purpose, it is assumed that a column of 1 km^2 cross-section contains, during the winter, about 7×10^{19} sodium atoms having a total mass of 2.7 mg. The model absorbing layer might then be considered to contain about 0.7 mg/km^2 of sodium. It is, therefore, tempting to speculate on the possibility of a connection between ionized airglow sodium and the well-known winter absorption anomaly. Sodium airglow and the population of atmospheric sodium are known to be maximum in winter [59, 58].

Nicolet [31] suggests that for $\lambda > 1$, $(\alpha_i)_s \ll 10^{-9}$ cm^3/sec for metallic ions of meteoric origin. Chapman and Little [15] use the value 10^{-9} cm^3/sec for α_i, but actually they are referring to $(\alpha_i)_a$, which would be expected to be larger than $(\alpha_i)_s$. For $(\alpha_i)_s = 10^{-10}$ cm^3/sec, (17) gives a value for the half-life of 46 hours, which is somewhat long. Thus, other removal or decay processes are likely to be present and may be dominant. The important point here is that the half-life for process (13) is not so short that the absorption would be required to disappear impossibly rapidly.

Turning then to other possible removal processes, wind transport and possibly turbulence are likely to lead to dilution, but there are photo-chemical processes which must be considered as well. While daytime photo-ionization is not thought to be very important, its effectiveness will be limited by such processes as associative detachment,

$$A + B^- \rightarrow AB + e \quad \ldots\ldots\ldots\ldots\ldots\ldots\ldots\ldots (18)$$

which according to Bates and Massey [60] is particularly important at thermal energies, and associative recombination,

$$A^+ + B^- \rightarrow AB \text{ (excited)} + h\nu \quad \ldots\ldots\ldots\ldots\ldots\ldots\ldots\ldots (19)$$

The latter process can also contribute directly to the removal of atomic ions. Both processes, as well as three-body processes, lead to the deactivation of the solar atoms or ions A or A^+ through the formation of molecules which are generally inert. Specifically, B^- is identified as O^- or O_2^- and the molecules are identified as oxides. It should be noted that while O^- is extremely rare compared with O_2^- in the 70- to 80-km region, it is not completely absent by any means. The part played by these processes in relation to mutual neutralization has not been sufficiently studied, though they may well predominate. Nicolet [31] has calculated the mean lifetime of a calcium atom before it becomes CaO as two months at 105 km, and four days at 70 km. When the O_2 molecule is involved, the time of molecular formation will be much less, particularly below about 90 km. At that height, Nicolet estimates the mean lifetime of a silicon atom to be about one day before it forms SiO_2. Bates [61] states that the mean life of a sodium atom at 70 km is about one second before it forms NaO_2.

The discussion of removal processes, while far from complete, does not indicate the likelihood of any serious inconsistency between the observed decay and the basic mechanism proposed to account for the observed absorption.

A final point must be made in connection with the continual arrival in the atmosphere of meteoric material which is at first deposited as atomic and ionic material almost entirely above 85 km. Considerations of vertical diffusion and other processes indicate that the time required for any appreciable number of meteoric atoms or ions to reach even 80 km from higher levels is likely to be measured by months or years. Thus, deactivation processes of the general kinds just discussed will have ample time to act, and as a result meteoric material is not expected to make any significant contribution to the normally observed ionospheric absorption. It may well play a significant part in summer sporadic-E ionization and night-time E-region ionization as already mentioned from the work of Kaiser and Nicolet.

(7) *Density of the incident particle stream*

It is important to have an estimate of the incident particle stream density in order to test the hypothesis proposed to account for the absorption effects against the evidence from published magnetograms [19] that the arriving ionic matter was insufficient to produce any significant magnetic disturbance. As far as is known, the arriving stream also failed to produce any noteworthy auroral activity [20]. This lack of high-latitude magnetic and auroral disturbance stands in marked contrast to events accompanying the large sudden-commencement geomagnetic storm which began shortly after 0300 UT on 25 February.

Consider first the solar ions taken to have been responsible for the long-enduring absorption effects. From what has already been shown, a column 10 km high centered at 75 km with a cross-section of 1 cm^2 contained about 6×10^{10} such ions at the end of the period of arrival. Since the ion ejection is presumed to have been associated with the great solar flare, it is probable that the ions arrived in a burst not lasting longer than the flare itself. For the purpose of calculation, it is assumed that the arriving burst lasted about half an hour and that the mean velocity of the stream was not greater than 0.14c or 4.2×10^9 cm sec. This velocity takes account of the probable overestimates of depth of penetration shown in Figure 4. It follows somewhat crudely then that in a period of half an hour, or 1.8×10^3 seconds, 6×10^{10} ions arrived, representing the contents of a column $4.2 \times 10^9 \times 1.8 \times 10^3$, or about 7.5×10^{12} cm in length and 1 cm^2 in cross-section. The positive-ion density of the arriving stream is thus seen to have been about 8×10^{-3} ion/cm^3.* To be safe, this density may be increased by a factor of about 10 to compensate for any possible underestimate of λ_D above, and by another factor of 10 to allow for the probable simultaneous presence of protons and possibly helium ions. With these safety margins, it would seem that the density of the incident stream of positive ions was probably less than one ion per cubic centimeter. Chapman [62] provides an estimate made by himself and Ferraro, which states that the minimum density of a neutral ionized gas sufficient to produce a moderate magnetic storm is 100 protons (plus 100 electrons) per cubic centimeter. Even allowing for an underestimate, as above, by a factor of 10^2, it seems unlikely that the arriving particles, among which were those responsible for the absorption effects, would have produced any significant magnetic or auroral activity. This is in satisfactory agreement with the facts.

Chapman [62] provides another criterion of some interest. He states that the single-particle theories as given by Störmer, LeMaître, and Vallarta, and the experimental results of Birkeland and Brüche are inapplicable to a cloud of neutral but ionized gas unless its density is far less than one particle per cubic centimeter. Thus, to the extent that the actual particle density is not much in excess of the lower limit of 8×10^{-3} ion cm^3, the geomagnetic limits shown in Figure 4 should provide a useful guide.

*Rough estimates indicate that the same absorption would have been observed from an absorbing layer formed between 80 and 90 km if the incident stream density had been 10 times as great. The velocity in this case would have been about 0.07c. Similarly, if the layer had formed between 60 and 70 km, the required incident stream density would have been about a tenth of this value, and the velocity about 0.2c.

(8) *Ionization produced by the incident particle stream*

The explanation thus far advanced for the observed absorption effects requires that moderately heavy solar ions be brought to rest (thermal equilibrium) in the *D* region. The ions, which arrive at the earth's atmosphere with energies possibly as high as 10^8 ev, must dissipate their kinetic energy in the stopping process. Radiation losses and, as stated earlier, nuclear interactions are assumed to be of negligible importance, so that the kinetic energy must be lost by ionizing collisions with air molecules. Most of the ionization thus produced occurs near the end of the path of an ion. For protons, such a concentration of the ionization will be more marked than for heavier ions which undergo stripping. If each incident ion is assumed to lose on the average 40 ev of its kinetic energy per ionizing collision, it can be shown on the basis of previous reasoning that a high rate of electron production will exist during the relatively short period of time assumed for the ion deposition. If the electron production is uniformly distributed throughout the absorbing region and normal recombination processes take place, a considerable absorption effect in the cosmic-noise intensities (probably exceeding that observed at midday on 23 February) should have been observed during the process of deposition. The absorption actually observed during the time when deposition is thought to have occurred was only a little greater than that observed on the following night, when, according to the present hypothesis, no deposition was taking place. From considerations of this kind, it is clear that other factors must be taken into account if the absorption actually observed before sunrise on 23 February is to be explained. Several ways out of this difficulty are available but their exploration has been deferred.

VII. CONCLUDING REMARKS

On the basis of the preceding account, it seems necessary to recognize a new class of signal-intensity enhancements for waves propagated by ionospheric scattering and a new kind of high-latitude absorption phenomenon. It would seem inappropriate to identify the observed absorption effects as merely a special case of the well-known polar blackout absorption. It is clear that an event such as that reported is rare. To the extent that such events are associated generally with outbursts of solar cosmic rays, they may on the basis of very meager statistics be expected to occur about once in four years. Actually, smaller events may occur more frequently, but are likely to be associated with important flares. The particle velocities thought necessary to account for the absorption effects are of the order of a tenth of cosmic-ray particle velocities, and the associated particle energies are correspondingly lower. The sun is, therefore, more likely to eject absorption-producing particles than particles having cosmic-ray energies.

It should be emphasized that the explanation suggested for the initial signal-intensity enhancement phenomenon has not been subjected to any detailed analysis and it may prove untenable. It is felt that the initial enhancement effect must be studied in detail together with the simultaneous or nearly simultaneous effects observed at LF and VLF.

The model absorbing layer employed in connection with the absorption effects is mainly a convenience which permits certain order-of-magnitude calculations.

It was placed between 70 and 80 km on the basis of height determinations in lower latitudes and on the basis of the explanation offered for the signal-intensity behavior during the daytime of 23 February and the days immediately following. Significant absorption may well have extended through a larger range of height. The important point which needs reiteration is that the circumstances of the VHF observations strongly suggest that some change in the composition of the lower ionosphere occurred fairly abruptly within a few hours of the solar-flare event. The observed effects, as argued, should be related to that change.

The presence in the *D* region of the moderately heavy ions of solar origin could, as has been shown, explain the absorption observations. Such ions probably arrive with energies of the order of 10^8 to 10^9 ev and on arrival at the top of the atmosphere are quite likely to be multiply ionized. If they are not too highly ionized on arrival, they will have magnetic rigidities of the order of 10^9 volts, and may thus perhaps tend to be deposited in favored impact zones [64, 65] in the *D* region. This point is but one of several requiring further study.

VIII. ACKNOWLEDGMENTS

Thanks are expressed to the U. S. Air Force, the National Bureau of Standards, and the U. S. Army Signal Corps for use of the observational material. Particular thanks are due to Mr. John Egbert who devoted much of his own time to the careful measurement of the recordings, and to Mr. John Creutz for illuminating discussions in connection with electrodynamic aspects of the problem. For very helpful discussions of various other aspects of the problem, thanks are offered to Dr. Felix Adler of the Carnegie Institute of Technology, Mr. R. M. Gallet of the National Bureau of Standards, Dr. S. A. Korff of New York University, and to the Department of Terrestrial Magnetism of the Carnegie Institution of Washington.

References

[1] H. V. Cottony, Trans. Inst. Radio Eng., **CS-4**, No. 1, 56 (1956).
[2] R. Bateman, D. K. Bailey, and J. A. Waldschmitt, Nation. Bur. Stan., No. 1R103 (1956); to be published.
[3] D. K. Bailey, R. Bateman, and R. C. Kirby, Proc. Inst. Radio Eng., **43**, 1181 (1955).
[4] F. Lied, J. Atmos. Terr. Phys., **10**, 48 (1957).
[5] C. M. Minnis, G. H. Bazzard, and H. C. Bevan, J. Atmos. Terr. Phys., **9**, 233 (1956).
[6] V. C. Pineo, J. Geophys. Res., **61**, 165 (1956).
[7] R. M. Gallet, private communication (1957).
[8] Nation. Bur. Stan., Rep. CRPL-F140, Pt. B, 5a (1956).
[9] S. E. Forbush, J. Geophys. Res., **61**, 155 (1956).
[10] H. I. Leighton, J. Geophys. Res., **62**, 483 (1957).
[11] Nation. Bur. Stan., Rep. CRPL-F139, Pt. A, 26 (1956)
[12] S. E. Forbush and B. F. Burke, J. Geophys. Res., **61**, 573 (1956).
[13] Geophysical Institute, University of Alaska, Abstr. of terrestrial phenomena observed following solar flare 23 February 1956, 0334 (cited from [12] above).
[14] H. S. W. Massey, Negative Ions, Cambridge Physical Tracts, No. 1, Cambridge University Press (1938). See pp. 96 and 97 for reference to possible application to the ionosphere of this idea, which is perhaps attributable originally to Prof. J. S. E. Townsend.
[15] S. Chapman and C. G. Little, J. Atmos. Terr. Phys., **10**, 20 (1957).
[16] P. Meyer, E. N. Parker, and J. A. Simpson, Phys. Rev., **104**, 768 (1956).
[17] R. R. Brown, J. Geophys. Res., **62**, 147 (1957).

[8] H. W. Wells, Terr. Mag., **52**, 315 (1947).
[9] T. Gold and D. R. Palmer, J. Atmos. Terr. Phys., **8**, 287 (1956).
[0] C. T. Elvey, private communication (1957).
[1] L. H. Meredith, M. B. Gottlieb, and J. A. Van Allen, Phys. Rev., **97**, 201 (1955).
[2] F. B. McDonald, private communication (1956).
[3] A. P. Mitra and R. E. Jones, J. Geophys. Res., **59**, 391 (1954); see their "References" for earlier papers by Bates and Massey, etc.
[4] M. Nicolet and P. Mange, J. Geophys. Res., **59**, 15 (1954).
[5] S. K. Mitra, The Upper Atmosphere, Asiatic Society, Calcutta, 2nd ed. (1952); p. 623. [Vol. 5, Asiatic Society Monograph Series.]
[6] L. M. Branscomb and S. J. Smith, Phys. Rev., **98**, 1127 (1955).
[7] T. R. Kaiser and J. S. Greenhow, Proc. Phys. Soc., B, **66**, 150 (1953).
[8] T. R. Kaiser, Advances in Phys. (Phil. Mag. Sup.), **2**, 495 (1953).
[9] D. R. Bates, Phys. Rev., **78**, 492 (1950).
[0] T. R. Kaiser, in Meteors, edited by T. R. Kaiser, Pergamon Press, London (1955); p. 119.
[1] M. Nicolet, in Meteors, edited by T. R. Kaiser, Pergamon Press, London (1955); p. 99.
[2] K. O. Kiepenheuer, J. Geophys. Res., **57**, 113 (1952).
[3] E.A. Milne, Mon. Not. R. Astr. Soc., **86**, 459 (1926).
[4] R. S. Richardson, Trans. Amer. Geophys. Union, 25th annual meeting, June 1–3, 1944, Pt. 4, 558 (1945).
[5] H. A. Brück and F. Rutllant, Mon. Not. R. Astr. Soc., **106**, 130 (1946).
[6] E. G. Bowen, in Report of Washington Conference on Radio Astronomy 1954, J. Geophys. Res., **59**, 163 (1954).
[7] H. W. Dodson, E. R. Hedeman, and J. Chamberlain, Astroph. J., **117**, 66 (1953).
[8] J. Cabannes, J. Dufay, and J. Gauzit, Astroph., J., **88**, 164 (1938).
[9] D. R. Bates, Terr. Mag., **52**, 71 (1947).
[0] M. Koomen, R. Scolnik, and R. Tousey, J. Geophys. Res., **61**, 304 (1956).
[1] F. S. Johnson, J. D. Purcell, and R. Tousey, J. Geophys. Res., **56**, 583 (1951).
[2] R. W. Ditchburn, P. J. Jutsum, and G. V. Marr, Proc. R. Soc., A, **219**, 89 (1953).
[3] P. J. Jutsum, Proc. Phys. Soc., A, **67**, 190 (1954).
[4] R. J. Havens, R. T. Koll, and H. E. LaGow, J. Geophys. Res., **57**, 59 (1952).
[5] H. E. LaGow and J. Ainsworth, J. Geophys. Res., **61**, 77 (1956).
[6] H. K. Kallmann, J. Geophys. Res., **58**, 209 (1953).
[7] W. Heitler, The Quantum Theory of Radiation, 3rd ed., Oxford University Press (1954); p. 376, Table 12...
[8] M. S. Livingston and H. A. Bethe, Rev. Mod. Phys., **9**, 245 (1937).
[9] B. Rossi, High-energy Particles, Printice-Hall, Inc., Englewood Cliffs, New Jersey (1952); pp. 40–41.
[0] J. Knipp and E. Teller, Phys. Rev., **59**, 659 (1941).
[1] C. Störmer, The Polar Aurora, Oxford University Press (1955); equation (29.4), p. 296.
[2] R. A. Alpher, J. Geophys. Res., **55**, 437 (1950); equation (26), p. 444.
[3] D. R. Bates and H. S. W. Massey, J. Atmos. Terr. Phys., 2, 1 (1951).
[4] A. P. Mitra, J. Atmos. Terr. Phys., **10**, 153 (1957).
[5] M. A. Biondi, Phys. Rev., **84**, 1072 (1951).
[6] H. S. W. Massey and E. H. S. Burhop, Electronic and Ionic Impact Phenomena, Oxford University Press (1952); p. 643, Table 5.
[7] S. K. Mitra, *op. cit.*, p. 309.
[8] F. E. Roach, private communication (1957).
[9] S. K. Mitra, *op. cit.*, p. 545.
[0] D. R. Bates and H. S. W. Massey, Phil. Mag., **45**, 111 (1954).
[1] D. R. Bates, in The Earth as a Planet, edited by G. P. Kuiper, University of Chicago Press, Chicago (1954); p. 576. [Vol. 2, The Solar System.]
[2] S. Chapman, J. Geophys. Res., **55**, 361 (1950).
[3] D. R. Barber, J. Atmos. Terr. Phys., **10**, 172 (1957).
[4] J. Firor, Phys. Rev., **94**, 1017 (1954).
[5] R. Lüst, Phys. Rev., **105**, 1827 (1957).

STRESS-INDUCED MAGNETIZATIONS OF SOME ROCKS WITH ANALYZED MAGNETIC MINERALS

BY JOHN W. GRAHAM (1), A. F. BUDDINGTON (2), AND J. R. BALSLEY (2)

(1) *Department of Terrestrial Magnetism, Carnegie Institution of Washington, Washington 15, D. C.*
(2) *U. S. Geological Survey, Washington 25, D. C.*

(Received July 15, 1957)

ABSTRACT

Magnetostriction can be of major importance in interpreting measurements of the residual magnetism of rock samples. A description is given of the experimental procedures that were used to determine the influence of axial compression on the natural magnetizations of a variety of rock core samples whose magnetic minerals have been analyzed. Changing the stress from 350 to 2,650 psi caused a marked decrease in magnetic intensity of rocks containing magnetite or ilmenomagnetite, and a slight increase when the magnetic minerals are in the system $FeTiO_3$-Fe_2O_3 . Directions of magnetization also changed, in a non-systematic manner. Inasmuch as many rocks acquire magnetization while under directed stress and are relatively stress-free when their magnetizations are measured, these results are offered as support of the opinion that many conclusions that have been offered on the basis of rock-magnetism data, relating to polar wandering, continental drift, secular variation, and reversal of the earth's magnetic field, are subject to serious doubt.

INTRODUCTION

In earlier publications [see 1 and 2 of "References" at end of paper], the question has been raised of the possible role of stress in establishing directions of residual magnetization of rocks. The basic idea there set forth, probably in oversimplified form, was that if a rock is in a state of non-hydrostatic stress at the time it is magnetized, and subsequently this stress is released, then as a result of the property of magnetostriction, the initial direction of magnetization can become deflected to some other direction and changed in intensity. Rocks that possess such compound magnetizations cannot be expected to be useful immediately for investigating problems such as the history of the earth's magnetic field in geologic time, polar wandering, continental drift, etc. Some evidence was presented to show that rocks may be significantly magnetostrictive, but there was insufficient basis for deciding whether magnetostriction should be considered of major or trivial importance in the subject of rock magnetism.

The present paper reports and discusses some reconnaissance measurements in the laboratory that have been directed at the basic question of the influence of

stresses on the magnetizations of typical rocks. In a sense, this study can be regarded as preliminary to more extensive work because it leaves many questions unanswered, but in another sense, the study is basic in that it establishes that the residual magnetization of many rocks is sensitive to directed stress to far more than a trivial extent.

THE BASIC EXPERIMENT

It can be imagined that, under natural conditions, many rocks were magnetized while they were in a state of non-hydrostatic stress (that is, elastically deformed) and that these stresses are essentially relieved by the time the sample is freed for measurement. Simple examples are provided by intrusive igneous rocks which solidified and became rigid at temperatures above the Curie point and then became magnetic while under vertical load, and by sediments which, while under a considerable load of younger sediments, were magnetized by the earth's field during the precipitation of magnetic minerals out of solution. More complicated, and very important, examples would be found in tectonically active regions. Laboratory experiments to duplicate probable geologic conditions reflecting these circumstances and to study the effect of the release of stress would be difficult to perform. However, the incomplete experiment of observing the change of the magnetization when the rock is taken from the non-stressed to the stressed state is straightforward and instructive. Judging from other studies [3, chap. 13] which show the reciprocal relationships of tension and compression on magnetically strain-sensitive material, it is believed that this incomplete experiment gives a significant measure of how much change of magnetization the rock might have experienced in a natural process of unloading.

EXPERIMENTAL TECHNIQUES

New equipment has been constructed at the Department of Terrestrial Magnetism specifically for these experiments. It consists of an astatic magnetometer and a device for applying axial compression to the sample while its magnetization is being observed.

It was planned originally to follow the elegant procedures of Blackett [4] to achieve high sensitivity and stability in the astatic magnetometer, but the requirements for a suitable foundation, temperature control, small magnetic field gradients and disturbances, etc., could not be easily met. Accordingly, sensitivity was sacrificed for the sake of stability, thus precluding observations on sediments and other weakly magnetized rocks. In the present experiments, observations were limited to samples whose natural magnetic moment exceeded 10^{-4}cgs/cc. Specimens were in the form of cylinders, an inch long by an inch in diameter. At a distance of 4 inches below the lower magnet of the suspension, the magnetic meridian of the sample could be located with an uncertainty of about 1/4°, and changes of intensity of 1/2 per cent could be detected.

Construction details of the magnetometer are as follows: Two magnets, 4-mm diameter by 10 mm long, of modified Ticonal X (ref. 5,*) at a spacing of 15 cm on a Lucite stick; trimmer magnets of Vicalloy wire to make it astatic; 25-cm quartz fiber; Lucite housing and lens support; copper damping plate below lower magnet;

*The kindness of Dr. K. J. de Vos in supplying these magnets is gratefully acknowledged.

optical path length 8 meters long (lamp to image). For nulling the earth's magnetic field at the magnetometer, two sets of Fanselau coils about 2 meters diameter maximum are used, one with a vertical axis, the other parallel to the meridian; current for Fanselau coils is from an electronic supply regulated to 1/10 per cent.

Axial compressive stress is applied to the sample by a device patterned after a nutcracker. Non-magnetic construction material was selected with care and tested in place. The sidearms are of 1½-inch Dural tube, and the force is applied to the sample by 1-inch diameter Lucite rods, which bear on pivots on the sidearms. The tension member adjacent to the sample is of 1-inch diameter Bakelite-impregnated cloth rod. The mechanical advantage of the nutcracker is 10 to 1; the ends of the sidearms are drawn together by a bronze turnbuckle. A measure of the force applied to the sample is given by a deflection gauge which shows the bending of one sidearm. Calibration is linear throughout the range of use. This device has been fully satisfactory for stresses up to 2,650 psi, but a different design would be needed for much greater values and further studies. It provides stress that is about the same as would be acting at the base of a column of rock only 2,000 feet high.

The cylindrical sample with its axis horizontal in the nutcracker is held centered below the magnetometer by a Lucite block that pivots about a vertical 2-inch diameter Lucite support piston. The azimuth of the sample is read to 1/4° by a plumb-line on an 8-inch diameter graduated circle, mounted at the top of the support cylinder. Vertical travel of 10 inches is controlled hydraulically at the reading scale by another cylinder-piston combination having a 30-inch stroke. The reset accuracy on a vertical setting can be a fraction of a millimeter; this is adequate to permit intensity comparisons to better than 1 per cent when samples are placed as close as 4 inches below the lower magnet.

The following method has been used to determine the direction of magnetization of a sample. The sample is mounted in a cubical holder following an adopted convention regarding orientation. For convenience, the holder is marked to indicate three particular orthogonal positions in which the orientations of the various components of magnetization are measured; these then are plotted on a projection net and solved graphically for the orientation of the magnetization axis. An estimate of the precision is given by the mutual consistency of the measurements. The axis of the strongly magnetized samples used in this study could be located with negligible uncertainty, and some comparisons made with induction-type magnetometers have confirmed the measurements.

The azimuth of an individual component is determined by revolving the sample in an exploratory way below the magnetometer until it is observed that the sample and the suspension are turning as if coupled together; the senses of magnetization of the sample and the lower magnet are now anti-parallel. The criterion that the magnetic meridian of the sample lies directly below the poles of the lower suspension magnet is met when it is possible to elevate the sample towards the lower magnet at its normal equilibrium position without causing a deflection (barring effects arising from the susceptibility of the sample). The angular position in which to place the sample for this condition can be determined (with the present samples to 1/4°) by making a plot of the magnetometer deflection *vs* azimuth setting with the sample kept at constant height; the desired angle is read off the curve at the scale reading given by the magnetometer with the sample absent.

Even though the magnetometer has not been calibrated for the measurement of absolute intensities of magnetization, it is immediately useful for comparison measurements. At the distance of 4 meters from the magnetometer mirror, a full-scale (40 cm) deflection of the light-spot corresponds to only a 3° rotation of the suspension. Hence, at a given height, with the magnetic meridian of the sample turned 90° from the zero position, the deflection is very nearly proportional to the horizontal component of the moment. Absolute intensities reported in this study were measured with an induction-type magnetometer.

The following procedure was used for measuring the influence of axial compression on the magnetization of samples. First, the orientation of the magnetic axis relative to the core axis and a scribe-line on the wall of the cylinder was determined. With this information, it was then possible to mount in the nutcracker the sample with its magnetic axis horizontal so that the total intensity could be measured by the magnetometer. To hold the sample and the nutcracker securely together at the start of the measurements, it was necessary to apply a compression of 350 lbs/in^2; further increase of compression caused no shift of the sample relative to the magnetometer. This practice was used on all samples, and changes produced by compression are considered here to have started from this initial setting. After having located the position of the magnetic meridian under these conditions, the sample and nutcracker were then turned 90° to produce the maximum magnetometer deflection, and the height was adjusted to give nearly a full-scale deflection. The total amplitude was read several times at two positions, 180° apart. Promptly, then, the turnbuckle was tightened to give a compression of 2,650 lbs/in^2, all the time the sample remaining in position for measurement (that is, in a region essentially free from a magnetic field). The readings were then made on the stressed sample at the same vertical setting as was used originally. Finally, the sample was removed from the magnetometer in order to read the instrument zero.

THE SAMPLES SELECTED FOR STUDY

For a number of years, the U. S. Geological Survey has fostered research on the problem of correlating the aeromagnetic and geologic data that have been gathered in the area of the Adirondack Mountains of upper New York State. The studies have emphasized the highly crystalline metamorphic Precambrian rocks that are extensively developed there [6]. As one part of the work, the magnetic ingredients of a large number of samples have been subjected to mineralogical and chemical analyses; from this suite of rocks, the present samples were selected on the basis of the variety of compositions represented rather than on the basis of their numerical importance as found in the field.

Table 1, with its appended explanation, summarizes data that are pertinent to these samples; bulk compositions of the magnetic ingredient are plotted in Figure 1. The following analytical procedures were used: The rock samples were crushed and the iron and iron-titanium oxide minerals separated from the silicates and other minerals by floatation in heavy liquids and by magnetic separation. The oxide minerals were then in turn separated into a strongly magnetic fraction (magnetite and ilmenomagnetite) and a weakly magnetic fraction (oxides of $FeTiO_3$-Fe_2O_3 system). Each fraction was then analyzed chemically and the chemical analyses recalculated in terms of total Fe_3O_4 and total oxides of the $FeTiO_3$-Fe_2O_3

Sample	Wt, per cent calculated as Fe_3O_4 in magnetite of rocks	Wt, per cent calculated as Fe_2O_3-FeO·TiO_2 system of magnetic oxides in rocks	Mineralogy (phases observed on polished surface)								Remanent magnetic moment[3]	Rock
			Mt	iMt	fIl	ifsMt	stHm[1]	tHm[1]	iHm	hIl		
A*(16)	77.90	.....	Excl	...	...	...	...	...	...	...	30.2	Magnetite ore
B (129)	2.90	2.87	...	Maj	Maj	....	...	...	...	...	4.6	Slightly garnetiferous pyroxene diorite gneiss
C (108)	2.70	0.88	...	Maj	Maj	...	...	...	...	...	3.7	Hornblende granite gneiss
D (107)	6.95	3.38	...	Maj	Maj	...	...	...	Li	...	1.4	Quartz-microcline granite gneiss
E (133)	2.05	6.39	...	...	Maj	Min	...	...	...	...	0.15	Garnetiferous pyroxene-oligoclase granulite
F (47)	57.50	.....	Excl	...	...	...	...	...	...	...	69.1	Magnetite ore
G (123)	0.10	5.25	Tr	...	...	...	...	...	Pred	Min	7.7	Pyroxene-plagioclase hornfels
H (98)	2.58	3.60	Maj	...	...	...	...	...	Pred	...	3.8	Pegmatite veined biotite quartz-plagioclase gneiss
I (87)	...	6.45	...	...	...	...	...	Excl	...	...	4.0	Pegmatite veined hornblende quartz-microcline-plagioclase gneiss
J[2] (56)	1.56	2.58	Maj	...	Maj	...	...	...	...	Li	...	Garnetiferous biotite quartz-plagioclase gneiss
K (162)	0.03	0.47	Tr	...	Pred	...	...	...	...	...	0.8	Hornblende-plagioclase gneiss; amphibolite
L (114)	19.82	21.73	Maj	...	...	...	Maj	...	...	...	5.7	Magnetite-subtitanhematite ore
M (242)	5.07	0.48	Pred	...	Tr	...	...	...	...	...	0.6	Hornblende microperthite granite
N (134)	...	0.49	...	Tr	Excl	...	...	...	...	...	0.1	Hornblende microcline granite gneiss

*The numbers following the letters are the original field numbers.
[1]stHm and tHm can be distinguished only by chemical analysis.
[2]The sample is so inhomogeneous that mineral analysis may not correspond to core sample stressed.
[3]In units of 10^{-3} cgs/cc.

Explanation of Table 1

Excl = nearly exclusive (97-100 per cent); *Pred* = predominant (75-97 per cent); *Maj* = major (35-75 per cent); *Min* = minor (10-34 per cent), *Li* = little (3-10 per cent); *Tr* = trace (0-3 per cent). *Mt* = magnetite; *iMt* = ilmenomagnetite (magnetite with microintergrowth of exsolved ilmenite); *ifsMt* = ilmenoferrous magnetite (magnetite with microintergrowths of both ilmenite and a little ulvöspinel); *fIl* = ferricilmenite (ilmenite with 6 per cent or more of Fe_2O_3 in solid solution); *hIl* = hemoilmenite (ferricilmenite with exsolved microintergrowths of hematite); *stHm* = subtitanhematite (hematite with 1.5 to 5 per cent TiO_2; as FeO·TiO_2, TiO, or both; in solid solution); *tHm* = titanhematite (hematite with 5-10 per cent TiO_2, as FeO·TiO_2 or TiO_2 or both, in solid solution); *iHm* = ilmenohematite (titanhematite with exsolved microintergrowths of ferricilmenite).

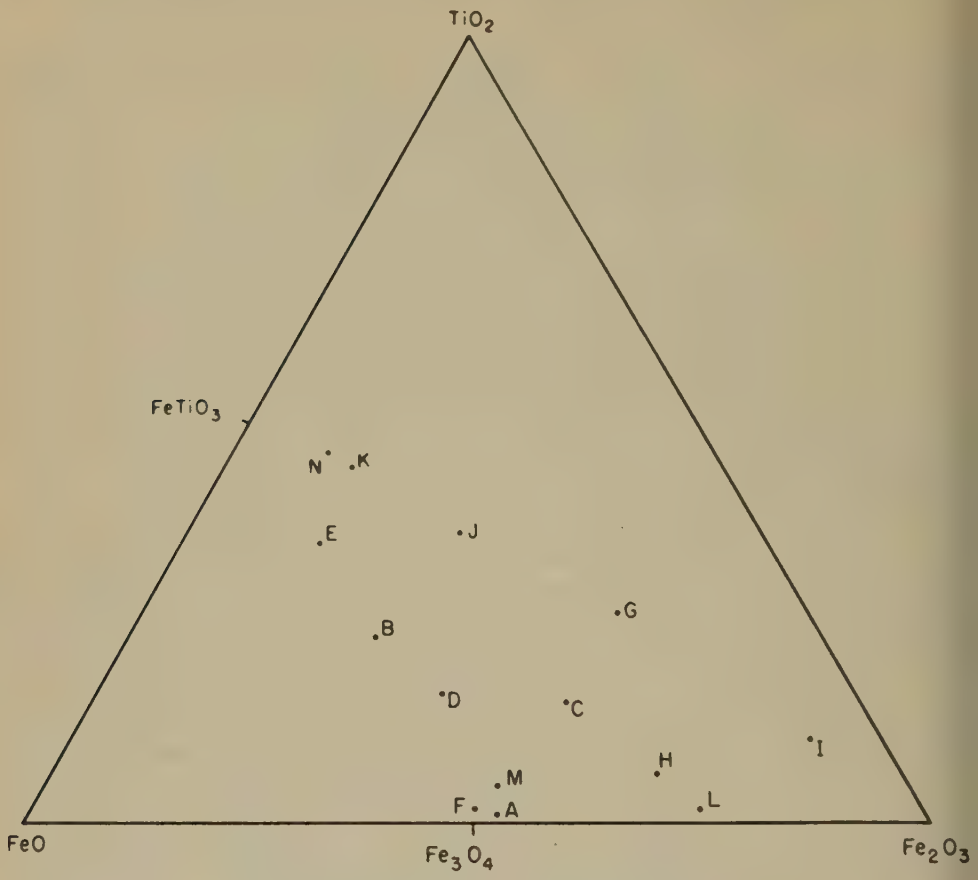

Fig. 1

system. In other words, the $FeTiO_3$ present in the strongly magnetic fraction is calculated and added to that of the weakly magnetic fraction. All mineral separations and chemical analyses were made by Joseph Fahey and Angelina Vlisidis of the U. S. Geological Survey. The nature of the oxides was checked by X-ray diffraction by Fred A. Hildebrand, also of the U. S. Geological Survey. Visual identification and evaluation of the opaque oxide phases were made by conventional observation techniques on polished surfaces at high magnification.

The magnetite and ilmenomagnetite occur exclusively as grains that are independent of the minerals of the Fe_2O_3-$FeTiO_3$ system. No magnetite has been found as exsolved microintergrowths in minerals of the Fe_2O_3-$FeTiO_3$ system.

With the exception of the ores *A* and *L*, and the granite *M*, all of the rock samples have a foliation and are gneisses inferred to have formed by recrystallization under stress at temperatures estimated to have been between perhaps 400° C and 600° C [7]. The magnetic minerals formed as solid solutions at this time. Since the metamorphism, the rocks have cooled through a period of scores of millions of years while erosion removed the original overlying rocks. The different magnetic

minerals of the rocks will thus have passed through their respective Curie points at very different times and under different loads. The exsolution of the microintergrowths must have taken place during an annealing process after the initial formation of minerals as solid solutions. The stress conditions during this history are unknown.

THE INFLUENCE OF COMPRESSIVE STRESS

Figure 2 summarizes the magnetic changes that were produced by increasing the axial compressive stress from 350 to 2,650 lbs/in^2. The results are plotted as vectors: the original intensity at 350 psi is taken as 100 per cent, and its angle relative to the direction of compression is plotted. The arrow end of the vector indicates the intensity and direction of magnetization of the stressed sample.

The measurements on these samples lead to the following generalizations, within the limitations of the experiments: Rocks containing either magnetite or ilmenomagnetite as their principal magnetic ingredient experience a reduction in intensity of magnetization on the application of axial compressive stress; in contrast, rocks with ferromagnetic minerals lying in the system $FeTiO_3$-Fe_2O_3 show an increase in magnetic intensity of smaller magnitude under the same conditions. Rocks containing a mixture of the two systems demonstrate an intermediate response. No simple rules can be formulated, from these measurements, for the orientation of the stress-induced vector of magnetic change, either relative to the stress axis, or to the original direction of magnetization.

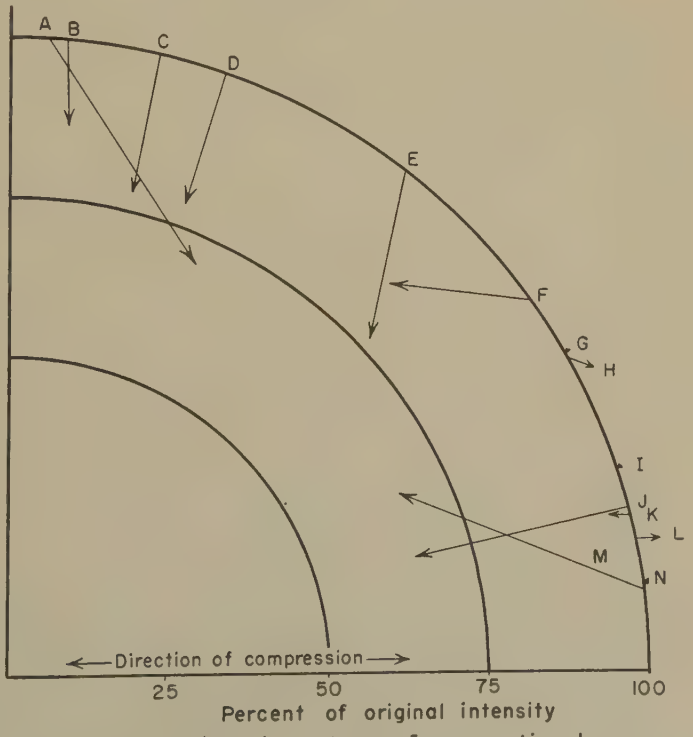

FIG. 2

THE QUESTION OF THE REVERSIBILITY OF THE STRESS-INDUCED VECTOR

For these observations, specimens were carefully selected for mechanical soundness. With the application of stress, none of them broke or showed any visible signs of damage. To an approximation, then, it can be said that they were not harmed by the experiment. And yet it was found that on the release of stress, some samples did not return to their original state of magnetization, either in direction or in magnitude. This effect was noted particularly in the case of samples containing a predominance of magnetite; it was not observed in samples of the $FeTiO_3$-Fe_2O_3 system. It is, of course, clear that the magnetization of any sample that is sensitive to cycling of directed stress is of little interest for the main purpose of rock magnetism.

It must be emphasized here that it is known that directed stress of a geologically important magnitude will not necessarily change the magnetizations of all rocks. Reference is made [8] to the magnetizations of a folded ferruginous Silurian sandstone at Pinto, Maryland. Here the angular relationship of the magnetization to the bedding is preserved throughout a complex fold. After the bed had been folded, it was transected by three sets of joints. Clearly, the forces that produced these joints did not cause important changes in the magnetization. How great these forces were is unknown.

THE LIMITATIONS OF THE PRESENT OBSERVATIONS

The scope of the present study was limited intentionally to the single basic question: do geologically reasonable non-hydrostatic stresses have any significant effect on the natural magnetizations of rocks? The answer is in the affirmative. All samples show a measurable sensitivity to stress-induced magnetic change—some greater than others—of sufficient magnitude that it must be taken into account when efforts are directed at the problem of explaining the natural magnetizations of rocks. It is now clear that any rock which was in a state of non-hydrostatic stress when it was magnetized, can be expected to have a modified magnetization when it is in the unstressed state. In the process of answering the basic question, a number of additional questions have come into view. These will afford abundant opportunity for further study.

The present observations are considered to be of little use in the challenging problem of attempting to eliminate, on the basis of adequate knowledge, the biasing effect of directed stress on the magnetizations. For one thing, the applied stresses, though producing significant magnetic effects, are far below the experimental elastic limit of rocks under confining pressures, and are far below the stresses which are known to have operated in nature. Additionally, all of the measurements have been made at room temperature without confining pressure. Under geological conditions, we can expect that changes of very large directed stress frequently took place at elevated temperature and under high confining pressure. The present observations give no basis for even guessing at the probable magnetic response of the rocks under these conditions, for in other studies [3, pp. 659 and 652] it has been shown that the magnitude of magnetostrictive changes can be a complex function of temperature. It is reasonable to expect that the magnetic ingredients of rocks may show similar characteristics. In the extreme, it can be imagined that at one

mperature a given rock would display one type of behavior, whereas at another mperature it would be distinctly different; self-reversal of the remanent moment ight result from such properties. For these reasons, the present observations are ot applicable to many interesting questions.

The present measurements do not provide adequate insight into the problem of xplaining the orientation of the stress-induced vector. It is seen that several amples show little change of magnetization direction with applied stress, and yet ther samples show a marked change. It seems reasonable that some of this com- lexity must be attributed to the elastic and dimensional anisotropy of the mineral ggregates. It is not known whether the unpredicability of the orientation of the tress-induced vector is characteristic of rocks in general, or merely of these samples particular. Clearly the problem deserves further study.

In the present work, no attempt has been made to carry out a systematic study f the possibility that stress-induced magnetization changes are time-dependent, ut some evidence suggests that this is so. In measuring the amplitude of the mag- etometer deflection produced by sample J while under stress, it was noticed that ver a 15-minute period of observation there was a quickly decelerating decrease in tensity amounting to 2 per cent of the original intensity. At the end of the 15 inutes, the accumulated decrease was 34 per cent of the original intensity. Sample was left for a two-week period under axial stress averaging 2,400 psi in the essen- ally field-free region below the magnetometer. Remeasurements at the end of is period showed an angular change of less than 1/4°, and a further intensity crease of 5.5 per cent. This added decrease with time is to be compared to the iginal decrease of 5 per cent when the stress was first applied. It is not known hether these two examples of time-dependent behavior are typical; the question ears investigation.

A puzzling effect, and doubtless one which merits careful study because of its heoretical and practical importance, was noticed with magnetite samples. It was bserved that if a sample, while under axial stress, was removed from the magneto- eter and exposed to the earth's magnetic field (for a minute or two) and then turned to the magnetometer, still under stress, there was an evident change in he magnetization. It seems that the response of some samples to stress depends not n stress alone, but also on weak applied magnetic fields (the earth's field) as well as n natural magnetization of the sample. It can be anticipated that this is a complex roblem, because the theories treating the behavior of magnetic materials in weak elds are inadequate and rocks are not made of simple materials.

AN APPRAISAL OF THE FUTURE OF ROCK MAGNETISM

It is worth while to make an estimate of some of the ways in which these findings an be related to what is known of the problem of the magnetization mechanism f rocks. The various ferromagnetic minerals that have been recognized in rocks re known to cover a considerable spread in the numerical values that can be ssigned to measurable properties; that is, Curie point, saturation magnetization, usceptibility, variation of various properties with temperature, etc. It is rare that n any given rock a single magnetic species occurs; in general, two or more coexist, nd they may be intimately intermingled or remotely separated as discrete units. Depending on the state of aggregation, there may be considerable, or little, magnetic

interaction of the different species on one another. At the time of formation, some ferromagnetic minerals may appear as metastable single phases which slowly during geologic time may break down into a mosaic of two or more mineral species. Some ferromagnetic minerals are prone to marked alteration by the simple process of oxidation. It is known that all of these features are important in the subject of rock magnetism. To this already complicated picture, we now add the question of the influence of stress. The reconnaissance measurements indicate that stresses, which geologically speaking are almost trivial, can have a marked influence on the magnetization. The response of the magnetizations to stress is such as to indicate that different species present are making different types of contributions to the change of the magnetization. It is likely that in a given sample it would be possible to describe the relative magnetostrictive contributions of the different ferromagnetic species present, but such knowledge gained today would not necessarily have any meaning to the problem of greater interest which we have had in view, namely, of attempting to infer the past directions, not to mention intensity, of the earth's magnetic field. This is so for two simple reasons: that we can give neither an accurate account of the stress history of the rock nor of the chemical and physical evolution of the magnetic species. It is, of course, clear that the older the rock, the greater will be the uncertainty. The only obvious way out of these difficulties is to have so many field observations from so many rocks of so many types in so many settings that the insidious influence of magnetostriction, either taken alone or in conjunction with (other?) time-dependent parameters, is eliminated. This is hardly an encouraging prospect.

The ultimate geophysical implications of these observations are not yet known, but they certainly do not further the hope that has prevailed for decades that by way of the techniques of rock magnetism it will be possible to deal effectively with such major geophysical questions as continental drift and polar wandering. The present observations do not assure that such hopes are beyond reach; however, they call for great caution in accepting rock-magnetism data, of the sort usually presented, as evidence bearing satisfactorily on major geophysical phenomena.

References

[1] J. W. Graham, Paleomagnetism and magnetostriction, J. Geophys. Res., **61**, 735-739 (1956).

[2] J. W. Graham, The role of magnetostriction in rock magnetism, Adv. Phys. (Quarterly supplement of Phil. Mag.), in press.

[3] R. M. Bozorth, Ferromagnetism, D. Van Nostrand Co., Inc., New York (1951).

[4] P. M. S. Blackett, A negative experiment relating to magnetism and the earth's rotation, Phil. Trans. R. Soc., A, **245**, 309-370 (1952).

[5] A. I. Luteijn and K. J. de Vos, Permanent magnets with $(BH)_{max}$ values over ten million gauss oersteds, Philips Res. Rep., **11**, 489-490 (1956).

[6] J. R. Balsley and A. F. Buddington, Remanent magnetism of the metamorphic rocks of the Border Belt, Adirondack Mountains, New York, Adv. Phys. (Quarterly supplement of Phil. Mag.), in press.

[7] A. F. Buddington, J. Fahey, and A. Vlisidis, Thermometric and petrogenic significance of titaniferous magnetite, Amer J. Sci., **253**, 497-532 (1955).

[8] J. W. Graham, The stability and significance of magnetism in sedimentary rocks, J. Geophys. Res., **54**, 131-167 (1949).

GEOMAGNETIC AND SOLAR DATA

INTERNATIONAL DATA ON MAGNETIC DISTURBANCES, FIRST QUARTER, 1957

This report continues the series which has appeared regularly in this JOURNAL nce Vol. 54, No. 3, 295 (1949). Please refer to that first report for an explanation the data given, and to Vol. 59, No. 3, 423 (1954) for the definition of *Ap*.

Preliminary Report on Sudden Commencements

S.c.'s given by five or more stations are in italics. Times given are mean values, th special weight on data from quick-run records.

Sudden commencements followed by a magnetic storm or a period of storminess (s.s.c.)

1957 January *02d 09h 10m*: forty-three.—21d 08h 00m: Si Me Ci SM.—*21d 12h m*: forty-one.—24d 10h 16m: Ci Hr (s.f.e.: Te Tn).—*24d 19h 10m*: thirty.—*d 13h 13m*: forty.

1957 February *04d 00h 03m*: six (s.f.e.: Si).—04d 11h 00m: V1 Ci.—*12d 18h m*: thirty-seven (s.f.e.: Si).—*13d 09h 39m*: twelve.—*23d 18h 07m*: forty-three.

1957 March *01d 16h 14m*: twenty-five.—*10d 00h 23m*: forty-four.—*15d 19h m*: seven.—*25d 01h 30m*: twenty-two.—*26d 10h 49m*: nine.—*27d 11h 36m*: neteen (s.f.e.: Te).—28d 04h 12m: Db? Ma?.—*29d 03h 36m*: forty-five.—*29d h 15m*: fifteen.

Sudden commencements of polar or pulsational disturbances (p.s.c.)

1957 January 01d 11h 11m: Ap To Am.—02d 22h 21m: V1 Cm.—06d 04h 52m: Te (s.f.e.: Tn).—06d 17h 00m: Ag SM.—06d 23h 11m: Hb IK.—*08d 00h 48m*: enty-one.—08d 20h 51m: Hb Ta.—09d 18h 58m: Wn Cm Fu Pr.—10d 05h 56m: e Ag.—*10d 23h 27m*: nine.—11d 23h 16m: Fu CF T1.—12d 21h 44m: So Bi.—d 23h 06m: Fu IK SM.—*15d 23h 20m*: six.—16d 12h 23m: Me Ap.—16d 20h 07m: Do Fu Hb.—17d 19h 19m: Fu CF.—19d 15h 17m: Ka Wa To Am.—21d 19h n: Fu Eb.—21d 22h 05m: Fu Eb.—23d 18h 19m: Wn V1 Hb IK.—*25d 20h 57m*: enty-one.—26d 21h 22m: So Do SM.—*31d 22h 12m*: nine.

1957 February 02d 17h 33m: So Do Qu.—02d 21h 46m: Tr So Do.—03d 12h m: Me Cm.—*03d 20h 23m*: seven.—06d 00h 42m: V1 T1.—09d 20h 43m: Do n Fu Qu.—09d 23h 39m: Fu Eb.—11d 02h 33m: Eb T1.—11d 16h 00m: IK Ka a Wa.—11d 16h 25m: Le Es V1.—*12d 07h 13m*: five.—14d 08h 32m: Me Ag.—*d 21h 26m*: five.—*15d 21h 38m*: eight.—18d 18h 19m: Es V1 T1 Te.—19d 18h m: Wn V1.—*19d 22h 10m*: five.—*20d 21h 20m*: sixteen.—21d 01h 29m: Fu Hb.—d 05h 22m: Ag Te.—22d 22h 41m: Pr Eb T1 Ta.—24d 07h 02m: Es V1 Cm Hr.—d 08h 37m: Te Ap.

TABLE 1—*Geomagnetic planetary three-hour-range indices Kp, preliminary magnetic character-figures C, average amplitudes Ap (unit 2γ), and final selected days, January to March, 1957*

January 1957									
E	1	2	3	4	5	6	7	8	Sum
1	0+	1−	1−	4−	3o	2o	2−	1−	13−
2	2+	2−	2+	5o	3−	2+	5+	5o	27−
3	4−	3−	2+	3o	2+	1+	1+	2−	18+
4	1+	2−	2o	2o	1−	1o	1−	1o	10+
5	1o	1o	1o	2−	1o	1o	2−	1−	9o
6	0o	3−	2−	2+	2o	1+	2−	2o	14−
7	2o	2o	2o	3−	3−	2o	1+	0+	15o
8	3−	3+	2o	4−	3+	3−	3−	3o	23+
9	2o	2o	2−	2−	3+	4−	3o	4−	21o
10	3+	4+	5o	4o	4o	4o	4+	5−	34−
11	4o	2−	4o	4−	4−	1o	2−	2o	22−
12	2+	4o	2o	1+	0+	0+	0+	1+	12o
13	2o	1−	1+	2−	1o	1o	1−	1+	10−
14	0+	0+	2−	2−	2−	1o	1−	0+	8−
15	1+	1o	1+	2−	3−	2+	2+	2o	15−
16	2+	2o	2o	2o	3o	1+	1+	1+	15+
17	2o	1+	1+	2o	2o	2−	2−	1+	13+
18	1o	0+	1+	1o	1o	1−	0+	0o	6−
19	0o	0+	2−	2+	2+	3+	2o	1+	13+
20	2−	1+	1−	1o	1+	1+	1−	0+	8+
21	2−	3+	4−	4−	5−	6−	8−	9−	39o
22	8+	7−	6+	5−	4o	4o	3o	2+	39+
23	3o	4−	4+	5o	4o	4−	4o	3+	31o
24	4o	5−	2−	3−	3+	3−	5+	5o	29+
25	5o	4−	5−	3o	2o	2o	2+	4o	27−
26	2+	3o	3−	3+	3−	3−	2−	3o	21+
27	2o	3−	2o	4o	3+	3−	2o	2−	20+
28	1−	2+	2−	1+	2o	2−	2+	2+	14+
29	1+	2+	2o	3−	5o	5o	4+	4o	27−
30	5o	6−	5+	5−	4−	3+	4−	3−	34o
31	2o	3o	3−	3−	3−	3o	3−	3−	21+

February 1957									
1	2	3	4	5	6	7	8	Sum
2o	2o	1+	3−	1+	2−	2o	1o	14o
1−	2o	2−	2o	3o	3−	3o	2+	17+
2−	2+	1−	1o	2o	2+	4−	4+	18o
4o	3+	3o	4−	5o	4+	4+	5+	33o
5o	6o	5−	5−	5o	4−	3o	3+	35+
3o	2+	3+	3−	2+	2−	1+	1o	18−
0o	1−	2−	3−	1o	1+	1+	2−	10+
2−	2o	3−	2−	2−	2−	2−	2o	15o
2o	3o	2−	1+	1o	1+	2o	2o	14+
3−	1o	1+	3−	0+	0+	0+	1−	9+
2−	2+	2−	2+	2+	4−	2o	2−	18−
2+	4+	3+	3−	2o	2o	4−	3−	23o
3+	5−	4−	5o	5+	5o	6+	3+	37−
3−	3−	3o	2−	1+	1o	1+	1−	14+
0o	1o	3+	4−	3o	3o	2−	3o	19−
0+	2−	2+	2o	2o	3−	2+	2o	15+
2o	1+	1o	3−	3+	3−	3−	3o	19−
3+	3o	3o	3o	3o	3o	4−	4−	26−
4−	3o	4o	3+	3−	3+	5−	4+	29o
4+	4o	3o	3−	3+	2+	2o	3+	25o
4o	4o	5+	4+	4o	5−	4−	5o	35o
4+	4+	4o	4−	4−	4−	3o	3+	30o
4−	4−	3o	2o	3−	3o	6o	6o	30o
7o	7o	6o	6o	5−	3−	3−	2o	38o
3o	3−	2+	3+	2−	1o	1−	0+	15o
2−	0+	1−	1o	1o	1o	1o	1+	8o
3−	3o	1+	1+	0o	1−	1+	1o	11+
1−	0o	0+	1o	1+	1+	1o	1o	7−

March 1957									
E	1	2	3	4	5	6	7	8	Sum
1	1−	1o	1+	2−	3+	4o	4o	5−	21−
2	6o	8+	8+	7o	7−	5+	6+	7−	55−
3	5o	5+	5+	3+	3o	4+	3+	3−	32+
4	4−	4o	3o	3−	3−	1−	2−	3o	21+
5	4−	3+	3o	3−	3+	3−	3+	3+	25+
6	4+	2o	2+	3o	3+	3+	2+	2−	22+
7	2−	2+	1+	2+	2+	3+	2+	2+	18o
8	4o	2−	3o	2o	3o	2o	3o	4o	23−
9	3+	4+	3+	2o	2+	3+	3o	3o	25−
10	4o	4+	5−	7−	7o	6o	6+	6−	45−
11	4o	3−	2+	1o	2o	1+	1o	1o	15+
12	2o	3+	3o	3−	2−	1o	0+	0o	14o
13	0+	1+	2o	3o	2+	4−	2o	2+	17o
14	1o	1−	1+	2+	1−	1+	0+	1−	8+
15	2+	2−	2o	2−	1+	2−	3−	4+	18+
16	5o	4+	4+	2+	3o	4−	6o	5+	34o
17	3−	3+	3+	2+	3o	4o	2+	3−	24−
18	2o	3o	2+	3+	4o	2−	2+	3−	21+
19	2+	2−	3−	3−	3−	2o	3o	3o	20o
20	3+	4−	4−	3−	1+	1o	2−	3+	21−
21	1+	3o	1+	1o	2+	5−	4+	5o	23o
22	4o	3o	4−	4−	4−	4−	3+	5−	30−
23	4+	4o	3o	4o	3o	3o	3−	2+	26+
24	3o	2o	2+	2−	1o	1o	4−	4−	18+
25	4+	6o	5−	5−	5−	2+	2−	1o	29+
26	1+	1+	1+	3o	4−	4−	2+	4−	20+
27	4+	4−	3o	4o	5−	4+	5+	7o	36+
28	7o	7−	6+	6−	3+	4o	2+	1+	37−
29	3+	5+	4+	4o	7o	8−	6+	6o	44o
30	6−	5−	3o	2−	2o	3−	2o	3+	25o
31	3o	3+	3+	3−	3o	4o	4+	4o	28−

Preliminary *C*, 1957			Average amplitude *Ap*		
Jan.	Feb.	Mar.	Jan.	Feb.	Mar.
0.3	0.3	1.0	8	7	16
1.3	0.5	2.0	25	9	132
0.6	0.9	1.2	10	12	32
0.1	1.4	0.7	5	31	14
0.1	1.3	0.8	4	39	17
0.3	0.4	0.9	6	10	14
0.3	0.2	0.6	7	5	9
0.9	0.2	0.8	14	7	15
1.0	0.2	0.9	13	7	16
1.4	0.2	1.9	31	5	73
0.6	0.7	0.4	15	9	9
0.3	0.9	0.3	7	15	8
0.1	1.6	0.6	5	43	10
0.1	0.4	0.0	4	8	4
0.4	0.6	0.7	7	12	11
0.3	0.3	1.4	8	7	37
0.1	0.7	0.8	6	11	15
0.0	1.0	0.7	3	17	13
0.4	1.2	0.7	7	23	11
0.1	0.9	0.7	4	17	13
1.9	1.3	1.0	82	35	20
1.8	1.0	1.2	70	24	23
1.3	1.4	0.9	26	32	19
1.2	1.5	0.6	27	62	11
1.1	0.3	1.2	22	9	31
0.6	0.0	0.8	12	4	13
0.6	0.1	1.5	12	6	44
0.2	0.1	1.6	7	3	58
1.4		1.8	24		77
1.3		1.0	36		21
0.6		1.0	f2		20

TABLE 1—(Concluded)—*Final magnetically selected days, January to March, 1957*

Month	Five quiet days	Ten quiet days	Five disturbed days
1957			
uary	5 13 14 18 20	4 5 6 12 13 14 17 18 20 28	10 21 22 23 30
ruary	7 10 26 27 28	1 7 8 9 10 14 16 26 27 28	4 5 13 21 24
ch	7 11 12 13 14	7 11 12 13 14 15 19 20 24 26	2 10 27 28 29

1957 March 01d 12h 44m: Sm Am.—03d 16h 52m: Es Eb Ta.— 03d 21h 29m: Ta.—04d 20h 36m: So Hb.—*06d 00h 02m*: sixteen.—06d 15h 55m: IK Ta —06d 16h 06m: Cm Hb.—07d 16h 24m: Do Cm Hb.—*07d 20h 28m*: nine.— *23h 53m*: eleven.—08d 18h 52m: So Qu.—*08d 23h 36m*: twenty-one.—*09d 17h* : six.—*09d 20h 53m*: eleven.—10d 23h 01m: Ks Ta.—15d 02h 28m: Eb T1 .—17d 13h 01m: Am To.—18d 03h 16m: T1 Sm.—18d 04h 10m: Ag Te.— 10h 36m: Me Hr.—18d 21h 07m: Do V1 E1.—19d 19h 25m: Hb E1.—19d 23h : Eb Ta.—20d 20h 56m: So Hb IK Qu.—*20d 21h 48m*: twenty-three.—22d 23h : T1 Ci.—*23d 20h 51m*: thirteen.—*24d 20h 31m*: eight.—26d 23h 40m: T1 SF E1.—27d 21h 39m: Wi Te.—*29d 02h 20m*: five.—*30d 23h 20m*: nine.—31d 15m: Tr Ta.

Sudden impulses found in the magnetograms (s.i.)

1957 January 03d 11h 01m: Ma Ks Hr.—*06d 19h 31m*: nine.—07d 00h 34m: IK Te.

1957 February 08d 15h 46m: Hu Va.—17d 10h 30m: So Cm Hb E1.—17d 22h : Hb IK Qu Hr.

1957 March *02d 05h 08m*: nine.—16d 05h 48m: Ma? Te.—16d 21h 12m: Tr Wi IK.

Preliminary Report on Solar-flare Effects

Effects confirmed by ionospheric or solar observations are in italics.

1957 January 01d 11h 39m: Cm.—02d 01h 36m: Ap.—*02d 12h 15m*: Es.— 11h 35m: Db(?).—*04d 15h 20m*: Es.—*05d 20h 22m*: Ho Hu.—06d 04h 53m: —*06d 11h 38m*: Es Ma(?).—06d 17h 00m–17h 48m: Tu Va Pi (p.s.c.: Ag SM).— 20h 21m: Ap.—07d 17h 26m–17h 54m: SJ.—*07d 17h 31m–18h 03m*: Hu Va .c.: Ag).—*10d 11h 00m–11h 30m*: Le V1 (s.s.c.: Ma).—*16d 09h 48m–10h 05m*: Es.—19d 09h 16m–09h 50m: E1 Tn.—*19d 10h 55m–11h 20m*: Le E1.—*20d 10h* : Es.—*21d 15h 13m–15h 35m*: Le.—*23d 10h 47m–12h 45m*: Le.—24d 10h 14m– 29m: Ci Te Tn (s.c.: Hr).—26d 14h 19m–14h 26m: Te.—26d 22h 27m–22h 33m: —*27d 07h 42m–08h 00m*: Tn Wa Hr.—*30d 09h 15m*: Es.

1957 February 01d 16h 57m: Hu.—04d 00h 03m: Si.—08d 14h 51m–15h 00m: —08d 15h 51m–16h 02m: Ch Hu Pi Hr(?) (s.i.: Va).—*10d 08h 14m*: Hr.—12d 50m: Si.—13d 22h 33m: Si.—17d 04h 31m–04h 41m: Tn(?).—17d 10h 28m– 55m: Te Tn (s.s.c.: So) (s.c.: E1).—22d 10h 17m–10h 21m: Te.—22d 11h 27m– 33m: Te.—22d 15h 09m–15h 19m: Te.—23d 08h 14m–08h 39m: Te.—*26d 13h* : Hu Hr(?).

1957 March 02d 17h 04m: Te.—03d 13h 46m: Te.—03d 15h 38m: Te.—07d

08h 00m: Tn(?).—09d 06h 50m: Tn(?).—10d 12h 53m: Te.—16d 18h 00m: Te.—17d 14h 39m: Te.—21d 15h 31m: Hu (s.i.: Te).—22d 20h 34m: Te.—26d 10h 50m: Bi.—27d 11h 35m: Te V1(??).—*29d 10h 26m*: Es.

Ionospheric or solar disturbances without clear geomagnetic effect

1957 January 08d 13h 40m–14h 00m: Hr.—10d 11h 12m–11h 30m: Hr.—20d 11h 00m–13h 00m: Hr.—24d 12h 40m–13h 00m: Hr.

1957 February: None.

1957 March: None

Minor disturbances reported by one station only are listed in the De Bilt quarterly circular, but omitted here.

Table 2—*Monthly mean values of Ci, Cp, and Ap*

Index	Jan. 1957	Feb. 1957	Mar. 1957
Mean *Ci*	0.67	0.70	0.96
Mean *Cp*	0.69	0.72	0.96
Mean *Ap*	17	17	26

Committee on Rapid Variations and Earth Currents
A. Romañá, *Chairman*, Observatorio del Ebro, Tortosa, Spain

Committee on Characterization of Magnetic Disturbances

J. Bartels, *Chairman*
University
Göttingen, Germany

J. Veldkamp
Kon. Nederlandsch Meteorologisch Instituut
De Bilt, Holland

ROVISIONAL SUNSPOT-NUMBERS FOR APRIL TO JUNE, 1957

ependent on observations at Zurich servatory and its stations at Locarno and Arosa)

Day	April	May	June
1	140	118	158
2	156	121	163
3	135	123	180
4	156	106	169
5	138	92	159
6	108	142	194
7	138	136	170
8	160	150	145
9	163	162	168
10	150	195	158
11	121	211	140
12	114	207	160
13	143	202	179
14	122	214	159
15	162	210	239
16	181	185	248
17	202	179	252
18	205	186	274
19	207	178	280
20	208	179	285
21	218	195	275
22	212	155	260
23	226	184	250
24	248	195	235
25	251	150	210
26	223	140	230
27	213	140	238
28	223	147	190
29	177	154	186
30	155	172	213
31		180	
ns....	175.2	164.8	205.6
days..	30	31	30

Mean for quarter: *181.7* (*91 days*)

M. WALDMEIER

SS FEDERAL OBSERVATORY
urich, Switzerland

FREDERICKSBURG THREE-HOUR-RANGE INDICES *K* FOR APRIL TO JUNE, 1957

[$K9 = 500\gamma$; scale-values of variometers in γ/mm: $D = 2.8$; $H = 2.6$; $Z = 3.0$]

Gr. day	April 1957		May 1957		June 1957	
	Values *K*	Sum	Values *K*	Sum	Values *K*	Sum
1	3443 3333	26	5434 2222	24	1111 2112	10
2	4123 2233	20	3333 3112	19	1211 1123	12
3	2133 2234	20	2214 2224	19	3333 4455	30
4	4322 3323	22	1223 3133	18	4443 2445	30
5	4235 5434	30	2211 2133	15	5333 2334	26
6	5444 1111	21	2325 3122	20	4455 2356	34
7	1111 1002	7	3432 2232	21	4212 1123	16
8	1222 2133	16	0233 3334	21	3431 2222	19
9	3443 3334	27	3433 3232	23	1211 1221	11
10	4465 4322	30	2322 2143	19	1001 0122	7
11	3224 4232	22	2222 2133	17	1111 1122	10
12	2331 2221	16	2111 1212	11	2121 2212	13
13	4342 2112	19	2223 2232	18	2112 2233	16
14	1100 0212	7	2311 2122	14	2211 2232	15
15	1222 3245	21	1001 2113	9	2322 2442	21
16	3323 2234	22	1010 1121	7	2021 2123	13
17	3423 5367	33	1322 2223	17	2332 3334	23
18	6333 2444	29	2211 2222	14	4442 2234	25
19	6664 4344	37	1111 2234	15	4523 4322	25
20	5432 2233	24	3443 3333	26	3422 2333	22
21	4433 2222	22	2333 3222	20	3433 2233	23
22	1011 1111	7	2222 2221	15	4224 3232	22
23	2322 3033	18	2231 2122	15	2112 3233	17
24	5424 3445	31	1123 2211	13	3333 2123	20
25	2112 2222	14	2333 3224	22	4334 4466	34
26	2344 4344	28	3544 3434	30	4565 5656	42
27	5333 3233	25	3333 2211	18	3234 3335	26
28	2232 2323	19	2132 2213	16	3334 4333	26
29	3322 2221	17	1232 1222	15	2122 2124	16
30	2422 2333	21	3135 4453	28	4657 6678	49
31			2513 2133	20		

ROBERT L. GEBHARDT
Observer-in-Charge

FREDERICKSBURG MAGNETIC OBSERVATORY
Corbin, Virginia, U. S. A.

PRINCIPAL MAGNETIC STORMS

(Advance knowledge of the character of the records at some observatories as regards disturbances)

Observatory (Observer-in-Charge)	Greenwich date	Storm-time		Sudden commencement				C-figure, degree of activity[4]	Maximal activity on K-scale 0 to 9			Ranges	
		GMT of begin.	GMT of ending[1]	Type[2]	Amplitudes[3]				Gr. day	Gr. 3-hr. period	K-index	D	H
					D	H	Z						
(1)	(2)	(3)	(4)	(5)	(6)	(7)	(8)	(9)	(10)	(11)	(12)	(13)	(14)
	1957	*h m*	*d h*		′	γ	γ					′	γ
College	Apr. 9	05 00	10 19	.....	.....	.....	.....	ms	10	3,4	7	200	1490
(C. J. Beers)	Apr. 18	15 00	20 00	.....	.....	.....	.....	ms	19	3	7	240	1490
	Apr. 21	04 00	21 20	.....	.....	.....	.....	ms	21	5,6	6	130	1000
	May	None											
	June 3	04 00	7 03	.....	.....	.....	.....	ms	3	7	6	200	1380
									6	2,3,4	6		
	June 25	00 45	27 03	s.c.*	−7	125	−7	ms	26	5	7	250	1510
	June 30	02 00	1 10	.....	.....	.....	.....	s	30	4	8	280	2280
Sitka	Apr. 5	10 ..	6 15	.....	.....	.....	.....	s	5	4	8	74	931
(J. E. Bottum)	Apr. 9	05 ..	10 21	.....	.....	.....	.....	s	10	2,3	8	179	1451
	Apr. 11	10 ..	11 16	.....	.....	.....	.....	ms	11	4,5	7	56	484
	Apr. 17	11 35	18 06	s.c.*	−10	+56	+15	ms	17	8	6	62	299
	Apr. 18	15 ..	20 13	.....	.....	.....	.....	s	19	3	8	96	1144
	Apr. 21	03 ..	21 19	.....	.....	.....	.....	ms	21	5	6	52	452
	Apr. 26	02 01	27 10	s.c.*	−1	+12	+4	ms	26	5,6	6	46	413
	May 8	17 ..	9 20	.....	.....	.....	.....	ms	9	2,3	6	47	365
	May 26	08 ..	27 08	.....	.....	.....	.....	ms	26	4,5	7	67	469
	May 30	08 23	31 06	s.c.*	−4	+5	+10	ms	30	4	6	41	371
	June 3	03 ..	7 03	.....	.....	.....	.....	ms	4	2	7	82	804
									6	3	7		
	June 18	18 ..	19 20	.....	.....	.....	.....	ms	19	1,2,5	6	37	593
	June 25	00 47	27 04	s.c.*	−3	+88	+9	s	26	3,4,5,6	8	179	1520
	June 29	23 46	1 10	s.c.*	−1	+28	+4	s	30	4	9	213	1660
									1	3	9		
Witteveen	Apr. 9	23 00	10 18	.....	.....	.....	.....	ms	10	2	6	30	190
(D. van Sabben)	Apr. 15	20 48	16 19	s.c.	−1	+38	0	ms	15	8	6	30	205
	Apr. 17	11 35	19 24	s.c.*	+5	+76	0	s	17	8	8	45	375
	May 30	08 22	30 22	s.c.*	+2	+27	0	ms	30	4	6	25	180
	June 3	08 00	4 05	.....	.....	.....	.....	m	3	4,5,6,7,8	5	25	145
									4	1	5		
	June 4	15 00	5 05	.....	.....	.....	.....	m	4	4,6,7,8	5	20	110
									5	1	5		
	June 5	14 00	6 07	.....	.....	.....	.....	m	5	8	5	25	135
									6	1,2	5		
	June 25	00 47	27 01	s.c.*	−4	+38	0	ms	25	4	6	30	285
									26	5,6	6		
	June 30	05 29	1 09	s.c.*	+6	+76	−4	s	30	6,7,8	8	75	730
Fredericksburg	Apr. 5	10 00	6 12	.....	.....	.....	.....	m	5	4,5	5	21	107
(R.E.Gebhardt)									6	1	5		
	Apr. 9	21 00	10 18	.....	.....	.....	.....	ms	10	3	6	30	116
	Apr. 15	20 48	19 10	s.c.	−2	+43	−3	ms	17	8	7	42	302
	May 29	08 22	31 06	s.c.	−1	+20	−1	m	30	4,7	5	28	124
									31	2	5		
	June 2	21 ..	6 12	.....	.....	.....	.....	m	3	7,8	5	26	145
									4	8	5		
									5	1	5		
									6	3,4	5		
	June 6	20 29	7 03	s.c.*	−2	+76	−10	ms	6	8	6	12	165
	June 25	00 47	27 01	s.c.*	+3	+45	−6	ms	25	7,8	6	30	290
									26	3,6,8	6		
	June 29	21 ..	1 09	.....	.....	.....	.....	s	30	8	8	41	514

[1]Approximate time of ending of storm construed as the time of cessation of reasonably marked disturbance movements in traces; more specifically, when the *K*-index measure diminished to 2 or less for a reasonable period.

[2]s.c. = sudden commencement; s.c.* = small initial impulse followed by main impulse (the amplitude in this case is that of *main impulse only*, neglecting the initial brief pulse); . . . = gradual commencement.

[3]Signs of amplitudes of *D* and *Z* taken algebraically; *D* reckoned positive if towards the east and *Z* reckoned positive if v cally downwards.

[4]Storm described by three degrees of activity: *m* for moderate (when *K*-index as great as 5); *ms* moderately severe (*K* = 6 or 7); *s* for severe (when *K* = 8 or 9).

PRINCIPAL MAGNETIC STORMS—Continued

vatory erver- harge))	Green-wich date	Storm-time GMT of begin.	Storm-time GMT of ending[1]	Sudden commencement Type[2]	Amplitudes[3] D	H	Z	C-figure, degree of activity[4]	Maximal activity on K-scale 0 to 9 Gr. day	Gr. 3-hr. period	K-index	Ranges D	H	Z
	(2)	(3)	(4)	(5)	(6)	(7)	(8)	(9)	(10)	(11)	(12)	(13)	(14)	(15)
	1957	*h m*	*d h*		′	γ	γ					′	γ	γ
White)	Apr. 9	04 ..	10 18	.....	.....	.....	.....	ms	10	3,4	6	15	172	72
	Apr. 15	20 48	16 12	s.c.	−2	+25	+	m	15	8	5	14	62	39
	Apr. 17	11 36	20 09	s.c.	+1	+46	+2	ms	17	8	7	31	245	59
									18	1	7			
	May 30	08 22	31 06	s.c.*	+1	....	+2	m	30	4	5	16	97	26
	June 3	03 ..	6 12	.....	.....	.....	.....	m	3	7,8	5	19	108	71
									6	3	5			
	June 6	20 29	7 08	s.c.*	+1	−9	−	m	6	8	5	10	121	25
	June 25	00 46	28 15	s.c.*	+	−4	−	m	25	1,4,7,8	5	18	135	53
									26	3,4,5,6	5			
	June 29	21 ..	1 12	.....	.....	.....	.....	ms	1	3	7	27	333	132
	June 30	05 28	.. ..	SD*	−2	−3	+3							
*(*Note*: SD indicates sudden displacement during storm not believed to be start of new storm)														
n quez)	Apr. 17	11 36	19 12	s.c.	+1	+15	−5	ms	17	8	6	17	194	65
									18	1	6			
	May	None												
	June 30	05 30	1 09	s.c.	+0	+48	−14	ms	30	4,8	6	24	275	66
	Apr. 9	22 00	10 17	.....	.....	.....	.....	ms	10	3	6	5	160	35
leven)	Apr. 17	11 37	20 12	s.c.	0	+34	+18	ms	17	8	6	10	235	90
									18	1	6			
	May	None												
	June 25	00 48	27 07	s.c.	0	+10	+8	m	26	1,2,4	5	8	130	100
	June 30	05 29	1 22	s.c.	−1	+26	+22	ms	30	8	6	10	240	75
ville/	Jan. 21	12 56	21 24	s.c.	−1	+53	−3	s	24	7,8	...	22	492	62
ndre)	Feb.	Pas d'orage important												
	Mar. 1	16 16	2 24	s.c.	−0	+47	....	ms	2	3,4	...	23	286	45
	Mar. 10	00 22	10 24	s.c.	−2	+35	....	s	10	4,5	...	22	342	43
s	Apr. 3	22 49	4 00	s.c.	(polar bay)			m	3	8	5	....	....	....
jk)	Apr. 5	09 ..	6 12	.....	.....	.....	.....	m	5	4	5	24	87	98
									6	1,2	5			
	Apr. 9	20 ..	10 20	.....	.....	.....	.....	m	10	2,3	5	14	124	68
	Apr. 17	11 36	20 04	s.c.	+3	+34	+34	ms	17	8	6	31	200	136
		(*Note*: Small initial impulse in *D*)							18	1,6	6			
									19	1	6			
	Apr. 27	00 27	27 06	s.c.	(polar bay)			m	27	2	5	....	....	....
	May 30	08 22	31 06	s.c.*	−3	+6	−4	ms	30	4	6	15	131	67
		(*Note*: Small initial pulses, positive in all three elements)												
	June 3	02 ..	7 03	.....	.....	.....	.....	m	3	7	5	17	103	100
									4	8	5			
									5	8	5			
									6	2,7	5			
	June 18	18 ..	19 19	.....	.....	.....	.....	m	18	8	5	....	....	....
		(*Note*: Minor disturbances, including polar bay)												
	June 25	00 47	27 01	s.c.	+2	+16	+18	m	25	4,8	5	23	162	101
									26	2,3,4	5			
	June 30	05 28	1 10	s.c.	+6	+23	+25	ms	30	4	7	43	265	195
		(*Note*: Initial negative impulse in *D*)												
	Jan. 21	12 45	23 11	s.c.	−1	+57	−7	s	21	7,8	...	11	510	56
)	Jan. 29	13 14	30 20	s.c.	−1	+21	−1	m	29	5,6	...	9	191	38
	Feb. 13	9 39	14 08	s.c.	−1	+20	−3	m	13	6,7	...	14	118	39
	Feb. 23	18 07	24 14	s.c.	−1	+46	−4	m	23	7	...	8	159	28
	Mar. 2	05 08	3 08	s.c.*	−0	+12	−1	ms	2	3	...	11	281	51
	Mar. 10	00 22	11 02	s.c.	−1	+34	−1	ms	10	4	...	9	324	39
	Mar. 27	11 37	29 00	s.c.	−1	+18	−2	m	27	7,8	...	6	219	30
	Mar. 29	03 35	30 04	s.c.	−1	+46	−1	m	29	5	...	7	162	30
	Apr. 9	21 00	11 16	.....	.....	.....	.....	ms	10	6	6	16	142	109
lott)	Apr. 17	11 36	20 05	s.c.*	+3	+42	+12	s	18	1	8	36	216	193
	May 30	08 22	31 01	s.c.*	+1	+6	+1	m	30	4	5	10	86	62
	June 25	00 46	26 24	s.c.*	−3	−6	−11	ms	26	5	6	20	216	165
	June 30	05 29	1 10	s.c.*	+4	+20	+18	s	30	7	8	38	188	294

PRINCIPAL MAGNETIC STORMS—Concluded

Observatory (Observer-in-Charge)	Greenwich date	Storm-time GMT of begin.	Storm-time GMT of ending[1]	Sudden commencement Type[2]	Sudden commencement Amplitudes[3] D	H	Z	C-figure, degree of activity[4]	Maximal activity on K-scale 0 to 9 Gr. day	Gr. 3-hr. period	K-index	Ranges D	H
(1)	(2)	(3)	(4)	(5)	(6)	(7)	(8)	(9)	(10)	(11)	(12)	(13)	(14)
	1957	*h m*	*d h*		′	γ	γ					′	γ
Toolangi	Apr.	None											
(I. B.	May	None											
Everingham)	June 25	17 00	27 02	.....	.....	.....	.....	m	26	5	7	38	234
	June 30	05 27	.. ..	s.c.*	+3	−54	−2	ms	..	....	...	....	....
				(*Note*: Storm in progress)									
Amberley	Apr. 9	05 05	10 17	s.c.	.....	.....	.....	ms	10	3	6	29	144
(A. L.	Apr. 17	11 36	20 11	s.c.	+2	+58	−10	m	17	8	5	20	158
Cullington)									18	1	5		
	Apr. 18	15 08	20 11	s.c.	+1	+20	−4	m	19	3,4	5	24	148
	Apr. 26	10 26	27 06	s.c.	−0	−16	+2	m	26	5	5	15	87
	May 30	08 24	31 00	s.c.*	+1	+31	−4	m	30	4	5	18	100
	June 25	00 46	26 18	s.c.*	+1	+16	−3	m	26	2,4,5,6	5	28	190
	June 30	05 29	1 11	s.c.*	−7	+97	+24	ms	30	5,6,7	6	41	315
				Reports added in galley-proof:									
Instituto	Apr. 5	10 33	6 06	.....	.....	.....	.....	ms	5	5,6	6	10	395
Geofisico de	Apr. 9	04 30	10 18	.....	.....	.....	.....	m	10	6	5	6	324
Huancayo	Apr. 17	11 37	19 20	s.c.	−2	+35	−5	ms	17	5,7	6	9	508
(A. A. Giesecke,	May 26	03 00	26 21	.....	.....	.....	.....	ms	26	6	6	5	253
Jr.)	May 30	08 22	30 19	s.c.	0	+18	−3	m	30	4,5	5	4	296
	June 3	04 57	4 06	.....	.....	.....	.....	m	3	6,7	5	5	278
	June 25	00 45	26 23	s.c.	0	+32	−5	ms	26	6,7	6	12	286
	June 30	04 00	1 22	.....	.....	.....	.....	s	30	6	9	12	588
Vassouras	Apr. 17	11 36	19 09	s.c.	1	37	16	m	18	1	5	15	328
(Lelio I.	May	None											
Gama)	June 30	05 29	1 09	s.c	2	54	17	m	30	6	5	23	342
Elisabethville/	Jan. 21	12 56	21 24	s.c.	−1	+53	−3	s	24	7,8	...	22	492
Karavia	Feb.	Pas d'orage important											
(A. Alexandre)	Mar. 1	16 16	2 24	s.c.*	−0	+7	...	ms	2	3,4	...	23	286
	Mar. 10	00 22	10 24	s.c.	−2	+35	...	s	10	4,5	...	22	342
	Mar. 29	03 36	30 04	s.c.	−1	+43	+2	ms	29	3,4,5	...	14	275
	Apr.	Pas d'orage important											
	May	Pas d'orage important											
	June 30	05 28	1 05	s.c.	−1	+51	−3	s	30	4,5	...	13	346
		(*Note:* Heures approchées; marque temps en panne)											
Apia	Apr. 8	03 20	13 11	.....	.....	.....	.....	ms	10	2	6	7	234
(A. A. Thomson)	Apr. 15	20 48	21 06	s.c.	+0	+29	−12	ms	17	8	6	7	282
									18	1	6		
	Apr. 23	03 40	25 01	.....	.....	.....	.....	m	24	5,7	5	6	75
	Apr. 30	14 54	5 01	.....	.....	.....	.....	m	1	4	5	5	100
	May 5	09 53	11 06	.....	.....	.....	.....	m	7	2	5	7	141
									9	1,2,3	5		
	May 25	10 53	27 14	.....	.....	.....	.....	m	26	3	5	6	132
	May 30	08 22	31 24	s.c.	+0	+18	−7	m	30	4	5	4	116
	June 16	19 ..	22 15	.....	.....	.....	.....	m	17	2	5	5	132
	June 25	00 46	28 09	s.c.*	+1	+10	−4	m	26	1,2,4,5	5	7	207
									28	3	5		
Binza	Apr. 17	11 34	19 24	s.c.	−2	+57	−5	m	17	8	...	10	242
(J. Leroy)									18	1	...		
	May 30	08 24	30 24	s.c.	+1	+37	−3	m	30	4	...	7	193
	June 25	11 16	26 24	s.c.*	−2	+50	−4	m	25	1,8	...	11	246
	June 30	05 28	1 24	s.c.	−1	+45	−2	ms	30	4	...	12	363

LETTERS TO EDITOR

FIELD-STRENGTH VARIATIONS RECORDED ON A VHF IONOSPHERIC SCATTER CIRCUIT DURING THE SOLAR EVENT OF FEBRUARY 23, 1956

It has been noted by D. K. Bailey, R. Bateman, and R. C. Kirby[1] that sudden ionospheric disturbances on the earth associated with flares (chromospheric eruptions) on the sun are in turn associated with enhanced signal strengths on ionospheric scatter circuits operating at 50 Mc. An SID is a phenomenon which occurs only on the daylight portion of the earth and, therefore, SID-type enhancements of VHF signal strengths are found to occur generally during daylight hours.

The records of signal strengths observed at Sterling, Virginia, of transmissions on 49.8 Mc at Cedar Rapids, Iowa, showed an SID-type occurrence during the night-time hours of February 22-23, 1956. This occurrence was in close time association with the flare seen at Tokyo and Kodaikanal, and cosmic-ray outburst reported from many locations, including the Chicago area by P. Meyer, E. N.

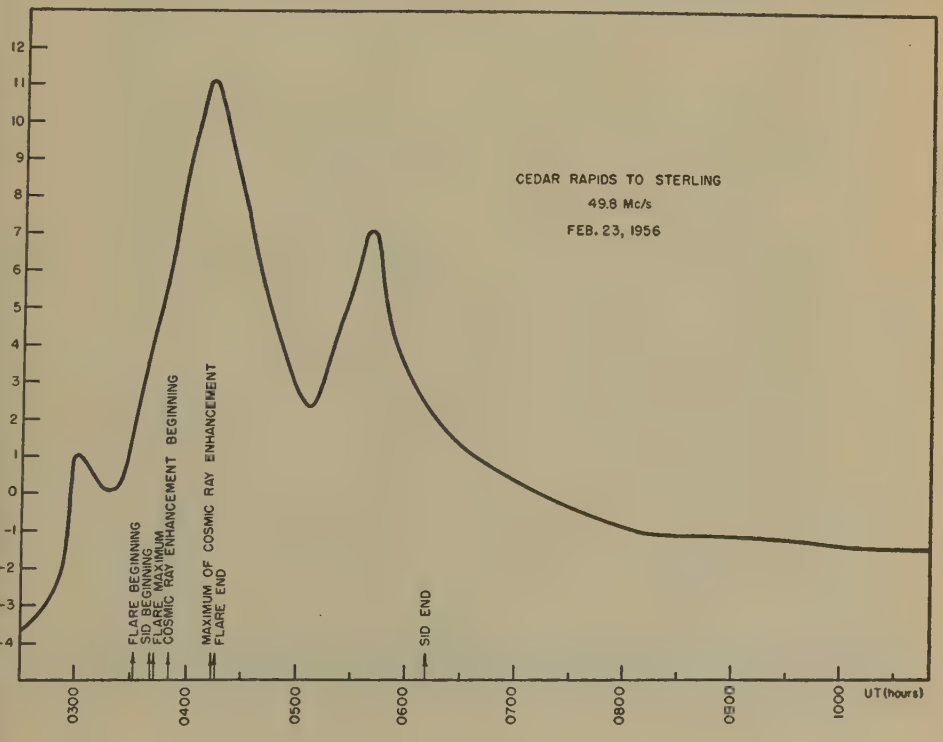

FIG. 1—Plot of signal-strength departures from hourly medians

[1]D. K. Bailey, R. Bateman, and R. C. Kirby, Radio transmission at VHF by scattering and other processes in the lower ionosphere, Proc. Inst. Radio Eng., **43**, 1181-1230 (1955).

Parker, and J. A. Simpson.[2] The VHF signal strength reached a maximum at 0413 UT.

Figure 1 shows a plot of signal-strength departures from hourly medians during this period. The times of occurrence of related phenomena are indicated across the bottom. It will be observed that the rise in signal strength on 49.8 Mc from Cedar Rapids began at about the same time as the flare. The maximum differences in signal strength occurred almost simultaneously with the maximum intensity of the cosmic-ray enhancement. The SID was reported from Okinawa and Japan to have begun at 0330 UT, which is the time of approximate flare onset, and to have continued after flare end. The return to nearly normal of the VHF signal strength lagged the ending of the flare and coincided closely with the end of the SID.

Some night-time enhancement of signal strength occurred for three days following the burst. There were no flares nor SID's reported for these times. Enhancement of the 25th was in time association with an intense magnetic storm.

Hope I. Leighton

National Bureau of Standards,
Boulder, Colorado, May 1, 1957
(Received May 6, 1957)

[2]P. Meyer, E. N. Parker, and J. A. Simpson, Solar cosmic rays of February, 1956 and their propagation through interplanetary space, Phys, Rev., **104**, 768-781 (1956).

COMPLETE NIGHT OF VERTICAL-INCIDENCE IONOSPHERE SOUNDINGS COVERING FREQUENCY RANGE FROM 50 KC/S TO 25 MC/S

The readers of this Journal will be interested in seeing the Figure on the following page. It is the first presentation, to my knowledge, of a group of vertical-incidence ionosphere soundings covering the entire frequency range from below 100 kc/s to 25 Mc/s. Each record is a composite made by joining at the 2-Mc/s marker one record made by a standard Model C-4 recorder and a record made at approximately the same time by the experimental low-frequency recorder in use at the Sunset Field Station, about 15 miles distant. The series shown includes a complete night with sunset and sunrise at half-hour intervals. Enlargements were made to secure an approximate match of the virtual-height scales. As one can see, the low-frequency section is made with a linear frequency sweep, and the high-frequency part uses the logarithmic scale.

The night shown is typical of moderately disturbed conditions, and it was chosen because it illustrates well the kinds of information that are missed by the conventional high-frequency recorders. Complicated traces from the *E*-region, as well as the extraordinary ray from the *F*-layer, are recorded below 1 Mc/s.

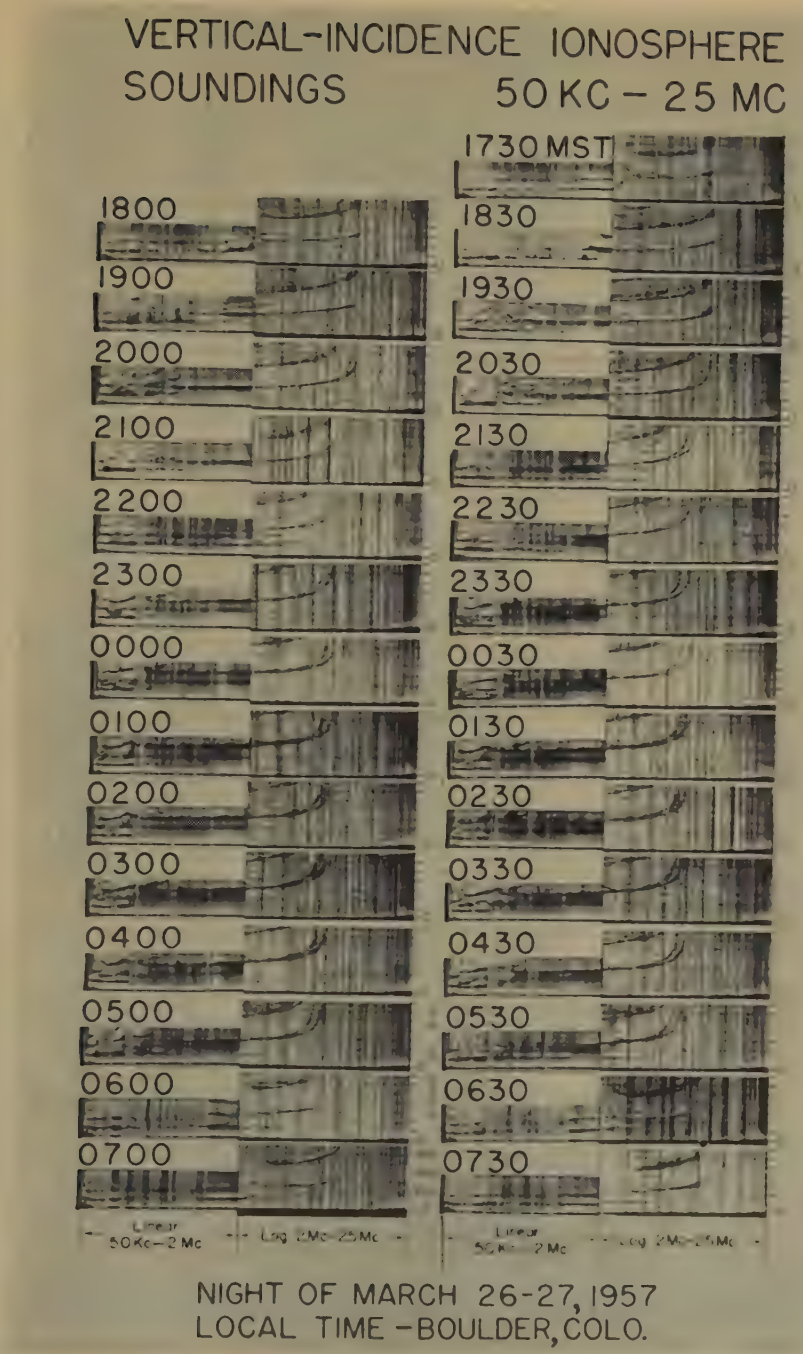

J. M. Watts

National Bureau of Standards,
Boulder, Colorado, April 19, 1957
(Received May 16, 1957)

THE FIGURE OF THE EARTH'S CORE AND THE NON-DIPOLE FIELD

The presence of longitude terms in the expression for the earth's external gravitational field, and therefore in the figure of the sea-level surface, has been suggested for some years. Heiskanen* found a harmonic term P_2^2 with amplitude 28 milligals, while Jeffreys'[1] expansion for the field contains terms P_2^2 and P_3^2. His terms are approximately equivalent to a longitudinal variation of amplitude 20 milligals, with maxima at longitude 0° and 180°. This corresponds to an elliptical equatorial section of the geoid, with a difference of some 200 metres in the length of the major and minor axes. There has not been a completely satisfactory explanation of these terms on the basis of known crustal structures, but Vestine[2] has recently called attention to the similarity in form of the gravitational field and the non-dipole part of the main magnetic field. He suggests that currents of material in the outer part of the core, responsible for this portion of the magnetic field, may distort the earth as a whole.

It appears unlikely that motion of material in the liquid core could distort elastically the 2,900-km thick rigid shell surrounding it, but it might be worth considering the effects of outflow at the base of the mantle. In other words, if the material in the lower part of the mantle can be assumed to have finite viscosity and zero strength, the core-mantle boundary may become warped as a result of stresses developed by currents in the outer part of the core. An equivalent surface distribution of mass, proportional to the difference in density between core and mantle, will result. There will be a direct effect of this at the surface, but in addition there may be a warping of surfaces of equal density in the mantle (if hydrostatic equilibrium is maintained), and there will be a distortion of the sea-level surface. An approximate evaluation of all effects suggests that a second-harmonic (P_2^2) warping of the boundary from its "normal" position with amplitude 2.5 km could produce the longitude variations of 20 milligals in sea-level gravity.

As a result of the differential motion between the outer part of the core and the mantle, the pattern of warping would have to be established in the relatively short time of 500 years. The viscosity in the lower part of the mantle is by no means well known, but it is almost certainly less than the value 10^{22} c.g.s. units suggested for the upper part. Even with this value, a simplified calculation, in which shearing stresses across the boundary are neglected, suggests that a second harmonic distribution at the boundary of normal stress of amplitude 1×10^9 dynes/cm^2 could produce the above warping. The stresses which would be produced by radial motions of material in the outer part of the core depend on the viscosity of the core itself, which is even less well known. Revelle and Munk[3] give 4×10^6 c.g.s. units as the maximum kinematic viscosity, but Bullard[4] has used a value as small as 10^{-3} c.g.s. units for the same quantity. It appears impossible at present to estimate even the

*The ideas outlined in this note, however, are based only on the presence of certain low harmonics in the external gravitational field, and not necessarily on the assumption of a triaxial ellipsoid for the reference spheroid.

[1]H. Jeffreys, Mon. Not. R. Astr. Soc., Geophys. Sup., **5**, 1 (1941), and **5**, 55 (1943).
[2]E. H. Vestine, Trans. Amer. Geophys. Union, **35**, 63 (1954).
[3]R. Revelle and W. Munk, Ann. Géophys., **11**, 104 (1955).
[4]E. C. Bullard, Proc. R. Soc., A, **197**, 433 (1949).

order of magnitude of velocity gradients required, but the point could be kept in mind when the kinematics of core motions are more completely determined. In any case, it appears that relatively high velocities in the outermost part of the core are required to explain the secular change, and considerable velocity gradients may result.

There is, of course, the well-known possibility that the material of the core is a high-pressure phase of the silicates of the mantle. If this is the case, the core boundary is determined by the critical pressure for the phase change, and warping of the boundary could result if the motions in the core alter the hydrostatic pressure around this boundary. The pressure gradient in the vicinity of the core boundary is about 0.5×10^9 dynes/cm^2 per kilometer, so that an increase in pressure over a portion of the core surface of 1×10^9 dynes/cm^2 would presumably cause the boundary to move out by the order of 2 km required.

The extreme difference in depth to the core boundary for the warping suggested above is 5 km. This would result in systematic variations in the times of the reflected elastic waves PcP and ScS of 0.8 second and 1.4 seconds, respectively, for observations at small focal distances in various longitudes. These variations might just be detectable if sufficiently good readings of the reflected phases were available. It is worth noting, in this respect, that the standard error of Jeffreys'[5] determination of core depth from these waves is 3 km, less than the warping suggested. The purpose of the present note is chiefly to draw the attention of geophysicists in the fields of geodesy, terrestrial magnetism, and seismology to what could be a problem of mutual interest.

G. D. Garland

Department of Physics,
University of Alberta,
Edmonton, Alberta, Canada, February 11, 1957
(Received February 14, 1957)

LATITUDE EFFECT OF NIGHT AIRGLOW

Night airglow from the zenith was observed aboard the *Soya*, the expedition ship of J.A.R.E.I. (Japan Antarctic Research Expedition I), which left Tokyo in November 1956 and sailed to the Prince Harald coast in Antarctica *via* Singapore and Cape Town, returning to Tokyo in April 1957.

The photometer, the field of view of which was 3°, was mounted on a stand similar to that of a navigating compass, which could keep the photometer in the direction of the zenith irrespective of the inclination of the ship's deck. The photometer itself consisted of a photomultiplier tube 1P21, with two interference filters (for λλ 5577A and 5300A). The output of the linear amplifier was recorded by an electric recorder.

The photometer was calibrated by a ZnS standard light source, which contained a small amount of Ra. The intensity of the light source decreased by 3 per cent during the expedition.

The result of the observation is shown in Figure 1. The full lines show the measurements during the outward (going) voyage (from Tokyo to the Prince Harald coast), while the dotted lines correspond to those during the homeward

[5] H. Jeffreys, Mon. Not. R. Astr. Soc., Geophys. Sup., 4, 537 (1939).

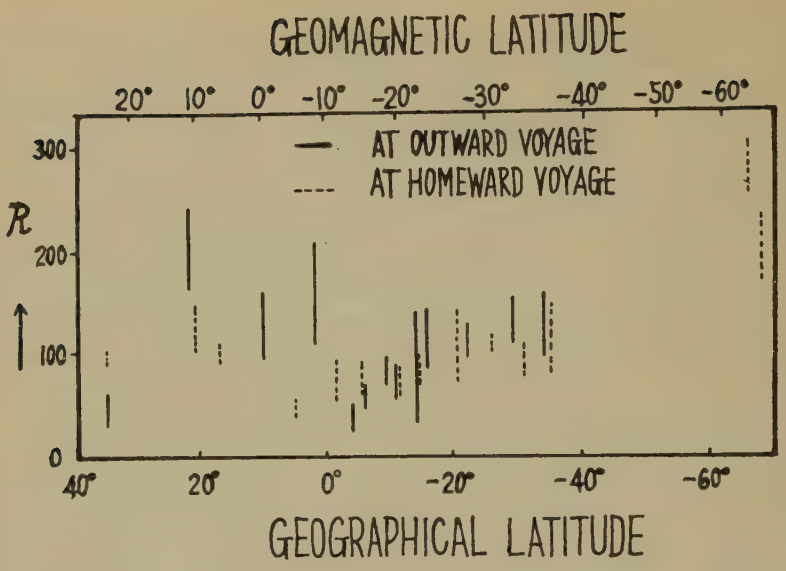

Fig. 1—Latitude effect of airglow; unit is the absolute intensity (Rayleigh)

voyage. Before plotting the measurements at −5°05′ (1956 March 30/31), −1°75′ (March 31/April 1), and +4°09′ (April 2/3), corrections were made due to the observations at Maruyama Observatory (near Tokyo), which showed abnormal activities of the sunspots at those dates. The measurements at +35°01′ were made at the Maruyama Observatory.

If we omit the 35°N values for the time, the general trend shows that a minimum of the intensity appears in the neighborhood of the geographical equator. It seems that a seasonal variation is superposed on this trend, because the minimum on the going away voyage (1956 December) is shifted to the south, and the minimum on the return trip (1957 April) is shifted to the north. If we take the 35°N values into consideration, however, it seems more reasonable to the author to assume that the intensity curve has three minima, at nearly 0° and ±20° of the geomagnetic latitude.

According to this consideration, the author is inclined to assume that there are two origins of the night airglow—the *ultraviolet rays* and the *charged particles* from the sun. The former is responsible for the conspicuous minimum at the geographical equator and the seasonal variation, while the latter causes the three minima which are found on both sides of the geomagnetic equator as well as on the geomagnetic equator. It would be worth while to note that this type of variation is very similar to the latitude effect of the ionosphere.

The author will repeat these observations on the next J.A.R.E., which starts in November 1957

Junji Nakamura

Department of Physics, College of General Education,
University of Tokyo, and Tokyo Astronomical Observatory,
Tokyo, Japan, June 8, 1957
(Received June 12, 1957)

SOLAR ACTIVITY AND ATMOSPHERIC TIDES*

The atmospheric tides, especially their semidiurnal components, are some of the most regular periodic phenomena occurring in the earth's atmosphere. They are, in the case of the solar semidiurnal oscillation S_2, largely caused by thermal action. Further, both S_2 and L_2, the lunar semidiurnal air tide, must depend on the over-all state of the oscillating system, namely, the atmosphere. Therefore, it has occasionally been suggested that the variations of S_2, and perhaps even L_2, may be correlated with solar parameters. This suggestion has been examined and a negative answer has been obtained. Since the whole problem is of some general interest and since the course of our investigation illustrates some of the pitfalls which have to be avoided, a brief account of our work is given here.

The lunar and solar semidiurnal oscillations are best known from atmospheric pressure observations at the ground, and the amplitudes of these pressure oscillations are largest near the equator. Therefore, two stations near the equator were used, namely, Batavia for which 80 years of surface pressure data, from 1866 to 1945 are available, and Manila with 49 years of data, namely, from 1890 to 1938. Correlation coefficients were determined between annual mean values of the Zurich relative sunspot numbers and the annual mean values of the amplitudes of S_2 and L_2. Annual mean values were chosen because for shorter time intervals the computed amplitudes of S_2, and of course even more L_2, are too much subject to accidental errors. The choice of sunspot numbers as the solar parameter was dictated by the necessity of a sufficiently long record.

In the case of all pairs of parameters which have been correlated, it has been determined from scatter diagrams that the relation is not non-linear, so that the correlation coefficient is a reasonable statistical measure of correlation. The following correlation coefficients with their standard errors were obtained between the annual sunspot numbers and the annual mean amplitudes of S_2 :

For Manila..... $+0.12 \pm 0.14$
For Batavia..... -0.028 ± 0.11

These coefficients are so small and their standard errors so large that they indicate clearly the absence of a correlation. It is also of interest to compute the correlation between the annual mean of the amplitudes of S_2 at Manila and Batavia. This figure turns out to be $+0.061 \pm 0.14$, which shows that the year-to-year variations of the amplitudes at both stations are unrelated, and suggests that they are not due to one and the same cause, terrestrial or extra-terrestrial.

There remains the possibility that sunspots and S_2 have a lag correlation. To explore this conjecture, the superposed-epoch method was used. For Batavia, data for seven sunspot cycles are available. The mean sunspot numbers and mean annual amplitudes of all the first, second, etc., years of each sunspot cycle were averaged. The resulting two curves are shown in Figure 1. The abscissa is the year of the sunspot cycle (counted from an arbitrary origin); the ordinate shows on the left side the relative sunspot number and on the right side the amplitude of S_2 in mm Hg.

*Sponsored by the Geophysics Research Directorate, Air Force Cambridge Research Center, Bedford, Massachusetts, under Contract AF 19(604)-1738.

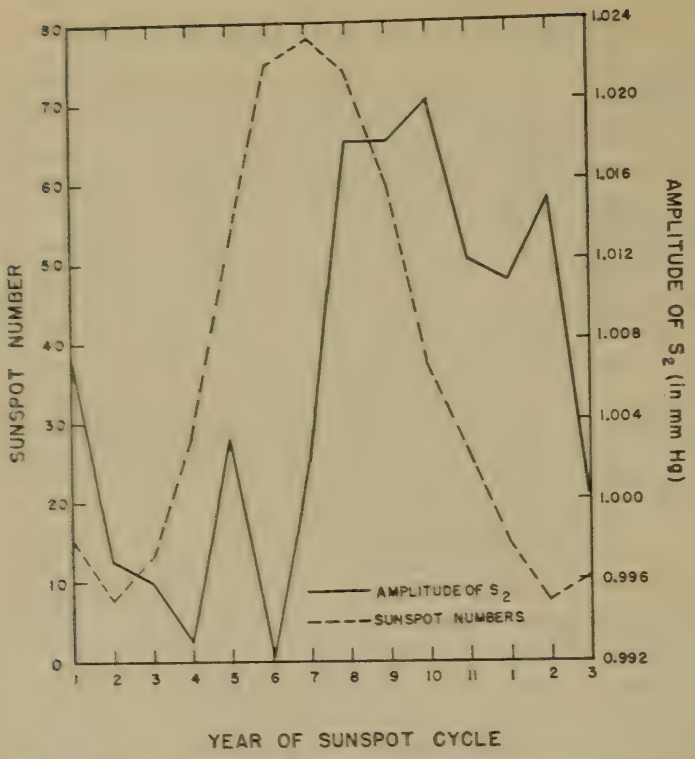

FIG. 1—Variation of sunspot numbers and amplitudes of S_2 at Batavia during the average sunspot period

The two curves exhibit a considerable amount of parallelism, with the extremes of the amplitudes lagging three years behind the extremes of the sunspot numbers.* Attention should be called to the small amount of variation of the amplitude of S_2 throughout the sunspot cycle, only 3 per cent of the mean value for the cycle, while the monthly normal amplitude of S_2 varies by 14 per cent throughout the year. Nevertheless, one might be inclined to believe that a lag relation between sunspot numbers and amplitude of S_2 exists. We have therefore computed the lag correlation coefficient between the two quantities assuming that the amplitude of S_2 lags three years behind the sunspot number, this amount being suggested by Figure 1. The correlation coefficient is then

$$+0.036 \pm 0.11$$

which indicates no correlation.

Although the correlation coefficient demonstrates clearly that the parallelism of the two curves is fortuitous, we have made two further tests which confirm this conclusion. In the first place, we have plotted in a harmonic dial the deviations from the mean vector within an 11-year cycle based on the years 1866-1945. The

*The amplitudes of S_2 on the right-hand side of Figure 1 where the first three years of the sunspot cycle are repeated are not identical with the corresponding values on the left-hand side because three years were omitted here in the computation of the means. The difference shows how much the curve is modified by merely suppressing 3 out of 80 values.

rve representing the end points of the deviation vector has a certain regularity. owever, if the three years 1866, 1867, 1945 are omitted in the computation so at only seven complete sunspot cycles are used, the end-point curve becomes ite different and much more irregular. It must be concluded that the apparent gularity of the first curve is entirely fortuitous if it is so greatly disturbed when out of 80 values are omitted. Secondly, we have applied an expectancy test (see, r instance, Conrad-Pollak, 1950, pp. 399-400).[1] This test shows that the amplitude the 11-year period contained in the curve representing the S_2 amplitudes of gure 1 is of a magnitude which would occur as often as 3 times in 10 cases in ndom data. Again, it must be concluded that the apparent 11-year period shown Figure 1 for S_2 is a statistical accident.

For Manila, curves analogous to those in Figure 1 for Batavia were also con- ucted by means of the superposed-epoch method. The resulting curves were nilar to those in Figure 1, but the parallelism was less pronounced. Therefore, it ld not seem necessary to apply the statistical tests to the Manila data.

Finally, a correlation coefficient was computed for the years 1866-1905, between e sunspot numbers and the amplitudes of the L_2 at Batavia, since values for e latter were available in a paper by Bartels (1927).[2] The correlation coefficient as found to be

$$-0.21 \pm 0.15$$

ere was no evidence of a non-linear or a lag correlation, so that this value of correlation coefficient demonstrates the absence of a statistical connection.

We are indebted to the Climatology Office of the U. S. Weather Bureau for ng the gaps in the pressure data for Manila and Batavia which were directly ailable to us.

B. Haurwitz
J. London
G. M. Sepúlveda
M. Siebert**

PARTMENT OF METEOROLOGY AND OCEANOGRAPHY,
NEW YORK UNIVERSITY,
New York 53, N.Y., June 21, 1957
(Received June 24, 1957)

[1] W. Conrad and L. W. Pollak, Methods in Climatology, Harvard University Press, Cambridge 50).

[2] J. Bartels, Über die atmosphärischen Gezeiten, Veröff. Preuss. Met. Inst., Vol. 8, No. 9 (1927).

**On leave from Geophysical Institute, Göttingen, Germany.

ON THE GEOMAGNETIC STORM EFFECT

In a recent paper,[1] an objection was raised against the "ring-current" hypothesis geomagnetic storm effects, and an alternative hypothesis based on atmosphere placements was advanced. The objection arose from the unacceptable delay, imated at 87 days, required for the passage of the storm through the outer aches of the earth's atmosphere. This delay was taken to be the diffusion time

$$T \sim L^2\mu\sigma/4 \quad \ldots\ldots\ldots\ldots\ldots\ldots\ldots\ldots\ldots\ldots (1)$$

[1] E. N. Parker, J. Geophys. Res., 61, 625 (1956).

appropriate to a medium having permeability $\mu(= \mu_0 = 4\pi \times 10^{-7}$ henry/m) and conductivity $\sigma(\sim 1$ mho/m), for penetration to a depth $L(\sim 5 \times 10^6$ m).

This relation fails to take into account the possible existence of a dominating magnetic field, such as the geomagnetic field in the present case. It fails, for example, to distinguish between the longitudinal and transverse components of the conductivity matrix (relative to the direction of the field), although the transverse components often determine the penetration properties of an electromagnetic disturbance. These components are almost certainly much less than 1 mho/m in the regions concerned, and, if inserted directly in (1), they lead to much more acceptable time delays. A criticism of a similar nature can be brought against the development of the proposed hypothesis of atmospheric displacements, though not against the hypothesis itself.

A second revision required by magnetic field considerations results from the fluidity of the atmosphere. In the special circumstances treated by Alfvén,[2] for example, the relations between the time scale τ and the spatial scale λ of a hydromagnetic disturbance can be written as

$$\lambda^2/\tau^2 = B_0^2\mu^{-1}\rho^{-1} + i2\pi\mu^{-1}\sigma^{-1}\tau^{-1} \quad \ldots\ldots(2)$$

where B_0 is the magnetic induction of the dominating field and ρ is the density of the medium. After a suitable reinterpretation and scaling of the symbols, (1) can be regained from (2) as a valid approximation whenever

$$\tau \ll 2\pi\rho\sigma^{-1}B_0^{-2} \quad \ldots\ldots(3)$$

However, if $\rho \sim 10^{-18}$ kgm/m^3 and $B_0 \sim 10^{-6}$ weber/m are accepted as representative of the regions concerned, this leads to the requirement $\tau \ll 10^{-5}$ sec. Clearly, in the case of geomagnetic storms, the alternative approximation

$$\lambda/\tau = B_0\mu^{-\frac{1}{2}}\rho^{-\frac{1}{2}} \sim 10^6 \text{ m/sec} \quad \ldots\ldots(4)$$

is more appropriate, and it leads to delay times of a few seconds at most. Generalizations of (2) have been developed for application when the conductivity is anisotropic,[3] and they lead to similar estimates of the delay.

Still further generalizations would be required before the actual circumstances of the storm process could be treated adequately, so the foregoing arguments can by no means be considered as final. But it does seem safe to conclude, even at this stage, that unacceptably long delay times do not constitute an inherent feature of the "ring-current" hypothesis.

C. O. HINES

RADIO PHYSICS LABORATORY, DEFENSE RESEARCH BOARD,
Ottawa, Ontario, Canada, June 21, 1957
(Received June 27, 1957)

[2]H. Alfvén, Cosmical Electrodynamics, Clarendon Press, Oxford (1950).
[3]C. O. Hines, Proc. Cambridge Phil. Soc., 49, 299 (1953).

SOME COMMENTS ON J. S. CHATTERJEE'S "INDUCTION IN THE CORE BY MAGNETIC STORMS AND EARTH'S MAGNETISM"

I have been asked by Dr. M. A. Tuve to comment on Dr. J. S. Chatterjee's rticle[1] entitled "Induction in the core by magnetic storms and the earth's magnetm," in which the author has proposed a theory that the earth's permanent agnetic field had been built up by the electromagnetic induction in the earth's eep interior by magnetic storms. Chatterjee has pointed out the importance of ie induced electric currents by the recovery phase of magnetic storms. The irrents, flowing from east to west in the lower mantle and the core, would not ecay until another storm took place. If this is so, successive occurrence of storms ould finally build up a system of electric currents strong enough to produce e earth's magnetic field.

Since no quantitative estimate of the induced currents has been given by hatterjee himself, I would here like to discuss the matter quantitatively. The agnetic potential of the inducing part of a magnetic storm may be expressed as $e^{-\alpha t}P_1$ (cos θ) ($t > 0$), provided the initial phase is ignored and the steep rise the beginning of the main phase is assumed to be instantaneous. In that case, coefficient of the harmonic can also be written in an operational form, such $e(t) = Ap(p + \alpha)^{-1}$. Corresponding to the inducing field of this type, the coefficit of the induced potential is given by an operational equation such as

$$i(t) = Ap(p + \alpha)^{-1}I(p) \quad \ldots\ldots(1)$$

ere $I(p)$ is to be determined by the distribution of the electrical conductivity thin the earth. On solving (1), we obtain

$$i(t) = e(t)h(0) + \int_0^t e(t - u)h'(u)\,du \quad \ldots\ldots(2)$$

ere $h(t)$ corresponds to $i(t)$ when $e(t) = 0 \quad (t < 0)$ and $=1 \quad (t \geq 0)$.

An instantaneous increase in the inducing field should produce a sheet-current the surface of the conductor, whence we obtain $h(0) = (A/2)q^3$, which is indedent of the conductivity. q designates the radius of the conducting sphere ided by the earth's radius. The explicit form of (2) becomes

$$i(t) = Ae^{-\alpha t}\left\{q^3/2 + \int_0^t e^{\alpha u}h'(u)\,du\right\} \quad \ldots\ldots(3)$$

The distribution of the electrical conductivity in the earth, which has been died by S. Chapman,[2] A. T. Price,[2,3] B. N. Lahiri,[3] and T. Rikitake,[4] suggests at $h'(t)$ is essentially negative, amounting to -10^{-6} sec^{-1} for a small value of t, h as $t = 0 \sim 10^4$ sec. Since α is of the order of 10^{-6} sec^{-1} for usual storms and

[1] J. S. Chatterjee, Science and Culture, **21**, 623 (1956).
[2] S. Chapman and A. T. Price, Phil. Trans. R. Soc., London, A, **229**, 427 (1930).
[3] B. N. Lahiri and A. T. Price, Phil. Trans. R. Soc., London, A, **237**, 509 (1939).
[4] T. Rikitake, Bull. Earthquake Res. Inst., Tokyo Univ., **28**, 45, 219, 263 (1950); **29**, 61, 539 51).

q amounts to 0.94, the right-hand side of (3) would be positive during the period from $t = 0$ to $t \sim 10^6$ sec. After this period, the decrease of $|h'(t)|$ with time would become very small, provided we assume a high conductivity such as 10^{-6} e.m.u. in the core, so that the right-hand side of (3) would become negative. In that case, the occurrence of the induced currents which intensify the earth's magnetic field may be expected, though their intensity is extremely small.

A rough estimate of $i(t)$ for a large value of t will be made in the following. Let us replace $h'(u)$ by $-(q^3/2)t^{-1}$, which approximately gives the mean value of $h'(t)$ during the period from $t = 0$ to $t = t$, whence we obtain

$$i(t) = (A/2)q^3(1 + (\alpha t)^{-1} - e^{\alpha t}(\alpha t)^{-1})e^{-\alpha t}$$

The expression leads to $i(t) \sim -(A/2)q^3(\alpha t)^{-1}$ for large t. From the last, we see that a magnetic storm, whose magnitude is designated by $A = 100$ gammas, leaves an effect $i(t) \sim 6$ gammas after 27 days (α is assumed to be 3×10^{-6} sec^{-1}). Suppose magnetic storms of the same magnitude occur every 27 days; the effect of the storm that occurred 54 days before becomes 3 gammas, 81 days 2 gammas, and so on. If all the earth's magnetic field is built up in this way as a result of n successive storms, the coefficient of the magnetic potential is to be $6(1 + \frac{1}{2} + \frac{1}{3} + \ldots + 1/n)$ gammas, so that we see that the field can increase indefinitely because the series is of divergent character, its sum being approximately equal to $\log_e n$ for a large value of n. Hence the number of storms which is necessary for building up the present magnetic field ($i = 3 \times 10^4$ gammas) is given by $\log_e n = 5 \times 10^3$, from which we obtain $n = 10^{2200}$. This means that a period of the order of 10^{2200} years is required in order to reach the present magnitude of the earth's magnetic field by the process suggested by Chatterjee. This time scale seems too much greater than the earth's age, which is widely believed to amount to the order of 10^{10} years. Even if one hundredth of the field is built up by Chatterjee's process, a period of 10^{20} years will be needed. It seems doubtful that the process suggested by Chatterjee has continued over such a long period.

In the light of the above discussion, it is not likely that the main part of the earth's magnetic field is built up by the induced one in the core by magnetic storms, though a very small part of it might be ascribed to the accumulation of the induced currents. I would also like to note that Chatterjee's theory cannot account for the secular variation and the supposed reversal of the earth's polarity, which might be explained by taking time-dependent dynamos into account.

T. RIKITAKE

EARTHQUAKE RESEARCH INSTITUTE,
TOKYO UNIVERSITY,
Tokyo, Japan, November 27, 1956
(Received November 30, 1956)

NOTES

(23) *National Academy of Sciences twelfth meeting of U. S. National Committee for the International Geophysical Year 1957-58*—A selected list of members of the press, radio, and television in the United States was invited to attend the 12th meeting at the National Academy of Sciences of the U. S. National Committee for the International Geophysical Year 1957-58. In this three-day meeting, efforts were made to give a full presentation to the people of the United States, whose tax funds have paid for the program of the U. S. activities in the International Geophysical Year. Technical information, reprints of talks and papers, and pictures were available at a series of desks and tables assigned to the different technical panels. Every effort was made to give a full exposition, in both general and technical terms, of the projects under each panel. In addition to the first day, devoted to general talks on each of the fields, a two-day symposium with technical exposition of the principal projects was held. The program which was presented will interest readers of the JOURNAL, especially by reason of the galaxy of speakers.

Thursday, June 27, 1957

The Chairman Presiding

Thursday Morning Session, Nine a.m.

Remarks by the Chairman, Joseph Kaplan
Remarks by the President of the Academy, Detlev W. Bronk
Remarks by the Director, National Science Foundation, Alan T. Waterman
Report by the Executive Director, Hugh Odishaw
Solar Activity, Walter Orr Roberts
Aurora and Airglow, C. T. Elvey
Cosmic Rays, Scott E. Forbush
Geomagnetism, E. O. Hulburt
Ionospheric Physics, Millett G. Morgan
World Days and Communications, A. H. Shapley

Twelve noon: Intermission

Thursday Afternoon Session, Two p.m.

Rocket Research, Fred L. Whipple
Satellite Program, Richard W. Porter
Meteorology, Harry Wexler
Glaciology, W. O. Field
Oceanography, Gordon G. Lill
Seismology and Gravity, Perry Byerly
Longitudes and Latitudes, William Markowitz

Reception, Academy Auditorium, Six p.m.

Reception of the President of the Academy for representatives of the communications media, the committee, panel chairmen, and symposium speakers. Cocktails and buffet supper.

Thursday Evening Session: Eight-thirty p.m.

The Academy Lecture Room

The IGY Antarctic Program, L. M. Gould
The IGY Arctic Program, John C. Reed

Symposium: Friday and Saturday, June 28-29, 1957

The Academy Auditorium

Friday Morning Session, Nine a.m.

Physics of the Upper Atmosphere: Solar Activity, Ionospheric Physics, Geomagnetism, Cosmic Rays, Aurora and Airglow
Solar Terrestrial Relationships, Walter O. Roberts
The High Atmosphere, N. C. Gerson
Instrumentation for Global Observations of the Sun during IGY, John W. Evans
Whistlers, Millett C. Morgan
Whistlers and VLF Emissions, Robert A. Helliwell
Probing the Ionosphere, Ralph J. Slutz
Upper Atmospheric Winds, Absorption and other Special Projects in the U. S. Program of Ionospheric Physics, Harry W. Wells
Background and Technical Objectives in Geomagnetism, Elliott B. Roberts

Twelve noon: Intermission

Friday Afternoon Session, Two p.m.

Significance of Cosmic Ray Monitor Observations, Robert L. Chasson
High Altitude Cosmic Ray Measurements, J. R. Winckler
Instrumental Observations of the Aurora, C. T. Elvey
Visual Observations of the Aurora, Carl W. Gartlein
Airglow Observations, Franklin E. Roach
Physics of the Upper Atmosphere: The IGY Rocketry and Satellite Programs
Rockets as a Research Tool, Peter H. Wyckoff
Pre-IGY Rocket Measurements, Herbert Friedman

Friday Evening Session, Eight-thirty p.m.

Presiding, the President of the Academy

Exploring Interplanetary Space with Cosmic Rays, John A. Simpson

Saturday Morning Session, Nine a.m.

Physics of the Upper Atmosphere: The IGY Rocketry and Satellite Programs (Continued)
The Satellite Launching Vehicle—Placing the Satellite in Orbit, John P. Hagen

The Satellite Tracking Program, W. H. Pickering
Scientific Instrumentation of the Satellite, James A. Van Allen
The Lower Atmosphere and the Earth itself: Meteorology, Oceanography, and Glaciology
The Heat and Water Budget of the Earth, Roger R. Revelle
Synoptic Meteorology and the IGY, Morton J. Rubin
Special Meteorological Studies for the IGY, Sigmund Fritz
Synoptic Studies in Oceanography, Columbus O'D. Iselin
Special Studies in Oceanography, Walter Munk
Mountain Glaciology, George P. Rigsby
U. S. Polar Snow and Ice Studies, Henri Bader

Twelve-forty: Intermission

Saturday Afternoon Session, Three p.m.

The Lower Atmosphere and the Earth itself: Seismology, Gravity, and Longitudes and Latitudes
The Crust and Mantle of the Earth, Maurice Ewing
Seismological Studies of the Earth, Jack E. Oliver
Gravity Observations during the IGY, George P. Wollard
The Moon Camera—Precision Determination of Terrestrial Coordinates, William Markowitz

(24) *IGY data centers in the United States*—For the United States, the data center will actually consist of 12 archives at institutions with a long history of interest and research in the field. They are as follows: Instrumental aurora at the University of Alaska, College, Alaska; visual aurora at Cornell University, Ithaca, New York; airglow and ionosphere at the Central Radio Propagation Laboratory, Boulder, Colorado; cosmic rays at the University of Minnesota; earth satellite at Smithsonian Astrophysical Observatory, Cambridge, Massachusetts; geomagnetism, gravity, and seismology at the U. S. Coast and Geodetic Survey; glaciology at the American Geographical Society, New York; latitude and longitude at the U. S. Naval Observatory; meteorology at the National Weather Records Center, Asheville, North Carolina; oceanography at Texas A. and M., College Station, Texas; rocketry at the State University of Iowa; and solar activity at the University of Colorado.

(25) *Annals of the International Geophysical Years*—A central record of the International Geophysical Year is to appear in the Journal of the Central Committee which guides the activities of the IGY. The Annals will indicate the inception, the planning, the preparations, and the programs, and in due course the progress and some of the main results of the IGY. Three volumes have been announced thus far, as follows: Vol. I, Introductory volume to International Year; Vol. II, Reports of Proceedings of International Geophysical Year; and Vol. III, Instruction manual for ionospheric studies in the International Geophysical Year. It is anticipated that a maximum of four to six volumes of approximately 400 pages of the Annals will be published during 1957 and 1958. Subscription rates are £6 or $17 per volume. Orders should be placed with the Pergamon Press, London, England, or New York, N. Y. Harold Spencer Jones will serve as general editor with the aid

of an editorial advisory board that consists of A. H. Shapley (world days), J. van Miegheim (meteorology), V. Laursen (geomagnetism), S. Chapman (aurora and airglow), W. J. G. Beynon (ionosphere), Y. Ohman (solar activity), J. A. Simpson (cosmic rays), A. Danjon (longitude and latitude), James Wordie (glaciology), G. Laclavère (oceanography,) L. V. Berkner (rockets and satellites), V. V. Beloussov (seismology), P. Lejay (gravity measurement), and M. Nicolet (nuclear radiation).

(26) *Establishment of magnetic observatory at Hartland, England*—The British Admiralty recently announced the establishment of a new magnetic observatory in the village of Hartland, Devonshire, England. It will operate as part of the Royal Greenwich Observatory, whose headquarters are at Herstmonceux Castle in Sussex. The function of the new station is to provide information relating to the earth's magnetic field, and to test and calibrate magnetic instruments intended for high precision investigations. The electrification of the railroad system and spread of industry necessitated this latest selection of observatory site in the south of England, following in succession the abandonment of Greenwich in 1925 and soon Abinger. The first observations at Hartland began in February 1957, although it will be some time before the observatory will be in full operation.

(27) *Publication of VLF symposium papers*—On January 23-25, 1957, the National Bureau of Standards, in conjunction with the IRE Professional Group on Antennas and Propagation, held a Symposium on the Propagation of Very-Low-Frequency Radio Waves, at which some 47 papers were presented. Thirteen of these papers were selected as being representative of important work in this field for publication in the "Proceedings of the Institute of Radio Engineers," Vol. 45, No. 6, pp. 739-811, 1957.

(28) *Measurement of the sun's magnetic field*—At the Cambridge University Laboratories an instrument is being built to record small magnetic fields on the surface of the sun. The instrument is modeled after the well-known Babcock solar magnetograph in Pasadena. The Cambridge spectrograph employs a Mount Wilson grating made by Babcock which is used in the fifth order green with a resolving power of about 600,000.

(29) *Recent monthly periodical, "Annals of Physics"*—The first issue of this journal (Vol. 1, No. 1, April 1957) has been published by the Academic Press, Inc., New York, N. Y., with Philip M. Morse, Department of Physics, Massachusetts Institute of Technology, its Editor. Its pages are to be devoted to the publication of papers describing original work in all areas of basic physics research.

(30) *New "Journal of Molecular Spectroscopy"*—This new periodical plans to publish original research papers dealing with molecular spectra in emission and absorption, molecular spectra in the ultraviolet, the visible, the near and far infrared, and in the microwave region. It will also contain contributions on Ramon spectroscopy and radiofrequency spectroscopy (including nuclear magnetic resonance spectroscopy). Volume 1, No. 1, June 1957, was the initial issue, published by the Academic Press, New York, N. Y. The editor is Harald H. Nielsen, Department of Physics, Ohio State University, Columbus, Ohio. It is planned to publish four issues during 1957, and in 1958 (Vol. 2) six issues.

(31) *Geomagnetic activities of the United States Coast and Geodetic Survey*—The

IGY program in geomagnetism is under way essentially as heretofore explained. The processing staff is being expanded to handle the increased volume of data that will be generated by the program.

Arrangements have been concluded by which the Coast and Geodetic Survey will conduct, for the disciplines of geomagnetism, seismology, and gravity, the IGY World Data Center serving the Western Hemisphere.

Mr. J. H. Nelson, Chief of Geomagnetism Branch, visited IGY geomagnetic installations in Alaska and the Pacific area during June 1957.

Messrs. J. Annexstad, J. Gniewek, and S. Borrello are now in training at Fredericksburg. Around the beginning of 1958, they will relieve geophysicists now in Antarctica.

(32) *Personalia*—Dr. *Ira S. Bowen*, Director of the Mount Wilson and Palomar Observatories, was the recipient of the Catharine Wolfe Bruce gold medal, awarded annually by the Astronomical Society of the Pacific to an astronomer distinguished for his outstanding work.

Dr. *S. A. Korff*, of New York University, an authority on cosmic rays, has been awarded the Order of Merit for Research and Invention by the Government of France. A professor of physics in the College of Engineering, Dr. Korff joined New York University in 1940. He has been engaged in cosmic-ray research since he was a National Research Fellow at Mount Wilson Observatory in 1932. Dr. Korff is executive secretary of the U. S. National Committee for the International Geophysical Year 1957-58.

Dr. *J. A. Jacobs*, Professor of Geophysics, University of Toronto, has accepted appointment as Research Professor in Geophysics at the University of British Columbia, Vancouver, Canada, beginning September 1957.

Two astronomers have retired from the staff of the Mount Wilson and Palomar Observatories: Dr. *Milton L. Humason*, whose observations have provided most of the evidence supporting the theory of the expanding universe, and Dr. *Seth B. Nicholson*, specialist in solar phenomena and discoverer of four of Jupiter's satellites. Both joined Mount Wilson Observatory around the same time; Humason in 1917 and Nicholson in 1915.

Dr. *Frank Press*, since 1955 professor of geophysics at the California Institute of Technology, has been named director of the Seismological Laboratory. He succeeds Dr. *Beno Gutenberg*, who is retiring to half-time status after 27 years at the Institute and 10 years as director of the Laboratory.

Mr. *J. M. Rayner*, Deputy Director of the Bureau of Mineral Resources, Geology and Geophysics, left Australia on August 9, 1957, to spend a period of about two months in the United States and Canada attending various scientific meetings. Mr. Rayner is Vice-President of the International Association of Geomagnetism.

LIST OF RECENT PUBLICATIONS

BY W. E. SCOTT

Department of Terrestrial Magnetism,
Carnegie Institution of Washington,
Washington **15**, *D. C.*

(Received July 3, 1957)

A—*Terrestrial Magnetism*

AKASOFU, S. Hydromagnetic relationships between the sun and the earth. Sci. Rep. Tôhoku Univ., Ser. 5, Geophysics, **8**, No. 2, 133-145 (1957).

BACKUS, G. The axisymmetric self-excited fluid dynamo. Astroph. J., **125**, No. 2, 500-524 (1957).

BARANOV, V. A new method for interpretation of aeromagnetic maps: Pseudo-gravimetric anomalies. Geophysics, **22**, No. 2, 359-383 (1957).

BARTELS, J., AND J. VELDKAMP. International data on magnetic disturbances—Part 2: *Kp*, *Ap*, *Ci*, and selected days, fourth quarter, 1956. J. Geophys. Res., **62**, No. 2, 315-318 (1957).

BARTELS, J., A. ROMAÑA, AND J. VELDKAMP. Geomagnetic indices *K* and *C*, 1955. Internat. Union Geod. Geophys., Assoc. Terr. Mag. and Aeronomy, Bull. No. 12j, 124 pp. (1957). 24 cm.

BEISER, A. Variations in the geomagnetic dipole in the past 15,000 years. J. Geophys. Res., **62**, No. 2, 235-239 (1957).

BUREAU, J. L. Confrontation entre la théorie du nuage ionisé de Chapman et Ferraro et l'enregistrement du debut d'un orage magnetique. Paris, C.-R. Acad. sci., **244**, No. 10, 1396-1398 (1957).

BURMEISTER, F. Die Berechnung des Normalfeldes. D. Hydrogr. Zs., **2**, 8-10 (1956). [Supp. Ser. *B* (4°), No. 2.]

BURMEISTER, F. Erdmagnetische Karten für die Epoche 1955.0 und ihre Bearbeitung. D. Hydrogr. Zs., **2**, 11-13 (1956). [Supp. Ser. *B* (4°), No. 2.]

COIMBRA. Observacões meteorológicas, magnéticas e sismológicas feitas no Instituto Geofisico (Observatorio Meteorológico, Magnético e Seismológico) no ano de 1953. 2ª Partie—Magnetismo terrestre, Vol. XCII. Coimbra, Tip. da Atlantida, 36 pp. (1955). [Received May 22, 1957.]

COX, A. Remanent magnetization of lower to middle Eocene basalt flows from Oregon. Nature, **179**, 685-686 (March 30, 1957). [Letter to Editor.]

DEUTSCH, E. R. The measurement of magnetic hysteresis in rocks and minerals at high temperatures. J. Geomag. Geoelectr., **8**, No. 3, 108-117 (1956).

DEUTSCH, E. R. The magnetic hysteresis of rocks and minerals at high temperatures. J. Geomag. Geoelectr., **8**, No. 3, 118-128 (1956).

ERRULAT, F. Einige Bemerkungen zu den Karten für die Epoche 1935.0 der erdmagnetischen Reichsvermessung. D. Hydrogr. Zs., **2**, 7-8 (1956). [Supp. Ser. *B* (4°), No. 2.]

FINCH, H. F. Royal Greenwich Observatory, Hartland. Nature, **179**, 994-995 (May 18, 1957).

FOSTER, F. G. Magnetography—The microscopy of magnetism. Bell Lab. Record, **35**, No. 5, 175-178 (1957).

GEBHARDT, R. L. Fredericksburg three-hour-range indices *K* for January to March, 1957. J. Geophys. Res., **62**, No. 2, 319 (1957).

GREENWICH ROYAL OBSERVATORY. Results of the magnetic and meteorological observations made at the Abinger Magnetic Station, Surrey, and the Royal Observatory, Greenwich, respectively, for the year 1947. London, H. M. Stationery Office, xx + 91 (1956). 30 cm.

HERZENBERG, A., AND F. J. LOWES. Electromagnetic induction in rotating conductors. Phil. Trans. R. Soc., A, **249**, No. 970, 507-584 (1957).

HOPE, E. R. Westward drift and cyclic secular variation. J. Geophys. Res., **62**, No. 2, 241-253 (1957).

DWELL, L. G., AND J. D. MARTINEZ. Polar movement as indicated by rock magnetism. Geophysics, 22, No. 2, 384-397 (1957).

ATO, Y., AND T. WATANABE. Studies on geomagnetic pulsation, Pc. Sci. Rep. Tôhoku Univ., Ser. 5, Geophysics, 8, No. 2, 111-132 (1957).

EEFE, J. A. C., S. H. WARD, AND J. T. WILSON. Report on survey of vertical magnetic intensity near Chubb Crater, July-August 1951. J. R. Astr. Soc. Can., 51, No. 2, 148-152 (1957). [This report is part of a paper entitled "Chubb Crater—a meteor crater," pp. 137-154 of same issue.]

HTI, H. Über das aufgetretenen der Magnetischen Pulsationen in Sodankylä und Vuotso in den Jahren 1935 und 1936. Helsinki, Veröff. Finn. Geod. Inst., No. 35, 15 pp. (1957).

ARSDEN, P. L., J. G. WILSON, AND D. C. ROSE. Geomagnetic variations in the cosmic-ray disturbance of 23 February 1956. J. Atmos. Terr. Phys., 10, No. 2, 117-119 (1957). [Research note.]

ORAIS, J. C. Observations of terrestrial magnetism made on the west coast of India by D. João de Castro in 1538-1539. Repr., Memórias e Noticias, No. 41, 8 pp. + 1 pl. (1956).

IKOL'SKI, A. P. Re the geographic distribution of magnetic activity in the antarctic. Doklady Akad. Nauk SSSR, 112, No. 5, 846-848 (1957). [Translation by E. R. Hope, Directorate of Scientific Information Service, Defense Research Board of Canada, Pub. No. T 244 R, May 1957.]

RŮHONICE OBSERVATORY. Výsledky Geomagnetických Měření na Observatoři Průhonice u Prahy za Rok 1955. Českoslov. Akad. Věd, Geofys. Ustav, 126 pp. (1957).

ZYBYSZEWSKI, E. Comparison of la Cour magnetometers at the Geophysical Observatory on the Hel Peninsula. Acta Geophys. Polonica, 5, No. 1, 22-33 (1957).

OMAÑÁ, A. International data on magnetic disturbances—Part 1: Sudden commencements and solar-flare effects, third and fourth quarters, 1956. J. Geophys. Res., 62, No. 2, 312-314 (1957).

NCORN, S. K. Rock magnetism. Nature, 179, 866 (April 27, 1957). [Letter to Editor.]

OTT, G. G. Compensation of the earth's magnetic field. Rev. Sci. Instr., 28, No. 4, 270-273 (1957).

NGER, S. F. A new model of magnetic storms and aurorae. Trans. Amer. Geophys. Union, 38, No. 2, 175-190 (1957).

NNO, K. On the origin of the long-lived solar corpuscular streams which appeared last solar cycle. J. Radio Res. Lab. Japan, 4, No. 15, 25-35 (1957).

NANARIVE (AMBOHIDEMPONA OBSERVATOIRE). Mesures magnetiqués, 1953-1954. Tananarive, Inst. Phys. Globe, 73 pp., mim. (rec'd April 17, 1957).

NNI, P. B., AND J. A. BROOKS. Magnetic results from Macquarie Island, 1953. Commonwealth of Australia, Bureau of Mineral Resources, Geology and Geophysics, Rep. No. 31, v + 3 pp. + 50 tables + 6 pls. (1956).

ELLIER, M. E. Progrès récents dans les mesures géomagnétiques. J. Phys. Radium, 18, No. 1, 9-10 (1957). [Utilisation de la résonance magnétique nucléaire.]

ILLIAMS, H. J., AND R. C. SHERWOOD. Magnetic domain patterns on thin film. J. Appl. Phys., 28, No. 5, 548-555 (1957).

NGST OBSERVATORIUM. Ergebnisse der erdmagnetischen Beobachtungen im Observatorium Wingst in den Jahren 1953 und 1954. D. Hydrogr. Inst., Hamburg, Jahrb. No. 9, 146 pp. (1956).

TTEVEEN MAGNETIC OBSERVATORY. Yearbook 1951. B—Geomagnetism. 'S-Gravenhage, K. Nederlands Met. Inst., No. 98, iv + 28 pp. (1954). [Contains hourly values of the magnetic elements for 1951 at Witteveen.]

ITTEVEEN MAGNETIC OBSERVATORY. Yearbook 1952. B—Geomagnetism. 'S-Gravenhage, K. Nederlands Met. Inst., v + 28 pp. (1955).

B—*Terrestrial Electricity*

HALMERS, J. A. Atmospheric electricity. Pergamon Press, New York and London, 335 pp. (1957).

LARENCE, N. D., AND D. J. MALAN. Preliminary discharge processes in lightning flashes to ground. Q. J. R. Met. Soc., 83, No. 356, 161-172 (1957).

Coroniti, S. C., and N. C. Gerson. Scatter-field strengths and large ion concentration. J. Atmos. Terr. Phys., **10**, No. 4, 237-239 (1957). [Research note.]

Kano, M., and K. Murai. On the velocity of the streamer in the lightning discharge. Pap. Met. Geophys., **7**, No. 3, 281-287 (1956).

Khastgir, S. R. Leader stroke current in a lightning discharge according to the streamer theory. Phys. Rev., **106**, No. 4, 616-617 (1957).

C—*Cosmic Rays*

Cachon, A., A. Daudin, et L. Jauneau. Les rayons cosmiques. Presses Universitaires de France, Paris, 116 pp. (1957).

Carmichael, H., and J. F. Steljes. Cosmic-ray bursts under lead at sea level. Phys. Rev., **105**, No. 5, 1626-1635 (1957).

Fowler, P. H., C. J. Waddington, P. S. Freier, J. Naugle, and E. P. Ney. The low energy end of the cosmic ray spectrum of alpha-particles. Phil. Mag., **2**, No. 14, 157-175 (1957).

Jacklyn, R. M., and A. G. Fenton. Changes in the high-latitude east-west asymmetry of cosmic rays. Phys. Rev., **106**, No. 4, 809-811 (1957).

Kawabata, K. On the magnetic storm on February 25, 1956. Rep. Ionosphere Res. Japan, **10**, No. 3, 148 (1956). [Short note.]

Legrand, J.-P., P. Chanson, et M. Bonpas. Variations de l'intensité du rayonnement cosmique les 21, 22 et 23 janvier 1957. Paris, C.-R. Acad. sci., **244**, No. 10, 1362-1364 (1957).

Lüst, R. Impact zones for solar cosmic-ray particles. Phys. Rev., **105**, No. 6, 1827-1839 (1957).

Manning, A. W. Measurements of the soft component of cosmic radiation by an absorption "well method." J. Atmos. Terr. Phys., **10**, No. 4, 189-193 (1957).

McDonald, F. B. Study of geomagnetic cut-off energies and temporal variation of the primary cosmic radiation. State University of Iowa, Phys. Dept., Rep. No. SUI-57-8, 24 pp. + 10 figs., mim. (April 1957).

Meyer, P., and J. A. Simpson. Changes in the low-energy particle cutoff and primary spectrum of cosmic rays. Phys. Rev., **106**, No. 3, 568-571 (1957).

Morrison, P. On the origins of cosmic rays. Rev. Modern Phys., **29**, No. 235-243 (1957).

Noon, J. H., A. J. Herz, and B. J. O'Brien. An observed cosmic-ray flux of light elements at 41° N. geomagnetic latitude. Nuovo Cimento, **5**, No. 4, 854-865 (1957).

Pfotzer, G. Solare Ultrastrahlung als Sonde für das Magnetfeld der Erde in grosser Entfernung. Mitt. Max Planck-Inst. Physik d. Stratosphäre, No. 9, 13 pp. (1956).

Shen, K. Y., and S. F. Singer. Intensity variation of vertical cosmic-ray air showers. Phys. Rev., **106**, No. 3, 555-557 (1957).

Stensland, B. On the phase and the amplitude of cosmic ray diurnal variation. Ark. Fys., **11**, No. 3, 253-258 (1956).

Yagi, T. Intensity problem in the deflection of cosmic rays in the solar magnetic field. J. Geomag. Geoelectr., **8**, No. 3, 87-92 (1956).

D—*Upper Air Research*

Aitchison, G. J. Ionospheric demodulation of radio waves at vertical incidence. Aust. J. Phys., **10**, No. 1, 204-207 (1957). [Short communication.]

Allan, A. H., D. D. Crombie, and W. A. Penton. Long-path V.L.F.—Frequency variations associated with the solar flare of 23 February 1956. J. Atmos. Terr. Phys., **10**, No. 2, 110-113 (1957).

Barber, D. R. Photoelectric observations of anomalously polarized twilight emission at 5893Å. J. Atmos. Terr. Phys., **10**, No. 3, 172-176 (1957).

Barbier, D. Observations de la luminescence atmosphérique nocturne de la raie rouge de l'oxygène. Paris, C.-R. Acad. sci., **244**, No. 13, 1809-1811 (1957).

Bates, D. R., and M. R. C. McDowell. Recombination in the ionosphere during an eclipse. J. Atmos. Terr. Phys., **10**, No. 2, 96-102 (1957).

Becker, W. Sporadische Ionisierung in der *E*-Region der Ionosphäre mittlerer Breiten. Archiv Elektr. Uebertrag., **11**, Heft 3, 101-104 (1957).

ECKER, W. Tabellierung der vertikalen Gruppengeschwindigkeiten ordentlicher Echos in der Ionosphäre. Archiv Elektr. Uebertrag., **11**, Heft 4, 166-172 (1957).

HAR, J. N. Relation between noon *F*2-layer ionization and magnetic dip. J. Atmos. Terr. Phys., **10**, No. 3, 168-172 (1957). [Research note.]

IBL, K., H. A. HESS, UND K. RAWER. Forward-scatter-Beobachtungen bei 50 MHz. Archiv Elektr. Uebertrag., **11**, Heft 2, 59-62 (1957).

UDDEN, K. G. The "waveguide mode" theory of the propagation of very-low-frequency radio waves. Proc. Inst. Radio Eng., **45**, No. 6, 772-774 (1957). [VLF Symposium paper.]

ULLINGTON, K. Radio propagation fundamentals. Bell System Tech. J., **36**, No. 3, 593-626 (1957).

HAPMAN, J., AND E. T. PIERCE. Relations between the character of atmospherics and their place of origin. Proc. Inst. Radio Eng., **45**, No. 6, 804-806 (1957). [VLF Symposium paper.]

HUBB, T. A., H. FRIEDMAN, R. W. KREPLIN, AND J. E. KUPPERIAN, JR. Rocket observation of X-ray emission in a solar flare. Nature, **179**, 861-862 (April 27, 1957). [Letter to Editor.]

RICHLOW, W. Q. Noise investigation at VLF by the National Bureau of Standards. Proc. Inst. Radio Eng., **45**, No. 6, 778-782 (1957). [VLF Symposium paper.]

ATTA, S. Recombination coefficient and electron production rate from total electron content in unit column below the level of maximum ionization. Indian J. Phys., **31**, No. 1, and Proc. Indian Assoc. Cultivation Science, **40**, No. 1, 43-52 (1957).

LVEY, C. T. Problems of auroral morphology. Proc. Nat. Acad. Sci., **43**, No. 1, 63-75 (1957).

SHLEMAN, V. R. The theoretical length distribution of ionized meteor trails. J. Atmos. Terr. Phys., **10**, No. 2, 57-72 (1957).

RSYTH, P. A., AND E. L. VOGAN. The frequency dependence of radio reflections from aurora. J. Atmos. Terr. Phys., **10**, No. 4, 215-228 (1957).

RIS, H. T., A. B. CRAWFORD, AND D. C. HOGG. A reflection theory for propagation beyond the horizon. Bell System Tech. J., **36**, No. 3, 627-644 (1957).

ADSDEN, M. The color of the zenith twilight sky: absorption due to ozone. J. Atmos. Terr. Phys., **10**, No. 3, 176-180 (1957). [Research note.]

ATES, W. L. A dynamical model for large-scale tropospheric and stratospheric motions. Q.J.R. Met. Soc., **83**, No. 356, 141-160 (1957).

BBONS, J. J., AND B. R. RAO. Calculation of group indices and group heights at low frequencies. Pennsylvania State University, Ionosphere Res. Lab., Sci. Rep. No. 92, 35 pp. mim. (April 1, 1957).

RIERSON, J. K. A technique for the rapid analysis of whistlers. Proc. Inst. Radio Eng., **45**, No. 6, 806-811 (1957). [VLF Symposium paper.]

ROVES, G. V. Velocity of a body falling through the atmosphere and the propagation of its shock wave to earth. J. Atmos. Terr. Phys., **10**, No. 2, 73-83 (1957).

ARANG, L., AND K. PEDERSEN. Drift measurements of the *E*-layer. J. Geophys. Res., **62**, No. 2, 183-198 (1957).

EPBURN, F. Wave-guide interpretation of atmospheric waveforms. J. Atmos. Terr. Phys., **10**, No. 3, 121-135 (1957).

ILL, E. L. Very low-frequency radiation from lightning strokes. Proc. Inst. Radio Eng., **45**, No. 6, 775-777 (1957). [VLF Symposium paper.]

OPE, E. R. The earth's exterior atmosphere and the counterglow (the counterglow as related to modern geophysical theories). Defense Scientific Information Service, Defense Research Board of Canada, Pub. No. T 65 R, 3rd ed., 52 pp., mim. (April, 1957). [Contains English translations of seven Russian papers translated by E. R. Hope.]

OSKING, R. H. The mean thickness of night-time E_s clouds at Brisbane. Aust. J. Phys., **10**, No. 1, 220-221 (1957). [Short communication.]

OUSTON, R. E., JR., W. J. ROSS, AND E. R. SCHMERLING. Some effects of intense solar activity on radio propagation. J. Atmos .Terr. Phys., **10**, No. 3, 136-139 (1957).

AISER, T. R. The geometry of auroral ionization. J. Geophys. Res., **62**, No. 2, 297-298 (1957).

ASUYA, I. Relationship between the semi-thickness of *F*2 layer at Tokyo and solar activity. J. Radio Res. Lab. Japan, **4**, No. 15, 49-57 (1957).

ELSO, J. M. The calculation of ionospheric electron density distributions. J. Atmos. Terr. Phys., **10**, No. 2, 103-109 (1957).

Landmark, B., and F. Lied. Note on a "QL-QT" transition level in the ionosphere. J. Atmos. Terr. Phys., **10**, No. 2, 114-116 (1957). [Research note.]

Lepechinsky, D. The Q.L.-Q.T. transition level. J. Atmos. Terr. Phys., **10**, No. 4, 243-244 (1957). [Letter to Editor.]

Maeda, K., and I. Kimura. A theoretical investigation on the propagation path of the whistling atmospherics. Rep. Ionosphere Res. Japan, **10**, No. 3, 105-123 (1956).

Mambo, M. On differences of f_0F2 between June and December viewed from a world-wide standpoint. J. Radio Res. Lab. Japan, **4**, No. 15, 59-71 (1957).

Mange, P. The theory of molecular diffusion in the atmosphere. J. Geophys. Res., **62**, No. 2, 279-296 (1957).

Mariani, F. The electron density in the *F*2 layer and its correlation with the solar activity. J. Atmos. Terr. Phys., **10**, No. 4, 239-242 (1957). [Research note.]

Matsushita, S. Lunar effects on the equatorial *Es*. J. Atmos. Terr. Phys., **10**, No. 3, 163-165 (1957). [Research note.]

McCrosky, R. E. Variations from a Poisson distribution of meteors recorded by radar techniques. Bull. Astron. Inst. Czechosl., **8**, No. 1, 1-5 (1957).

McKerrow, C. A. Some recent measurements of atmospheric noise in Canada. Proc. Inst. Radio Eng., **45**, No. 6, 782-786 (1957). [VLF Symposium paper.]

Minnis, C. M. Ionospheric changes at Singapore during the solar eclipse of 20 June 1955. J. Atmos. Terr. Phys., **10**, No. 4, 229-236 (1957).

Mitra, A. P. Night-time ionization in the lower ionosphere—I. Recombination processes. J. Atmos. Terr. Phys., **10**, No. 3, 140-152 (1957).

Mitra, A. P. Night-time ionization in the lower ionosphere—II. Distribution of electrons and positive and negative ions. J. Atmos. Terr. Phys., **10**, No. 3, 153-162 (1957).

Mitra, N. Investigation of discrete sources of radiation from solar eclipse observations. Indian J. Phys., **31**, No. 2, and Proc. Indian Assoc. Cultivation Science, **40**, No. 2, 69-82 (1957).

Mitra, S. N., and R. B. L. Srivastava. Fading and random motion of ionospheric irregularities. Indian J. Phys., **31**, No. 1, and Proc. Indian Assoc. Cultivation Science, **40**, No. 1, 20-42 (1957).

Montgomery, G. F., and G. R. Sugar. The utility of meteor bursts for intermittent radio communication. Nation. Bur. Stan., Boulder, NBS Rep. No. 5064, 16 pp. + 1 table + 14 figs., mim. (April 1, 1957).

Munro, G. H. Anomalies of ionosonde records due to traveling ionospheric disturbances. J. Geophys. Res., **62**, No. 2, 325-326 (1957). [Letter to Editor.]

Nakata, Y. Sweep-frequency *ft* and *h'f* records of the ionosphere at the time of solar flares on February 14 and 23, 1956. Rep. Ionosphere Res. Japan, **10**, No. 3, 149-151 (1956). [Short note.]

Nikol'ski, A. P. On the high-latitude geographic distribution of anomalous absorption of radio waves in the ionosphere. Doklady Akad. Nauk SSSR, **112**, No. 4, 628-631 (1957). [Translation by E. R. Hope, Directorate of Scientific Information Service, Defense Research Board of Canada, Pub. No. T 244 R, May 1957.]

Omholt, A. Considerations regarding the sodium lines in the nightglow and twilight. J. Geophys. Res., **62**, No. 2, 207-212 (1957).

Pierce, J. A. Intercontinental frequency comparison by very low-frequency radio transmission. Proc. Inst. Radio Eng., **45**, No. 6, 794-803 (1957). [VLF Symposium paper.]

Poincelot, P. Sur la réflexion ionosphérique en présence de chocs. Paris, C.-R. Acad. Sci., **244**, No. 18, 2298-2299 (1957).

Price, R., and P. E. Green, Jr. Measurement of ionospheric path-phase for oblique incidence. Nature, **179**, 372-373 (Feb. 16, 1957). [Letter to Editor.]

Rastogi, R. G. Thunderstorms and sporadic *E* layer ionisation. Indian J. Met. Geophys., **8**, No. 1, 43-54 (1957).

Regener, V. H. The vertical flux of atmospheric ozone. J. Geophys. Res., **62**, No. 2, 221-228 (1957).

Revellio, K. Die atmosphärischen Störungen und ihre Anwendung zur Untersuchung der unteren Ionosphäre. Mitt. Max Planck-Inst. Physik d. Stratosphäre, No. 8, 56 pp. (1956).

Rowden, R. A., and J. W. Stark. Long-distance propagation at 94.35 Mc/s over the North Sea. Proc. Inst. Elec. Eng., B, **104**, No. 15, 210-212 (1957).

ECHRIST, C. F., JR. Theory and design of a traveling wave antenna system for long wave sweep frequency investigation of the ionosphere at vertical incidence. Pennsylvania State University, Ionosphere Res. Lab., Sci. Rep. No. 91, 49 pp. (March 1, 1957).

EKERA, Z. Light scattering in the atmosphere and the polarization of sky light. J. Optical Soc. Amer., **47**, No. 6, 484-490 (1957).

HIMAZAKI, T. The characteristics of the *F*2 regions as deduced from the daily variations in the ionospheric layer. Rep. Ionosphere Res. Japan, **10**, No. 3, 124-142 (1956).

HIMAZAKI, T. Effect of the *Sq* current system on the ionospheric *E* and *F*1 regions. J. Radio Res. Lab. Japan, **4**, No. 15, 37-48 (1957).

LVERMAN, R. A. Fading of radio waves scattered by dielectric turbulence. J. Appl. Phys., **28**, No. 4, 506-511 (1957).

MMONS, G. J. Comments concerning the Kallmann-White-Newell article, "Physical properties of the atmosphere from 90 to 300 kilometers." J. Geophys. Res., **62**, No. 2, 327-328 (1957). [Letter to Editor.]

NGER, S. F., AND R. C. WENTWORTH. A method for the determination of the vertical ozone distribution from a satellite. J. Geophys. Res., **62**, No. 2, 299-308 (1957).

NGLETON, D. G. A study of "spread-*F*" ionospheric echoes at night at Brisbane. Aust. J. Phys., **10**, No. 1, 60-76 (1957).

NNO. K. On radio propagation disturbances. Rep. Ionosphere Res. Japan, **10**, No. 3, 143-147 (1956).

AO, K. On the relationship between the scattering of radio waves and the statistical theory of turbulence. J. Radio Res. Lab. Japan, **4**, No. 15, 15-24 (1957).

AIT, J. R. The geometrical optics of VLF sky wave propagation. Proc. Inst. Radio Eng., **45**, No. 6, 754-760 (1957). [VLF Symposium paper.]

AIT, J. R. The mode theory of VLF ionospheric propagation for finite ground conductivity. Proc. Inst. Radio Eng., **45**, No. 6, 760-767 (1957). [VLF Symposium paper.]

AIT, J. R. The attenuation *vs* frequency characteristics of VLF radio waves. Proc. Inst. Radio Eng., **45**, No. 6, 768-771 (1957). [VLF Symposium paper.]

ALTON, G. F. The relation between an *umkehr* curve and the vertical distribution of atmospheric ozone. Q.J.R. Met. Soc., **83**, No. 356, 173-180 (1957).

ATT, A. D., AND E. L. MAXWELL. Characteristics of atmospheric noise from 1 to 100 kc. Proc. Inst. Radio Eng., **45**, No. 6, 787-794 (1957). [VLF Symposium paper.]

ATTS, J. M. An observation of audio-frequency electromagnetic noise during a period of solar disturbance. J. Geophys. Res., **62**, No. 2, 199-206 (1957).

AYNICK, A. H. The present state of knowledge concerning the lower ionosphere. Proc. Inst. Radio Eng., **45**, No. 6, 741-749 (1957). [VLF Symposium paper.]

AYNICK, A. H. The present state of knowledge concerning the lower ionosphere. Pennsylvania State University, Ionosphere Res. Lab., Sci. Rep. No. 90, 34 pp. (Feb. 1, 1957).

EISS, A. A. The distribution of the orbits of sporadic meteors. Aust. J. Phys., **10**, No. 1, 77-102 (1957).

HEELON, A. D. Diurnal variations of signal level and scattering heights for the VHF propagation. J. Geophys. Res., **62**, No. 2, 255-266 (1957).

HEELON, A. D. Spectrum of turbulent fluctuations produced by convective mixing of gradients. Phys. Rev., **105**, No. 6, 1706-1710 (1957).

HITE, M. L. On the atmospheric dynamo theory. J. Geophys. Res., **62**, No. 2, 329-330 (1957). [Letter to Editor.]

ABROFF, I. W. Reflection at a sharply-bounded ionosphere. Proc. Inst. Radio Eng., **45**, No. 6, 750-753 (1957). [VLF Symposium paper.]

ONEZAWA, T. A new theory of formation of the *F*2 layer. II. The effect of the vertical movement of electrons and ions on the electron density distribution. J. Radio Res. Lab. Japan, **4**, No. 15, 1-14 (1957).

E—*Radio Astronomy*

LON, I., M. R. KUNDU, ET J.-L. STEINBERG. Dispositif interférométrique pour l'étude des sources solaires localisées centimétriques. Paris, C.-R. Acad. sci., **244**, No. 13, 1726-1729 (1957).

Arsac, J. Application of mathematical theories of approximation to aerial smoothing in radio astronomy. Aust. J. Phys., **10**, No. 1, 16-28 (1957).

Avignon, Y., É. J. Blum, A. Boischot, R. Charvin, M. Ginat, et P. Simon. Observation des orages radioélectrique solaires avec le grand interféromètre de Nançay. Paris, C.-R. Acad. sci., **244**, No. 11, 1460-1463 (1957).

Conway, R. G., and P. A. O'Brien. The distribution of brightness at metre wave-lengths across the sun's disk. Mon. Not. R. Astr. Soc., **116**, No. 4, 386-394 (1956).

Costain, C. H., B. Elsmore, and G. R. Whitfield. Radio observations of a lunar occultation of the Crab Nebula. Mon. Not. R. Astr. Soc., **116**, No. 4, 380-385 (1956).

Dagg, M. The correlation of radio-star-scintillation phenomena with geomagnetic disturbances and the mechanism of motion of the ionospheric irregularities in the *F* region. J. Atmos. Terr. Phys., **10**, No. 4, 194-203 (1957).

Dagg, M. Diurnal variations of radio-star scintillations, spread *F*, and geomagnetic activity. J. Atmos. Terr. Phys., **10**, No. 4, 204-214 (1957).

Davies, R. D. The relation between interstellar gas, dust and the emission from neutral hydrogen at 21 cm. Mon. Not. R. Astr. Soc., **116**, No. 4, 443-452 (1956).

Davis, R. J. 21-centimeter observations near galactic longitude 120°. Astroph. J., **125**, No. 2, 391-407 (1957).

Ellis, G. R. Cosmic radio-noise intensities below 10 Mc/s. J. Geophys. Res., **62**, No. 2, 229-234 (1957).

Ellis, G. R., and G. Newstead. Discrete sources of cosmic radio noise at 18.3 and 10.5 Mc/s. J. Atmos. Terr. Phys., **10**, No. 4, 185-188 (1957).

Erickson, W. C. Generation of polarized light in the Crab Nebula. Nature, **179**, 773 (April 13, 1957). [Letter to Editor.]

Harrower, G. A. Radio star scintillations and interstellar hydrogen. Nature, **179**, 608-610 (March 23, 1957).

Head, A. K. A new form for a giant radio telescope. Nature, **179**, 692-693 (April 6, 1957).

Kerr, F. J., and C. A. Shain. Reflexion of radio waves from the moon (with comment of J. D. Kraus). Nature, **179**, 433 (Feb. 23, 1957).

Kraus, J. D. Relation of 11-metre solar system phenomena to solar disturbances. Nature, **179**, 371-372 (Feb. 16, 1957). [Letter to Editor.]

Link, F. Preuves possible de l'ionosphère jovienne. Bull. Astron. Inst. Czechosl., **8**, No. 1, 4-5 (1957).

Mills, B. Y., and O. B. Slee. A preliminary survey of radio sources in a limited region of the sky at a wavelength of 3.5 M. Aust. J. Phys., **10**, No. 1, 162-194 (1957).

Rowson, B. Measurements of the angular diameters of two galactic radio sources at a wavelength of 10.7 cm. Proc. Phys. Soc., B, **70**, No. 447, 328-330 (1957). [Research note.]

Shain, C. A. Galactic absorption of 19.7 Mc/s radiation. Aust. J. Phys., **10**, No. 1, 195-203 (1957).

Whitehurst, R. N., J. Copeland, and F. H. Mitchell. Solar radiation and atmosphere attenuation at 6-millimeter wavelength. J. Appl. Phys., **28**, No. 3, 295-298 (1957).

F—*Earth's Crust and Interior*

Aggarwala, B. D., and E. Saibel. A hypothesis of formation of mountains and continents. Trans. Amer. Geophys. Union, **38**, No. 2, 245-247 (1957).

Antevs, E. Geological tests of the varve and radiocarbon chronologies. J. Geol., **65**, No. 2, 129-148 (1957).

Båth, M. A note on the measure of seismicity. Bull. Seis. Soc. Amer., **46**, No. 3, 217-218 (1956).

Båth, M. An earthquake catalogue for Fennscandia for the years 1891-1950. Stockholm, Sv. Geol. Unders., Ser. C, No. 545 (1956). [Årsbok 50, No. 1, 1956.]

Burke-Gaffney, T. N., and K. E. Bullen. Seismological and related aspects of the 1954 hydrogen bomb explosions. Aust. J. Phys., **10**, No. 1, 130-136 (1957).

Cole, G. H. A. Hydromagnetics and the earth's inner core. Observatory, **77**, No. 896, 17-19 (1957).

Du Toit, A. L. Our wandering continents. Hafner Publishing Co., New York, xiii + 366 (1957). [A re-issue; originally published in 1937.]

EARDLEY, A. J. The cause of mountain building—an enigma. Amer. Scientist, **45**, No. 3, 189-217 (1957).

GILVARRY, J. J. Temperatures in the earth's interior. J. Atmos. Terr. Phys., **10**, No. 2, 84-95 (1957).

HURLEY, P. M. Test on the possible chondritic composition of the earth's mantle and its abundance of uranium, thorium, and potassium. Bull. Geol. Soc. Amer., **68**, No. 3, 379-382 (1957). [Short note.]

INGLIS, D. R. Shifting of the earth's axis of rotation. Rev. Modern Phys., **29**, No. 1, 9-19 (1957).

LAPINA, M. I. Geomagnetism and seismic phenomena. Ottawa, Defense Research Board, No. T211R, 9 pp., mim. (March 1957). [Translation by E. R. Hope, from Izv. Akad. Nauk SSSR, Geophys. Ser., **5**, 393-404 (1953).]

NEW ZEALAND. Crustal structure project. (The Wellington profile, by G. A. Eiby; The seismic energy and magnitude of the explosion, by R. R. Dibble; The Pencarrow profile, by G. A. Eiby). Wellington, Department of Scientific and Industrial Research, R. E. Owen, Govt. Printer, Geophys. Mem. No. 5, 40 pp. (1957).

NUTTLI, O. W. Tentative velocities of seismic crustal waves in the central United States. Earthquake Notes, **27**, No. 4, 41-44 (1956).

SACKS, I. S. A low-noise transistorized seismic preamplifier. J. Geophys. Res., **62**, No. 267-278 (1957).

TARDI, P. Expériences séismique dans les Alpes occidentales en 1956; résultats obtenus par le "Groupe d'Études des Explosions Alpines." Paris, C.-R. Acad. sci., **244**, 9, 1114-1119 (1957).

G—*Miscellaneous*

ABETTI, G. The sun. The Macmillan Co., New York, 325 pp. (1957).

ATHAY, R. G., D. H. MENZEL, AND F. Q. ORRALL. Variations in the thermodynamic state of the chromosphere over the sunspot cycle. Smithsonian Contributions to Astrophysics, **2**, No. 4, 35-50 (1957).

BERKNER, L. V. The instrumented earth satellite. Science and Culture, **22**, No. 10, 553-554 (1957).

DOBRIN, M. B. Geophysical research and progress in exploration. Geophysics, **22**, No. 2, 412-433 (1957).

DUFAY, J. Gas and dust in interstellar space (translated by A. J. Pomerans). Hutchinson's Scientific and Technical Publications, London, 352 pp. + 24 pls. (1957).

DUGAS, R. A history of mechanics. Central Book Co., Inc., New York, 671 pp. (1957).

GREENWICH OBSERVATORY. Results of measures made at the Royal Greenwich Observatory of photographs of the sun taken at Greenwich, the Cape, and Kodaikanal in the year 1948. London, H. M. Stationery Office, vii + 216 pp. (1956). 30 cm.

GREENWICH OBSERVATORY. Results of measures made at the Royal Greenwich Observatory of photographs of the sun taken at Greenwich, the Cape, and Kodaikanal in the year 1949. London, H. M. Stationery Office, vii + 203 pp. (1956). 30 cm.

IONOSPHERE RESEARCH COMMITTEE, SCIENCE COUNCIL OF JAPAN. Catalogue of disturbances in ionosphere, geomagnetic field, field intensity of radio wave, cosmic ray, solar phenomena and other related phenomena. Rep. Ionosphere Res. Japan, **10**, No. 3, 163-226 (1956).

MARTRES, M. J., G. OLIVIERI, ET J. RAYROLE. Éruptions chromosphériques remarquables associées à des disparitions brusques de filaments. Paris, C.-R. Acad. sci., **244**, No. 13, 1724-1725 (1957).

PLUMPTON, C. Axially symmetric torsional oscillations of a star in the presence of a poloidal magnetic field. Astroph. J., **125**, No. 2, 494-499 (1957).

ST. AMAND, P., F. K. ODENCRANTZ, H. B. PETTIT, AND R. G. WELDON. A nomogram for solving spherical triangles and transforming astronomical coordinate systems. J. Geophys. Res., **62**, No. 2, 213-219 (1957).

SHEPPARD, P. A. Natural and artificial trace elements in geophysical research. Nature, **179**, 996-997 (May 18, 1957).

WALDMEIER, M. Final relative sunspot-numbers for 1956. J. Geophys. Res., **62**, No. 2, 309-311 (1957).

WALDMEIER, M. Provisional sunspot-numbers for January to March, 1957. J. Geophys. Res., **62**, No. 2, 319 (1957).

NOTICE

When available, single unbound volumes can be supplied at $6 each and single numbers at $2 each, postpaid.

Charges for reprints and covers

Reprints can be supplied, but prices have increased considerably and costs depend on the number of articles per issue for which reprints are requested. It is no longer possible to publish a schedule of reprint charges, but if reprints are requested approximate estimates will be given when galley proofs are sent to authors. Reprints without covers are least expensive; standard covers (with title and author) can be supplied at an additional charge. Special printing on covers can also be supplied at further additional charge.

Fifty reprints, without covers, will be given to institutions paying the publication charge of $8 per page.

Alterations

Major alterations made by authors in proof will be charged at cost. Authors are requested, therefore, to make final revisions on their typewritten manuscripts.

Orders for back issues and reprints should be sent to Editorial Office, 5241 Broad Branch Road, N.W., Washington 15, D. C., U.S.A.

Subscriptions are handled by The Editorial Office, 5241 Broad Branch Road, N.W., Washington 15, D. C., U.S.A.

CONTENTS—Concluded

JOURNAL OF GEOPHYSICAL RESEARCH